

Copper, Gold, Sulphurets,  
Northwestern British Columbia

802362

R. W. KIRKHAM

THE DEFORMED EARLY JURASSIC KERR COPPER - GOLD PORPHYRY DEPOSIT,  
SULPHURETS GOLD CAMP, NORTHWESTERN BRITISH COLUMBIA

by

DAVID JULIAN BRIDGE

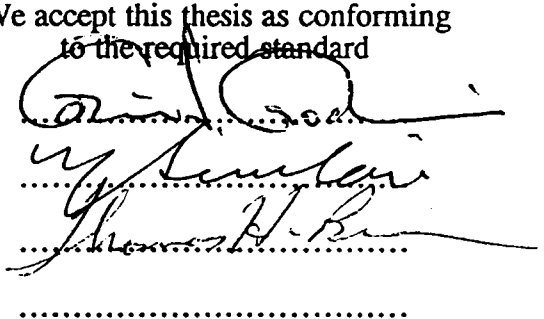
BASc., The University of British Columbia, 1990

A THESIS SUBMITTED IN PARTIAL FULFILLMENT OF  
THE REQUIREMENTS FOR THE DEGREE OF  
MASTER OF APPLIED SCIENCE

in

FACULTY OF GRADUATE STUDIES  
(Department of Geological Sciences)

We accept this thesis as conforming  
to the required standard

  
.....

THE UNIVERSITY OF BRITISH COLUMBIA

November 1993

© David Julian Bridge



## ABSTRACT

The Early Jurassic Kerr copper - gold porphyry deposit is hosted within a northerly striking, highly deformed and metamorphosed alteration zone in Late Triassic Stuhini Group sedimentary and volcanic rocks. Mineralization is related to west dipping calc-alkaline monzonite, syenodiorite ( $197 \pm 3$  Ma, U-Pb zircon) and K-Ba-feldspar megacrystic plagioclase hornblende porphyry ( $194 \pm 1.5$  Ma, U-Pb zircon) dykes. The Late Triassic sedimentary rocks exposed along the footwall form an east dipping, upright sequence of well bedded mudstone with conglomerate lenses overlain by conglomerate, sandstone and argillite. Feldspar fragments in the conglomerate indicate a local volcanic provenance.

see  
p. 28  
& p. 25

Copper and gold mineralization is concentrated in a region of early, texturally destructive potassic alteration, which is flanked by lower grade propylitic alteration. The potassic alteration was cut by monzonite dykes that were subsequently altered to sericite - quartz - pyrite. Alteration of the monzonite dykes coincided with widespread retrograde alteration of the potassic assemblage during the development of a banded quartz vein stockwork followed by pyrite - chalcopyrite veins and finally anhydrite - quartz - siderite - pyrite - chalcopyrite veins. The retrograde alteration of the deposit resulted in a core of chlorite - sericite - quartz - anhydrite - pyrite - chalcopyrite - magnetite, which has a halo of yellow sericite - quartz - pyrite - rutile alteration.

Structural fabrics in the deposit record southwesterly directed shortening coupled with southeasterly directed extension. A whole rock K-Ar age of  $124 \pm 4$  Ma from deformed sericite - quartz - pyrite monzonite suggests that the deposit was deformed and metamorphosed in the Cretaceous. This age and style of deformation correlates with widespread deformation in the Skeena Fold belt during the Late Jurassic to Early Tertiary. The deformation caused widespread recrystallization of the deposit with only local redistribution into extension gashes. Boudinaged dykes and left lateral displacement of the fabric across westerly dipping faults suggest that this deformation was followed by additional southeasterly directed contraction. Undeformed kersantite dykes ( $51.5 \pm 2$  Ma, whole rock K-Ar) intrude these westerly dipping faults.

Supergene alteration was focused where anhydrite occurred in the chlorite core of the deposit. Hydration of the anhydrite to gypsum caused the rock to fracture parallel to foliation, and resulted in a flaky rubble zone once the gypsum dissolved. Three supergene alteration zones developed in this permeable rubble: (i) leached hematite/jarosite, (ii) minor native copper and coatings of chalcocite/covellite, and (iii) stable chalcopyrite and pyrite without gypsum or anhydrite. The supergene alteration developed in the chlorite core mainly in response to the dissolution of the gypsum.

## TABLE OF CONTENTS

ABSTRACT	ii
TABLE OF CONTENTS	iii
LIST OF FIGURES	vi
LIST OF PLATES	xii
LIST OF TABLES	xiii
ACKNOWLEDGEMENTS	xv
1.0 INTRODUCTION	1
1.1 Focus of Study	3
1.2 Physiography and Vegetation	3
2.0 REGIONAL GEOLOGY	6
3.0 LOCAL GEOLOGY	9
3.1 Economic Geology	10
4.0 PROPERTY GEOLOGY	11
4.1 Volcanic and Sedimentary Rock Units Exposed Along the Footwall	13
4.2 Intrusive Rock Units	20
4.3 Geochemical Petrogenesis of Intrusive Rocks	30
4.3.1 Introduction	30
4.3.2 Major and minor element plot	35
4.3.3 Trace element spiderdiagram plots	35
4.4 Discussion of the Geological Setting of the Kerr Deposit	42
4.4.1 Sedimentary and volcanoclastic rock units	42
4.4.2 Intrusive rock units	43
5.0 STRUCTURAL GEOLOGY OF THE KERR DEPOSIT	45
5.1 Introduction	45
5.2 Local Structural Setting of the Kerr Deposit	47
5.3 Bedding in Sedimentary and Volcanoclastic Rocks in Domains 1 and 5	48
5.4 Penetrative Fabrics, Deformed Dykes, and Extension and Shear Veins in Domains 1 to 5	51
5.4.1 Domain 1	51
5.4.2 Domain 2	51
5.4.3 Domain 3	62
5.4.4 Domain 4	63
5.4.5 Domain 5	63
5.5 Discussion of Structural Features Related to $S_1$ and $S_2$	64

5.5.1 Orientation of S <sub>1</sub> and S <sub>2</sub> fabric in domains 1 to 5	64
5.5.2 Deformation of porphyry copper veins by S <sub>1</sub>	66
5.6 Timing of Major Deformation	70
5.7 Westerly Dipping Left Lateral Faults	72
5.8 Discussion Major Deformation of the Kerr Deposit	72
6.0 HYPOGENE ALTERATION AND MINERALIZATION IN THE KERR DEPOSIT	76
6.1 Introduction	76
6.2 Methodology for Selection of Alteration Zones	83
6.3 Alteration Zone Characteristics	84
6.3.1 Summary of copper and gold ratios	87
6.4 Description of Alteration Minerals and Veins	87
6.5 Description of Vein Assemblages	100
6.6 Alteration of Late Syn- and Post-Mineralization dykes	104
6.6.1 Alteration in augite and hornblende porphyry dykes	104
6.6.2 Alteration in albite and K-Ba-feldspar megacrystic plagioclase hornblende porphyry dykes	104
6.7 Effects of Deformation and Metamorphism on the Distribution of Minerals in the Three Alteration Zones	105
6.7.1 Core alteration zone	105
6.7.2 Halo alteration zone	106
6.7.3 Periphery alteration zone	109
6.8 Alteration of Tertiary Dykes	112
6.9 Late Gypsum Veins	112
6.10 Magmatic and Hydrothermal Alteration of the Kerr Deposit	112
6.11 Discussion of the Effects of Deformation on the Mineralogy of the Kerr Deposit	116
6.12 Discussion of Hydrothermal Alteration After Deformation	119
7.0 DESCRIPTION OF SUPERGENE ALTERATION IN THE KERR DEPOSIT	121
7.1 Introduction	121
7.2 Supergene Mineralogy	124
7.3 Geochemical Modeling	126
7.3.1 PCPATH computer program	128
7.3.2 Assumptions required for modelling the reactions between host rock and fluid	128
7.3.3 Geochemical model results	130
7.4 Application of Model Results to Formation of the 'Rubble Zone' in the Kerr Deposit	138
7.5 Discussion of Supergene Alteration	140
8.0 SUMMARY AND CONCLUSIONS	141
9.0 REFERENCES	146
APPENDIX A.0 GEOLOG DATABASE	150
A.1 Introduction	150
A.2 Methodology of Collecting Data from the Drill Core	150
A.2.1 Methodology for collection of alteration minerals and veins	151
A.3 Analysis of Visually Estimated Mineral Data	155
A.3.1 Probability plots	156
A.3.2 Discussion of probability plots	156

A.3.3 Plots of mineral populations	172
APPENDIX B.0 SAMPLE PREPARATION AND ANALYSIS OF ROCK SAMPLES	178
B.1 Sample Preparation	178
B.2 Sample Analysis	179
B.3 Precession and Accuracy of Results from XRAL	179
B.4 Precession of Cu and Au assays analyzed by Placer Dome Inc.	193
APPENDIX C.0 SCANNING ELECTRON AND MICROPROBE ANALYZES	199
C.1 Introduction	199
C.2 Preparation of Samples	199
C.3 Analysis of Electron Microprobe Results	199
C.4 Analysis of Scanning Electron Microprobe Results	203
C.4.1 Core alteration zone	203
C.4.2 Halo alteration zone	211
APPENDIX D.0 LIST OF VISUALLY ESTIMATED ALTERATION MINERALS AND MEASURED AMOUNTS OF VEINS	220
D.1 List of Abbreviations	220
D.2 Table of Visually Estimated Percentages of Alteration Minerals and Veins	223

## LIST OF FIGURES

Figure 1.1.	Location and regional geology of the Kerr deposit, northwestern British Columbia.	2
Figure 1.2.	Physiography of the Kerr deposit, northwestern British Columbia.	4
Figure 4.1.	Geology of the Kerr porphyry deposit, northwestern British Columbia.	12
Figure 4.2.	Geological cross-sections for sections 9700N and 10600N on the Kerr deposit.	17
Figure 4.3.	AFM diagram from Irvine and Barager (1971) showing least altered intrusive units on the Kerr deposit, northwestern British Columbia.	36
Figure 4.4.	Spiderdiagram of major and trace elements normalized to MORB for plagioclase augite diorite, monzonite and syenodiorite rock units from the Kerr deposit, northwestern British Columbia.	37
Figure 4.5.	Spiderdiagram of major and trace elements normalized to MORB for augite porphyry, hornblende porphyry, K-Ba-feldspar megacrystic plagioclase hornblende porphyry and albite megacrystic plagioclase hornblende porphyry rock units from the Kerr deposit, northwestern British Columbia.	38
Figure 4.6.	Spiderdiagram of major and trace elements normalized to MORB for trachytic plagioclase porphyry, aphanitic intermediate dyke and kersantite rock units from the Kerr deposit, northwestern British Columbia.	40
Figure 5.1.	Outline of structural domains and variation in penetrative fabric orientation across the Kerr deposit, northwestern British Columbia.	46
Figure 5.2.	Detailed geological map along section 9700N Kerr deposit, northwestern British Columbia.	49
Figure 5.3.	Detailed geological map along section 10600N Kerr deposit, northwestern British Columbia.	50
Figure 5.4.	Equal area stereonet of poles to weighted foliation $S_1$ in domain 1, Kerr deposit, northwestern British Columbia.	53
Figure 5.5 (A to D).	Equal area stereonets of poles to weighted foliation $S_1$ for domains 2 to 5.	54



Figure 5.6 (A to C).	Equal area stereonet of poles to weighted lineation for domains 2 to 4.	55
Figure 5.7.	Equal area stereonet of poles to $S_1$ and $S_2$ foliations along sections 9700N and 10600N. A) Domain 2 $S_1$ foliation, B) domain 2 $S_2$ foliation, C) domain 4 $S_1$ foliation, D) domain 4 $S_2$ foliation.	58
Figure 5.8 (A to B).	Equal area stereonet of poles to extension quartz veins along section 9700N in domains 2 and 3.	61
Figure 5.9 (A to B).	Equal area stereonet of poles to weighted lineation and foliation $S_1$ for all domains.	65
Figure 5.10.	Two cross - sections, 9700N and 10600N showing the distribution of deformed mineralized quartz veins in the Kerr deposit, northwestern British Columbia.	67
Figure 5.11 (A to C).	Equal area stereonet of poles to mineralized porphyry copper - gold veins along sections 9700N and 10600N in domains 2 to 3 on the Kerr deposit, northwestern British Columbia.	68
Figure 5.12.	Cross - sections 9700N and 10600N showing the distribution and orientation with respect to foliation $S_1$ of deformed sulphide veins.	71
Figure 5.13.	Average foliation $S_1$ orientation for each domain on the Kerr deposit, northwestern British Columbia.	74
Figure 6.1.	Distribution of core, halo and periphery alterations zones in the Kerr deposit, northwestern British Columbia.	82
Figure 6.2.	Copper and copper to gold ratios on sections 9700N and 10600N, Kerr deposit, northwestern British Columbia.	88
Figure 6.3.	Distribution of visually estimated chlorite and sericite and chlorite on sections 9700N and 10600N, Kerr deposit, northwestern British Columbia.	89
Figure 6.4.	Distribution of visually estimated grey and blue sericite and illite on sections 9700N and 10600N, Kerr deposit, northwestern British Columbia.	91
Figure 6.5.	Distribution of visually estimated silicification and yellow sericite on sections 9700N and 10600N, Kerr deposit, northwestern British Columbia.	94
Figure 6.6.	Distribution of visually estimated total magnetite and hematite and total tetrahedrite-tennantite on sections 9700N and 10600N, Kerr deposit, northwestern British Columbia.	97
Figure 6.7.	Distribution of measured mineralized quartz veins (type 1 and type 3) and sulphide veins (type 4) on sections 9700N and 10600N, Kerr deposit, northwestern British Columbia.	102

Figure 6.8.	Distribution of minerals filling fractures and pressure shadows in bull and banded quartz veins (type 1 and type 3), Kerr deposit, northwestern British Columbia.	107
Figure 6.9.	Distribution of early pervasive potassic and propylitic alteration across an idealized cross section 10600N, Kerr deposit, northwestern British Columbia.	114
Figure 6.10.	Distribution of pervasive phyllic alteration and syn-mineralization monzonite dyke across an idealized cross section 10600N, Kerr deposit, northwestern British Columbia.	115
Figure 6.11.	Distribution of sulphate and carbonate veins across an idealized cross section 10600N, Kerr deposit, northwestern British Columbia.	117
Figure 7.1.	Distribution of supergene minerals on sections 9700N and 10600N, Kerr deposit, northwestern British Columbia.	122
Figure 7.2.	Four supergene regions A to D in the pervasive chlorite alteration zone on sections 9700N and 10600N, Kerr deposit, northwestern British Columbia.	123
Figure 7.3 a).	Variation of log molality of $\text{Cu}^{2+}$ , $\text{Fe}^{2+}$ , $\text{Mn}^{+}$ , $\text{Au}^{+}$ ions versus Log XI.	131
Figure 7.3 b).	Variation of log molality of $\text{H}^{+}$ , $\text{HCO}_3^{-}$ , $\text{Ca}^{2+}$ and $\text{SO}_4^{2-}$ versus Log XI.	131
Figure 7.4.	Variation in log $f(\text{S}_2)$ and log $[\text{SO}_4^{2-}/(\text{OH}^{-})^2]$ during the PCPATH model.	132
Figure 8.1	Major alteration zones in the Kerr deposit, northwestern British Columbia. Data is from Tables 6.1 and 6.2.	144
Figure A.1.	Log histograms of averaged Cu (%) from intervals on cross - sections 9700N and 10600N in the Kerr deposit, northwestern British Columbia.	157
Figure A.2.	Log probability plot of averaged Cu (%) from intervals on cross sections 9700N and 10600N in the Kerr deposit, northwestern British Columbia.	158
Figure A.3.	Log histograms of averaged ratio of total chalcopyrite to pyrite (CP/PY) over intervals on cross - sections 9700N and 10600N in the Kerr deposit, northwestern British Columbia.	161
Figure A.4.	Log probability plot of averaged ratio of total chalcopyrite to pyrite over intervals on cross - sections 9700N and 10600N in the Kerr deposit, northwestern British Columbia.	162

Figure A.5.	Log histograms of averaged intergrown chlorite and sericite over intervals on cross - sections 9700N and 10600N in the Kerr deposit, northwestern British Columbia.	163
Figure A.6.	Log probability plot of averaged intergrown chlorite and sericite over intervals on cross - sections 9700N and 10600N in the Kerr deposit, northwestern British Columbia.	164
Figure A.7.	Log histograms of averaged chlorite envelopes to sulphide and sulphate veins over intervals on cross - sections 9700N and 10600N in the Kerr deposit, northwestern British Columbia.	165
Figure A.8.	Log probability plot of averaged chlorite envelopes to sulphide and sulphate veins over intervals on cross - sections 9700N and 10600N in the Kerr deposit, northwestern British Columbia.	166
Figure A.9.	Log histograms of averaged sericite envelopes to sulphide veins over intervals on cross - sections 9700N and 10600N in the Kerr deposit, northwestern British Columbia.	167
Figure A.10.	Log probability plot of averaged sericite envelopes to sulphide veins over intervals on cross - sections 9700N and 10600N in the Kerr deposit, northwestern British Columbia.	168
Figure A.11.	Log histograms of averaged total tetrahedrite-tennantite over intervals on cross - sections 9700N and 10600N in the Kerr deposit, northwestern British Columbia.	169
Figure A.12.	Log probability plot of averaged tetrahedrite-tennantite over intervals on cross - sections 9700N and 10600N in the Kerr deposit, northwestern British Columbia.	170
Figure A.13.	Log histograms of averaged total magnetite and hematite, total gypsum and anhydrite and carbonaceous material over intervals on cross - sections 9700N and 10600N in the Kerr deposit, northwestern British Columbia.	171
Figure A.14.	Cross - sections 9700N and 10600N showing the distribution of the high, medium and low populations in averaged Cu (%) and total chalcopyrite to pyrite ratio.	173
Figure A.15.	Cross - sections 9700N and 10600N showing the distribution of the high, medium and low populations in averaged intergrown chlorite and sericite and total magnetite and hematite.	174
Figure A.16.	Cross - sections 9700N and 10600N showing the distribution of the high, medium and low populations in averaged chlorite envelopes and sericite envelopes.	175
Figure A.17.	Cross - sections 9700N and 10600N showing the distribution of the	

	high, medium and low populations in averaged carbonaceous material and total tetrahedrite - tennantite.	176
Figure A.18.	Cross - sections 9700N and 10600N showing the distribution of the high, medium and low populations in averaged total gypsum and anhydrite.	177
Figure B.1.	Precision control graphs for: SiO <sub>2</sub> , Al <sub>2</sub> O <sub>3</sub> , K <sub>2</sub> O, Na <sub>2</sub> O, CaO and Fe <sub>2</sub> O <sub>3</sub> (wt%).	184
Figure B.2.	Precision control graphs for: MgO, TiO <sub>2</sub> , MnO and P <sub>2</sub> O <sub>5</sub> (wt%).	185
Figure B.3.	Precision control graphs for: Cr, As, Sb, U, W and Th (ppm).	186
Figure B.4.	Precision control graphs for: Sr, Ba, Cl, Rb, Zr and Nb (ppm).	187
Figure B.5.	Precision control graphs for: B, Co, Ni, Cu, Zn and V (ppm).	188
Figure B.6.	Precision control graphs for: Y (ppm), Sc (ppm), Au (ppb), Pd (ppb), Hg (ppb) and S (wt%).	189
Figure B.7.	Precision control graphs for: La, Ce, Pr, Nd, Sm and Eu (ppm).	190
Figure B.8.	Precision control graphs for: Gd, Tb, Dy, Ho, Er and Tm (ppm).	191
Figure B.9.	Precision control graphs for: Yb, Lu and Tl (ppm).	192
Figure B.10.	Precision control graphs for assayed Cu (wt %) and Au (ppb) for intervals on cross - sections 9700N and 10600N in the Kerr deposit, northwestern British Columbia.	194
Figure C.1.	Energy dispersive spectrometry (EDS) spectra for a) siderite in sample KS-125 190.6m, b) disseminated magnetite, c) chlorite and d) siderite.	204
Figure C.2.	EDS spectra for a) chlorite neighbouring anhydrite, b) sericite, c) anhydrite and d) gypsum in veinlet.	206
Figure C.3.	EDS spectra for a) chlorite intergrown with chalcopyrite and sericite, b) same chlorite as a but with minor K, c) chlorite intergrown with chalcopyrite, d) same as c but with Fe contamination, and e) barite in contact with chlorite.	208
Figure C.4.	EDS spectra for a) point B on a chlorite grain with minor intergrown rutile, b) point C on the chlorite grain, c) point D on the chlorite grain, d) point E on the chlorite grain showing minor K in it, and e) sericite in the matrix surrounding the chlorite grain.	209
Figure C.5.	EDS spectra for a) chlorite intergrown with ilmenite, b) ilmenite intergrown with a, c) sericite intergrown with ilmenite, d) ilmenite intergrown with c, and e) gold with a minor silver content intergrown with chalcopyrite.	210

- Figure C.6. EDS spectra for a) tetrahedrite - tennantite grain in quartz vein in sample KS-125 16 m, b) Ti phase inclusions in pyrite, c) chalcopyrite inclusion intergrown with pyrrhotite in pyrite, d) pyrrhotite with c, e) yellow sericite grain, and f) radiating chlorite in extensional quartz vein. 212
- Figure C.7. EDS spectra for a) pale brown calcite with trace Mn b) calcite fibres near a, c) calcite fibres away from a with no Mn peak, and d) chlorite along pyrite veinlet. 214
- Figure C.8. EDS spectra for a) sphalerite in carbonate vein, b) tennantite with a, c) Br-Sr-Ca sulphate mineral with a, d) Ba-Sr-sulphate mineral with a, and e) recrystallized calcite in the carbonate vein. 215
- Figure C.9. EDS spectra for a) clintonite in yellow sericite altered mudstone, b) Zn mineral in rock which may be zincite or smithsonite, and c) sericite in the matrix. 215a
- Figure C.10. EDS spectra for a) chalcopyrite inclusion in pyrite, b) bornite inclusion in pyrite grain in a, c) disseminated tennantite, d) yellow sericite grain and e) grey sericite grain. 217
- Figure C.11. EDS spectra for a) olive green sericite intergrown with rutile and b) rutile intergrown with a). 218
- Figure C.12. EDS spectra for a) yellow sericite intergrown with rutile and b) rutile intergrown with a). 219



# LIST OF PLATES

Plate 4.1.	Mudstone with graded bedding and ripple marks exposed along the footwall on section 9700N.	15
Plate 4.2.	Conglomerate with clasts of fine grained tuffaceous rock, chert, and minor feldspar porphyritic rock.	18
Plate 4.3.	Conglomerate with clasts of argillite, tuffaceous rock, feldspar porphyry and trace chert in a matrix of broken feldspar grains.	18
Plate 4.4.	Well bedded argillite with normal grading of coarse sand to clay sized particles.	19
Plate 4.5.	Volcanic conglomerate exposed immediately above fault contact with argillite in plate 4.4.	19
Plate 4.6.	Photomicrograph of oscillatory zoned augite (bright second order colours) and sericite altered plagioclase with rims of K-feldspar.	23
Plate 4.7.	Breccia between buff weathering tuff and white to tan weathering syenodiorite.	23
Plate 4.8.	Photomicrograph of sericite altered, oscillatory zoned plagioclase, chlorite altered hornblende and euhedral orthoclase poikilitically enclosing subhedral plagioclase in a matrix of quartz, chlorite and sericite.	26
Plate 4.9.	Chill contact between K-Ba-feldspar megacrystic porphyry and syenodiorite on the ridge below Kerr Peak.	26
Plate 5.1.	Photomicrograph of intensely deformed sericite-quartz-pyrite alteration, Kerr deposit.	57
Plate 5.2.	Stockwork of quartz veins in chlorite alteration.	57
Plate 5.3.	Boundinaged quartz veins with rotated segments.	69
Plate 5.4.	Photograph of a deformed sulphide vein with quartz filled pressure shadows in domain 2.	69
Plate 5.5.	West directed view of apparent left lateral faults deforming well developed S <sub>1</sub> and S <sub>2</sub> fabric.	73
Plate 6.1.	Sample from KS-94 40.8m, Figure 4.2, stained for K-feldspar (bright yellow) patches.	93
Plate 6.2.	Broken pyrite grains in a matrix of Fe - chlorite grains, quartz and minor sericite.	93

# LIST OF TABLES

Table 4.1.	Modal composition of volcanoclastic and sedimentary units exposed on the Kerr deposit, northwestern British Columbia.	14
Table 4.2.	Modal mineralogy of intrusive rocks exposed on the Kerr deposit, northwestern British Columbia.	21
Table 4.3.	Timing relationships among the dykes, mineralization and deformation in the Kerr deposit, northwestern British Columbia.	25
Table 4.4.	Whole rock K-Ar data from two samples on the Kerr deposit, northwestern British Columbia.	31
Table 4.5.	Primary and alteration mineralogy of the least altered of each intrusive rock unit submitted for whole rock geochemical analysis.	32
Table 4.6.	Whole rock geochemical results of least altered intrusive rocks on the Kerr deposit, northwestern British Columbia.	34
Table 5.1.	Structural measurements from different domains on the Kerr deposit, northwestern British Columbia.	52
Table 5.2.	Calculated strike and dip of the edge of the contact between highly and weakly deformed rock in the Kerr deposit, northwestern British Columbia.	60
Table 6.1.	Percentages of alteration minerals in the core, halo and periphery of the Kerr deposit, northwestern British Columbia.	77
Table 6.2.	Summary of mineralogical and vein characteristics of each alteration zone, Kerr deposit, northwestern British Columbia.	80
Table 6.3.	Effect of deformation and metamorphism on minerals in the core alteration zone, Kerr deposit, northwestern British Columbia.	108
Table 6.4.	Effect of deformation and metamorphism on minerals in the halo alteration zone, Kerr deposit, northwestern British Columbia.	110
Table 6.5.	Effect of deformation and metamorphism on minerals in the peripheral alteration zone, Kerr deposit, northwestern British Columbia.	111
Table 7.1.	Percentages of alteration and supergene minerals intersected by a hypothetical flow path through the Kerr deposit, northwestern British Columbia.	125
Table 7.2.	Starting and equilibrium solutions for geochemical modeling of supergene process in the Kerr deposit, northwestern British Columbia.	127

Table 7.3.	List of chemical reactions for supergene processes on the Kerr deposit, northwestern British Columbia. (Specified reactions are referred to in text and on figures).	133
Table A.1.	Table of minerals recorded during detail core logging of the Kerr deposit, northwestern British Columbia.	152
Table A.2.	Table of thresholds and means of mineral populations.	160
Table B.1.	Methodology for sample digestions use for analysis by X-ray Assay Labs, (Levin, personal communication 1992)	180
Table B.2.	Precision control graph data from duplicates submitted to X-ray Assay Lab.	182
Table B.3.	Table of geochemistry for an internal standard WP1.	195
Table B.4.	Table of geochemistry for an internal standard P1.	197
Table C.1.	Table of calculated composition of K-feldspars analyzed by electron microprobe from three different dykes	201
Table C.2.	Table of calculated composition of sericite analyzed by electron microprobe from three samples.	202

## ACKNOWLEDGEMENTS

Fieldwork for this study was supported by financial and technical assistance provided by Placer Dome Inc. and the Mineral Deposit Research Unit (MDRU), Department of Geological Sciences at The University of British Columbia. Special thanks are extended to E. Kimura, J. Kowalchuk, R. Pease, S. Price, G. Ditson, B. Fowler and G. Shevchenko of Placer Dome Inc. P. Lewis, T. Brown and J. Ross of the Department of Geological Sciences at The University of British Columbia are thanked for technical discussions; C. Godwin supervised the thesis; Y. Douma and B. Cranston prepared polished thin sections and gave photographic advice, respectively. This project is part of the Mineral Deposit Research Unit study "Metallogeny of the Iskut River Area, Northwestern B.C.", funded by thirteen companies, a Science Council of British Columbia Research and Technology grant, and a National Science and Engineering Research Council Collaborative Research and Development grant.

## 1.0 INTRODUCTION

The Kerr copper - gold porphyry deposit, owned by Placer Dome Inc., has a northerly strike length of 1600 metres and an average width of 100 metres. It contains a resource of 135 million tonnes grading 0.76% copper and 0.34 g/t gold (Ditson, personal comm. 1993). The deposit, located on Figure 1.1 (NTS 104B/8: 56°28'30" north, 130°16' west), is in the Sulphurets gold camp in the Boundary Ranges of the Coast Mountains, 60 km north-northwest of Stewart, British Columbia. This camp has been active for over 100 years. Recent activity has concentrated on precious and base metal deposits associated with Early Jurassic monzonite intrusions. The Sulphurets gold camp is at the eastern edge of a metallogenic belt that stretches from the Galore Creek gold camp in the northwest to the Stewart gold camp.

Geological mapping by Grove (1986), Alldrick and Britton (1988), Anderson and Thorkelson (1991) and Kirkham (1991) shows that the Sulphurets gold camp is within a Late Triassic to Early Jurassic volcanoplutonic arc along the western margin of the Stikine terrane.

The Kerr deposit was first staked by the Alpha Joint Venture in 1982 to cover ground south of gold showings along Sulphurets Creek held by Esso Minerals Canada Limited (Epp, 1985). Brinco Limited optioned the property and conducted a surface geochemistry and drill program from 1984 to 1986. Western Canadian Mining Corporation optioned the property in 1986; during diamond drilling in 1987 they recognized the porphyry style mineralization in the deposit (Kowalchuk and Jerema, 1987). Subsequent drilling in 1988 and 1989 by Western Canadian Mining Corporation and Sulphurets Gold Corporation outlined a region of copper and gold mineralization hosted by foliated sericitic and chloritic quartz - pyrite schist cut by a stockwork of quartz, sulphide and sulphate veins. In 1989 Placer Dome Inc. purchased the property. Their diamond drilling in 1990 and 1992 was designed to define the continuity of mineralization in this highly deformed copper - gold porphyry deposit.



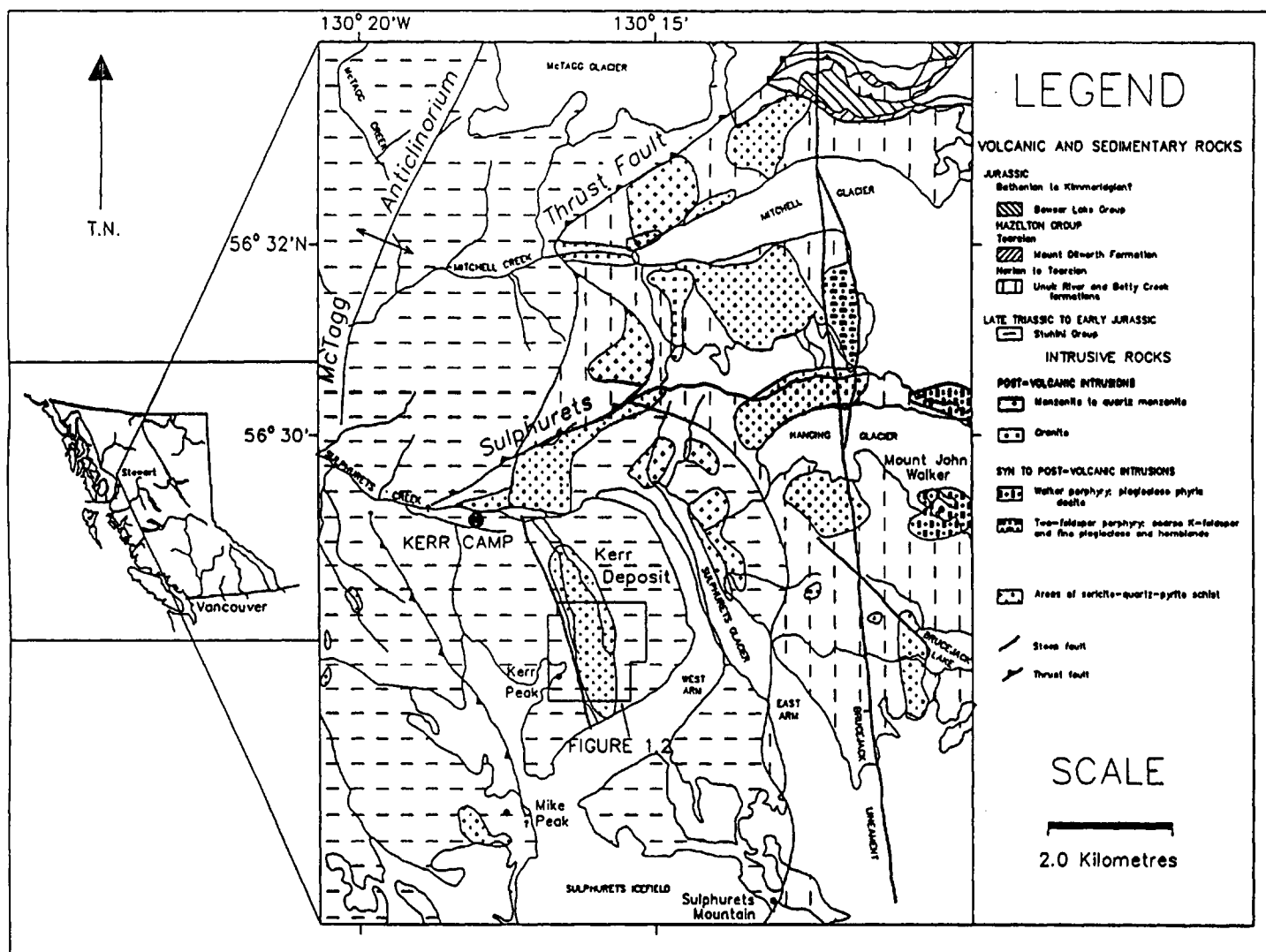


Figure 1.1. Location and regional geology of the Kerr deposit, northwestern British Columbia. Geology was compiled from maps by Alldrick and Britton (1988), Kirkham (1991), Alldrick and Britton (1991) and Lewis (1992).

### 1.1 Focus of Study

This study focuses on the geology, timing of intrusive events, alteration mineral assemblages and structure of the Kerr deposit. Spatial and temporal relationships among pre- to post-mineralization intrusions and their host rocks were determined by core logging coupled with detailed geological mapping along two cross-sections of the deposit. Modal mineralogy of the intrusions, whole rock geochemistry and U-Pb zircon geochronometry provide a framework for determining the magmatic and hydrothermal activity responsible for the formation of the Kerr deposit. Preliminary results of this study have been published by Bridge and Godwin (1992).

Quantative estimates of the hypogene and supergene alteration mineral assemblages were used to outline their spatial distribution and relationship to the copper and gold content of the porphyry deposit. Textural and cross-cutting relationships among alteration minerals and veins were also used to determine their sequence of formation.

Relationships between the deformation, and the spatial distribution of copper and gold mineralization were investigated. Petrographic analysis and examination of the distribution of shear and extensional veins showed that they represent precipitation by fluids during metamorphism and deformation of the deposit.

### 1.2 Physiography and Vegetation

The Kerr porphyry copper - gold deposit straddles the east shoulder of Kerr Peak (Fig. 1.2). Most of the mineralization crops out between elevations of 1200 m and 1850 m. The north facing slope of the deposit is partly covered by a permanent snowfield. Part of the deposit at the base of the cirque is covered by ground moraine that is buried by recent debris from the cliffs below Kerr Peak.

No vegetation grows on mineralized outcrops of the Kerr deposit except where covered by moraine. Stunted alpine fir and hemlock grow below 1450 m elevation on the east dipping

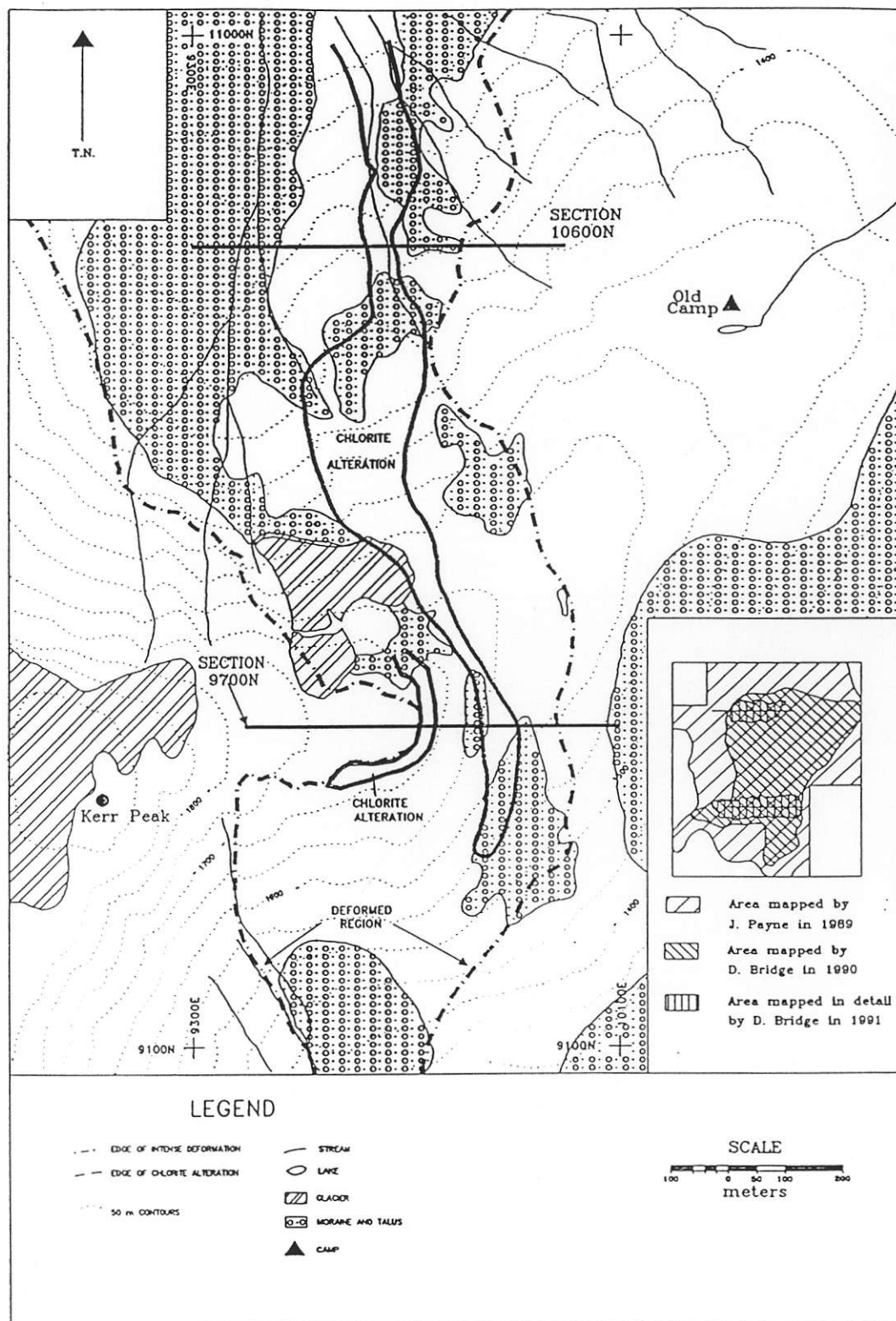


Figure 1.2. Physiography of the Kerr deposit, northwestern British Columbia. The outline of the central chlorite alteration and limit of intense deformation is shown. Insert shows areas of compiled geology from mapping in 1990-1991 and Payne (1989).

slope above the Sulphurets glacier. Tall stands of hemlock, alpine fir and spruce grow below 900 m elevation on the east side of the north facing bowl below the cirque, and above the trim line of the Sulphurets Glacier. Alpine meadows cover moraine and talus slopes above the Sulphurets Glacier.

## 2.0 REGIONAL GEOLOGY

The Kerr deposit is hosted in a Late Triassic to Early Jurassic volcanoplutonic complex situated along the western margin of the Stikine terrane (Anderson and Thorkelson, 1991). The Stikine terrane is a Devonian to Jurassic volcanic island arc that was amalgamated with another volcanic island arc, the Quesnellia terrane, in the Triassic. This composite terrane was later accreted to the North American craton by the Middle Jurassic (Monger 1990).

The stratigraphy of the Stikine terrane in the metallogenic belt from the Galore Creek to Iskut to Sulphurets to Stewart gold camps (GISS) consists of Late Triassic Stuhini Group sedimentary rocks and augite phyric volcanic rocks unconformably overlying folded Paleozoic strata. The Stuhini Group sediments are divided into a western facies that overlies the Paleozoic strata around the Stikine River and an eastern facies exposed in the core of the McTagg anticlinorium six kilometres west of the Sulphurets gold camp. The eastern facies consists of two sequences of laminated argillaceous siltstone and mudstones separated by pyroxene phyric flows, breccia and conglomerate. This sequence lacks the coralline limestone and felsic volcanic rocks of the western facies (Anderson and Thorkelson, 1991).

The Hazelton Group unconformably overlies the Stuhini Group. The lowermost strata, the Jack formation, consists of cobble to boulder conglomerate with limestone clasts overlain by fossiliferous limy sandstone and siltstone (Henderson et al., 1992). Overlying the Jack formation is the Unuk River Formation consisting of andesitic tuffs to breccias interbedded with argillaceous shales. The volcanic rocks are temporally and spatially related to the Early Jurassic, calc-alkaline Texas Creek plutonic suite of sub-volcanic and epizonal intrusions. Most intrusions are wholly or in part K-feldspar megacrystic with a matrix of subordinate plagioclase and hornblende phenocrysts. These intrusions are spatially and possibly temporally related to all major porphyry and shear vein deposits in the GISS metallogenic belt. The intrusions range in age from 195 to 189 Ma (Anderson, 1993).



Late phases of the Texas Creek plutonic suite (K-feldspar megacrystic porphyry stocks) are cogenetic with the Betty Creek Formation that conformably overlies the Unuk River Formation. The Betty Creek Formation is composed of volcanic conglomerate, breccia and siltstone. Mount Dilworth Formation is exposed extensively in the metallogenic belt as a pyritic, felsic tuff and breccia unconformably above the Betty Creek Formation. The formation is cogenetic with silicic flow domes near the Eskay Creek volcanic massive sulphide deposit (Bartsch, 1993).

The Lower Jurassic to Middle Jurassic Salmon River Formation unconformably overlies the Mount Dilworth Formation and Stuhini Group rocks. This formation is exposed in three northerly trending belts in the GISS metallogenic belt, and it represents sedimentation in a back-arc following the quiescence of the Early Jurassic volcanic arc (Anderson and Thorkelson, 1991). The central, Eskay Creek facies, is exposed as a northerly thickening sequence of fossiliferous, calcareous siltstone and overlying pillowed mafic flows (Anderson and Thorkelson, 1991). Rhythmically banded, siliceous shale and tuff occur in easternmost facies exposed 15 km north of the Premier gold mine.

Conformably overlying the Salmon River Formation is the Middle to Upper Jurassic Bowser Lake Group clastic rocks. These rocks fill the Bowser Basin that adjoins the GISS metallogenic belt to the east.

Regional deformation, related to the development of the Skeena fold and thrust belt during the Late Jurassic to Early Tertiary, deformed the Stuhini, Hazelton and Bowser Lake group rocks into north to northwest trending folds (Evenchick, 1991) with a moderate to strong axial plane foliation (Lewis, 1992). These folds are synchronous with widespread sub-greenschist to greenschist metamorphism of the rocks. The westerly dipping Sulphurets thrust fault and sinistral, South Unuk/Harrymel fault formed during this regional compression (Lewis, 1992). Motion on the Sulphurets thrust fault was directed to the southeast.

Hyder plutonic suite of Tertiary plutons (44 - 54 Ma) intrude the southern margin of the GISS metallogenic belt along the Canadian and United States border (Anderson and Bevier,

1990). All of the intrusions cut the regional fabric and contain biotite as the dominant mafic mineral. Locally, they form dykes swarms that may be related to Tertiary crustal extension (Brown, 1987).

### 3.0 LOCAL GEOLOGY

The Sulphurets gold camp is centered on epizonal, Early Jurassic plutons that intruded Late Triassic Stuhini Group and Early Jurassic Hazelton Group sedimentary and volcanic rocks (Fig. 1.1). Lowermost units of the Stuhini Group rocks consist of rhythmically banded siltstones and arkosic wackes with interbeds of volcanic clasts (Britton and Alldrick, 1988; Henderson et al., 1992). Overlying these rock units are pyroxene phyric lava flows, breccia and tuff. Topmost units are thin bedded siltstone, mudstone and conglomerate with possible granitoid clasts (Henderson et al., 1992).

Unconformably overlying the Stuhini Group sediments are the Jack formation sedimentary rocks, and the Unuk River Formation and Betty Creek volcanoclastic rocks, which are coeval with calc-alkaline, sub-volcanic intrusions exposed two kilometres north of Brucejack Lake (Fig. 1.1; Alldrick, 1989) and a flow dome south of the lake (Roach and Macdonald, 1992). Volcanoclastic rocks, tuffs, lapilli tuffs and breccias in the Unuk River Formation are intermediate in composition, and they are interbedded with minor siltstone beds. Betty Creek volcanoclastic rocks around Mount John Walker are dominated by purple to maroon volcanic conglomerate.

Calc-alkaline post-volcanic intrusions range in composition from equigranular monzonite to granodiorite, and locally, they are cut by porphyritic alkali-feldspar phyric andesitic dykes (Alldrick and Britton, 1991). Aphanitic, mafic dykes trending easterly cut the intrusive rocks on the ridge between Sulphurets and Mitchell creeks. These dykes are basaltic andesite in composition and have a groundmass of hornblende, plagioclase and clinopyroxene crystals (Margolis, 1992; Kirkham, 1963).

Fold and thrusting during the Late Jurassic to Early Tertiary deformed the Stuhini and Hazelton group rocks (Lewis, 1992). The western edge of the Sulphurets gold camp is covered by Stuhini Group rocks on the hanging wall of the southeasterly vergent Sulphurets

thrust fault. Peak metamorphism in the Sulphurets gold camp is at least lower greenschist in grade and occurred during deformation of the region (Alldrick and Britton, 1988). A northerly penetrative fabric, parallel to the trend of the McTagg anticlinorium, developed in the Stuhini Group rocks to the west of the Sulphurets thrust fault (Lewis, 1992). East of the thrust fault and north of the Sulphurets Creek, the penetrative fabric is orientated easterly and dips steeply north (Margolis, 1992; Kirkham, 1963).

### 3.1 Economic Geology

Published geological mapping completed by Kirkham (1991), Britton and Alldrick (1988), and Roach and Macdonald (1992) have documented porphyry copper - gold, porphyry gold, shear - hosted gold and silver and possible epithermal gold deposits in the Sulphurets gold camp. All deposits are spatially associated with the Early Jurassic Texas Creek suite of intrusions.

Porphyry copper - gold deposits are associated with potassic alteration with superimposed phyllic alteration around monzonite to quartz monzonite intrusions. Mineralization in these deposits consists of disseminated pyrite, chalcopyrite and minor molybdenite with hematite and magnetite throughout and adjacent to the intrusive contact. Along the trace of the Sulphurets fault, 1.5 km north of the terminus of the Sulphurets Glacier, remnants of hydrothermal biotite occur in foliated sericite - quartz alteration with disseminated chalcopyrite and molybdenite (Kirkham, 1963).

Base and precious metal quartz - carbonate veins crop out between the Hanging Glacier and Brucejack Lake (Kirkham, 1963), and around the southern shore of the lake in the West zone (Roach and Macdonald, 1992). Veins in the West zone are in a silica flooded alteration zone which strikes 140°.

#### 4.0 PROPERTY GEOLOGY

The Kerr Property is underlain by volcanic and sedimentary units of the Late Triassic Stuhini Group. These were intruded by Early Jurassic and Eocene dykes. Intense hydrothermal alteration and deformation has partially obliterated the identity of the units in the centre of the deposit so that individual contacts of rock units cannot be traced across the deposit with confidence. This highly altered and deformed region hosts the porphyry copper-gold deposit. The porphyry deposit strikes northward and dips steeply west (Fig. 4.1). The elongate core of the porphyry deposit consists of chlorite and sericite altered tuffaceous rocks with disseminated pyrite and minor chalcopyrite (Fig. 4.1). The chlorite alteration hosts a stockwork of magnetite and specular hematite, bull and banded quartz, pyrite - chalcopyrite, anhydrite - quartz - siderite - pyrite - chalcopyrite, and pink anhydrite - pyrite - chalcopyrite veins.

Rock units 50 metres or more from either side of the chlorite core can be identified because they are relatively unaltered. The footwall of the Kerr deposit is defined as the region to the east of the chlorite alteration marked on Figure 4.1. West of the chlorite alteration intersected by section 9700N, there is a region of weakly deformed mineralization and tuffaceous rocks. The mineralization in this region is known as the upper lense.

Detailed geological mapping along 200 m wide panels centered along sections 9700N and 10600N was completed in 1991 (Fig. 1.2). Traverses in 1990, guided by mapping by Payne (1989), outlined the geology between the two cross-sections and the surrounding area.

Bedding in the sedimentary units strikes parallel to the chlorite core, but it dips steeply to the east along the footwall and gently to the west in the hanging wall (Fig. 4.1). Plagioclase augite diorite to aphanitic intermediate dykes are concentrated in the deformed alteration zone (Fig. 4.1).

Sedimentary rock units are described from the oldest to youngest for both the hanging wall and the footwall separately because contacts across the deposit have not been observed.

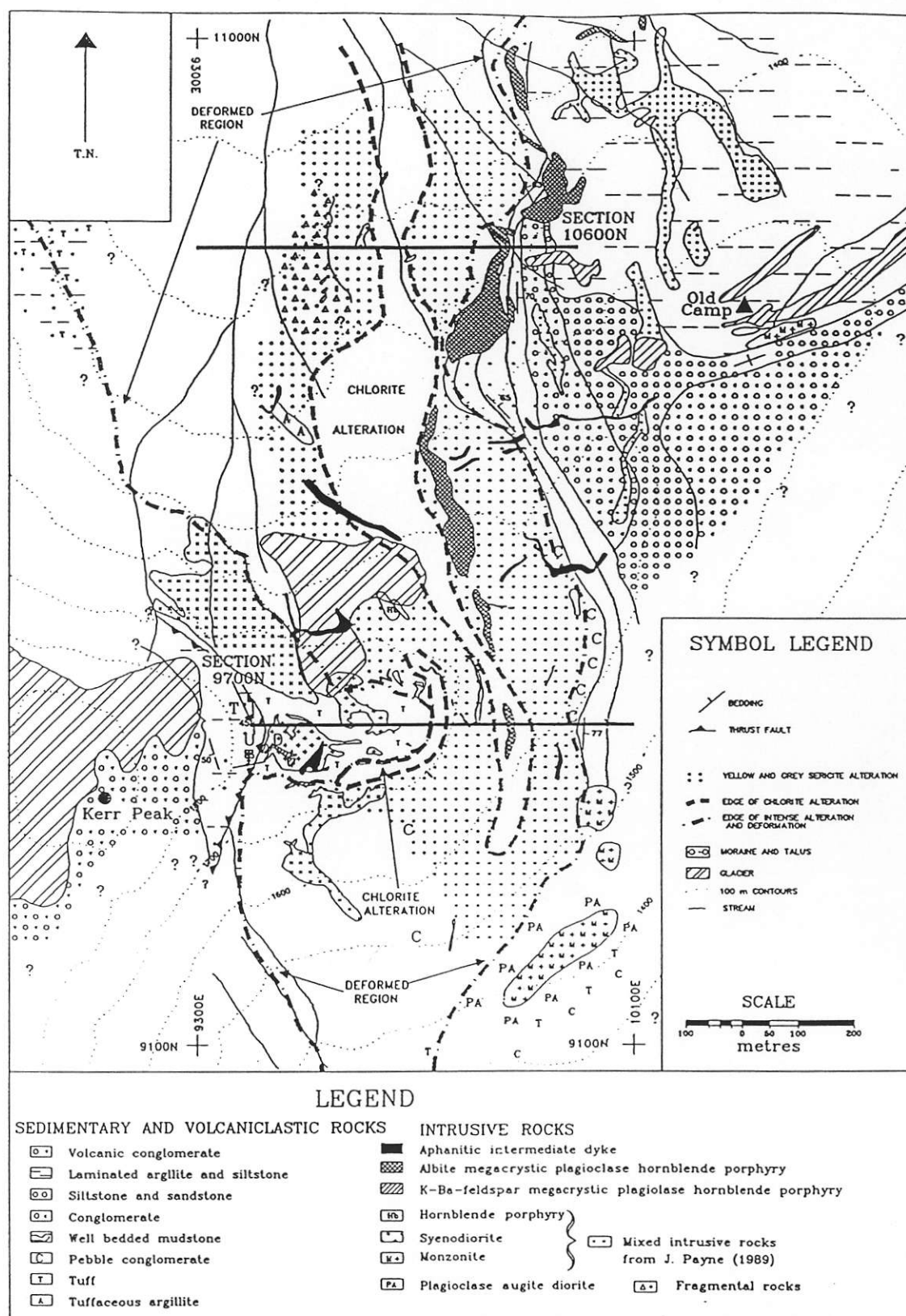


Figure 4.1. Geology of the Kerr porphyry deposit, northwestern British Columbia. Surface geology between deformation lines is omitted due to the intense alteration that obliterated contacts between the tuffaceous and sedimentary units. Thin biotite lamprophyre (kersantite) and trachytic plagioclase porphyry dikes are omitted.

Intrusive rock units are described in temporal order determined from cross-cutting relationships, style of deformation, intensity of hydrothermal alteration and geochronometry. Timing of the various intrusive events with respect to mineralization can be deduced from cross-cutting relationships of the different veins and alteration assemblages.

#### **4.1 Volcanic and Sedimentary Rock Units Exposed Along the Footwall**

Massive tuff, exposed along the footwall and above the upper mineralized lense (Fig. 4.1), is a uniform, crystal rich unit with occasional beds of volcanic conglomerate and mudstone. Faint graded bedding is observed on pale brown weathered outcrops outside the area of intense mineralization. The graded bedding suggests that the unit may represent reworked submarine tuffaceous deposits. Due to the intense surface weathering, volcanic conglomerate was observed only in drill core.

The mineralogy of the massive tuff exposed on the eastern end of section 9700N is dominated by broken perthitic orthoclase and quartz grains (Table 1); in the hanging wall it consists of broken grains of quartz, plagioclase and hornblende. The original constituents of the matrix could not be identified due to alteration.

Well bedded mudstone, exposed along the footwall, has prominent graded bedding with rare ripple marks (Fig. 4.1, Plate 4.1). The unit dips steeply to the east along the footwall of the deposit where it is at least 200 metres thick. The mudstone weathers pinkish brown or yellow-brown, depending upon the degree of hydrothermal alteration.

Bedding in each layer consists of 1 to 2 millimetre laminations of very fine grained quartz and feldspar, and graded coarser layers 5 to 20 mm thick consisting of fragments of feldspar and amphibole (Table 4.1). The size of clasts in the coarser layers in the footwall section decrease up section from cobble to sand size. Samples of the unit with ripple marks indicate that the unit does not have reverse graded bedding (Plate 4.1).

Table 4.1. Modal composition of volcanoclastic and sedimentary units exposed on the Kerr deposit, northwestern British Columbia.

Legend: Qtz. = quartz, Ser. = sericite, Chl. = chlorite, Carb. = carbonate

Rock Unit	Location	Mineralogy						Matrix			
		Quartz	Plagioclase	K-feldspar	Amphibole	Ilmenite	Apatite	Qtz.	Ser.	Chl.	Carb.
Laminated argillite	footwall, hanging wall	20% 0.1-0.2 mm	5% 0.1 - 0.3 mm	5% 0.1 mm			1%		Major	Major	1%
Sandstone (Arkose)	footwall, hanging wall	trace	50-70% 0.05-0.2 mm An33	10% perthitic		5% 0.015 mm		Minor		20%	10%
Conglomerate	footwall										
Well bedded mudstone	footwall, hanging wall	20% 0.005 mm							80%		
Massive tuff											
Plagioclase dominant	hanging wall	2-30% 0.1-0.3 mm	40% 0.2-1.5 mm broken		10% 0.1-0.4 mm subhedral	2% 0.015 mm	trace - 0.5% 0.01-0.2 mm	40-50%	30%		
K-feldspar dominant	footwall	10% 0.5 mm	minor broken	30-50% 2 mm broken	10%				Minor		Minor



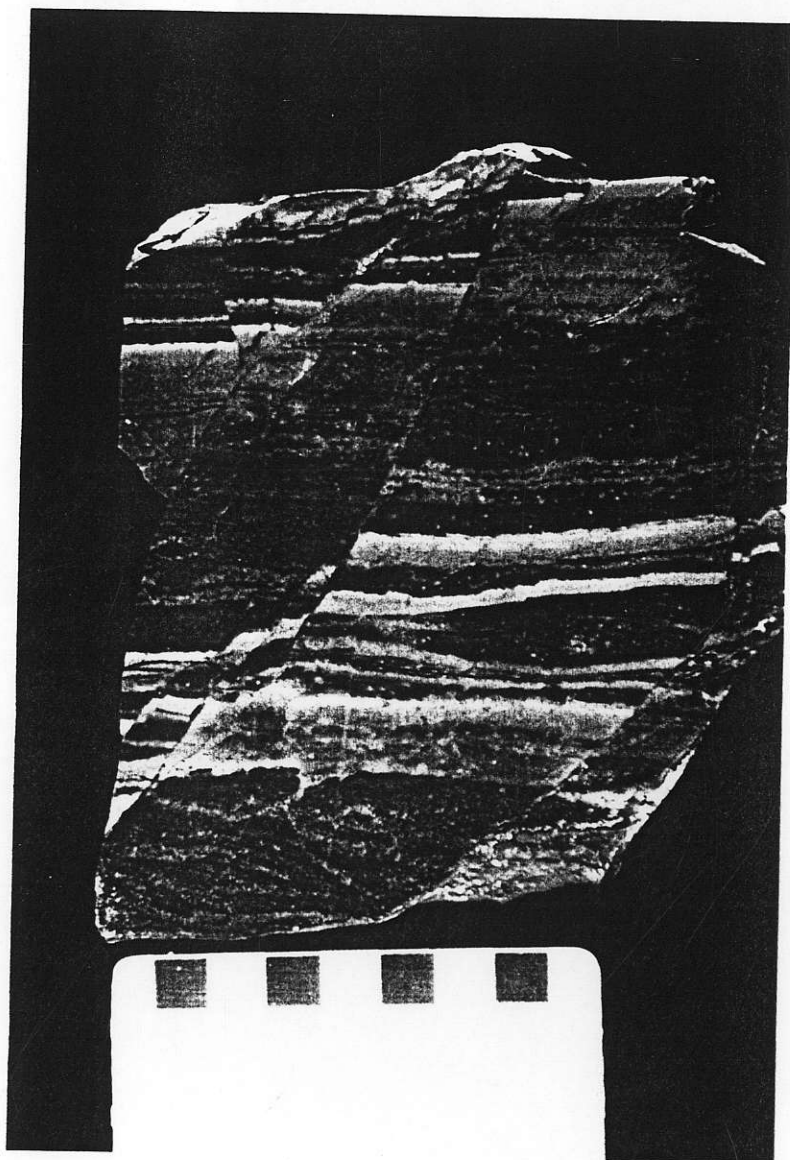


Plate 4.1. Mudstone with graded bedding and ripple marks exposed along the footwall on section 9700N. Pale pink colour is due to microcrystalline K-feldspar in the matrix of the rock. Sample is located at 9900N, 10075E on Figure 4.1.

Conglomerate is clast supported, and is only exposed along the footwall of the deposit where it overlies the tuffaceous units (Fig. 4.2). The clasts vary in composition upward from: (i) tuff, crystal tuff and fine grained siliceous rock, to (ii) shale, porphyritic andesite, rare fossiliferous limestone and granitoid clasts (Plates 4.2 and 4.3). The abundance of feldspar crystals and carbonaceous material in the matrix generally increases up section.

Interbedded sandstone and siltstone with limy concretions 20 to 30 mm in diameter stratigraphically overlie the conglomerate exposed along the footwall of the deposit (Fig. 4.2). This unit weathers dull grey exposing prominent graded bedding. It consists of rounded, broken grains of plagioclase, K-feldspar and minor quartz with minor carbonaceous material in finer grained laminations. The composition of the crystal fragments in the rock unit makes this unit an arkose. Another similar sandstone is exposed in a structurally bound wedge below Kerr Peak (Figs. 4.1 and 4.2).

Black laminated argillite and rusty weathering siltstone conformably overlie the interbedded sandstone on the footwall (Figs. 4.1 and 4.2, Plate 4.4). Abundant load casts and graded bedding exposed in drill core on section 10600N define a steep easterly dip to the unit parallel to the dip of the mudstone. The siltstone layers consist of broken crystals of K-feldspar, plagioclase and quartz (Table 4.1). Minor lenses of bedded limestone interbedded with the argillite outcrop below Kerr Peak. Samples of the limestone yielded no micro fossils (G. Nadaraju, U.B.C., personal comm., 1992).

Volcanic conglomerate with minor interbedded black argillite underlies Kerr Peak southwest of the deposit (Fig. 4.1, Plate 4.5). This unit is in fault contact with the underlying laminated argillite and siltstone. Clasts in this conglomerate, 1 to 30 cm in diameter, comprise: plagioclase porphyry (30% of unit), hornblende porphyry (10%), aphanitic felsic volcanic rock (10%) and epidotite (5%). The clasts are supported by a matrix consisting of

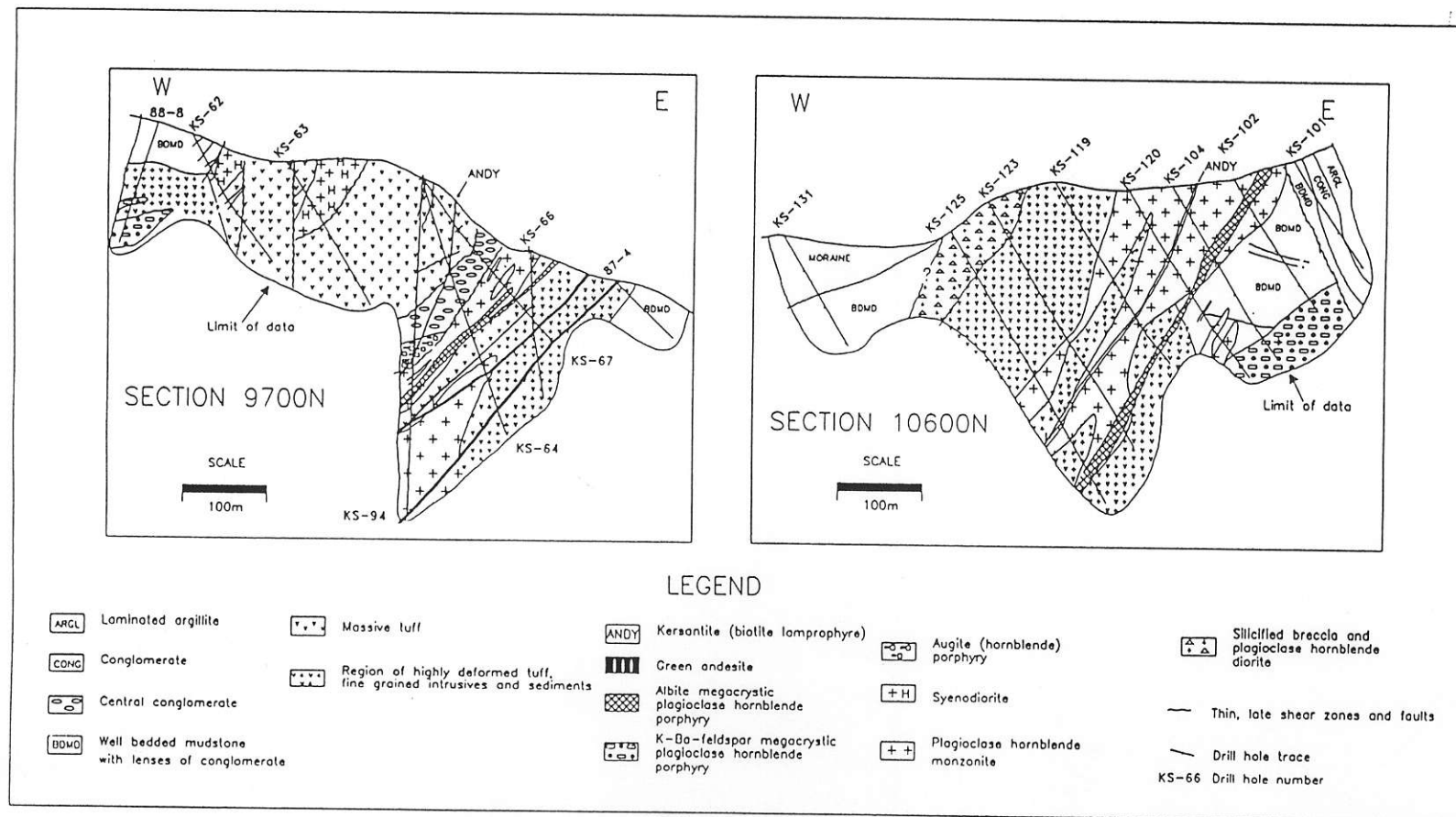


Figure 4.2. Geological cross-sections for sections 9700N and 10600N on the Kerr deposit. Trace of cross-section corresponds to line on Figures 1.2 and 4.1.



Plate 4.2. Conglomerate with clasts of fine grained tuffaceous rock, chert, and minor feldspar porphyritic rock. Sample is located at 9750N, 10000E on Figure 4.1.

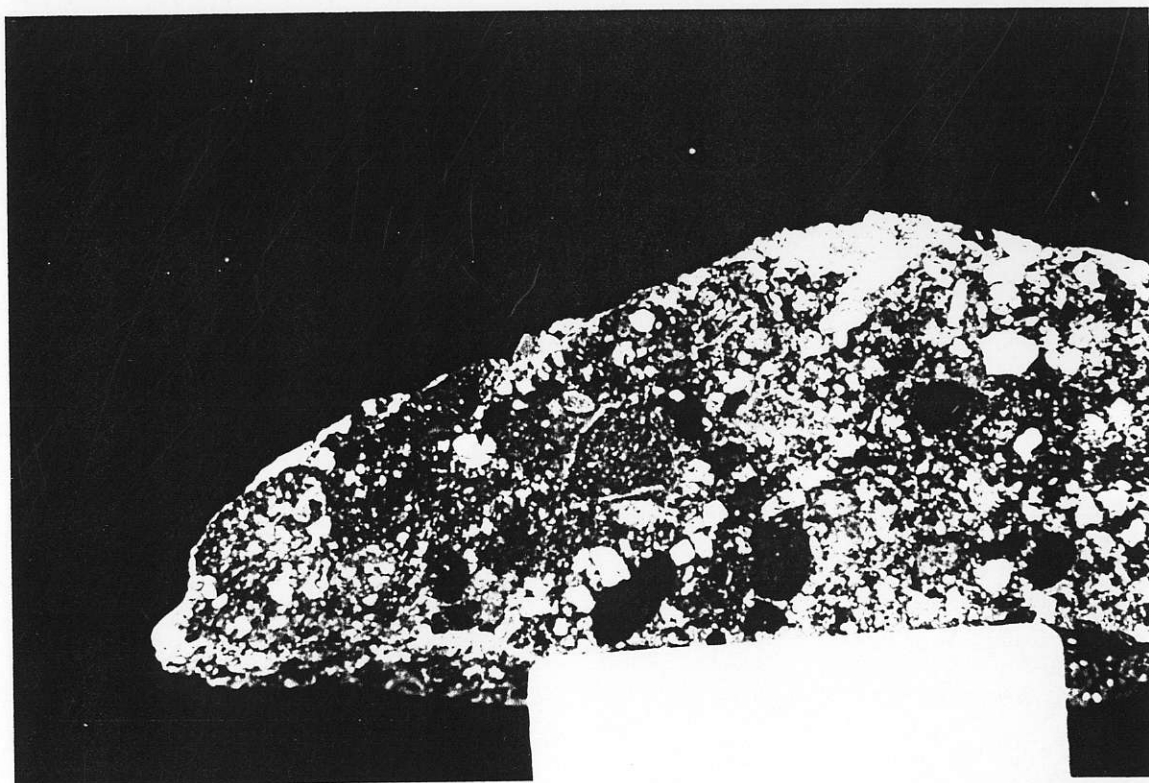


Plate 4.3. Conglomerate with clasts of argillite, tuffaceous rock, feldspar porphyry and trace chert in a matrix of broken feldspar grains. The black colour in the matrix is due to carbonaceous material. Sample is located at 10350N, 10300E on Figure 4.1.



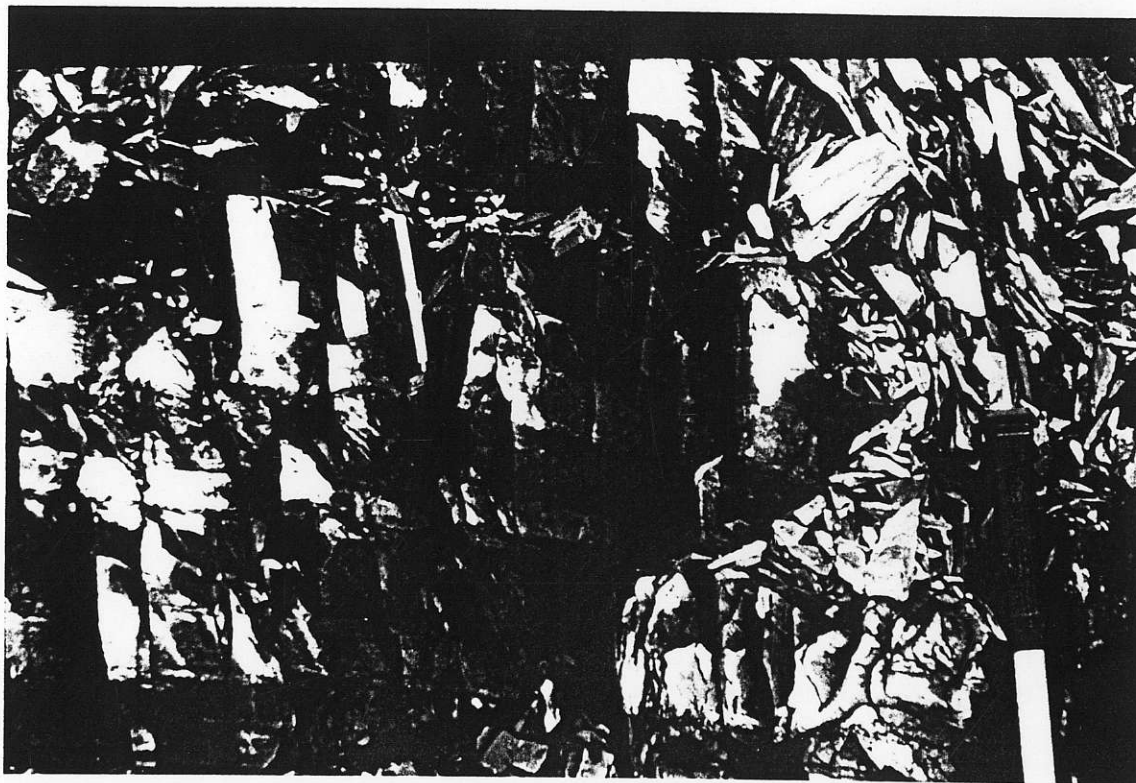


Plate 4.4. Well bedded argillite with normal grading of coarse sand to clay sized particles. Photograph of unit below Kerr Peak. Yellow magnet is 12 centimeters long. Sample is located at 9700N, 9450E on Figure 4.1.

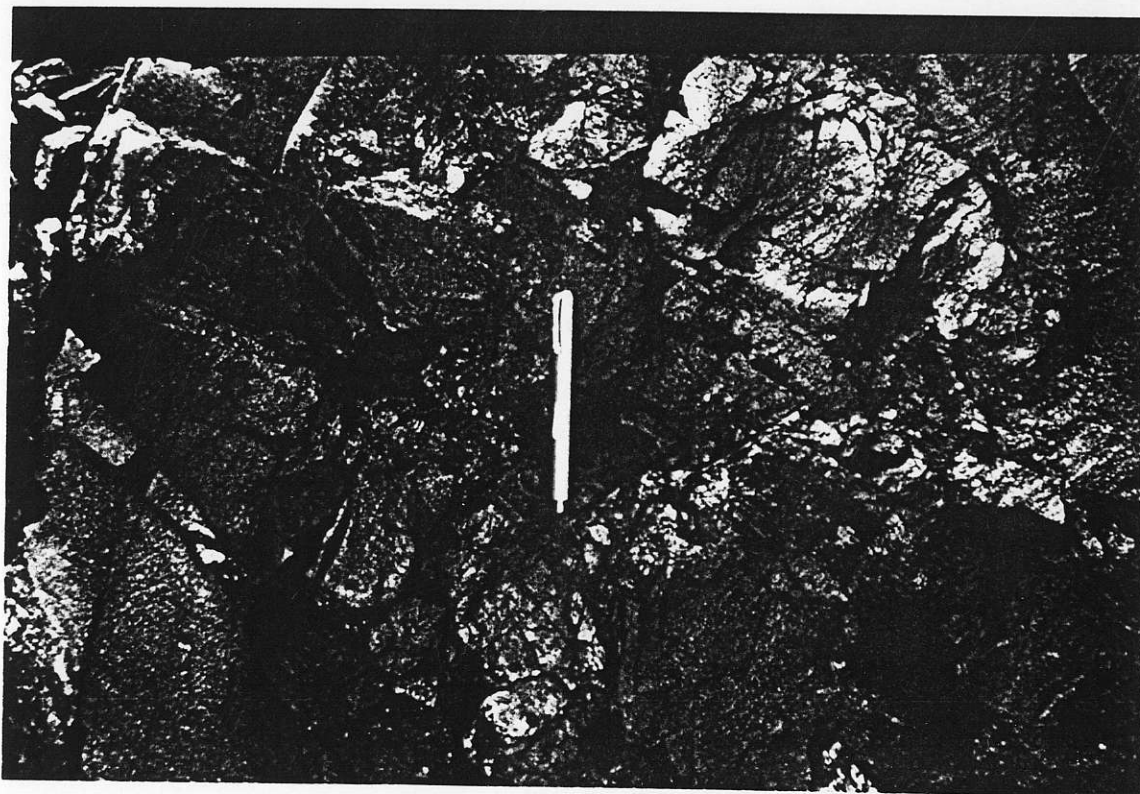


Plate 4.5. Volcanic conglomerate exposed immediately above fault contact with argillite in plate 5. Monolithic clasts are supported by a matrix of broken plagioclase grains. Sample is located at 9700N, 9490E on Figure 4.1.

fragments of plagioclase crystals (20%) and very fine grained crystals (25%) that are altered. The proportion of clasts to matrix varies throughout the unit. Beds without clasts have a weak bedding that is emphasized on weathered surfaces.

## 4.2 Intrusive Rock Units

Intrusive rock units are described from oldest to youngest. Their mineralogy is in Table 4.2 and their timing relationships to mineralization and deformation are in Table 4.3.

Plagioclase augite diorite is exposed along the footwall of the deposit (Fig. 4.1). It has also been observed as a dyke cutting bedded and massive K-feldspar tuff on the eastern edge of section 9700N. It has not been observed cutting sedimentary rock units along either the footwall or hanging wall of the deposit.

The unit is euhedral - granular with oscillatory zoned plagioclase (An<sub>37</sub>) and augite laths in a very fine grained matrix of K-feldspar (Plate 4.6, Table 4.2). Cobble sized clasts of massive, very fine grained tuff occur sporadically throughout it.

This intrusive rock is interpreted to be a pre-mineralization intrusion because it hosts mineralization associated with early stage K-feldspar alteration (see below, Table 4.3). Intrusion relationships with the host tuffs and its mineralogy suggest that this unit may be related to the Late Triassic Stuhini Group pyroxene phyric lava flows and breccias.

Monzonite to syenodiorite dykes are the most voluminous in the deposit area. They bifurcate at depth and parallel the westerly dip of the deposit (Fig. 4.2). They have chilled contacts with sedimentary and volcanoclastic units and the plagioclase augite diorite. Their composition varies with the various stages of mineralization in the Kerr deposit. Early monzonite dykes and highly altered equivalents in the deposit host banded quartz, pyrite - chalcopryrite and sulphate veins. The monzonite dykes parallel pervasive chlorite alteration

Table 4.2. Modal mineralogy of intrusive rocks exposed on the Kerr deposit, northwestern British Columbia.

Legend: Qtz. = quartz, Plag. = plagioclase, K-spar. = K-feldspar, ilm. = ilmenite, an. = anhedral, sub. = subhedral, eu. = euhedral, oscil. = oscillatory zoning, por. = porphyry.

Rock unit	Region/Timing	Mineralogy							Matrix / Interstitial phases		
		Quartz	Plagioclase	K-feldspar	Amphibole	Biotite	rutile/sphene ilm./magnetite	Apatite	Qtz.	K-spar.	Plag.
Kersantite	North-south striking	trace embayed	60% 0.6 mm	trace	20% brown	Biotite 20% 0.02 x 0.4 mm	Magnetite 2%			Minor	Major
Aphanitic intermediate dykes	East-west striking						Minor sphene and ilmenite		Minor 0.25 mm		
Tractytic plagioclase porphyry	Footwall	trace 0.25 mm	50% An22 1.0 x 2.0 mm subhedral	trace subhedral	5 - 40% brown subhedral		Sphene 10%			10%	
Feldspar megacrystic plagioclase hornblende porphyry											
Albite	North-south striking	trace - 2%	35% An27-An33 0.4 - 3.2 mm subhedral albite trace - 2% 4.0 - 40 mm euhedral		10% subhedral			trace 0.02 mm euhedral	Minor an		
Ba - K-feldspar	East-west striking	trace euhedral	30% 2.0 x 5.0 mm subhedral	10% perthitic 20 x 30 mm euhedral	10% 2.4 x 1.0 mm anhedral			trace	Minor		

Table 4.2. cont'd

Rock unit	Region/Timing	Mineralogy							Matrix / Interstitial phases		
		Quartz	Plagioclase	K-feldspar	Amphibole	Pyroxene	rutile/sphene ilm./magnetite	Apatite	Qtz.	K-spar.	Plag.
Augite and Hornblende porphyry	Western portion of deposit	trace 0.2 mm	20% 0.5 mm anhedral		20% 0.1 - 4.0 mm subhedral		Magnetite 2%				
Augite and hornblende por.	Centre of section 9700N		5% oscil. 1.4 x 2.2 mm		trace	20% ophite 2.0 mm	2% magnetite with rutile exsol.	2% 0.2 mm			
Augite porphyry	Footwall		50% 0.2 - 0.4 mm subhedral			20% 2.0 - 4.0 mm subhedral			Minor	10%	
Monzonite to syenodiorite											
Monzonite	Early central dikes		30% 1.0 x 2.0 mm eu., oscil.	10% 4.0 x 5.0 mm anhedral	30% brown 3.0 mm subhedral		sphene 0.5 % 0.4 mm subhedral	0.1% 0.5 mm subhedral	2%	10 - 50%	Minor
Syenodiorite	Late dikes along western margin		40% 3.2 x 0.6 mm subhedral		30%				30%		
Plagioclase Augite Diorite	Footwall		50% An37 0.04 x 0.1 mm subhedral			10 - 20% 0.08 - 0.4 mm subhedral				Minor	



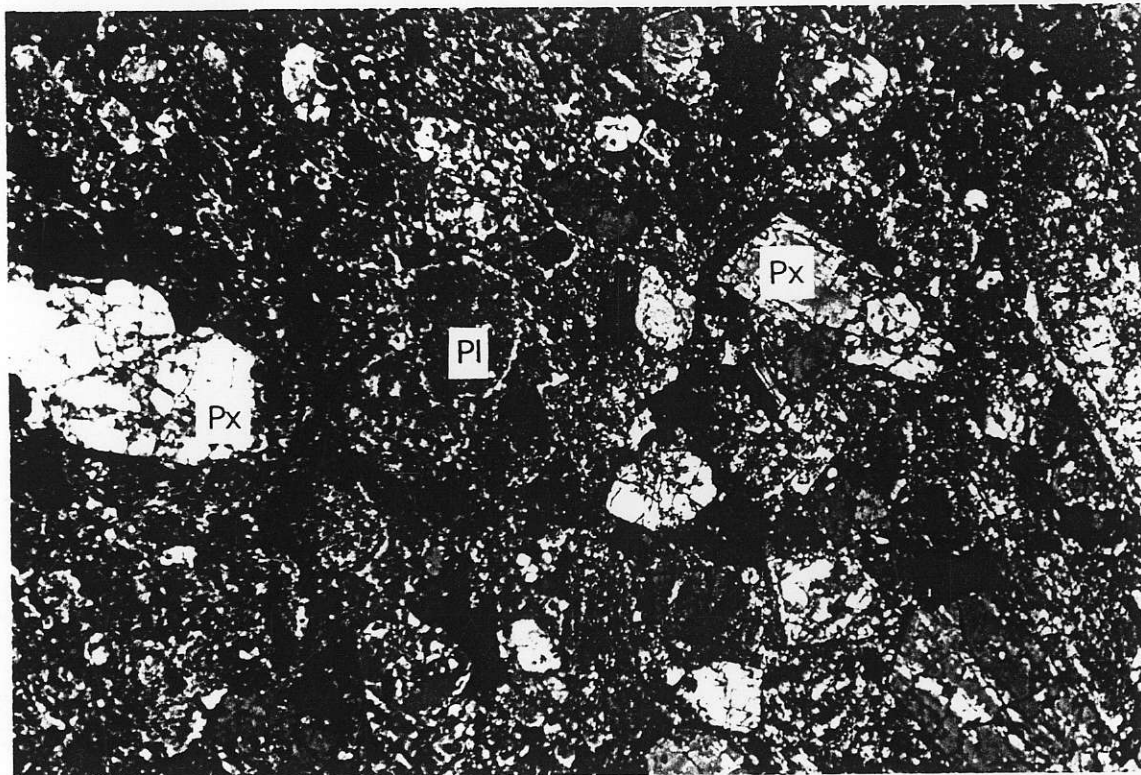


Plate 4.6. Photomicrograph, cross nicols, of oscillatory zoned augite (bright second order colours) and sericite altered plagioclase with rims of K-feldspar. Sample is located at 9950N, 9300E on Figure 4.1. Field of view is 1.25 mm. Legend: Px - augite, and Pl - plagioclase.

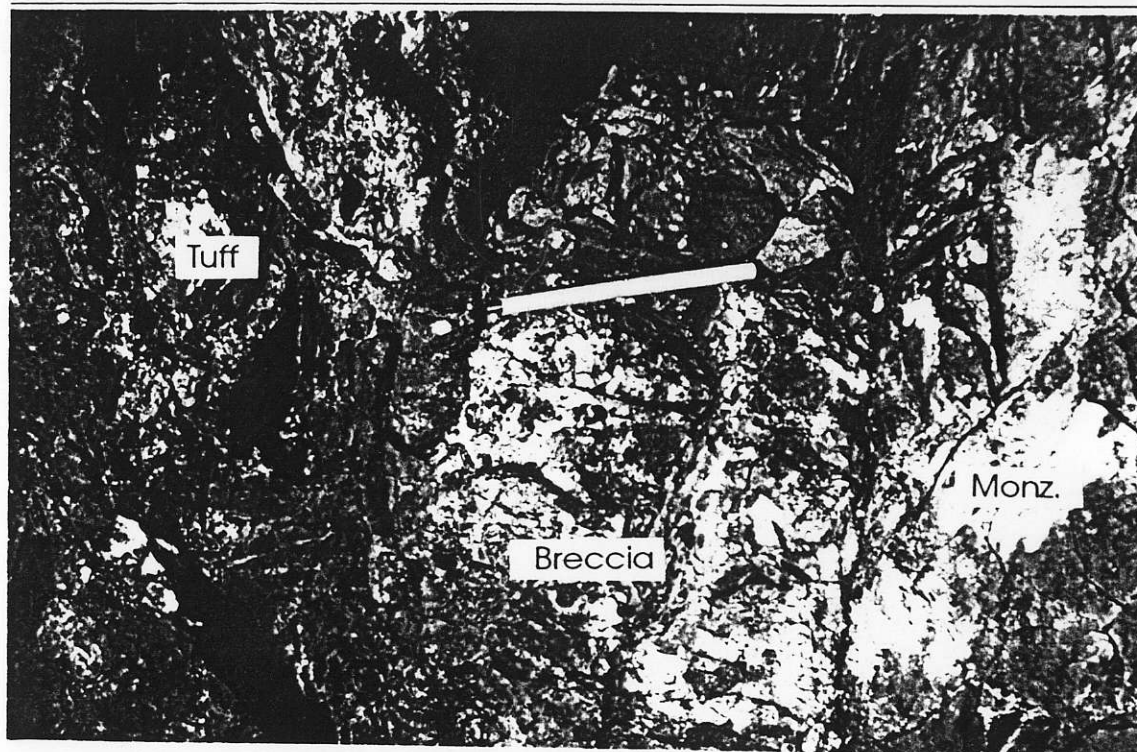


Plate 4.7. Breccia between buff weathering tuff and white to tan weathering syenodiorite. Magnet points to a sub-angular tuff fragment in a matrix of altered syenodiorite. Sample is located at 9705N, 9590E on Figure 5.2.

with minor specular hematite and magnetite veins; syenodiorite dykes cut banded quartz veins and host pyrite - chalcopyrite veins (Table 4.3). These syenodiorite dykes occur above the upper lense of mineralization on section 9700N; they are interpreted to be late-mineralization intrusions because they cut mineralized quartz veins, but host later sulphide veins. Monzonite and syenodiorite dykes are both deformed, which indicates that they are pre- to syn-deformational.

Margins of these dykes have incorporated fragments to form intrusion breccias from 5 cm to 20 m wide. These breccias are wider along syenodiorite dykes, and they consist of cobble sized angular blocks of tuffaceous rock in a matrix of euhedral plagioclase and hornblende grains (Plate 4.7). The volume of fragments decreases toward the centres of the dykes.

Monzonite dykes are distinguished by their porphyritic texture of oscillatory zoned plagioclase (An<sub>32</sub>), and zoned hornblende and minor perthitic orthoclase in a matrix of K-feldspar, plagioclase and quartz with trace sphene and apatite (Plate 4.8, Table 4.2). Orthoclase crystals, with up to 4.6 wt% BaO (electron microprobe data in Appendix C), poikilitically enclose euhedral plagioclase laths. The crystallization sequence in the monzonite, deduced from petrography, is early crystallization of apatite and sphene, plagioclase, K-feldspar, hornblende and quartz followed by crystallization of plagioclase, K-feldspar and quartz. Interstitial quartz grains have phyllosilicate and actinolite inclusions. Plagioclase phenocrysts are locally rimmed by K-feldspar.

Syenodiorite dykes are characterized by an absence of K-feldspar and a greater proportion of hornblende micro-phenocrysts in the matrix than the monzonite. The syenodiorite dykes have an age of  $197 \pm 3.0$  Ma (U-Pb zircon: D. Ghosh, U.B.C., pers. comm., 1992). The zircons exhibit <sup>207</sup>Pb loss that may be due to lead contamination or to a

Table 4.3. Timing relationships among the dykes, mineralization and deformation in the Kerr deposit, northwestern British Columbia.

Intrusive Unit	Age (Ma)	Mineralization				Deformation	
		Pre	Syn	Late Syn	Post	Pre	Post
Kersantite (biotite lamprophyre)	51.5 +/- 2 K-Ar w.r.				X		X
Aphanitic intermediate dyke	?				X	X	
Trachytic plagioclase porphyry	?				X	X	
Albite megacrystic plagioclase hornblende porphyry	195 +/- 1.5 U-Pb zircon				X	X	
K-Ba-feldspar megacrystic plagioclase horn- blende porphyry				X		X	
Hornblende porphyry				X		X	
Augite porphyry				X		X	
Syenodiorite				X		X	
Plagioclase hornblende monzonite	197 +/- 3.0 U-Pb zircon		X			X	
Plagioclase augite diorite		X				X	
	Late Trassic?						

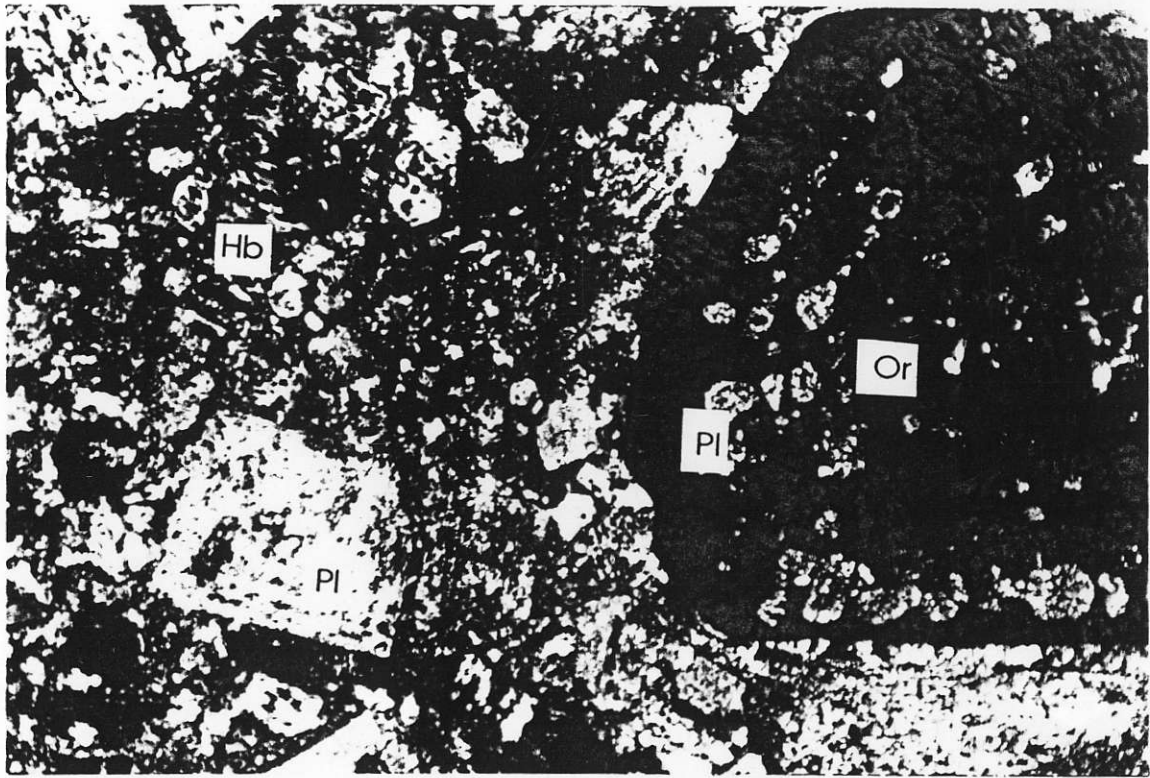


Plate 4.8. Photomicrograph, cross nicols, of sericite altered, oscillatory zoned plagioclase, chlorite altered hornblende and euhedral orthoclase poikilitically enclosing subhedral plagioclase in a matrix of quartz, chlorite and sericite. Sample is located at 9500N, 10050E on Figure 4.1. Field of view is 1.25 mm. Legend: Hb - hornblende, Or - orthoclase, and Pl - plagioclase.

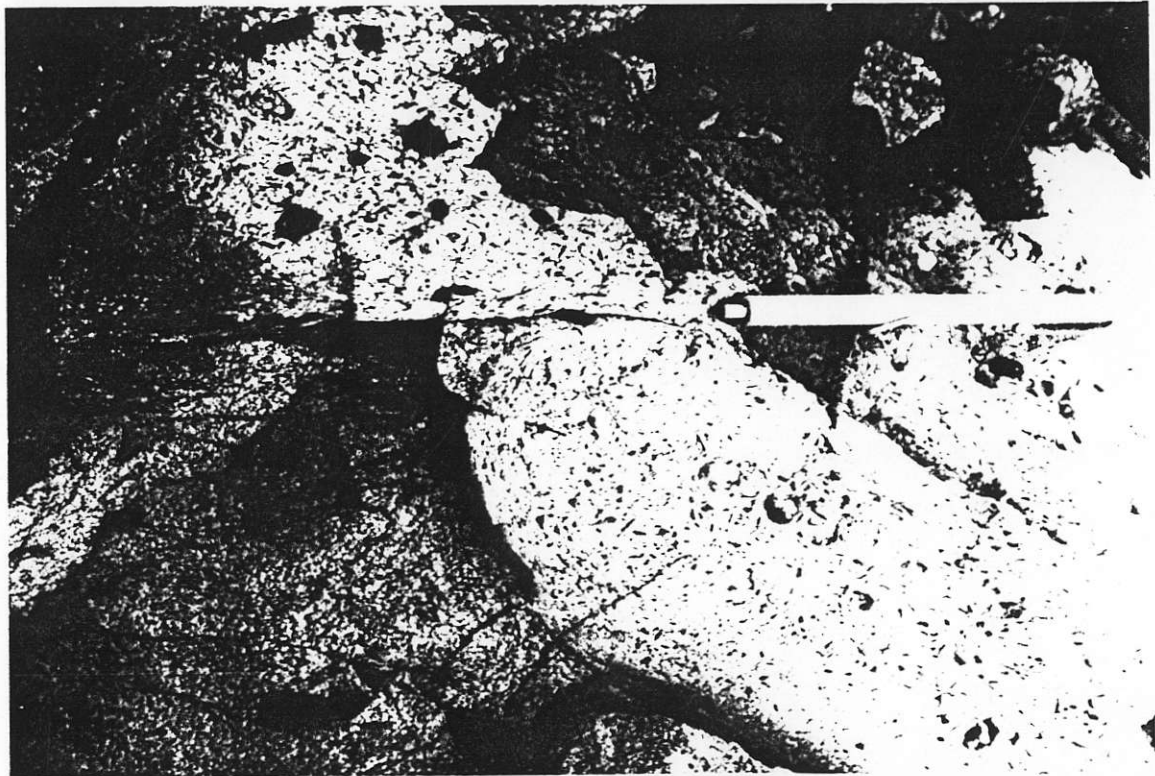


Plate 4.9. Chill contact between K-Ba-feldspar megacrystic porphyry and syenodiorite on the ridge below Kerr Peak. Sample is located at 9650N, 9510E on Figure 5.2.

contribution from an older terrane. These dykes only host pyrite - chalcopyrite veinlets where they cut chlorite - sericite - quartz altered tuffaceous rocks.

Augite and hornblende porphyry dykes parallel the strike of the Kerr deposit and range in thickness from 2 to 20 m (Fig. 4.1). They are hosted by relatively unaltered sedimentary units along the footwall and intensely altered and deformed sericitic tuffaceous rocks in the centre of the deposit (Fig. 4.2). Dykes vary in composition across the deposit from augite porphyry with trace hornblende along the footwall, to hornblende porphyry in the west (Table 4.2). These dykes are interpreted to be late syn-mineralization because they host pyrite - chalcopyrite veinlets, which are characteristic of late stages of mineralization in the Kerr deposit (Table 4.3), and they cut syenodiorite dykes along the western portion of section 9700N.

The augite porphyry dykes have knots of radiating augite crystals and oscillatory zoned plagioclase laths supported by a matrix of K-feldspar and quartz. These dykes have early crystallization of apatite, followed by augite and plagioclase. Dykes exposed in the centre of the deposit have hornblende laths intergrown with the augite clusters and have accessory magnetite with ilmenite exsolution lamellae. Hornblende porphyry dykes along the western edge of the deposit have hornblende megacrysts (20 mm long) with magnetite and ilmenite grains along growth zones. These megacrysts crystallized before matrix plagioclase, K-feldspar and quartz.

K-Ba-feldspar megacrystic plagioclase hornblende porphyry dykes (K-Ba-feldspar megacrystic porphyry), up to 10 m thick, trend east-west and dip vertically in syenodiorite below Kerr Peak and in the footwall east of the Old Camp (Fig. 4.1, Plate 4.9). Megacrysts of hyalophane  $[(K,Ba)(Al,Si)_2Si_2O_8]$  (electron microprobe analysis, Appendix C) up to 25 mm in diameter are in a fine grained groundmass of euhedral plagioclase, amphibole and trace

reabsorbed quartz (Table 4.2). The megacrysts have minor perthitic exsolution albite lamellae and partial albite rims. Quartz occurs as euhedral grains within amphibole. The matrix, possibly aphanitic originally, has been altered to sericite, quartz and chlorite. The crystallization sequence in the unit is early apatite?, plagioclase, quartz, K-Ba-feldspar and finally hornblende.

This dyke is  $195 \pm 1.5$  Ma old (U - Pb zircon: D. Ghosh, U.B.C., pers. comm., 1992). Each zircon fractionation exhibits  $^{207}\text{Pb}$  loss. This may be due to contamination by excess  $^{206}\text{Pb}$  from the magma before zircon crystallized, or to addition of older lead from crustal material incorporated during intrusion.

This unit is interpreted to be a late syn-mineralization intrusion because it hosts small, but high grade gold poly-metallic veins below Kerr Peak (Table 4.3). Altered plagioclase and hornblende grains near the mineralized veins exhibit a weak fabric, which suggests that this late stage mineralization occurred before deformation.

Albite megacrystic plagioclase hornblende porphyry dyke (albite megacrystic porphyry), up to 15 m thick, parallels the trend of the deposit. The dyke is boundinaged parallel to the foliation in the deposit (Fig. 4.1). It passes from the hanging wall in the southern portion of the deposit to the footwall in the northern portion. The unit consists of rare albite, 5 to 40 mm in length, in a groundmass of 4 mm laths of plagioclase ( $\text{An}_{27}$ ) and hornblende with minor interstitial quartz (Table 4.2). Undeformed portions of this unit show that the albite phenocrysts and groundmass crystals have a random orientation in an originally aphanitic matrix. The crystallization sequence of phenocrysts in the dyke is: early plagioclase and hornblende, albite and finally quartz.

Megacrysts in this dyke are concentrated in the centre of the dyke; whereas, in the K-Ba-feldspar dykes they are evenly distributed. Concentration of large crystals in the centre of the albite dyke may be due to flow segregation known as the Bugnolli effect (Marsh, 1985).

The dyke is post-mineralization because it cuts the porphyry copper - gold deposit. However, traces of pyrite and chalcopyrite occur in syntaxial, extension veins close to the margins of the dyke. The presence of these sulphides in gash veins suggests that the fluid present during deformation was remobilizing mineralization.

Trachytic plagioclase porphyry dykes are up to 1 m thick, and trend easterly and dip steeply in the footwall of the deposit. Relatively unaltered dykes consist of radiating knots of brown amphibole in a groundmass of aligned subhedral plagioclase (An<sub>23</sub>), K-feldspar and trace biotite in a cryptocrystalline matrix (Table 4.2). This dyke is post-mineralization but pre-deformation because it is deformed and cuts sericite - quartz - pyrite altered tuffaceous rocks.

Aphanitic intermediate dykes, up to 2 m thick, strike east and dip steeply north or south (Fig. 4.1). They are dark green on fresh and weathered surfaces. Carbonate filled, flow aligned vesicles are concentrated at dyke margins. The dykes were microcrystalline but are now altered to sericite, chlorite, quartz and minor rutile and sphene.

These dykes are abundant in the highly deformed portion of the Kerr deposit where they cut altered syn- to late syn-mineralization dykes. They are intensely folded where they strike perpendicular to foliated sericitic tuffaceous rocks, or are boundinaged where they parallel the foliation.

Kersantite (biotite lamprophyre) dykes follow post-foliation fault zones that dip steeply west (Fig. 4.2). This unit consists of biotite books up to 20 mm in diameter in a fine grained groundmass of ferromagnesian minerals (biotite and hornblende), plagioclase and magnetite. Biotite grains and magnetite grains are enclosed by plagioclase laths. The matrix also contains rare orthoclase and embayed quartz crystals. Minor pyrite and chalcopyrite clots occur in the centre of the dykes. Mirolitic cavities up to 5 mm in diameter are encrusted with K-feldspar.



Disseminated hematite occurs in chill contacts with foliated sericite - quartz - pyrite host rock. This unit is kersantite (Streckeisen, 1979) based on its mineralogy.

An Eocene whole rock K-Ar age of  $51.5 \pm 2$  Ma was obtained from a sample of relatively unaltered dyke (Table 4.4).

### 4.3 Geochemical Petrogenesis of Intrusive Rocks

#### 4.3.1 Introduction

The least altered equivalent of each different intrusive rock was analyzed for 12 major elements plus 49 minor and trace elements (Table 4.5). These data (Appendix B) were used to constrain the geochemical relationships between the rock units, and to investigate if sub-units based upon the modal mineralogy are supported by analytical geochemistry. Descriptions of the analytical methods used to analyze the rock samples for major and trace elements, and the precision and accuracy of the whole rock geochemical data are in Appendix B.

Spiderdiagrams of the trace elements are normalized to mid-ocean ridge basalt (MORB) (Figs. 4.4, 4.5 and 4.6) so that the additions and losses can be related to magma processes above the subducting ocean plate (Pearce, 1982) beneath the volcanoplutonic arc, which is thought to represent the Early Jurassic magmatic setting of the Sulphurets gold camp (Anderson, pers. comm., 1992). The normalizing factors for MORB are described in Pearce (1982). The spiderdiagrams show large ion lithophile elements (LILE: K, Rb, Ba, Th, U, Cs, Sr, Zr and Hf) on the left and centre, rare earth elements (REE: La, Ce, Nd, Sm, Eu, Gd, Dy, Y, Er, Yb and Lu) in the centre and on the right. High field strength elements (HFSE: Nb and Ti) occur in the centre of diagram.

Plots of major element trends in the suite of intrusives are affected by propylitic, argillic and phyllic alteration (see Chapter 6.0 and Table 4.6). Propylitic alteration resulted in



Table 4.4. Whole rock K-Ar data from two samples on the Kerr deposit, northwestern British Columbia.

Sample Number	K (wt%) Average of two by AAS	$^{40}\text{Ar}$ ( $10^{-6}$ cc/gm)	% total Ar	Age(+/- 1s.dMa)
1	3.21 +/- 0.02	6.521	83.1	51.5 +/- 1.8
2	5.67 +/- 0.02	28.246	96.1	124 +/- 4

#### LEGEND

s.d - standard deviation

AAS - Atomic absorption spectrometry

#### Sample descriptions:

##### Sample 1

Biotite kersantite collected from 89-12 58 m at UTM (zone 9) 62659900N; 421800E. Sample fraction analyzed was between -80 and 100 mesh. Dykes with the same degree of alteration consist of chlorite and sphene replacing biotite, sericite replacing plagioclase, trace K-feldspar, quartz, magnetite and gypsum .

##### Sample 2

Sericite altered monzonite dike from KS-125 220.5 m at UTM (zone 9) 6259450N; 421825E. Sample analyzed was between -80 and 100 mesh, and it consisted of phengite and quartz. Pyrite was removed from the sample by using a heavy liquid separation. The composition of the phengite was determined by electron microprobe.

Table 4.5. Whole rock geochemical results of least altered intrusive rocks on the Kerr deposit, northwestern British Columbia.

SAMPLES Rock Unit	Plagioclase augite diorite	Monzonite	Syenodiorite	Augite porphyry	Hornblende porphyry	K-Ba-feldspar megacrystic plagioclase hornblende porphyry	Albite megacrystic plagioclase hornblende porphyry	Trachytic plagioclase porphyry	Aphanitic intermediate dykes	Biotite kersantite (lamprophyre)
Location	9240N 9860E	9230N 9940E	9660N 9550E	DDH 87-9 7.9m	9730N 9525E	9635N 9472E	9973N 9778E	9880N 10055E	DDH 87-9 37.2m	DDH 89-12 58m
(wt %)										
SiO <sub>2</sub>	48.6	57.8	58.7	51.3	53.6	60.8	59.1	47.5	56.5	48.2
Al <sub>2</sub> O <sub>3</sub>	16.3	17.1	17.9	15.1	17.6	17.1	16.2	15.9	14.8	15.8
Fe <sub>2</sub> O <sub>3</sub>	10	5.61	8.3	9.55	8.95	4.07	4.91	9.96	13.4	8.12
MgO	4.67	1.78	3.56	6.54	3.34	1.81	1.67	8.2	3.02	5.52
CaO	8.06	5.22	0.64	4.74	3.29	3.74	4.74	5.98	2.06	5.5
Na <sub>2</sub> O	2.41	4.06	2.79	1.4	3.25	3.27	3.64	3.98	4.35	3.62
K <sub>2</sub> O	3.33	3.85	3.13	4.42	4	3.64	2.67	1.21	0.61	3.43
NiO	0.37	0.18	0.18	0.62	0.17	0.17	0.2	0.28	0.27	0.15
TiO <sub>2</sub>	0.763	0.671	0.549	0.707	0.691	0.28	0.537	1.55	1.42	2
P <sub>2</sub> O <sub>5</sub>	0.68	0.28	0.34	0.36	0.45	0.2	0.22	1.21	0.56	0.97
CO <sub>2</sub>	0.09	0.55	0.04	0.08	0.67	2.4	3.34	0.37	0.22	2.23
H <sub>2</sub> O	2.2	1.3	2.4	2.6	2.4	1.9	2.2	4.1	3.8	2.8
TOTAL	97.7	98.4	98.5	97.4	98.4	99.4	99.4	100.2	101.0	98.3
(ppm)										
H	24	27	47	26	35	39	30	21	24	28
S	12000	11400	5400	18500	1800	790	200	750	2150	1460
Cl	183	146	<100	303	<100	<100	115	182	<100	146
Sc	30.5	11.2	13.3	41.5	20.6	10.6	7.3	24.6	19.6	13.8
V	298	129	175	281	168	105	98	253	48	175
Cr	48	51	38	160	36	35	45	89	37	96
Co	18	6	3	20	10	<1	2	15	10	12
Ni	4	2	4	32	<1	<1	56	78	0.1	67
Cu	215	81.3	179	84.4	131	50.8	10.2	79.8	25.2	33.8
Zn	90	51.9	58.4	142	53.3	79.5	77.2	202	163	103
Ag	0.01	0.2	0.01	1	0.01	0.01	0.3	0.8	0.7	0.9
Cd	0.02	0.02	0.02	0.02	0.02	0.02	0.02	0.02	0.02	0.02
Sb	4.8	2.2	6.2	4.2	9.2	4.6	1.5	2.6	2.4	2.2
Te	0.04	<0.02	<0.02	<0.02	<0.02	<0.02	<0.02	<0.02	<0.02	<0.02
Mo	2	<1	<1	<1	<1	<1	<1	<1	<1	<1
Ge	30	<10	18	<10	13	22	<10	<10	<10	13
As	13	3.3	30	5.2	5.5	1.5	3.4	17	23	22
Se	0.5	<0.5	<0.5	<0.5	<0.5	<0.5	<0.5	<0.5	<0.5	<0.5
W	3	0.1	4	0.1	0.2	0.1	0.1	0.1	4	2
Tl	0.6	0.8	0.8	1.4	1.5	0.6	1.3	0.3	0.4	0.5
Pb	<2	<2	<2	<2	<2	17	2	<2	<2	<2

Table 4.5 cont'd

SAMPLES Rock Unit	Plagioclase augite diorite	Monzonite	Syenodiorite	Augite porphyry	Hornblende porphyry	K-Ba-feldspar megacrystic plagioclase hornblende porphyry	Albite megacrystic plagioclase hornblende porphyry	Trachytic plagioclase porphyry	Aphanitic intermediate dykes	Biotite kersantite (lamprophyre)
Location	9240N 9860E	9250N 9940E	9660N 9550E	DDH 87-9 7.9m	9750N 9523E	9635N 9472E	9975N 9778E	9880N 10055E	DDH 87-9 37.2m	DDH 89-12 58m
(ppm)										
Rb	73	74	83	106	83	97	66	18	11	52
Sr	861	808	119	409	1010	496	229	746	89	1120
Y	17	26	4	15	29	8	11	20	48	19
Zr	36	133	81	45	64	58	96	94	327	292
Nb	11	14	9	10	6	8	14	25	20	38
Cs	1	1	4	3	3	4	2	2	1	1
Ba	1970	2100	1760	2680	5800	7490	1390	480	414	1440
La	12.6	18.6	5.3	7.1	12.6	9.3	11.9	51	29.7	70.1
Ce	23.2	39.3	9.8	13.7	22.6	14.8	29.9	107	65.2	136
Pr	3.4	4.8	1.4	1.8	2.9	2.1	2.9	12.3	8.1	14.5
Nd	15	19.7	7.1	8.9	13.8	9.6	12.4	50.7	36	57.8
Sm	3.5	4.8	1.1	2.2	3.3	2	2.4	9.5	9.6	9.7
Eu	0.99	1.43	0.5	0.89	1.3	1.4	0.72	2.46	2.01	2.2
Gd	3.6	4.7	1	2.8	3.7	1.2	2.2	6.8	10.5	6.3
Tb	0.5	0.8	0.1	0.5	0.7	0.3	0.3	0.9	1.6	0.9
Dy	3.5	4.6	1.4	2.9	4.4	1.6	1.3	4.3	8.7	4.1
Ho	0.56	0.98	0.21	0.59	0.89	0.3	0.17	0.8	1.52	0.68
Er	2.1	3.2	0.9	1.9	2.8	0.9	1.2	2.3	4.6	2
Tm	0.2	0.5	0.01	0.2	0.5	0.2	0.2	0.3	0.6	0.2
Yb	1.6	2.7	0.9	1.4	2.6	1.1	0.8	1.5	3.1	1.4
Lu	0.23	0.34	0.17	0.21	0.43	0.23	0.14	0.19	0.43	0.26
Bi	<1	<1	<1	<1	<1	<1	<1	<1	<1	<1
Th	1.7	2.7	2.3	1.2	1.9	2.2	3.5	1.6	4.6	6.4
U	1	1.6	1.4	0.3	1.1	2	3.3	0.4	2.5	2.2
(ppb)										
Au	53	13	63	130	21	6	<1	5	13	<1
Pd	15	3	6	13	4	7	<1	2	<1	1
Pt	<10	<10	<10	<10	<10	<10	<10	<10	<10	<10
Hg	27	11	38	20	16	27	11	27	27	7900
(wt %)										
LOI	3.23	1.75	4	3.75	3.39	4.23	5	3.95	2.95	4.8
SUM	98.9	98.6	100.3	98.8	99.5	100.2	99.1	99.9	100.0	98.4

Table 4.6. Primary and alteration mineralogy of the least altered of each intrusive rock unit submitted for whole rock geochemical analysis.

Legend: Ser = sericite, ill = illite, chl = chlorite, clay = unidentified clay minerals, qtz = quartz, cal = calcite, leu = leucoxene, epi = epidote, act = actinolite, hm = hematite, ilm = ilmenite and rut = rutile.

ROCK UNIT	MINERALOGY							Alteration/Veins
	Plagioclase (Percentage of mineral altered, mineralogy)	Quartz	K-feldspar	Hornblende	Augite	Minor phases	Matrix	
Kersentite	50% (2%, ill, ser)	Trace	Trace fresh	20%		Biomite 20% (100%, chl, rut) Magnetite 5%		Pyrite with minor chalcopyrite Carbonate and gypsum filled vesicles
Apatitic intermediate dykes							100% (ser, chl, ilm ill, qtz)	
Trachytic plagioclase porphyry	40% (50%, ill)		10% fresh	40% fresh		Sphene 10%	Trace calcite	
Albite megacrystic plagioclase hornblende porphyry	30% (100%, ill)	2%	Trace	5% (100%, chl)			60% (100%, ser chl, qtz, hm)	Disseminated hematite 2%
Ba-K-feldspar megacrystic plagioclase hornblende porphyry	30% (100%, ser)	Trace	10% (2%, carb, ser)	10% (80%, chl)			50% (100%, qtz ill, carb)	Minor carbonate veinlets
Hornblende porphyry	20% (100%, ser, qtz)	10%	5% fresh	20% (70%, chl, ep, ilm)			50% (100%, ser, chl, ilm)	Pyrite 2%, epidote veinlets
Augite porphyry	60% (20% ser)				15% (50%, clay, act)		5% (100%, chl, ser leu, cal)	Disseminated pyrite and trace chalcopyrite
Syenodiorite	40% (80%, ser, qtz)			20% (100%, chl, ilm)			40% (100%, qtz ser, chl)	Pyrite 2%, trace chalcopyrite with chalcocite rims
Monzonite	(20%, ser, ill)	5%? alteration	fresh	brown fresh		Apatite 1% Sphene 0.1%	(100%, ser, olino, chl)	Pyrite 2%
Plagioclase augite diorite	50% (100%, ser)				20% fresh		(100%, ser)	Minor K-feldspar veins 5% pyrite cubes

the partial alteration of the anorthite component of plagioclase to clinozoisite and calcite. Widespread argillic and phyllic alteration is characterised by clays and sericite replacing plagioclase and abundant calcite. The alteration of the plagioclase is accompanied by loss of Na from the sample. Concentrations of iron and magnesium may be approximately constant because pyrite and chlorite replace hornblende and augite in phyllic altered samples.

#### 4.3.2 Major and minor element plots

A plot of major elements on the AFM diagram of Irvine and Barager (1971) show that most of the intrusive rock units are calc-alkaline while the aphanitic intermediate dyke is tholeiitic (Fig. 4.3). Samples of each unit that have a higher proportion of ferromagnesian minerals, or contain augite instead of hornblende, plot on the primitive side of the more evolved sample. This indicates that the alteration of the intrusive rocks has not significantly affected the distribution of the major elements in these least altered samples.

#### 4.3.3 Trace element spiderdiagram plots

The spiderdiagram in Figure 4.4 is normalized to MORB for plagioclase augite diorite, monzonite and syenodiorite rock units. It shows that the intrusive units are enriched in LILE and depleted in heavy REE with respect to MORB. The absence of an Eu anomaly in the three rock units indicates that feldspar fractionation did not occur or was not an important process in the magma chamber before intrusion of the rock units. The marked trough in Zr for the plagioclase augite diorite reflects a lack of differentiation that concentrates Zr in the magma. Both the plagioclase augite diorite and the monzonite exhibit a marked trough in Ti. This indicates that the magma source may have a residual Ti phase that did not melt during magma generation, or that Ti bearing phases had previously fractionated before intrusion of the magma. The lower heavy REE in the syenodiorite relative to the monzonite is possibly caused by the unit being derived from a source from which hornblende had been removed by either fractionation or crystal settling.

# PRE-, SYN- AND POST-MINERALIZATION DYKES

▽ Kersantite (biotite lamprophyre)

▲ Aphanitic intermediate dykes

\* Trachytic plagioclase porphyry

◆ Albite megacrystic plagioclase hornblende porphyry

◇ K-Ba-feldspar megacrystic plagioclase hornblende porphyry

● Hornblende porphyry

○ Augite porphyry

■ Syenodiorite

□ Monzonite

x Plagioclase augite diorite

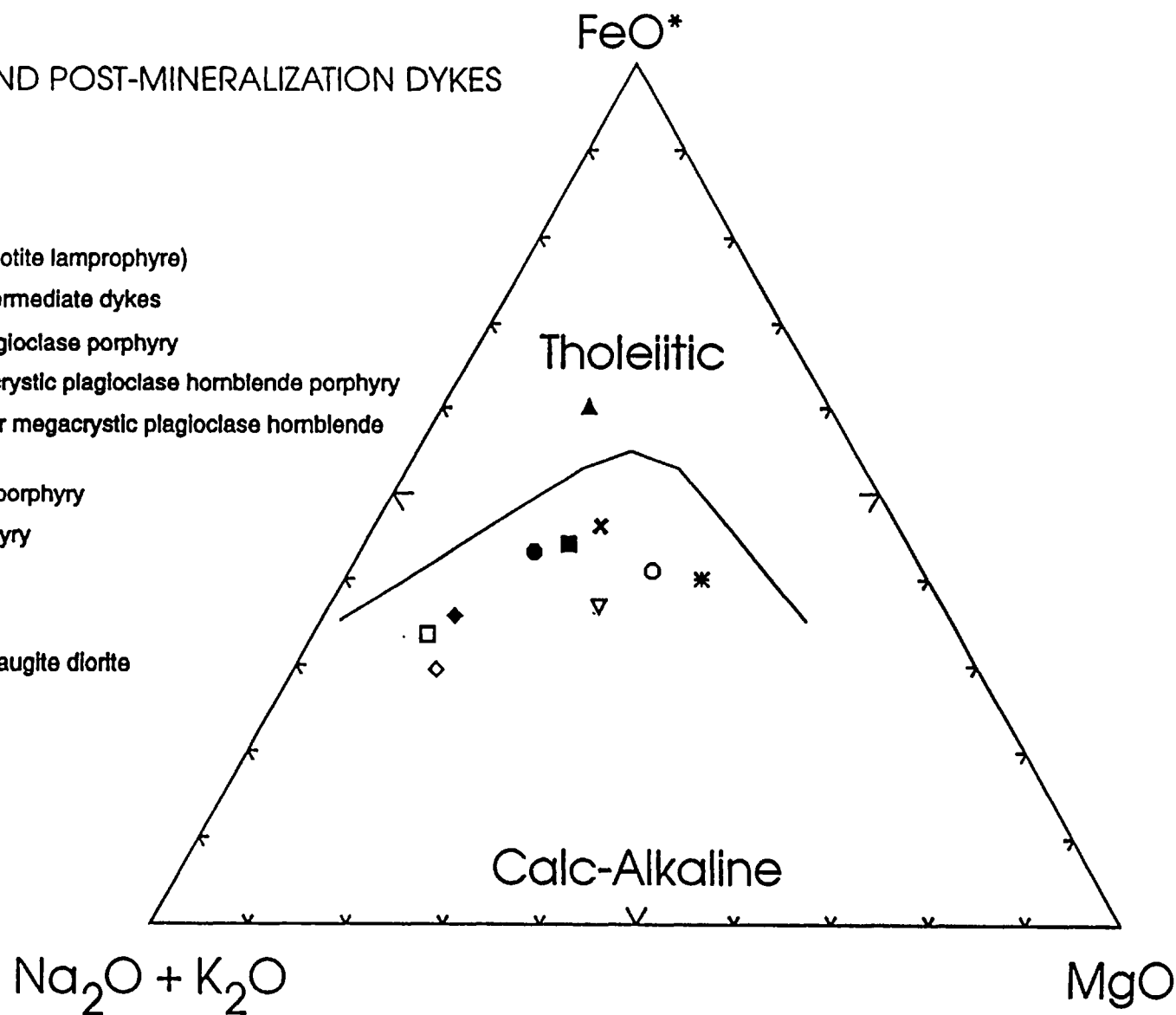


Figure 4.3. AFM diagram from Irvine and Barager (1971) showing least altered intrusive units on the Kerr deposit.  $\text{FeO}^*$  is total iron. All major units, except the aphanitic intermediate dykes, plot in the calc-alkaline field.

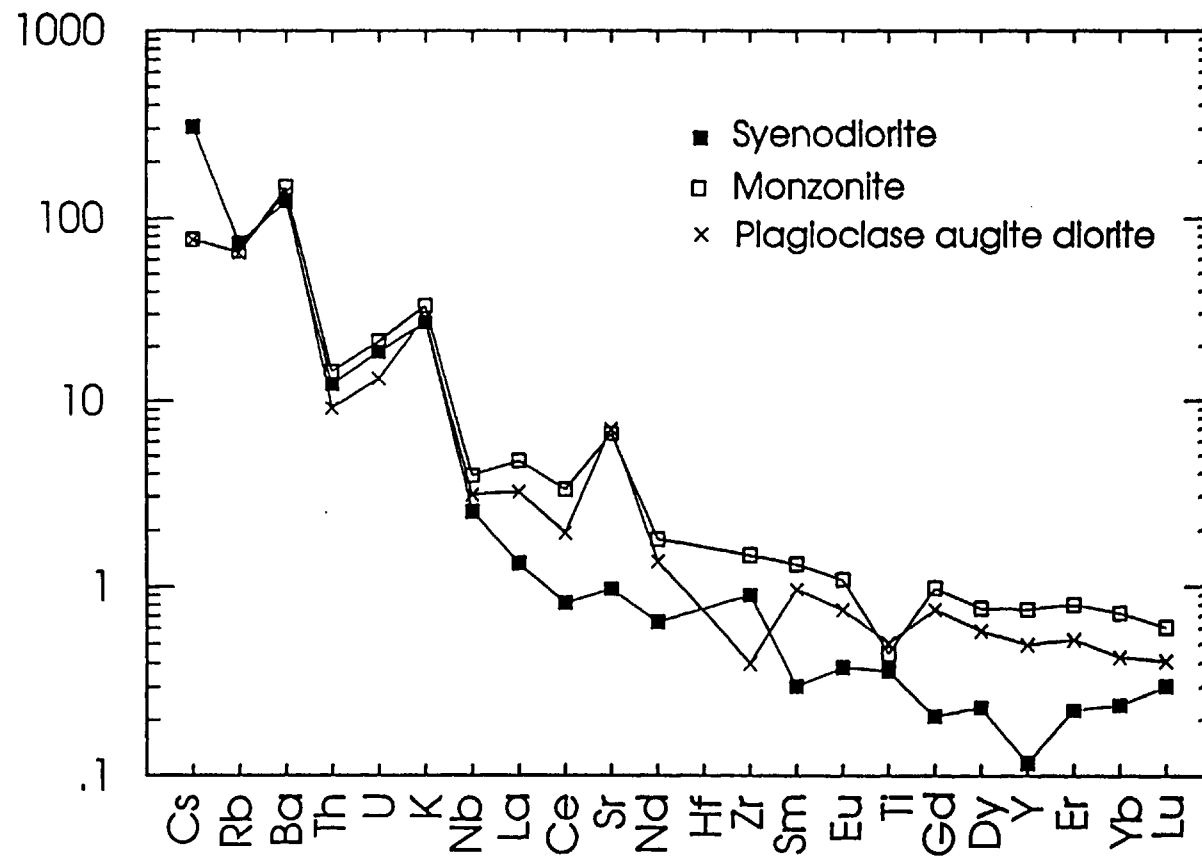


Figure 4.4. Spiderdiagram of major and trace elements normalized to MORB for plagioclase augite diorite, monzonite and syenodiorite rock units from the Kerr deposit, northwestern British Columbia.

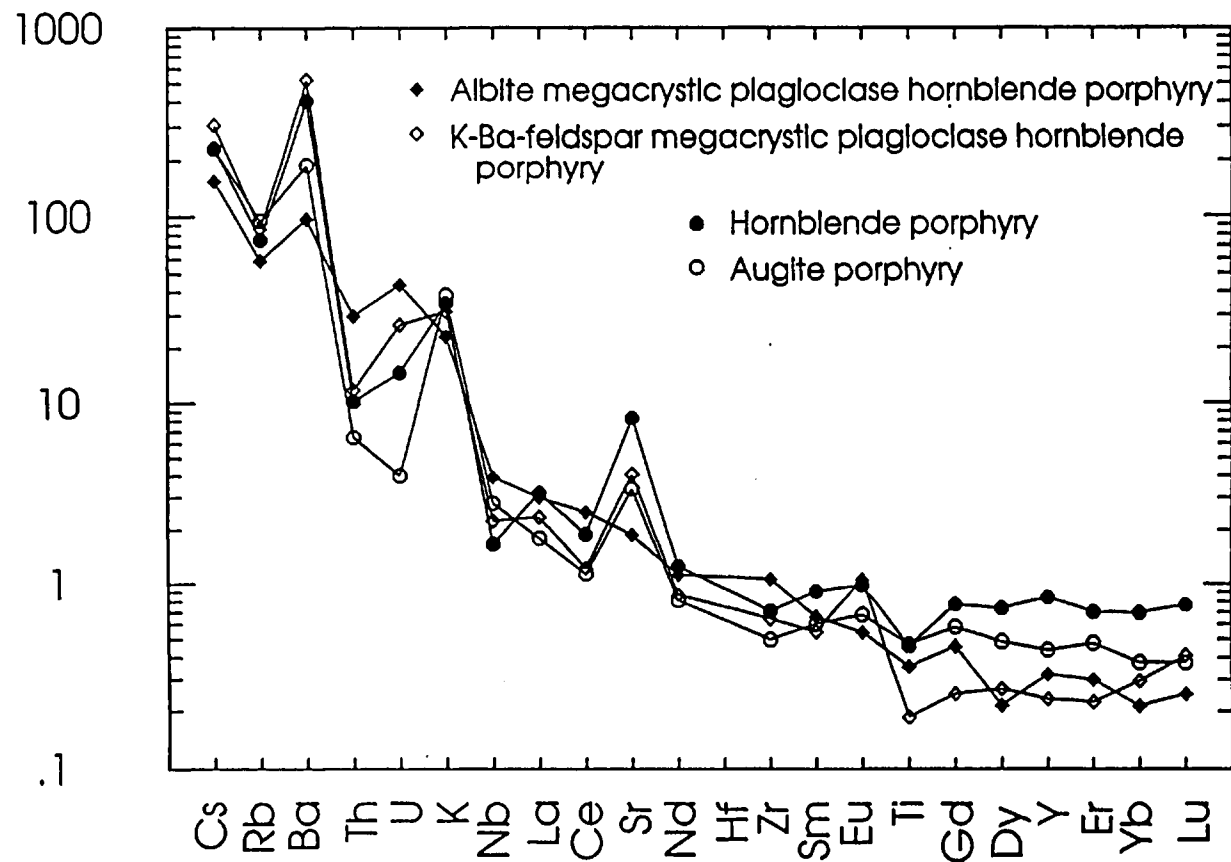


Figure 4.5. Spiderdiagram of major and trace elements normalized to MORB for augite porphyry, hornblende porphyry, K-Ba-feldspar megacrystic plagioclase hornblende porphyry and albite megacrystic plagioclase hornblende porphyry rock units from the Kerr deposit, northwestern British Columbia.



Spiderdiagrams normalized to MORB indicate that the augite porphyry from the footwall and hornblende porphyry from the hanging wall have similar patterns except that augite porphyry has lower concentrations of heavy REE, Th and U (Fig. 4.5). The lower U and Th may be due to variations in magma chemistry, or reflect poor analytical precision (Appendix B). The lower HREE in the augite porphyry compared to the hornblende porphyry is possibly due to preferential partitioning of HREE into hornblende rather than augite. Both samples have Ti depletion similar to that in plagioclase augite diorite and monzonite.

Spiderdiagrams of trace elements in albite megacrystic porphyry and K-Ba-feldspar megacrystic porphyry dykes have normalized patterns (Fig. 4.5) that are similar to those for augite and hornblende porphyry. The albite megacrystic porphyry dyke (Fig. 4.5) has higher concentrations of the incompatible elements Th, U and Zr, and less Rb, Ba and Sr, which are concentrated in K-feldspar. The higher concentrations of incompatible elements indicate that this dyke may be slightly more evolved than the K-Ba feldspar dykes. This conclusion is consistent with the observation that the albite megacrystic dyke was intruded after the K-Ba-feldspar dyke. The lower concentrations of Rb, Ba and Sr in the albite dyke are possibly due to absence of K-feldspar megacrysts in the sample analyzed. The high Eu content of the K-Ba-feldspar dyke may be due to the early crystallization of feldspars. The albite megacrystic dyke with less Eu may have been derived from a source that had previously undergone feldspar fractionation. Both dykes have Ti depletion, possibly due to Ti-phase fractionation before intrusion.

The spiderdiagram plot of trachytic plagioclase porphyry shows that the sample is depleted in Zr, Rb and K compared to the previous rock units (Fig. 4.6). These depletions support the conclusion drawn from the petrography and AFM diagram that the sample is quite primitive and has not been strongly differentiated. A plot of the tholeiitic aphanitic intermediate dyke shows that it is enriched in heavy REE compared to the other calc-alkaline

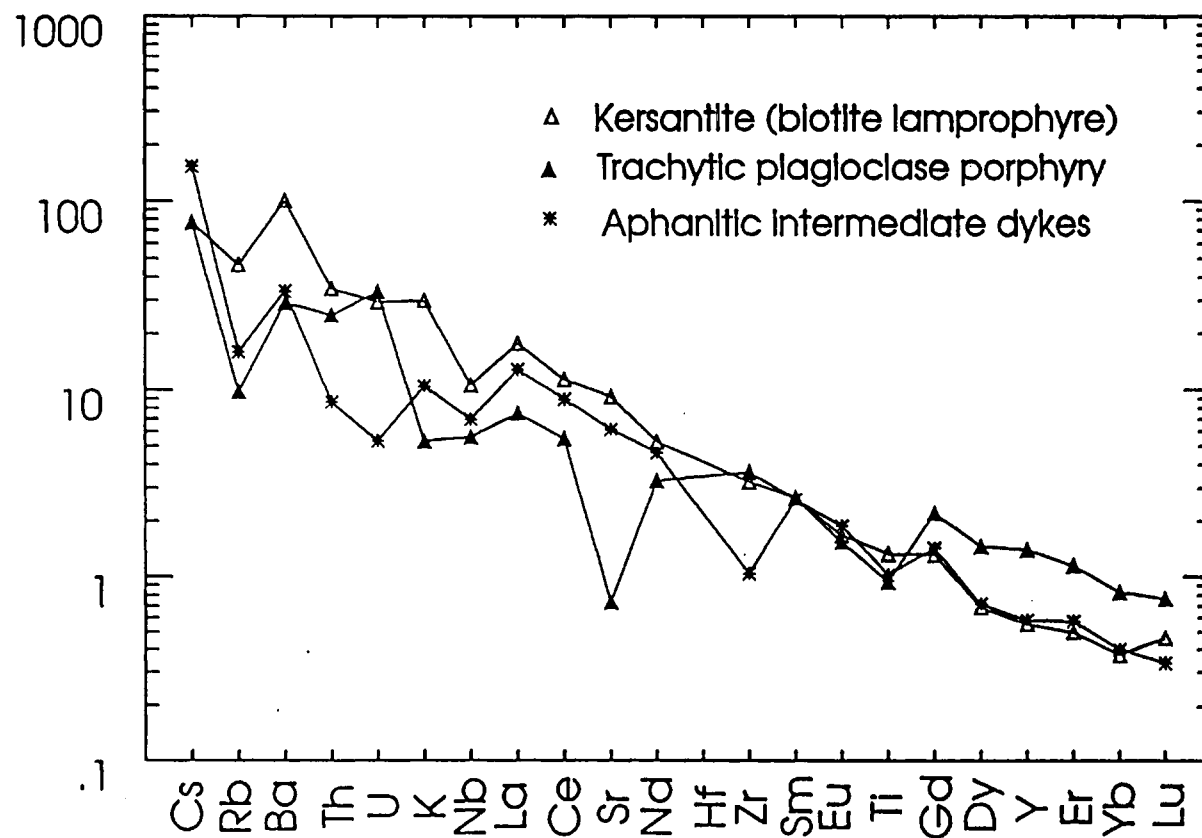


Figure 4.6. Spiderdiagram of major and trace elements normalized to MORB for trachytic plagioclase porphyry, aphanitic intermediate dyke and kersantite rock units from the Kerr deposit, northwestern British Columbia.

rocks. A plot of trace elements in kersantite (calc-alkaline biotite lamprophyre) show little variation from the normal crustal concentrations of trace elements, which is typical of lamprophyric rocks (Rock, 1987).

#### **4.4 Discussion of the Geological Setting of the Kerr Deposit**

##### **4.4.1 Sedimentary and volcanoclastic rock units**

The presence of bedding and ripples in sedimentary and volcanic rock units exposed on the Kerr deposit suggest that they were deposited in a subaqueous environment. Along the east side of the northerly trending deposit, the stratigraphic sequence coarsens upward from well laminated mudstone with minor conglomerate lenses to heterolithic conglomerate. The sequence subsequently fines upward to well bedded argillites that have graded beds of broken plagioclase grains. Large, subhedral K-feldspar grains in the central conglomerate unit suggest that their provenance was close, otherwise these grains would have been destroyed. The overlying, well laminated argillites and siltstones probably represent volcanoclastic deposits that either slumped off the shoulders of volcanoes, or represent ash and tuff that fell into the ocean and subsequently flowed down the submerged flanks of a volcano.

Well-bedded mudstone to heterolithic conglomerate strata correspond to descriptions of the eastern facies of the Late Triassic Stuhini Group (Anderson and Thorkelson, 1991; Lewis, 1992). The K-feldspar megacrysts in the conglomerate are typical of megacrysts from the Early Jurassic Texas Creek plutonic suite. Their occurrence in a conglomerate units suggest that it was deposited during volcanism in the Sulphurets gold camp (Alldrick and Britton, 1988). Overlying argillites with beds of broken plagioclase grains around the Old Camp (Fig. 4.1) suggest that they were also deposited during the onset of volcanism in the Sulphurets gold camp.

#### 4.4.2 Intrusive rock units

Monzonite, syenodiorite and alkali-feldspar megacrystic dykes in the Kerr deposit are spatially and temporally related to the mineralization. With one exception (Fig. 4.3) all of these dykes are calc-alkaline in composition and were once quartz saturated either before (i.e. K-Ba-feldspar megacrystic porphyry) or after emplacement (monzonite). These characteristics and their Early Jurassic ages suggest that they are related to the Early Jurassic, calc-alkaline Texas Creek plutonic suite. The mineralogy of the monzonite and syenodiorite dykes correspond to other mineralized intrusions between the Sulphurets and Mitchell glaciers (Alldrick and Britton, 1991; Alldrick and Britton, 1988).

Intrusion breccias related to the monzonite to syenodiorite dykes appear to be confined to the hanging wall of the deposit. They are restricted to an intermediate phase of this suite characterized by more abundant plagioclase than hornblende laths, and possibly by less K-feldspar in the matrix than the earlier monzonite phases along the footwall.

The megacrystic dykes vary in orientation. Early K-Ba-feldspar megacrystic porphyry dykes are thin and trend easterly. They are concentrated in the area below Kerr Peak and also crop out 70 m south of drill hole KS-101 on the eastern edge of section 10600N. These dykes are not intersected by the relatively thick, albite megacrystic dykes that strike northerly and dip west underneath the K-Ba-feldspar dykes. The albite megacrystic porphyry dyke cuts the deposit following the trend of the earlier mineralized monzonite intrusions. No magmatic breccias have been observed along the margins of these dykes.

Major and trace element geochemistry of the augite and hornblende porphyry dikes indicate that they are calc-alkaline. The variation in phenocrysts from augite to hornblende may reflect a source magma that was becoming water saturated (Cline and Bodnar, 1991).

The tholeiitic aphanitic intermediate dykes are similar to those described by Margolis (1992) from the ridge between the Sulphurets and Mitchell creeks. The tholeiitic composition of the dykes is typical of magma produced in an extensional environment (Wilson, 1989). This evidence suggests that the tholeiitic aphanitic intermediate dykes may have intruded into the Kerr deposit during Early to Middle Jurassic regional extension of the Iskut area.

The modal mineralogy and age of the kersantite dykes suggests that they are temporally related to the Tertiary Hyder plutonic suite in the Stewart mining camp.

## 5.0 STRUCTURAL GEOLOGY OF THE KERR DEPOSIT

### 5.1 Introduction

The Kerr deposit is in the footwall of the Sulphurets thrust fault which outcrops about two kilometres west of the deposit (Fig. 1.1; Lewis, 1992). Mapping by Alldrick and Britton (1988) and Lewis (1992) indicate that this thrust has southeasterly vergence and possibly formed during lower greenschist metamorphism of the Late Triassic Stuhini Group and Early Jurassic Hazelton Group. The thrust fault dominates the geology along the western edge of the Sulphurets gold camp. Motion along the thrust fault was concentrated along the main fault trace. West of the Sulphurets thrust fault is the McTagg anticlinorium (Fig. 1.1). Axial plane foliation, in the anticlinorium west of the Kerr deposit, strikes northwesterly with steep dips (Lewis, 1992). Three kilometres north of the Kerr deposit, foliation strikes east-west and dips north in sericite - quartz - pyrite altered Hazelton Group rocks in the footwall to the Sulphurets thrust fault (Margolis, 1992).

The two, regional foliation directions in the vicinity of the Kerr deposit reflect differences in the regional shortening direction. This is possibly due to local variations in the orientation of principal stresses or they may relate to different deformation events (Lewis, personal comm., 1993). The McTagg anticlinorium and the southeasterly vergent Sulphurets thrust fault correlates with similar Late Jurassic to Early Tertiary structural features in the Skeena fold belt, 150 km to the northwest (Evenchick, 1991).

Geological mapping by Payne (1989) showed that the Kerr deposit is hosted in a well foliated north-trending alteration zone where a strong stretching lineation on foliation planes consistently plunges northwest. This study combines detailed geological mapping across sections 9700N and 10600N, and structural measurements by Payne (1989) over a larger area

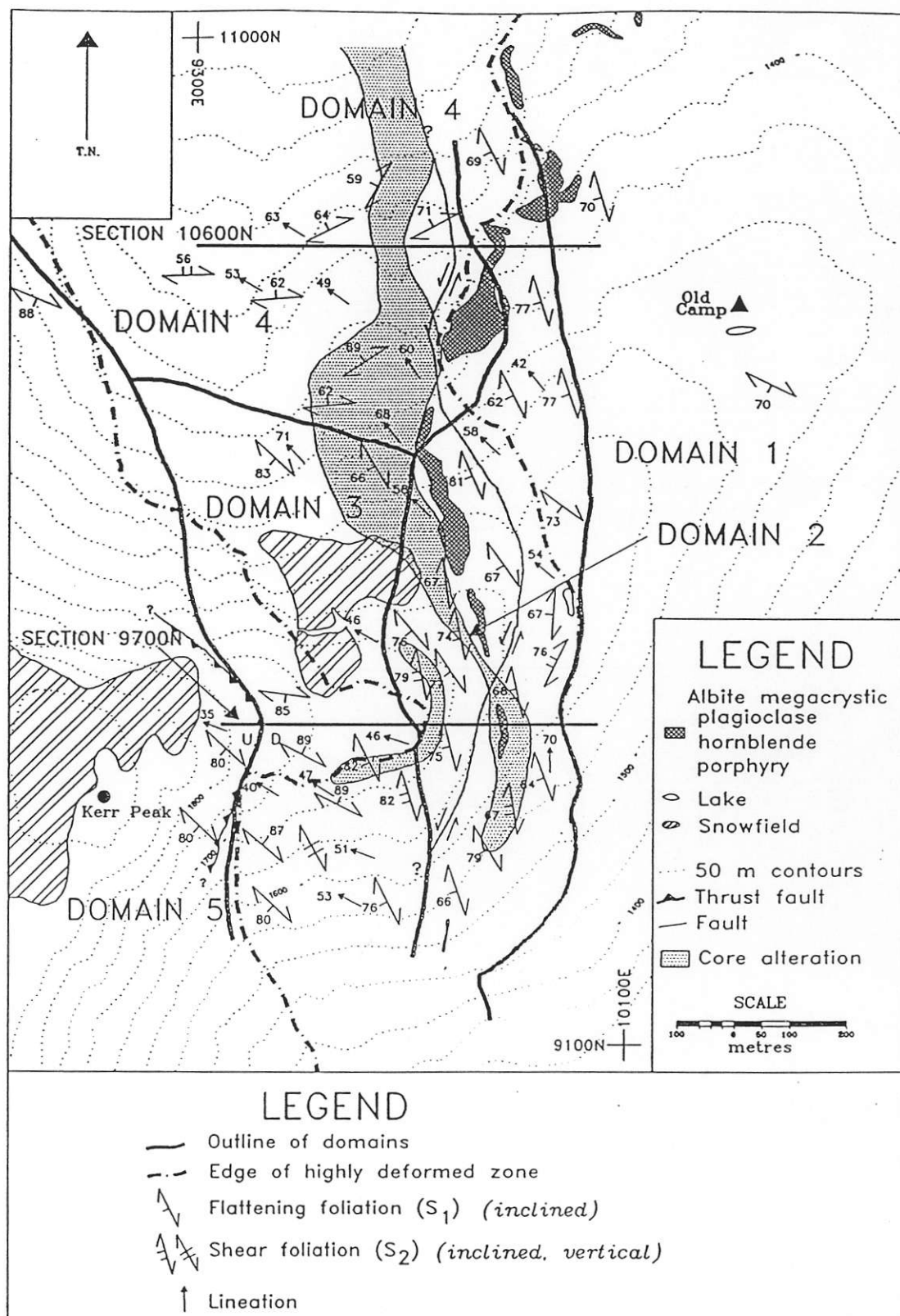


Figure 5.1. Outline of structural domains and variation in penetrative fabric orientation across the Kerr deposit, northwestern British Columbia. Each symbol represents the average orientation from at least five measurements. Data outside of the 1990-1991 mapping area (Fig. 1.2) is from Payne (1989).

(Fig. 5.1). Post-mineralization dykes are deformed in the same style as the alteration zone except for Eocene lamprophyre dykes, which are undeformed and locally follow fault zones.

The effects of deformation on mineralization and alteration mineral assemblages in the Kerr deposit were recognized after analysis of the variation in orientation of penetrative fabrics, mineral elongation lineation, quartz fibres and deformed post-mineralization dykes along sections 9700N and 10600N. Detailed description of the effects of deformation on mineralized veins follows the discussion of penetrative fabrics.

## 5.2 Local Structural Setting of the Kerr Deposit

The region covered by Figure 4.1 was split into five major structural domains (Fig. 5.1). Each domain has a characteristic orientation of penetrative fabric elements and intensity of deformation. Domain 1 forms the weakly deformed footwall of the deposit. The sedimentary rocks are weakly altered and have a northwesterly striking spaced cleavage parallel to the axial plane of open folds. Weak alteration replaces the matrix to the sedimentary rocks, but not the mineral fragments. Domain 2 lies west of the footwall domain, and it is characterized by northward striking, west dipping foliation. Foliation is most pronounced in intensely altered tuffaceous rocks surrounding the chlorite core of the Kerr deposit, and it decreases in intensity northward. Domain 3 is west of domain 2, and it is distinguished from domain 2 by the northwesterly strike of the foliation and a pronounced northwesterly plunging mineral lineation. Tuffaceous rocks are not as altered as in domain 2, except along its northern boundary with domain 4. Domain 4, north of domain 3, has foliation that strikes northeasterly and dips north. The penetrative fabric is dominated by a northwesterly plunging mineral elongation. Domain 5 forms the weakly deformed hanging wall above a minor thrust fault exposed along section 9700N. The sedimentary rocks have a weak northwesterly striking foliation.



Penetrative fabrics are most pronounced in the yellow and grey sericite - quartz - pyrite alteration surrounding the chlorite core of the Kerr deposit (domains 2 and 4; Figs. 4.1 and 5.1). In this area, most of the original rock textures are obliterated. Outside of this region, rock units are less deformed and their lithologies can be identified.

Structural measurements in each domain were averaged so that areas with a higher density of measurements do not bias the stereonet plots. Each domain was divided into 100 m squares or a modified shape of equal area, and the structural measurements were averaged in each area. Structural measurements were first plotted on equal area stereonet and then contoured using the Kamb method (Kamb, 1959). Relationships among extensional quartz veins, mineralized veins, quartz slickensides and penetrative fabrics were determined from detailed mapping along two cross - sections, 9700N and 10600N (Figs. 5.2 and 5.3).

If primary, lithological layering in the rock was observed, it was recorded as  $S_0$ . Penetrative fabric was recorded as  $S_1$ . Microscopically,  $S_1$  corresponds to either anastomosing cleavage in sericite - quartz - pyrite altered rock with abundant quartz grains or planar cleavage in rock with abundant phyllosilicates. A fabric would be designated  $S_2$  if it cut  $S_1$  and was continuous at outcrop scale. This fabric consists of parallel bands of phyllosilicates that cut the  $S_1$  fabric.

### 5.3 Bedding in Sedimentary and Volcaniclastic Rocks in Domains 1 and 5

Prominent graded bedding and ripples act as good tops indicators along both the footwall and hanging wall of the Kerr deposit. Bedding in the well bedded mudstone and interbedded sandstone and siltstone units along the footwall dip steeply east (Fig. 4.1). Bedding in the overlying laminated argillite is contorted into irregular folds around the Old Camp, but it parallels well bedded mudstone near their contact with the underlying sediments.

Hanging wall sandstone and argillite beds dip gently southwest (Fig. 4.1). Below a minor thrust fault, bedding in the well bedded mudstone is tightly folded and locally overturned adjacent to relatively undeformed syenodiorite dikes. Weakly deformed K-Ba-

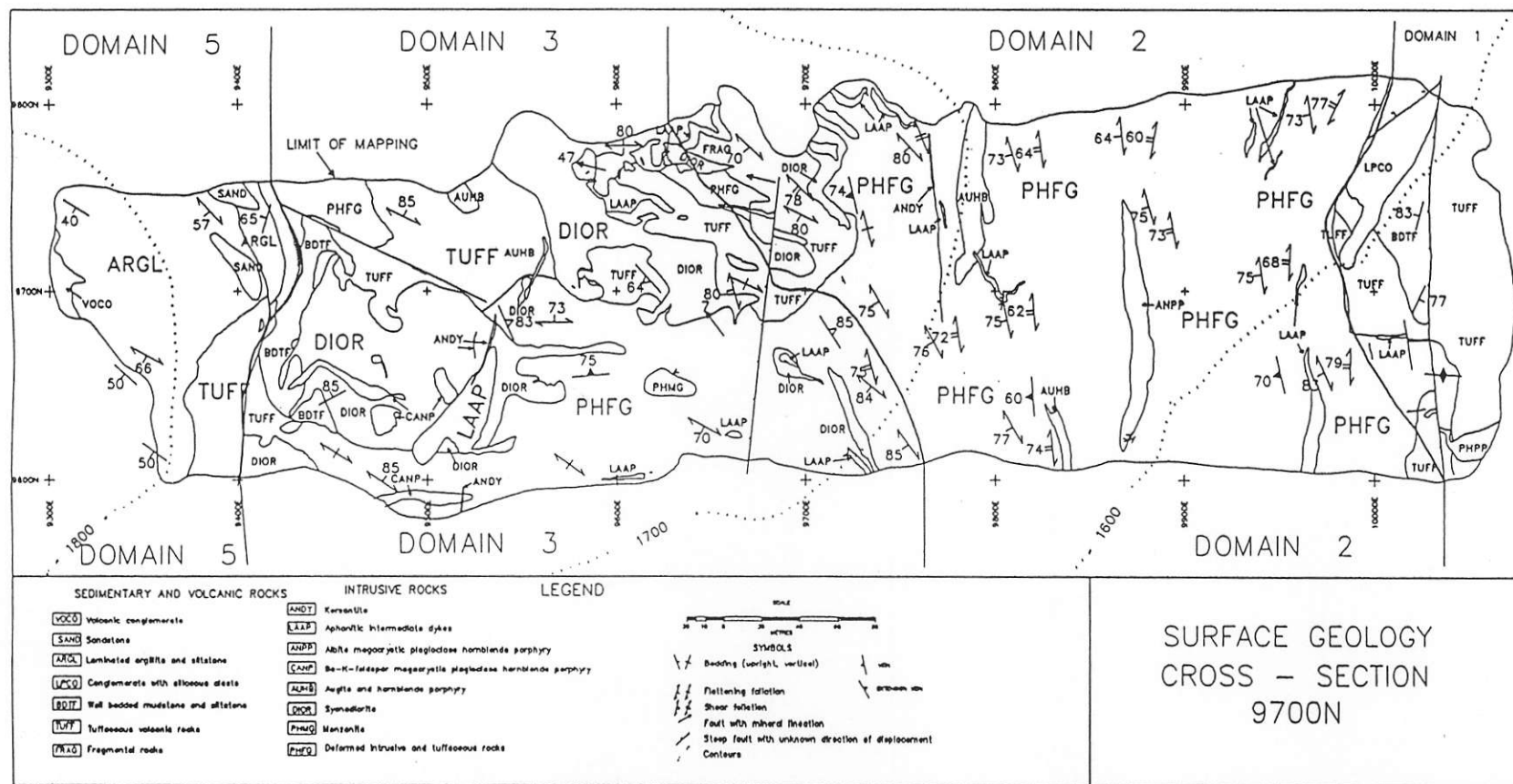


Figure 5.2. Detailed geological map along section 9700N Kerr deposit, northwestern British Columbia, shows the variation in orientation of foliation, lineation, mineralized quartz veins and extension quartz veins across the deposit. Structural domains on the section are indicated.

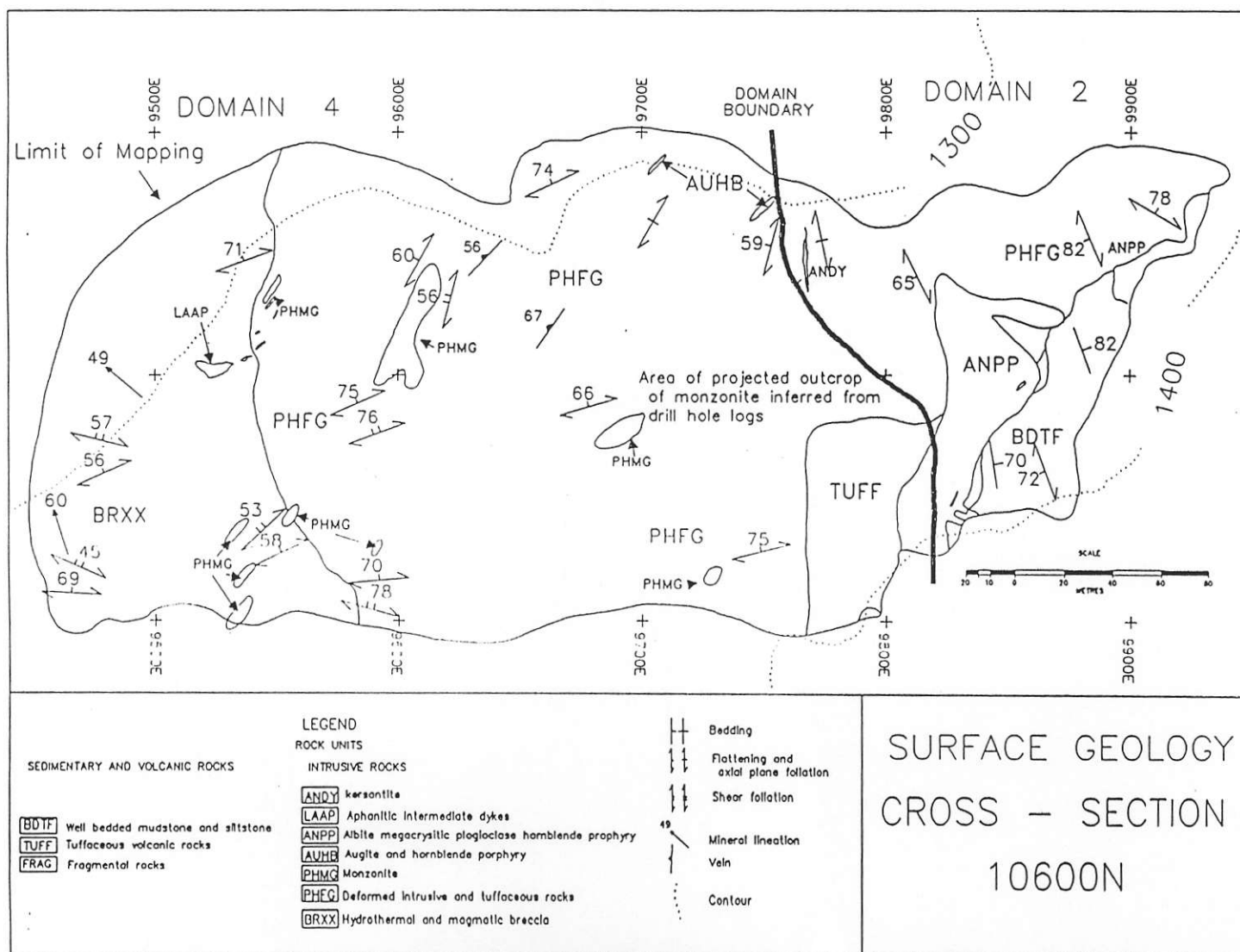


Figure 5.3. Detailed geological map along section 10600N Kerr deposit, northwestern British Columbia, shows the variation in orientation of foliation, lineation, mineralized quartz veins and extension quartz veins across the deposit. Structural domains on the section are indicated.

feldspar megacrystic dykes intrude this tightly folded, well bedded mudstone. These relationships suggest that either the mudstone accommodated most of the strain during deformation (Ramsay and Huber, 1983) or it was deformed prior to intrusion of the dyke. Lithological layering in the massive tuff unit could not be traced on surface due to the intensity of hydrothermal alteration, deformation and weathering.

#### **5.4 Penetrative Fabrics, Deformed Dykes and Extension and Shear Veins in Domains 1 to 5.**

##### **5.4.1 Domain 1**

Domain 1 covers the weakly to undeformed footwall of the Kerr deposit. Average orientation of the penetrative fabric in the domain is  $118^{\circ}/84^{\circ}\text{W}$  (Fig. 5.4 and Table 5.1). Penetrative fabrics in the northern portion of the domain are more pronounced than in the region 300 m south of the Old Camp (Fig. 5.1). Spaced vertical cleavage in the conglomerate 100 m south of the camp strikes  $110^{\circ}$  and is characterized by stylolitic contacts between cobbles. At the eastern end of section 9700N (Fig. 5.1), the penetrative fabric consists of stylolites in monzonite. These stylolites cut plagioclase, hornblende and quartz crystals, and are normal to 5 mm thick quartz - chlorite - calcite extension veins. Plagioclase phenocrysts in the monzonite are kinked where the trace of extension veins intersect them.

##### **5.4.2 Domain 2**

Domain 2 covers the region immediately west of the weakly to undeformed footwall. This domain has a pronounced steep penetrative fabric at  $157^{\circ}/74^{\circ}\text{W}$  and a mineral lineation at  $310^{\circ}/54^{\circ}$  (Figs. 5.5 and 5.6; Table 5.1). This fabric parallels the contact with domain 1. Within domain 2 the foliation changes in orientation such that it parallels the fabric in domains 3 and 4. The northern portion of the domain contains weakly to moderately deformed rocks.

Table 5.1. Structural measurements from different domains on the Kerr deposit, northwestern British Columbia.

WEIGHTED AVERAGE ORIENTATION		
DOMAIN	FOLIATION S1	LINEATION
1	118/84W	
2	157/74W	310/54
3	133/83W	300/53
4	247/61N	304/57
5	140/76W	

DOMAIN	FOLIATION S1	FOLIATION S2	LINEATION	MINERALIZED QUARTZ VEIN	EXTENSION QUARTZ VEINS
<b>SECTION 9700N</b>					
2	153/76W			169/69W	177/80W 49/15E
PAIRED MEASUREMENTS					
2	155/76W	173/73W			
3	117/89N		292/40	298/83N	168/87W 166/79W
PAIRED MEASUREMENTS					
3	122/87S	157/84W			
<b>SECTION 10600N</b>					
2	160/72W				
4	243/64N		300/53		
PAIRED MEASUREMENTS					
4	245/63N	269/56N			

## WEIGHTED FOLIATION FOR DOMAIN 1

A

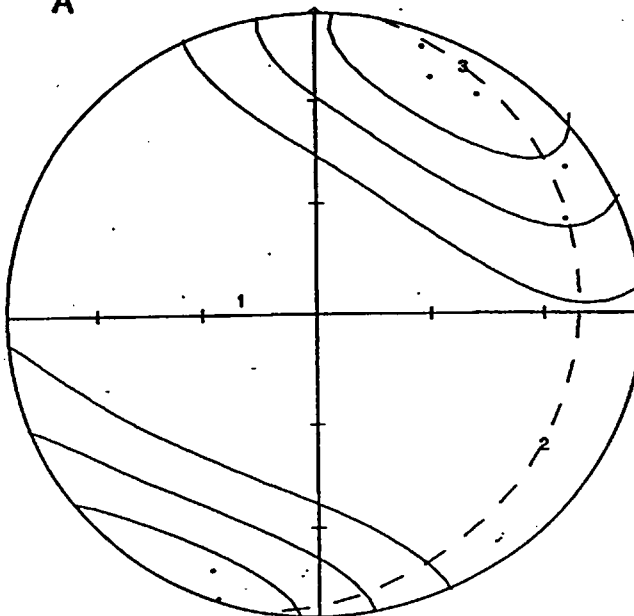
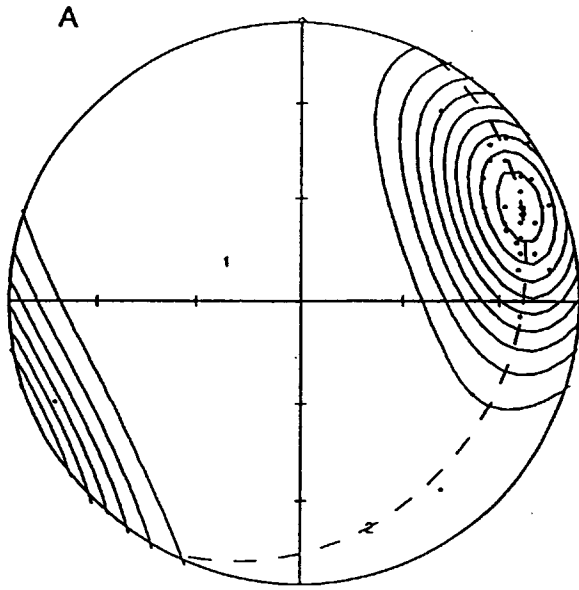
 $N = 8$  $E = 2.12$  $k = 3.78$  $\text{Sigma} = 0.71$  $(\text{Peak} - E)/\text{Sigma} = 5.9$ Peak position :  $28.1^\circ / 6.2^\circ$ 

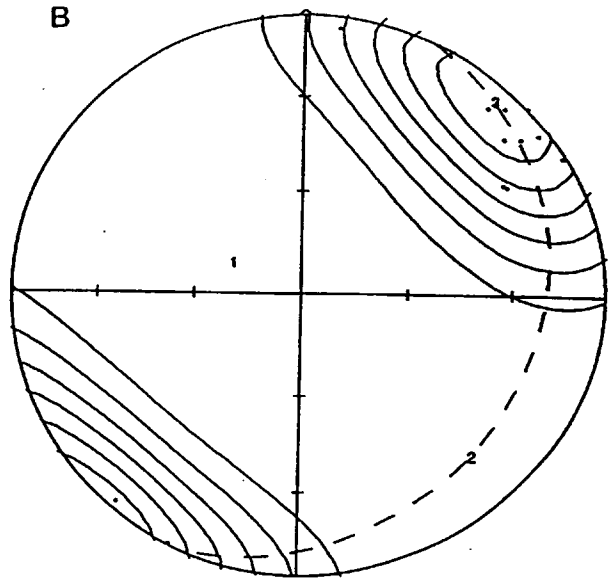
Figure 5.4. Equal area stereonet of poles to weighted foliation ( $S_1$ ) in domain 1, Kerr deposit, northwestern British Columbia.  $N$  = number of data points,  $k$  = kurtosis of the Gaussian bell weighting function. Lowest contour is  $E$  with each successive contours at multiples of  $\text{Sigma}$  -- the coefficient of statistical dispersion of the data.

## WEIGHTED DATA FOR DOMAIN 2



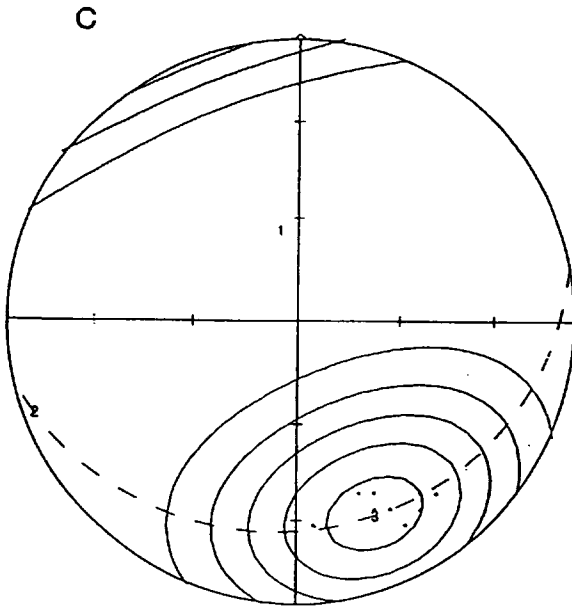
$N = 32$                        $E = 3.51$   
 $k = 9.11$                        $\text{Sigma} = 1.17$   
 $(\text{Peak} - E)/\text{Sigma} = 17.5$   
 Peak position :  $66.8^\circ / 16.5^\circ$

## WEIGHTED FOLIATION DATA FOR DOMAIN 3



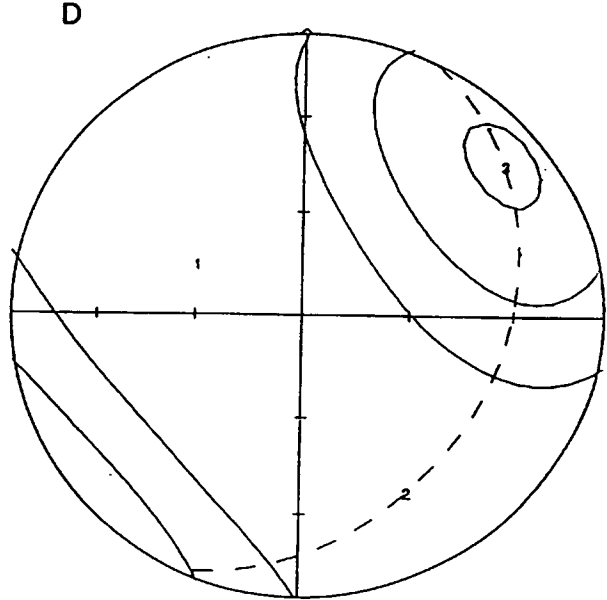
$N = 19$                        $E = 3.05$   
 $k = 6.22$                        $\text{Sigma} = 1.02$   
 $(\text{Peak} - E)/\text{Sigma} = 12.0$   
 Peak position :  $42.9^\circ / 7.3^\circ$

## WEIGHTED FOLIATION DATA FOR DOMAIN 4



$N = 11$                        $E = 2.47$   
 $k = 4.44$                        $\text{Sigma} = 0.83$   
 $(\text{Peak} - E)/\text{Sigma} = 9.0$   
 Peak position :  $157.4^\circ / 28.6^\circ$

## WEIGHTED FOLIATION FOR DOMAIN 5 BELOW KERR PEAK

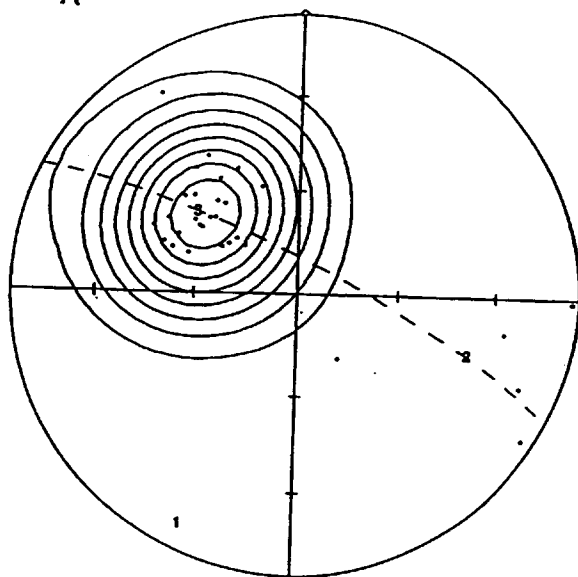


$N = 3$                        $E = 1.13$   
 $k = 2.67$                        $\text{Sigma} = 0.38$   
 $(\text{Peak} - E)/\text{Sigma} = 4.3$   
 Peak position :  $50.2^\circ / 14.3^\circ$

Figure 5.5 (A to D). Equal area stereonets of poles to weighted foliation ( $S_1$ ) for domains 2 to 5. See caption of Figure 5.4 for legend.

## LINEATION ON DOMAIN 2

A

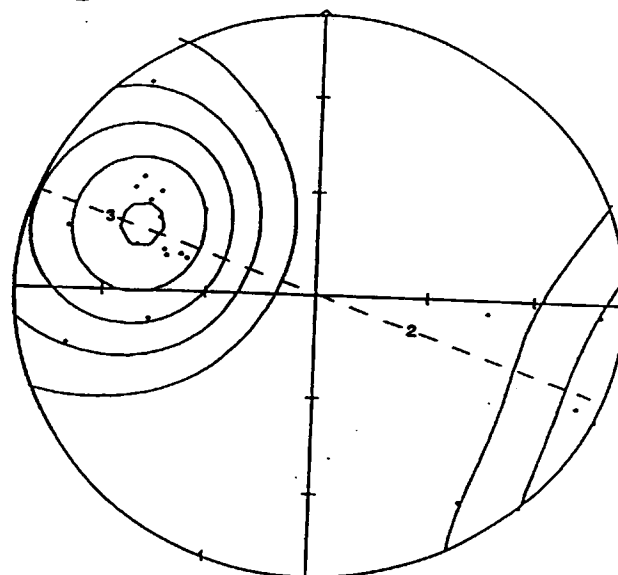


$N = 32$   
 $k = 9.11$   
 $(\text{Peak} - E)/\text{Sigma} = 16.0$   
 $\text{Peak position} : 309.8^\circ / 54.3^\circ$

$E = 3.51$   
 $\text{Sigma} = 1.17$

## LINEATION ON DOMAIN 3

B

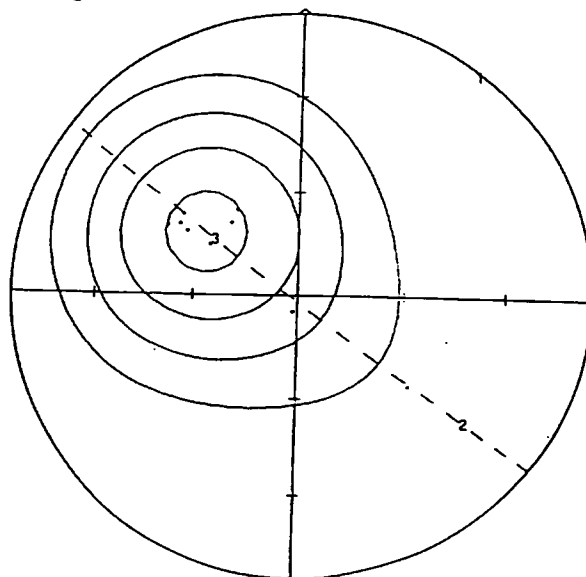


$N = 21$   
 $k = 6.67$   
 $(\text{Peak} - E)/\text{Sigma} = 8.3$   
 $\text{Peak position} : 291.8^\circ / 39.9^\circ$

$E = 3.15$   
 $\text{Sigma} = 1.05$

## LINEATION ON DOMAIN 4

C



$N = 9$   
 $k = 4.00$   
 $(\text{Peak} - E)/\text{Sigma} = 6.7$   
 $\text{Peak position} : 303.7^\circ / 57.1^\circ$

$E = 2.25$   
 $\text{Sigma} = 0.75$

Figure 5.6 (A to C). Equal area stereonet of poles to weighted lineation for domains 2 to 4. See caption of Figure 5.4 for legend.



Lithological layering can be recognized in the weakly deformed sericite altered rocks, but it is obliterated in moderately deformed ones. The southern portion of the domain (around the eastern end of 9700N) contains moderately to highly deformed sericite - quartz - pyrite and chlorite altered tuffaceous and sedimentary units.

The northern portion of domain 2 has  $S_1$  foliation oriented  $160/72^\circ\text{W}$  at an acute angle to bedding in sericite altered well bedded mudstone (Fig. 5.3). Bedding in the well bedded mudstone is weakly transposed by the penetrative fabric.

The southern portion of the domain 2, surrounding a boudinaged albite megacrystic plagioclase hornblende porphyry dyke, has two penetrative fabrics,  $S_1$  and  $S_2$ .  $S_1$  is defined by elongate quartz grains and anastomosing foliation.  $S_2$  is defined by parallel bands of sericite flakes that rotate into the plane containing the elongate quartz grains (Plate 5.1). The orientation and appearance of  $S_1$  and  $S_2$  in hand samples and in thin sections indicate that the  $S_1$  defines a flattening foliation and  $S_2$  a shear foliation. Pancake shaped sericite and quartz altered feldspar phenocrysts in monzonite and hornblende porphyry are parallel to the  $S_1$  flattening foliation. Post-mineralization dykes in this region are boudinaged where they parallel the foliation, or are folded where they cut it.

Average orientation of  $S_1$  and  $S_2$  around section 9700N in the southern portion of domain 2 is  $155^\circ/76^\circ\text{W}$  and  $173^\circ/73^\circ\text{W}$  respectively (Fig. 5.7). The shear foliation,  $S_2$ , is 18 degrees clockwise to  $S_1$ . Average mineral lineation in the southern portion of domain 2 plunges at  $300^\circ/63^\circ$  parallel to elongated quartz grains and quartz fibres in pressure shadows around pyrite grains.

In the southern portion of domain 2, the angle between the flattening and shear foliations gradually decreases towards the contact with domain 1. Along this contact, as defined from drill hole intersections, both fabrics steepen by about 10 degrees to parallel the contact. The shear foliation parallels the contact with relatively undeformed domain 1;



Plate 5.1. Photomicrograph of intensely deformed sericite-quartz-pyrite alteration, Kerr deposit. Parallel bands of sericite flakes define shear foliation ( $S_2$ ). In between the bands, sericite flakes surrounding elongate quartz grains rotate parallel to the layers of sericite flakes. Field of view is 1.25 mm. Legend: s - foliation  $S_1$ , and c - foliation  $S_2$ .

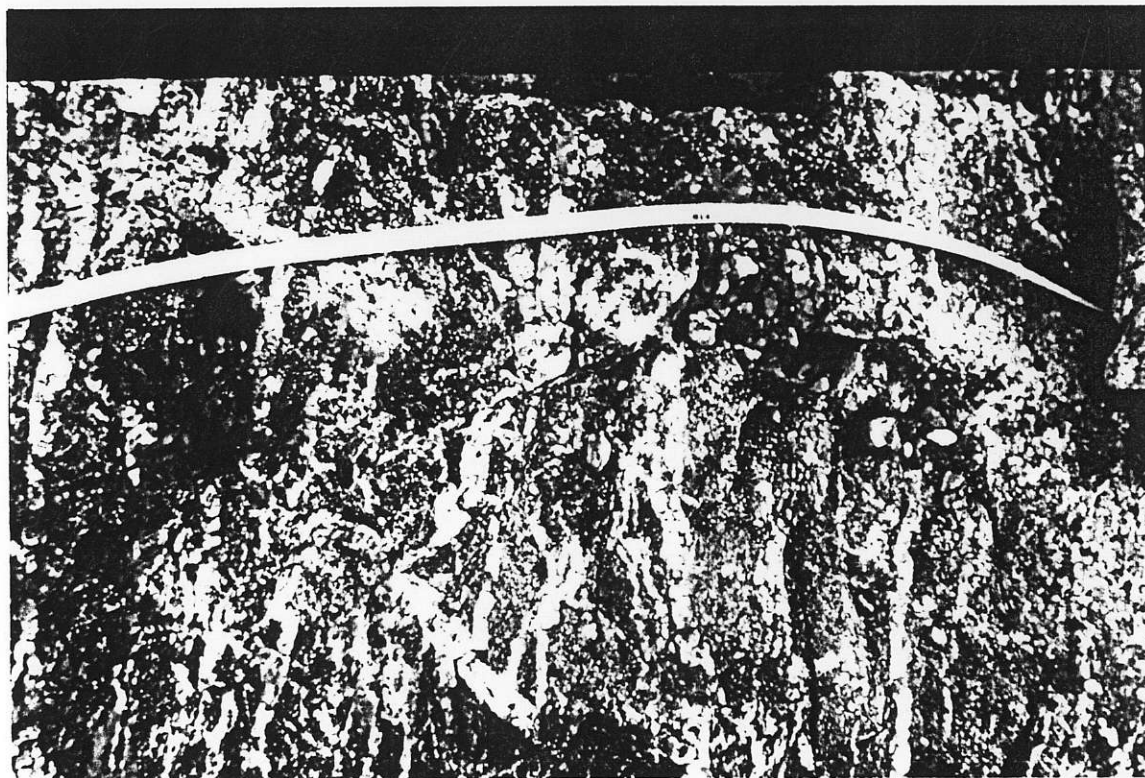
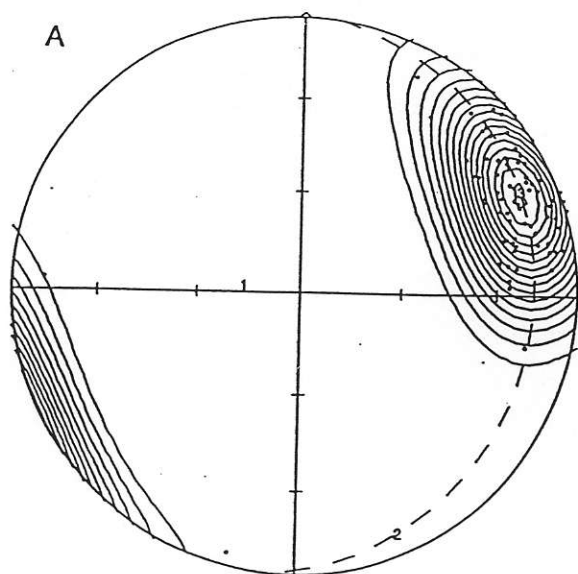
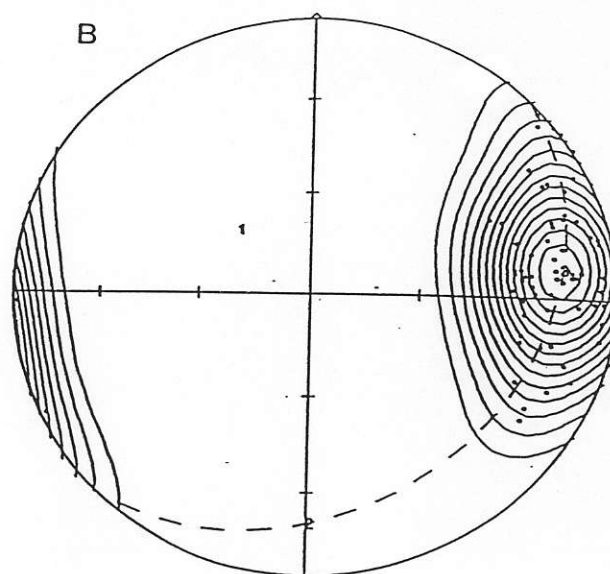


Plate 5.2. Stockwork of quartz veins in chlorite alteration. Yellow tape measure has centimeters on top and inches on bottom. Sample is located at 9660N, 9580E on Figure 5.2.



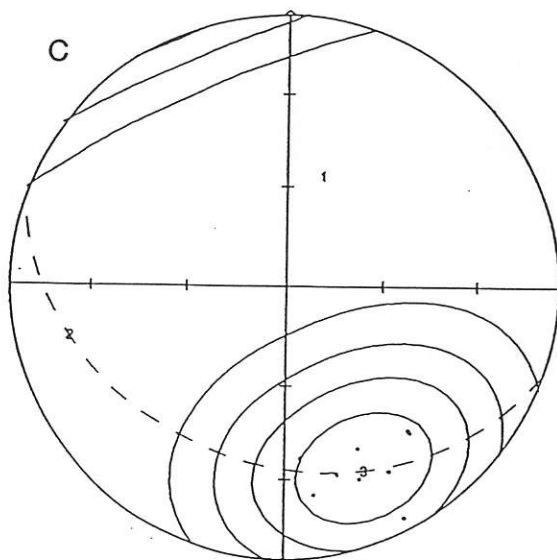
$N = 76$   
 $k = 18.89$   
 $(\text{Peak} - E)/\text{Sigma} = 30.5$   
 Peak position :  $63.4^\circ / 14.1^\circ$

$E = 4.02$   
 $\text{Sigma} = 1.34$



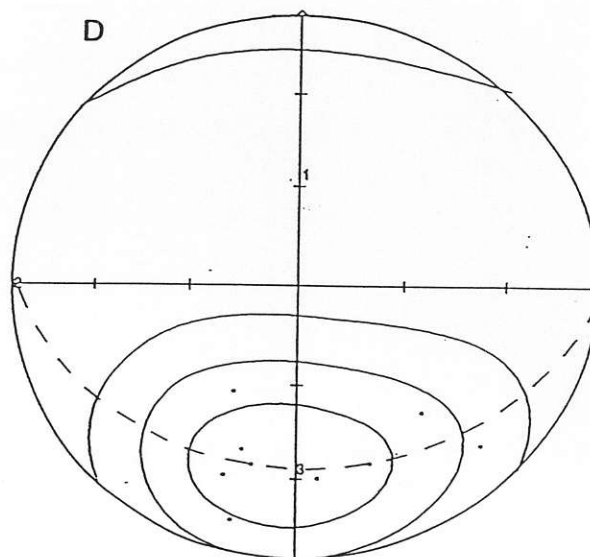
$N = 76$   
 $k = 18.89$   
 $(\text{Peak} - E)/\text{Sigma} = 25.9$   
 Peak position :  $82.4^\circ / 17.1^\circ$

$E = 4.02$   
 $\text{Sigma} = 1.34$



$N = 9$   
 $k = 4.00$   
 $(\text{Peak} - E)/\text{Sigma} = 7.7$   
 Peak position :  $157.4^\circ / 28.6^\circ$

$E = 2.25$   
 $\text{Sigma} = 0.75$



$N = 9$   
 $k = 4.00$   
 $(\text{Peak} - E)/\text{Sigma} = 5.7$   
 Peak position :  $184.8^\circ / 33.5^\circ$

$E = 2.25$   
 $\text{Sigma} = 0.75$

Figure 5.7. Equal area stereonets of poles to  $S_1$  and  $S_2$  foliations along sections 9700N and 10600N. A) domain 2  $S_1$  foliation, B) domain 2  $S_2$  foliation, C) domain 4  $S_1$  foliation, D) domain 4  $S_2$  foliation. See caption of Figure 5.4 for legend.

whereas, the flattening foliation forms an acute angle to it (Table 5.2). Drill core from the boundary shows a gradual loss of the penetrative fabric in the rock; there is no indication of a major fault.

Dykes in domain 2 are intensely deformed by the flattening and shear foliations. Contacts between the highly altered tuffaceous and sedimentary rocks and post-mineralization dykes are always deformed. The intensity of deformation inside the dyke decreases rapidly from its contact. The albite megacrystic porphyry dyke is boudinaged parallel to the shear foliation in the southern portion of domain 2. Aphanitic intermediate dykes trending easterly across the foliation are folded such that their axial plane parallels the orientation of the flattening foliation (Fig. 5.1). West dipping aphanitic intermediate dykes are deformed into Z shapes when viewed down plunge (Fig. 5.1).

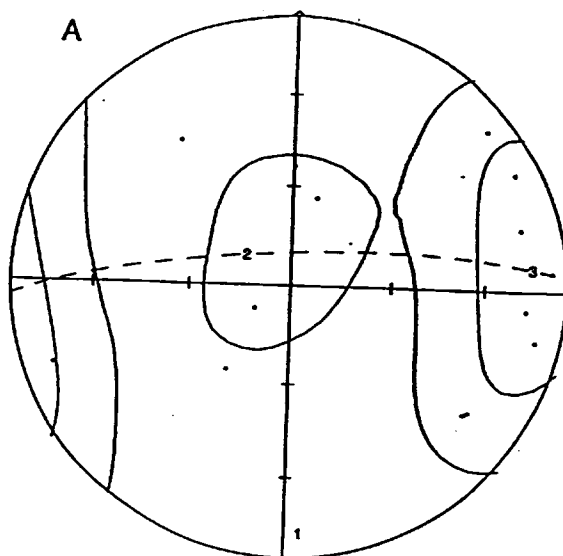
Two sets of extensional quartz veins are exposed on the cliffs west of the boudinaged albite megacrystic porphyry dyke in the southern portion of domain 2 (Fig. 5.1). These veins are 0.5 cm to 2.0 cm thick and are oriented at  $177^{\circ}/80^{\circ}\text{W}$  and  $49^{\circ}/15^{\circ}\text{SE}$  in weakly silicified sericitic tuffaceous rock (Table 5.1 and Fig. 5.8). The steep quartz veins are at an acute angle to the  $S_1$  and  $S_2$  fabrics (Table 5.1). Quartz fibres in these veins parallel slickensides on shallowly, west dipping faults in domains 2 and 3. These veins are also concentrated in the albite megacrystic plagioclase hornblende porphyry dyke. The orientation of these slickensides on these faults are scattered on a great circle that intersects the average mineral lineation orientation in domain 2. This suggests that the quartz fibres on the faults and the mineral lineation record the same direction of elongation; otherwise, they would not define a great circle (Ramsay and Huber, 1983).

In the remainder of the domain, shallowly dipping extension veins predominate over steeply dipping ones. These veins are well exposed in drill core where they occur normal to the flattening fabric in the altered rock.

Table 5.2. Calculated strike and dip of the edge of the contact between highly and weakly deformed rock in the Kerr deposit, northwestern British Columbia. Data is from drill hole intersections in the deposit.

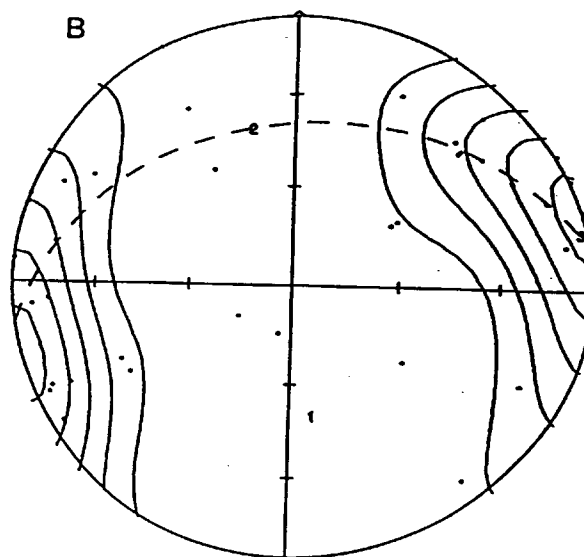
REGION	DOMAIN	FLATTENING FOLIATION (S1)	SHEAR FOLIATION (S2)	EDGE OF DEFORMED ZONE	TOP OF ALBITE MEGACRYSTIC DYKE
A	2	159/84W	198/77W	180/62W	NA
B	2	153/76W	168/68W	143/62W	NA
C	2	169/74W	207/76W	200/59W	NA
D	2	160/72W	NA	125/67S	NA
E	3	135/84S	NA	200/62W	205/55W
F	4	230/68N	NA	235/55N	210/70W
G	4	270/72N	NA	215/75W	225/68W

EXTENSION QUARTZ VEINS ON DOMAIN 2  
SECTION 9700N



$N = 16$   
 $k = 5.56$   
 $(\text{Peak} - E)/\text{Sigma} = 3.9$   
 Peak position:  $82.9^\circ / 11.4^\circ$   
 $E = 2.88$   
 $\text{Sigma} = 0.96$

EXTENSION QUARTZ VEINS ON DOMAIN 3  
SECTION 9700N



$N = 40$   
 $k = 10.89$   
 $(\text{Peak} - E)/\text{Sigma} = 8.8$   
 Peak position:  $73.6^\circ / 1.8^\circ$   
 $E = 3.67$   
 $\text{Sigma} = 1.22$

Figure 5.8 (A to B). Equal area stereonets of poles to extension quartz veins along section 9700N in domains 2 and 3. See caption of Figure 5.4 for legend.

Shear veins of calcite with fibres normal to calcite extension gashes are concentrated in weakly deformed sediments in the footwall. Shear veins of anhydrite and calcite are concentrated in sericite - quartz - pyrite altered monzonite intersected along section 9700N. Fibres in these veins are 45 to 55 degrees to the foliation in the rock. This angle between the fibres and the flattening foliation suggests that they formed synchronously.

#### 5.4.3 Domain 3

Domain 3 is located east of a shallow, westerly dipping thrust fault on section 9700N (Fig. 5.1) and west of domain 2. Most of this domain contains weakly altered and deformed tuffaceous rocks, and well bedded mudstone that can be readily identified, especially along the western edge of the domain. Hornblende porphyry dykes trend northerly and dip steeply west. K-Ba-feldspar megacrystic porphyry and aphanitic intermediate dykes strike easterly with vertical dip.

The  $S_1$  fabric in this domain consists of stretched sericite altered plagioclase laths and flattened quartz grains. The grains, elongated at  $284^\circ/47^\circ$ , are flattened parallel to  $122^\circ/87^\circ S$  (Table 5.1, Figs. 5.1, 5.5 and 5.6). The intensity of the penetrative fabric along section 9700N increases towards the eastern boundary as the foliation rotates from  $110^\circ/90^\circ$  to  $134^\circ/75^\circ SW$ .

$S_2$  fabric was recognized along the eastern boundary of the domain. The fabric is orientated at  $157^\circ/84^\circ W$ , which is clockwise to  $S_1$  (Table 5.1).

Extensional quartz - calcite veins, 0.5 mm to 20 mm thick in the tuffaceous rocks and post-mineralization dykes, are normal to the plane of apparent flattening in individual outcrops in domain 3. Their average orientation,  $168/87^\circ W$ , parallels the plane of flattening in domain 2, 50 m to the east (Fig. 5.8). Quartz fibres in these veins are parallel to the elongation of grains in the rock. Northerly striking, westerly dipping faults displace vertical features

upward. This displacement indicates that the faults have west side up movement. This sense of movement is in the same direction as the Sulphurets thrust fault 2 km to the west.

#### 5.4.4 Domain 4

Domain 4 is immediately north of domain 3. This domain has as an average  $S_1$  fabric orientation of  $275^\circ/56^\circ\text{N}$  and a pronounced mineral elongation at  $304^\circ/57^\circ$  (Figs. 5.5 and 5.6; Table 5.1). This fabric is dominated by the mineral elongation consisting of sericite altered elongate grains with lesser sericite laths parallel to the flattening plane. Aphanitic intermediate dykes are boudinaged where they strike parallel to the  $S_1$  fabric (Fig. 5.3). No extensional quartz veins were recognized on surface in this domain. Extension veins in the subsurface are rare in drill core. These veins were perpendicular to the flattening fabric.

$S_2$  foliation was recognized along section 10600N. The average orientation is  $247^\circ/61^\circ\text{N}$  (Fig. 5.7). This fabric cuts  $S_1$  and it is oriented at an acute angle clockwise to  $S_1$  (Table 5.1). The fabric was only recognized in the western half of the detailed map area on section 10600N (Fig. 5.1).

The contact between domains 2, 3 and 4 is an area of several foliations overprinting each other. The contact between domains 2 and 4 in the intensely deformed rock region consists of lozenges of foliated rock with foliation striking  $065^\circ/70^\circ\text{N}$  cut by a pronounced foliation striking  $180^\circ/90^\circ$ . The region between domains 3 and 4 has a strong mineral lineation that parallels the intersection of the two flattening foliation directions.

#### 5.4.5 Domain 5

Domain 5 covers the region below Kerr Peak and above the west dipping minor thrust fault. Motion on this fault was determined to be reverse from the closing direction of the acute angle between the shear and flattening foliation. Domain 5 has a weak foliation oriented



at  $140^{\circ}/76^{\circ}\text{SW}$  defined by radiating cleavage fans in folded argillite and siltstone, and an elongation lineation defined by elongate clasts in the volcanic conglomerate trending  $110^{\circ}$  (Fig. 5.5). Intersection of the radiating cleavage and bedding in argillaceous layers is at  $270^{\circ}/40^{\circ}$ . Cobbles in the volcanic conglomerate unit are elongate so that their long axis is oriented at  $20^{\circ}$  to the intersection of cleavage with bedding in the argillite and sandstone.

Calcite extension veins in this domain are 0.5 cm wide and 3.0 cm long and they form a conjugate set. Foliation bisects the obtuse angle between the veins. Rare galena blebs occur in these veins where they cut argillite and siltstone beds.

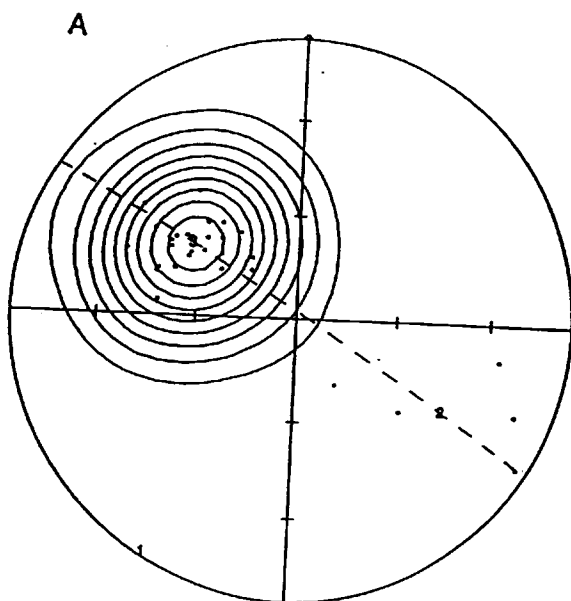
## 5.5 Discussion of Structural Features Related to $S_1$ and $S_2$

### 5.5.1 Orientation of $S_1$ and $S_2$ fabric in domains 1 to 5

Figure 5.1 shows the distribution of  $S_1$  and  $S_2$  foliations and mineral elongation lineation across all domains in the Kerr deposit relative to the outline of the central core alteration. The footwall of the Kerr deposit parallels the boundary between the domains 1 and 2 (Fig. 5.1) except in the northern portion immediately south of section 10600N. In this area, the footwall of the Kerr deposit is in domain 4. The line separating intensely deformed rock with less deformed marks the transition between pervasive, texturally destructive sericite alteration from non-texturally destructive sericite alteration.

A plot of the data weighted by area on a stereonet for domains 2 to 4 shows that the  $S_1$  foliation plots on a great circle and that the mineral elongation lineation is the pole to this plane (Fig. 5.9). This relationship is confirmed by the field observations that the mineral lineation is parallel to the plane of the flattening foliation.  $S_2$  foliation is oriented consistently clockwise from  $S_1$  and the trace of it in domain 2 follows the boundary between domains 1 and 2 (Fig. 5.1). The  $S_2$  foliation is not synchronous with the development of  $S_1$ . The orientation of  $S_2$  and its relationship to the boundary between domains 1 and 2 suggest that  $S_2$

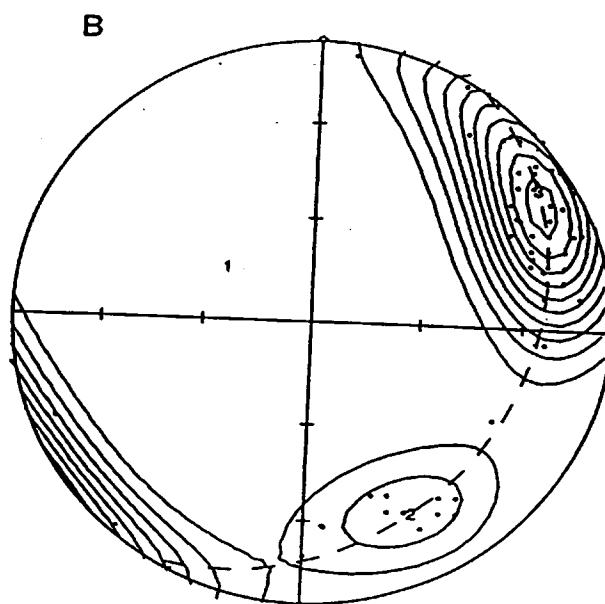
## WEIGHTED LINEATION FOR ALL DOMAINS



$N = 35$   
 $k = 9.78$   
 $(\text{Peak} - E)/\text{Sigma} = 17.5$   
 Peak position :  $305.5^\circ / 50.5^\circ$

$E = 3.58$   
 $\text{Sigma} = 1.19$

## WEIGHTED FOLIATION FOR ALL DOMAINS



$N = 66$   
 $k = 16.67$   
 $(\text{Peak} - E)/\text{Sigma} = 18.8$   
 Peak position :  $63.4^\circ / 14.1^\circ$

$E = 3.96$   
 $\text{Sigma} = 1.32$

Figure 5.9 (A to B). Equal area stereonets of poles to weighted lineation and foliation  $S_1$  for all domains. See caption of Figure 5.4 for legend.

represents slip planes in the deposit that accommodated apparent right-lateral slip during deformation of the deposit.

### 5.5.2 Deformation of porphyry copper veins by S<sub>1</sub>

All mineralized, porphyry copper veins (Chapter 6.0) in the Kerr deposit exhibit weak to strong deformation depending upon their orientation, location and host rock alteration mineralogy. The composition of the shear and mineralized quartz veins was found to be similar to the earlier porphyry copper veins; therefore composition differences between veins in the deposit is not a reliable indicator of age. Mineralized quartz veins can be distinguished from later extensional and shear quartz veins by their

- (1) orientation at an acute angle to the foliation,
- (2) transparent grey colour compared to milky white of extension quartz veins, and
- (3) coxcomb quartz compared to quartz fibres.

Weakly deformed mineralized quartz veins (banded and bull quartz; see section 6.0) in domain 3 have a variable attitude to the flattening plane of the constrictional fabric (Plate 5.2, Table 5.1). In sericitic altered tuffaceous rocks they are oriented at an anti-clockwise acute angle to S<sub>1</sub> when looking northward onto a horizontal plane. These veins are boudinaged with calcite, chlorite, pyrite and trace chalcopryrite filling fractures in them.

Mineralized quartz veins in domain 2 are nearly parallel to the flattening foliation (Fig. 5.11, Table 5.1) or are at a small clockwise angle to the flattening foliation when viewed looking north. These veins are strongly boudinaged when they parallel the flattening plane. Veins perpendicular to the flattening plane are tightly folded with carbonate infilling the voids between separated quartz segments (Plate 5.3). If the vein occurs at an acute angle to the

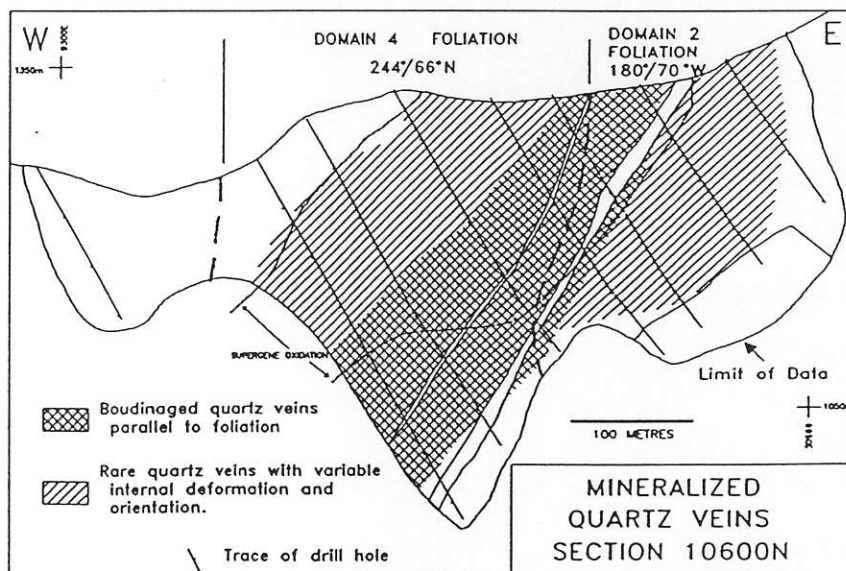
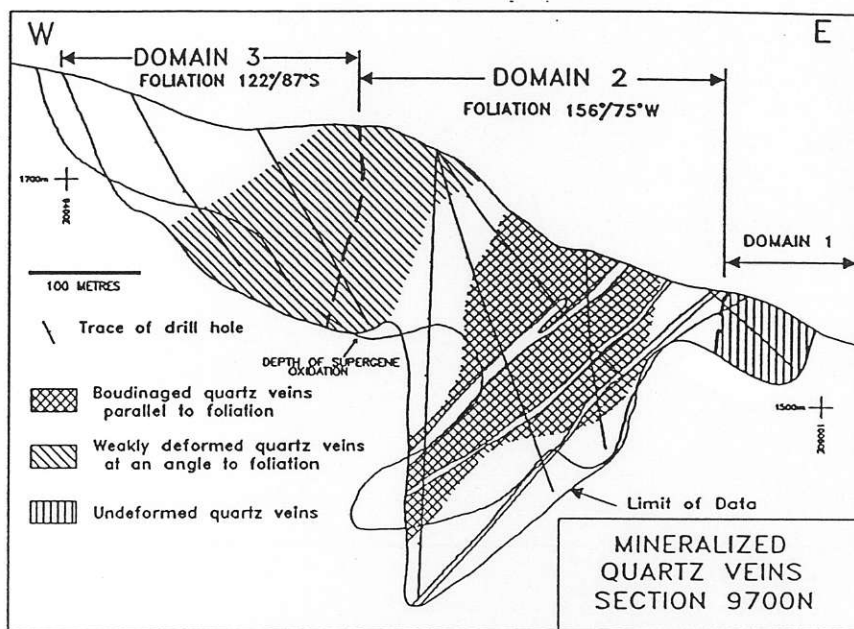
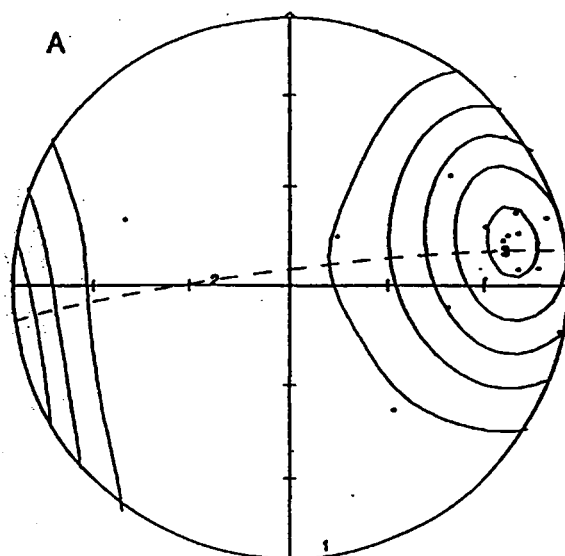


Figure 5.10. Two cross sections, 9700N and 10600N showing the distribution of deformed mineralized quartz veins in the Kerr deposit, northwestern British Columbia.

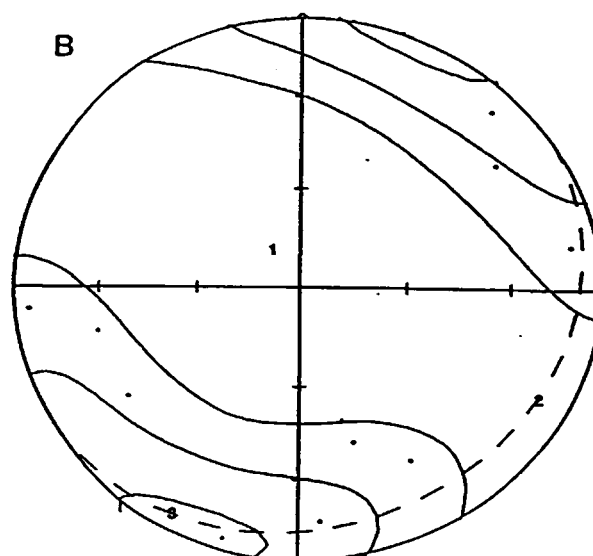
MINERALIZED QUARTZ VEINS ON DOMAIN 2  
SECTION 9700N



$N = 18$   
 $k = 6.00$   
 $(\text{Peak} - E)/\text{Sigma} = 8.6$   
 Peak position :  $78.7^\circ / 16.1^\circ$

$E = 3.00$   
 $\text{Sigma} = 1.00$

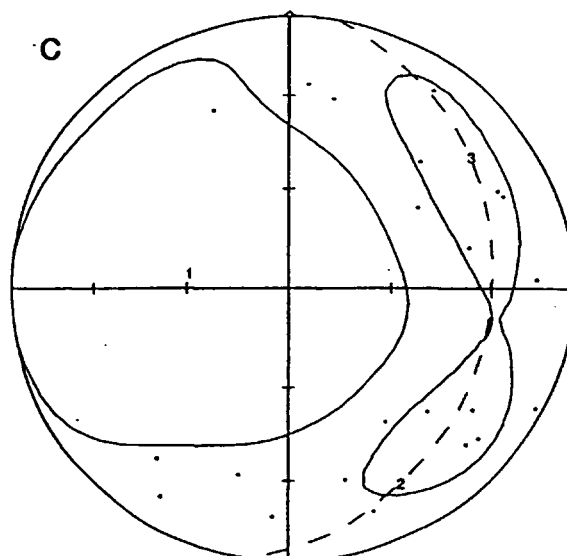
MINERALIZED QUARTZ VEINS ON DOMAIN 3  
SECTION 9700N



$N = 15$   
 $k = 5.33$   
 $(\text{Peak} - E)/\text{Sigma} = 4.5$   
 Peak position :  $202.4^\circ / 2.5^\circ$

$E = 2.81$   
 $\text{Sigma} = 0.94$

MINERALIZED QUARTZ VEINS ON DOMAIN 4  
SECTION 10600N



$N = 24$   
 $k = 7.33$   
 $(\text{Peak} - E)/\text{Sigma} = 2.8$   
 Peak position :  $135.0^\circ / 22.5^\circ$

$E = 3.27$   
 $\text{Sigma} = 1.09$

Figure 5.11 (A to C). Equal area stereonets of poles to mineralized porphyry copper - gold veins along sections 9700N and 10600N in domains 2 to 3 on the Kerr deposit, northwestern British Columbia. See caption of Figure 5.4 for legend.



Plate 5.3. Boundinaged quartz veins with rotated segments. Sample is from KS-64 177.0m on Figure 4.2.



Plate 5.4. Photograph of a deformed sulphide vein with quartz filled pressure shadows in domain 2. Sample is from KS-94 34.9 m on Figure 4.2.

flattening plane, it is either split into equant squares or rectangles. Each rectangle is bounded by shears that appear to displace the quartz vein segments so that the trace of the vein parallels the flattening plane. The original banded quartz growth textures are preserved in these vein segments. Fractures are infilled with either calcite, siderite or anhydrite (see Chapter 6.0).

Sulphide veins are more randomly oriented with respect to the flattening plane than are the mineralized quartz veins (Fig. 5.12). Sulphide veins have been deformed such that they now consist of disaggregated pyrite grains with chalcopyrite and quartz fibres that fill pressure shadows. Plate 5.4 shows a pyrite stockwork with quartz fibres that parallel the fabric in the rock. Most of the veins have not rotated into the foliation, but have broken into discrete grains separated by quartz fibres in pressure shadows.

Sulphate and carbonate veins related to the porphyry mineralization are rarely boudinaged even in highly deformed rock. They are parallel with weak to pronounced flattening planes in the host rock. The mineral grains in the veins do not exhibit any deformation so they may have recrystallized immediately after or during deformation.

## 5.6 Timing of Major Deformation

Whole rock K-Ar dating of deformed, sericite - quartz - pyrite altered syn-mineralization plagioclase hornblende monzonite dyke from domain 4 along section 10600N gave an age of 124  $\pm$  4 Ma (Table 4.4). The age represents either the closure temperature of phengite (350°C) or the end of ductile deformation in the rock (Dunlap et al., 1991). The presence of undeformed phengite flakes in the rock and patches of radiating grains suggest that the date represents a minimum age representing the end of recrystallization.

This age is consistent with the timing of the regional deformation determined by analysis of major folds and thrust faults in the Bowser Basin (Evenchick, 1991).

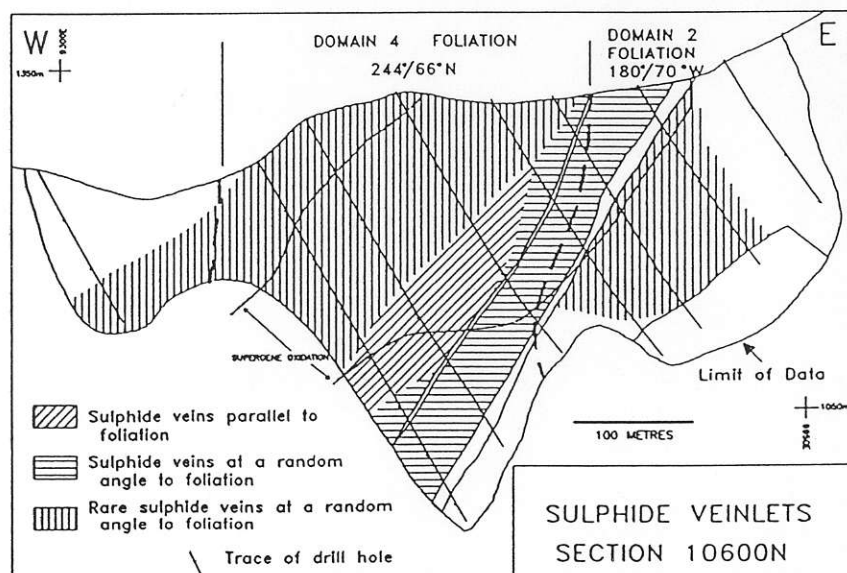
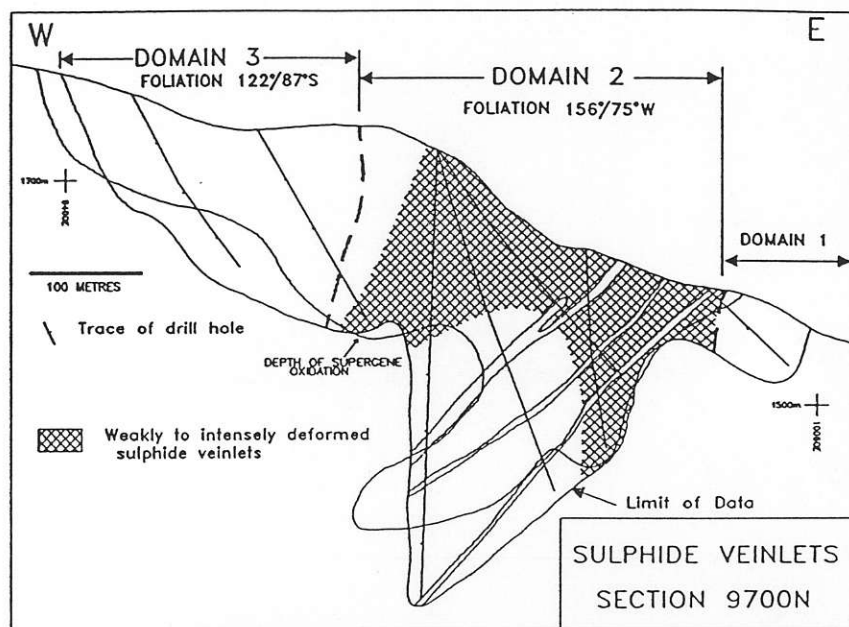


Figure 5.12. Cross sections 9700N and 10600N showing the distribution and orientation with respect to foliation  $S_1$  of deformed sulphide veins.



### 5.7 Westerly Dipping Left Lateral Faults

The Kerr deposit is cut by steep, west dipping faults that host undeformed Eocene kersantite dykes. The most continuous fault passes through the centre of the deposit (Fig. 5.1). Foliation along this major fault is contorted, and cut by numerous minor fault planes (Plate 5.5). This major fault has an apparent left lateral sense of displacement. Albite megacrystic porphyry and aphanitic intermediate dykes are displaced to the left across the major faults (Fig. 5.1). Intrusion of relatively undeformed Eocene biotite kersantite along these major faults indicate that they predate the dyke.

There are also numerous vertical faults in all the domains. The sense of displacement and timing of their formation is unknown; most are probably post-mineralization in age.

### 5.8 Discussion on Major Deformation of the Kerr Deposit

The orientation of the coincident northwest plunging mineral lineation and flattening foliation in the region of intense deformation on the Kerr deposit suggests that the deposit was extended to the southeast by southwesterly directed shortening (Fig. 5.13). The direction of extension in the Kerr deposit is parallel to the direction of transport of the southeasterly vergent Sulphurets thrust fault whose trace is projected to overlie the Kerr deposit (Lewis, personal comm., 1993).

The combination of shortening from the southwest coupled with extension to the southeast deformed the southwestern portion of the Kerr deposit such that intensely deformed rock lies beside the weakly deformed footwall. The northern portion of the deposit deformed parallel the strike of the albite megacrystic plagioclase hornblende porphyry dyke. Most of the deformation was accommodated by the sericite - quartz - pyrite alteration located above the dyke; therefore the dyke was only weakly deformed. Rock beneath the dyke is only weakly

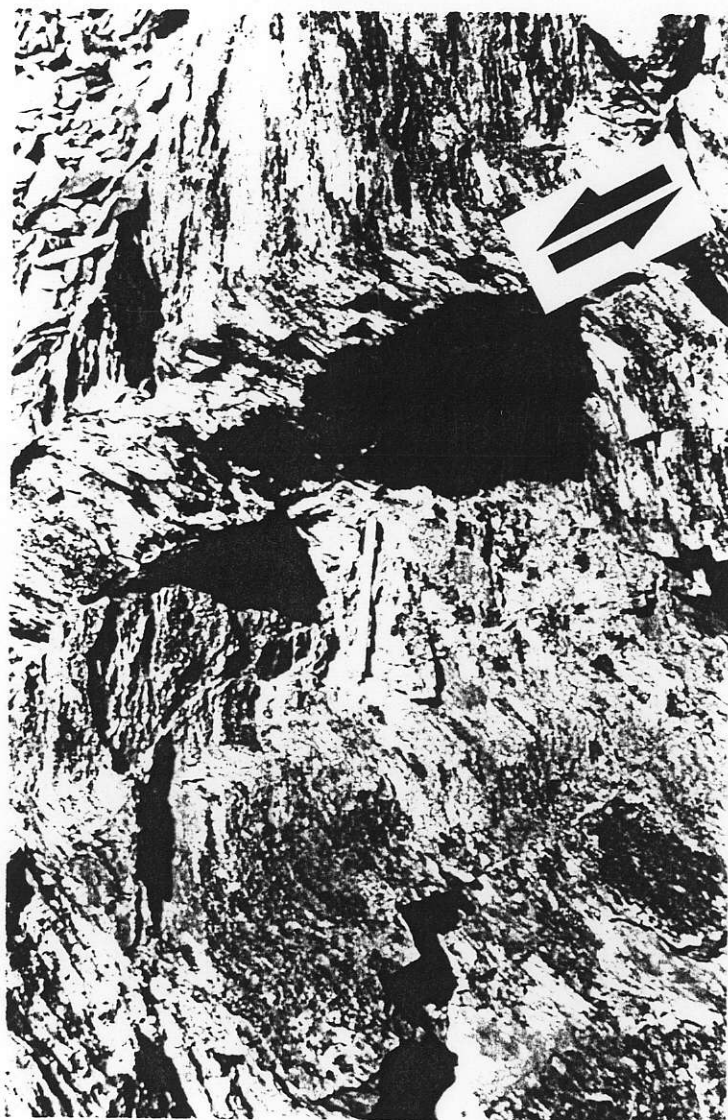


Plate 5.5. West directed view of apparent left lateral faults deforming well developed  $S_1$  and  $S_2$  fabric. Photograph taken at 9635N, 9820E on Figure 5.1.

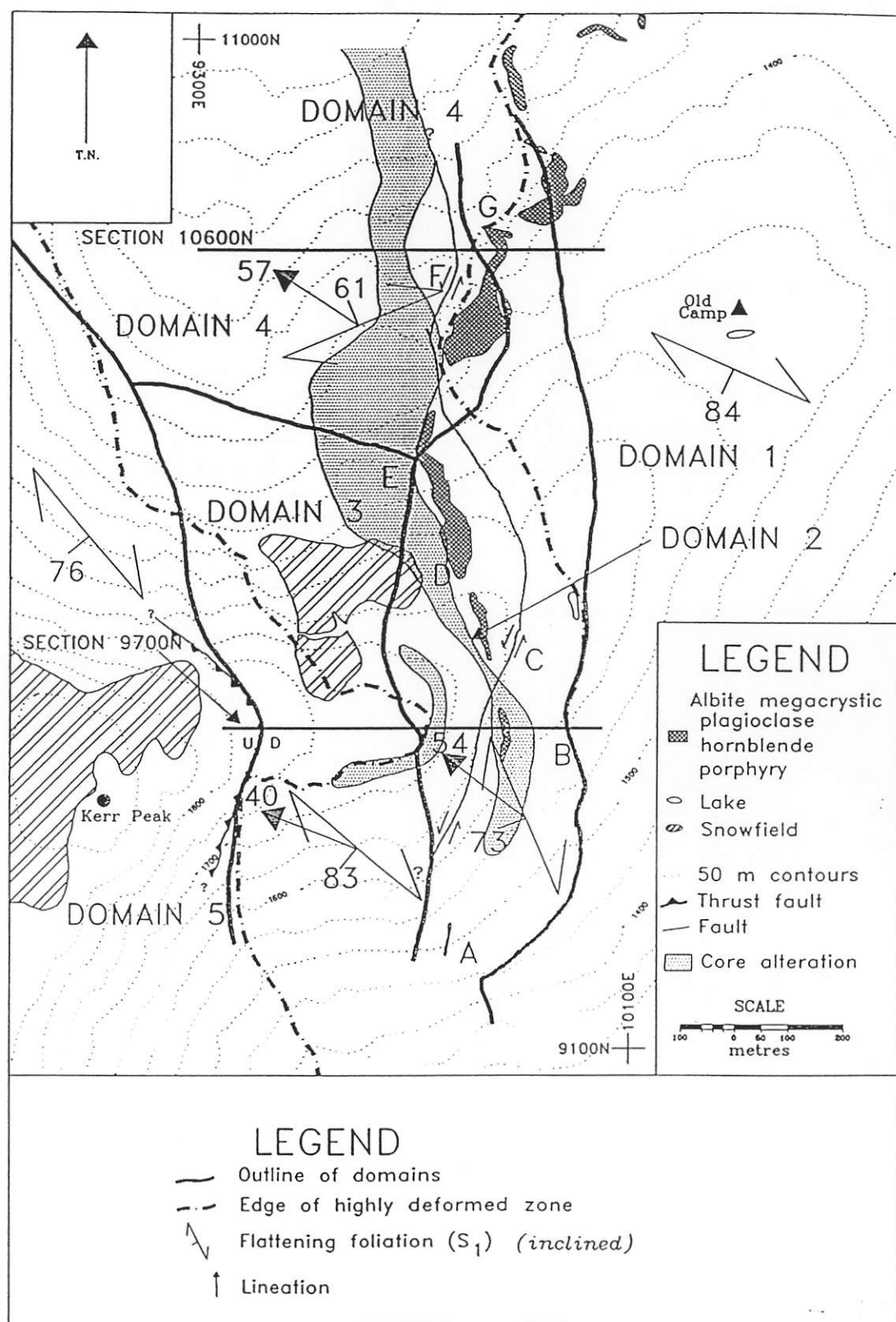


Figure 5.13. Average foliation  $S_1$  orientation for each domain on the Kerr deposit, northwestern British Columbia. Lettre symbols are located where the contact between highly and weakly deformed rock was calculated from drill hole intersections.

deformed because it was not extensively altered during the development of the porphyry deposit.

Continued deformation of the southwestern portion of the Kerr deposit resulted in a second foliation parallel to the contact between highly deformed sericite - quartz - pyrite altered rocks and weakly deformed rock. This motion may have caused the right-lateral shear along the footwall that deformed aphanitic intermediate dyke into Z shapes.

Deformation of the mineralized quartz veins in domains 2 and 3 has oriented them parallel to the flattening fabric in the rock. The flattening deformation compressed the altered rock between individual veins, and the component of shear caused veins at an angle to the flattening foliation to separate into segments. Each segment of the vein rotates such that its long axis parallels the foliation plane. Thus, rotation of these blocks is due to rotational stresses developed during strain (Ramsey and Huber, 1983).

The abundance of weakly deformed mineralized quartz veins parallel to the foliation in the chlorite centre of the deposit suggests that the orientation of the penetrative fabric was caused by the original trend of the deposit. This conclusion is supported by the strike and dip of the foliation in domain 2, which parallels the trend of the sericite - quartz - pyrite altered rocks.

## 6.0 HYPOGENE ALTERATION AND MINERALIZATION IN THE KERR DEPOSIT

### 6.1 Introduction

Three alteration zones, core, halo and periphery, have been identified in the deformed and metamorphosed Kerr deposit. They were recognized after the analysis of averaged, visually and petrographically estimated percentages of major alteration minerals on cross - sections 9700N and 10600N (Table 6.1). Table 6.2 summarizes the major mineral and vein characteristics of each zone. The three alteration zones are:

- (1) core: texturally destructive, pervasive chlorite, sericite, anhydrite and magnetite alteration,
- (2) halo: texturally destructive, sericite and quartz without anhydrite and chlorite, and
- (3) periphery: chlorite and sericite replacement of primary minerals in volcanic and sedimentary rocks in the hanging wall and footwall of the deposit. Carbonaceous material is also characteristic of the peripheral alteration in the footwall and the central conglomerate unit in the centre of section 9700N.

Seven veins related to the porphyry copper deposit have been identified in the Kerr deposit. They are in paragenetic order from oldest to youngest :

- Type 1: bull quartz, minor pyrite,
- Type 2: magnetite and specular hematite,
- Type 3: banded quartz, minor pyrite,
- Type 4: sulphide (pyrite - chalcopyrite - quartz),
- Type 5: anhydrite - quartz - siderite - pyrite - chalcopyrite - molybdenite,
- Type 6: pink anhydrite - pyrite - chalcopyrite - molybdenite, and
- Type 7: calcite - quartz - sphalerite - tetrahedrite - galena - sphalerite.

Table 6.1. Percentages of alteration minerals in the core, halo and periphery of the Kerr deposit, northwestern British Columbia. The percentages are estimated from drill core along two cross sections 9700N and 10600N.

MINERALS AND ANALYSES Number of intervals in each alteration zone	UNITS	CORE 32			HALO 23			PERIPHERY 18		
		Average	Range Min Max		Average	Range Min Max		Average	Range Min Max	
Copper	(%)	0.59	0.057	1.4	0.18	0.015	0.49	0.086	0.011	0.49
Gold	(ppm)	0.33	0.071	0.74	0.19	0.09	0.74	0.20	0.021	0.88
Copper / gold		18900	4700	48000	10300	841	30000	6800	330	25000
Silicification	(%)	3.4	0	24.6	6.0	0	36.6	2.6	0	17.8
Quartz veins	(%)	7.4	0	38.4	2.7	0.3	10.7	1.1	0	6.4
Pervasive anhydrite	(%)	2.9	0	20.9						
Anhydrite veins	(%)	0.7	0	2.4						
Total anhydrite	(%)	3.3	0	20.9						
Pervasive gypsum	(%)	0.6	0	2.7						
Gypsum veins	(%)	1.4	0	2.5						
Total gypsum	(%)	2.0	0	5.1						
Total gypsum and anhydrite	(%)	5.3	0	22.6						
Grey and blue sericite	(%)	22.2	6.4	40.0	23.0	0	44.4	24.8	0	51.6
Grey sericite envelopes	(%)	0.2	0	1.8	0.8	0	10.0	0.017	0	0.22
Total grey and blue sericite	(%)	22.4	6.4	40.0	23.8	8.0	44.5	24.8	0.014	51.6
Pervasive yellow sericite	(%)	5.1	0	27.1	8.5	0	30.0	0.52	0	24.7
Yellow sericite envelopes	(%)	0.026	0	0.71	0.0054	0	0.1		0	0.13
Total yellow sericite	(%)	5.1	0	27.1	8.6	0	30.0	0.52	0	24.8
Intergrown chlorite and sericite	(%)	6.1	0	30.0	1.7	0	18.7	0.17	0	4.1
Chlorite and sericite envelopes	(%)	0.011	0	0.36	0.013	0	0.30		0	0
Total chlorite and sericite	(%)	6.1	0	30.0	1.7	0	19.0	0.17	0	4.1
Total sericite and minor chlorite	(%)	29.1	17.9	47.3	31.4	20.1	46.0	23.9	0.014	52.9
Pervasive clay alteration	(%)	4.5	0	20	2.3	0	12.8	6.6	0	15.8
Pervasive chlorite	(%)	2.8	0	15.8	0.3	0	2.8	2.4	0	10.5
Chlorite envelopes and selvages	(%)	0.40	0	1.8	0.085	0	0.54	0.23	0	1.1
Total chlorite	(%)	3.2	0	17.6	0.38	0	3.1	2.7	0	10.9

Table 6.1 cont'd

MINERALS Number of intervals in each alteration zone	UNITS	CORE 32			HALO 23			PERIPHERY 18		
		Average	Range		Average	Range		Average	Range	
			Min	Max		Min	Max		Min	Max
Pervasive calcite	(%)	0.035	0	0.47	0.012	0	0.29	0.48	0	3.3
Vein calcite	(%)	0.26	0	1.3	0.63	0	5.0	0.68	0	1.4
Total calcite	(%)	0.30	0	1.3	0.65	0	5.0	1.2	0	4.7
Pervasive siderite	(%)	0.006	0	0.14		0	0	0.0032	0	0.06
Vein siderite	(%)	0.092	0	2.0	0.025	0	0.22	0.016	0	0.15
Total siderite	(%)	0.098	0	2.0	0.025	0	0.22	0.019	0	0.20
Pervasive magnetite	(%)	0.011	0	0.36				0.015	0	0.27
Vein magnetite	(%)	0.01	0	0.16				0.000008	0	0.00015
Total magnetite	(%)	0.021	0	0.50				0.015	0	0.27
Pervasive hematite	(%)	0.09	0	1.4		0	0	0.016	0	0.28
Vein hematite	(%)	0.38	0	3.7	0.006	0	0.14	0.000005	0	0.00010
Total hematite	(%)	0.47	0	5.1	0.006	0	0.14	0.016	0	0.28
Total hematite and magnetite	(%)	0.50	0	5.1	0.800	0	3.50	0.03	0	0.28
Pervasive carbonaceous material	(%)				0.12	0	2.8	0.99	0	12.1
Carbonaceous veins	(%)				0.033	0	0.76	0.26	0	1.1
Total carbonaceous material	(%)				0.15	0	3.5	1.3	0	12.3
Disseminated pyrite	(%)	6.0	0.87	12.3	6.6	3.1	10.7	5.9	1.3	11.7
Pyrite in veins	(%)	2.3	0	8.7	1.8	0.13	7.1	0.46	0	7.1
Total pyrite	(%)	8.4	0.87	20.9	8.4	3.8	13.3	6.4	1.5	13.1
Disseminated chalcopyrite	(%)	0.28	0	1.0	0.065	0	0.35	0.024	0	0.31
Chalcopyrite in veins	(%)	0.64	0	2.5	0.17	0	1.2	0.017	0	1.2
Total chalcopyrite	(%)	0.92	0	3.5	0.23	0	1.5	0.041	0	1.5
Total chalcopyrite/total pyrite		0.10	0	0.23	0.024	0	0.12	0.0056	0	0.12
Disseminated tetrahedrite-tennantite	(%)	0.0054	0	0.14	0.021	0	0.20	0.0068	0	0.12
Tetrahedrite-tennantite in veins	(%)	0.013	0	0.18	0.034	0	0.18	0.00049	0	0.025
Total tetrahedrite-tennantite	(%)	0.019	0	0.20	0.055	0	0.38	0.0073	0	0.13

Table 6.1 cont'd

MINERALS Number of intervals in each alteration zone	UNITS	CORE 32			HALO 23			PERIPHERY 18		
		Average	Range Min	Max	Average	Range Min	Max	Average	Range Min	Max
Bornite in veins	(%)	0.019	0	0.36	0.000019	0	0.00030	0.000006	0	0.00013
Molybdenite in veins	(%)	0.0034	0	0.030	0.0025	0	0.028	0.00081	0	0.014
Sphalerite in veins	(%)	0.0068	0	0.17	0.004	0	0.091	0.0008	0	0.014
Galena in veins	(%)	0.0096	0	0.030	0.000022	0	0.00042	0.000034	0	0.00035
Gypsum filled fractures	(%)	0.37	0	3.5	0.018	0	0.40			
MINERALIZED VEINS										
Type 1 and 3 Qz - Py	(%)	7.4	0	35.8	1.6	0	10.6	0.64	0	7.4
Type 2 Mg / Hc - Cp	(%)	0.4	0	3.7						
Type 4 Py - Cp - Qz	(%)	1.2	0	5.6	1.1	0	5.6	0.15	0	5.6
Type 5 An - Sd - Qz - Py - Cp - Tt	(%)	0.23	0	1.9	0.008	0	0.18			
Type 6 An - Cp - Mo	(%)	0.45	0	4.3	0.00054	0	0.013			
Type 7 Cb - Qz - Py - Tt - Sl - Gn	(%)	0.084	0	2.5	0.016	0	0.32	0.0022	0	0.038
DEFORMATION VEINS										
Carbonate	(%)	0.25	0	4.2	0.58	0	4.2	0.072	0	0.50
Quartz-calcite	(%)	0.16	0	1.2	0.28	0	1.2	0.92	0	3.1



Table 6.2. Summary of mineralogical and vein characteristics of each alteration zone, Kerr deposit, northwestern British Columbia.

METAL	UNITS	CORE (MS-GS-CL-SI- AN+GY-MG+HE)	HALO (MS-YS-SI-PY)	PERIPHERY (MS-CY-PY-SI- CL-GR-CA)
Copper	(%)	0.59	0.18	0.086
Gold	(ppb)	330	190	200
Copper/Gold		18900	10300	6800
<b>ALTERATION MINERAL</b>				
Sericite (phengite) (MS)	(%)	22	23	25
Yellow sericite (YS)	(%)	5.1	8.5	0.5
Intergrown chlorite and sericite (GS)	(%)	6.1	1.7	0.2
Chlorite (CL)	(%)	2.8	0.3	2.4
Silification (SI)	(%)	3.4	6	2.6
Disseminated quartz (petrography)	(%)	30	30	(rock type) (dependent)
Clay minerals (CY)	(%)	4.5	2.3	6.6
Carbonaceous material (GR)	(%)	0	0.15	1.3
Calcite (CA)	(%)	0.04	0.012	0.5
Total magnetite and hematite (MG+HE)	(%)	0.5	0.01	0
Total anhydrite and gypsum (AN+GY)	(%)	5.5	0	0
Total pyrite (PYT)	(%)	8.4	8.4	0.4
Total chalcopryrite (CPT)	(%)	0.9	0.23	0.041
Total tetrahedrite-tennantite (TTT)	(%)	0.02	0.06	0.007
<b>VEINS</b>				
Type 1 (Bull quartz) + Type 3 (Banded quartz)	(%)	7.4	1.6	0.6
Type 2 (Magnetite and specular hematite)	(%)	0.4	0.01	
Type 4 (PY - CP - QZ)	(%)	1.2	1.1	0.15
Type 5 (AN - QZ - SD - PY - CP - MO)	(%)	0.23	0.08	
Type 6 (AN - CP - MO)	(%)	0.45	0.00054	
Type 7 (QZ - CA - SI - TT - GN)	(%)	0.084	0.066	0.022

Shear veins (Chapter 5.0) are related to deformation and cut these veins. The texturally destructive nature of the core and halo alteration obliterates primary lithologies; however, projection of the rock units from outside the highly deformed region into the core of the deposit indicates that the pervasive alteration probably replaced massive tuff, mudstone with lenses of conglomerate, and possibly, minor plagioclase augite diorite dykes (Fig. 4.2). Syn- and post-mineralization dykes can be identified in these two alteration zones. The periphery alteration enhances the texture of the rock and each rock unit has a different alteration mineral assemblage.

All three alteration assemblages can be mapped at surface and traced at depth in drill holes (Fig. 6.1). The core alteration is pancake shaped, and it strikes north and dips 60° west. It has a west facing bulge that is coincident with the marked curvature in the albite megacrystic plagioclase hornblende porphyry dyke (Fig. 6.1). Below Kerr Peak on the western edge of section 9700N (Fig. 6.1), the core alteration crops out as a northwesterly dipping wedge. The halo alteration assemblage is absent from this area. Otherwise, the halo and periphery alteration generally parallel the trend of the core. A region of sericitic periphery alteration occurs in the centre of the section 9700N. This region is bounded by faults, which indicate that it has been faulted into its present position.

Mineral assemblages in the region of intense deformation marked on Figure 4.1 represent the recrystallized and deformed products of the original assemblages in altered tuff, in mudstone with lenses of conglomerate and in monzonite dykes. This region of intense deformation covers the core and halo alteration zones, except for a portion of the core along the western edge of section 9700N. Periphery alteration is generally external to the region of intense deformation. Comparison of relatively undeformed mineralization and alteration, and highly deformed equivalents, indicate that there has been minor changes in bulk mineralogy during deformation (see below). Minerals that grew before, during or after deformation show a variety of habits. Primary igneous mineral grains, such as apatite, are boudinaged in

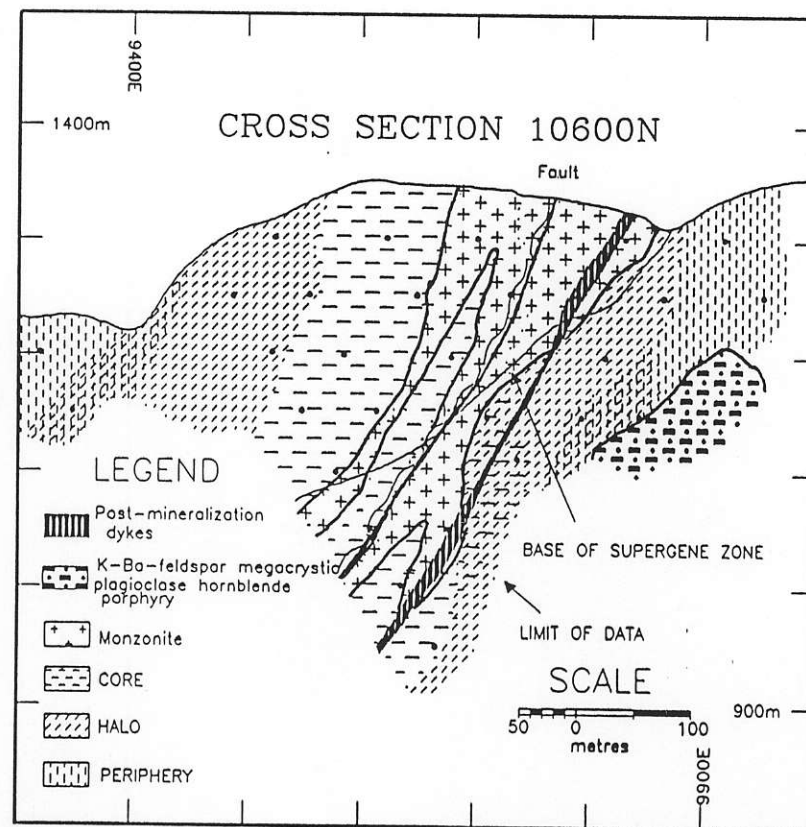
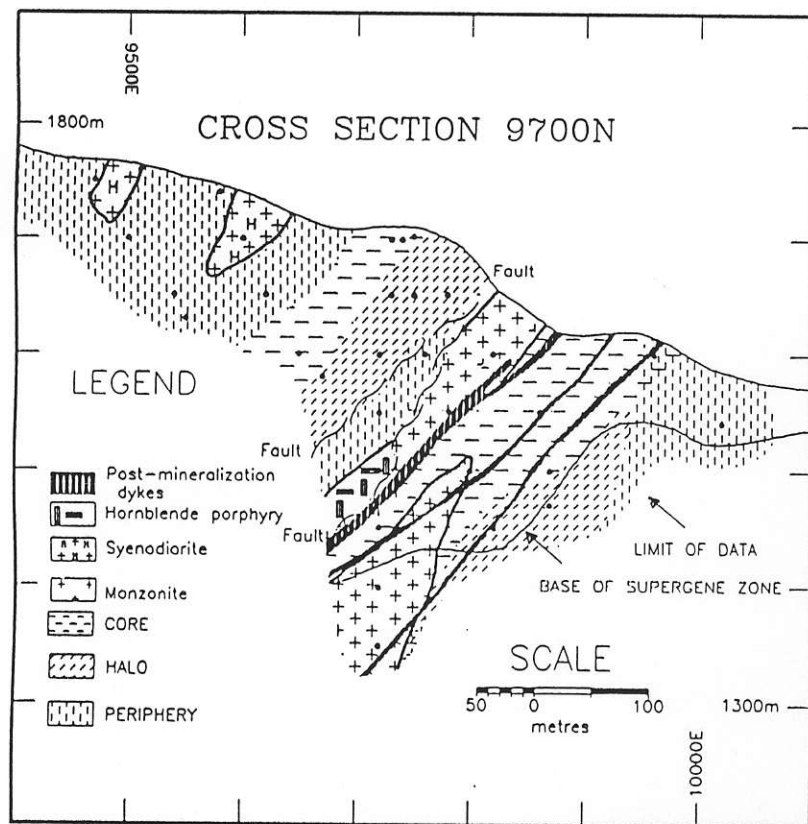


Figure 6.1. Distribution of core, halo and periphery alterations zones in the Kerr deposit, northwestern British Columbia. Dots mark the centre of the 20 metre averaged intervals. Outline of syn-mineralization and post-mineralization dykes have been added.

intensely deformed rock. Alteration minerals that survived deformation and recrystallization are either boudinaged or form porphyroblasts surrounded by grains parallel to the foliation. Minerals, especially sericite, which crystallized during deformation, parallel the penetrative fabric in the rock. Minerals that recrystallized after deformation grew across the fabric in the rock. Recrystallized chlorite and sericite occur as radiating clusters replacing parallel flakes of chlorite and strained hornblende crystals.

The distribution and mineralogy of veins in the deposit have survived the intense deformation. Cross-cutting relationships among veins are preserved because recrystallization of the vein material does not change the temporal relationships among them; whereas, recrystallization of the pervasive alteration can obliterate the original mineral assemblage.

## 6.2 Methodology for Selection of Alteration Zones

The spatial distribution and composition of the three alteration zones was analyzed by first plotting the average concentration of visually estimated minerals on cross - sections using bubble plots. Bubble plots consist of circles whose diameter is proportional to the concentration of the mineral. Each circle represents the concentration averaged over 20 m of drill core centred on 50 m bench intervals (Appendix A). Three alteration zones were outlined on the two cross - sections by comparing and contrasting the distribution of distinct populations in averaged copper grade, intergrown chlorite and sericite, total magnetite and hematite, anhydrite, carbonaceous material and tetrahedrite-tennantite. The computer program PROBPLOT (Stanley, 1988) was used to define the distinct populations in each mineral (Appendix A). The seven minerals and Cu assays were known from hand samples and petrographic descriptions to be concentrated either in a specific alteration zone in the Kerr deposit, or with a pervasive habit, but locally concentrated in one of the zones.

Accuracy of the visual estimate of percentage of alteration minerals was verified with petrography of 16 representative samples from the 20 metre intervals. Comparison between

the amounts of alteration minerals estimated visually and petrographically indicated that errors in over or under estimation were consistent throughout the data. All visual estimates of major silicate minerals were within an order of magnitude except for clay minerals, which could not be estimated petrographically or easily distinguished from sericite. Visual estimates of pyrite were consistent with petrography, and chalcopryite was consistently under estimated.

Petrographic estimates of tetrahedrite-tennantite, galena, sphalerite and molybdenite were higher than visual estimates because these minerals were disseminated evenly throughout the drill core, but were too fine grained to be visible. Several minerals: barite, rutile and clintonite were not identified visually because of their small grain size and physical properties that made them indistinguishable from more commonly occurring minerals such as calcite and sericite.

### 6.3 Alteration Zone Characteristics

The core alteration zone is dominated by: chlorite, sericite, quartz, pyrite, chalcopryite with bull and banded quartz veins, magnetite and specular hematite veins, and sulphide veins (Table 6.2). Anhydrite is disseminated and occurs in anhydrite - quartz - siderite veins and pink anhydrite - chalcopryite - molybdenite veins in the core alteration zone except for the upper lense on section 9700N. The pervasive portion of this mineral assemblage forms alternating, one to five metre thick bands of: (i) texturally destructive chlorite and sericite with minor pyrite, chalcopryite and variable amounts of disseminated magnetite, and (ii) grey sericite and quartz with minor pyrite and chalcopryite. Anhydrite alters by hydration to gypsum, resulting in a rock cut by late gypsum filled fractures. Dissolution of the gypsum by groundwater results in typically flaky, pieces of altered rock with mineralized veins. The sequence of alteration parallels the margins of the highly altered monzonite dykes. Percentages of minerals in this zone are given in Table 6.1.

Grey sericite and quartz bands consist of interconnecting 0.5 mm to 30 mm siliceous kidney shaped masses, that consist of intergrown sericite and quartz, which become progressively more oval shaped with increasing deformation. This alteration varies from dark grey to white. Dark grey patches contain abundant finely disseminated pyrite, which may be responsible for their dark colour.

Syn-mineralization monzonite dykes are parallel to the pervasive core alteration and to magnetite veins. These dykes host type 3 to 7 veins along their margins, especially along their lower contacts. The dykes are altered to sericite - quartz - pyrite. The sericite - quartz - pyrite alteration consists of blue sericite replacing feldspar grains, and grey sericite with trace chlorite replacing the ferromagnesian minerals and matrix. The outline of the altered feldspar grains are enhanced in comparison to feldspars in propylitically altered monzonite. Apatite grains appear to be unaltered.

The halo alteration zone is distinguished from the core and periphery by the absence of anhydrite and chlorite (Table 6.2). The zone has pervasive yellow sericite with rutile, sericite, quartz and pyrite. The concentration of type 4 veins in the halo is the same as in the core, but it has fewer type 1 and 3 veins and no type 2, 6 and 7 veins (Table 6.2). Overlap of the core and halo on Figure 6.1 is due to averaging of observations over 20 m intervals, and to gradual changes in the alteration assemblages. Concentrated along the outside edges of this alteration are rare patches of bright apple green fuchsite (Cr-Ti-muscovite).

Altered monzonite in the halo zone of section 10600N has blue sericite altered plagioclase laths, which retain outlines of oscillatory zoning, and fresh orthoclase grains. Hornblende is altered to chlorite, sericite and rutile.

Periphery alteration surrounds the texturally destructive yellow sericite halo and chlorite core (Fig. 6.1). Three regions of this alteration have been identified on section 9700N and two occur on section 10600N (Fig. 6.1). These regions are located in the hanging wall

and footwall of the deposit, and in a structurally bound region in the centre of section 9700N. This alteration is characterized by enhanced primary rock textures and trace carbonaceous material in calcite veins near argillite or conglomerate beds. Primary rock textures can be identified readily where they only have a weak penetrative fabric. The periphery alteration zone has roughly the same concentration of chlorite and sericite as the core, but it does not have abundant chalcopyrite.

Propylitically altered monzonite in the undeformed footwall consists of fresh orthoclase and sphene grains with epidote, calcite and sericite replacing plagioclase, and chlorite and rutile replacing hornblende. The alteration can vary from propylitic to phyllic within 10 centimetres. Banded quartz veins without alteration envelopes cut the monzonite in the footwall of section 9700N.

Well bedded mudstones in the hanging wall of section 10600N are completely altered to sericite, clay minerals and quartz with rare cross-cutting calcite veins. The same mudstone unit in the footwall of 9700N is composed of small grains of quartz and plagioclase in a very fine grained K-feldspar matrix. In both altered rocks, delicate sedimentary laminations are preserved.

Alteration minerals in pebble conglomerates in the footwall of section 10600N vary depending upon the composition of the clasts. Bright apple green fuchsite with pale grey sericite occasionally replace whole clasts in the conglomerate. Carbonaceous veins with minor calcite occur in carbonaceous argillites, overlying conglomerates and tuffaceous units. This alteration also occurs in the centre of section 9700N where the carbonaceous veins form a stockwork in sericite altered rock, which originally may have been a conglomerate.

The undeformed footwall rocks of section 9700N preserve the contact between original K-feldspar flooding and propylitic alteration. K-feldspar flooding replaces the matrix and rims clay altered plagioclase grains. Micron sized grains of chalcopyrite occur in the K-feldspar matrix. Ragged patches of pyrrhotite, sphalerite with intergrown chalcopyrite ("chalcopyrite's disease") and overgrowths of euhedral pyrite occur in the tuff.

### 6.3.1 Summary of copper to gold ratios

Each of the three alteration zones has a distinct copper and copper to gold ratio (Tables 6.1 and 6.2). The pervasive chlorite core has the highest copper content (0.59%) and a ratio of copper to gold of 18900. The halo has intermediate values and the periphery the lowest (Table 6.1). Thus, gold is weakly enriched in the core alteration zone. The variation in the copper reflects the changes in the total chalcopyrite to pyrite ratio in the three alteration zones because total amount of pyrite is approximately equal in all alteration zones.

### 6.4 Description of Alteration Minerals

The distribution and habit of each major alteration mineral is described below for each of the alteration zones. The descriptions first concentrate on the major silicate minerals and end with the minor sulphide minerals and sulphates.

*Chlorite* occurs as clots of radiating grains or as parallel flakes intergrown with pervasive sericite in the core alteration zone. Chlorite also occurs in the periphery alteration zone replacing the matrix to tuffaceous rocks in the footwall and hanging wall of section 9700N (Fig. 6.2) and replacing hornblende phenocrysts.

Pervasive intergrown chlorite and sericite are pale green and individual flakes of the two minerals cannot be identified except with the aid of a microscope. Most of the intergrown flakes of chlorite and sericite parallel the foliation in the rock, but they also form clusters of radiating grains in areas of less deformation.



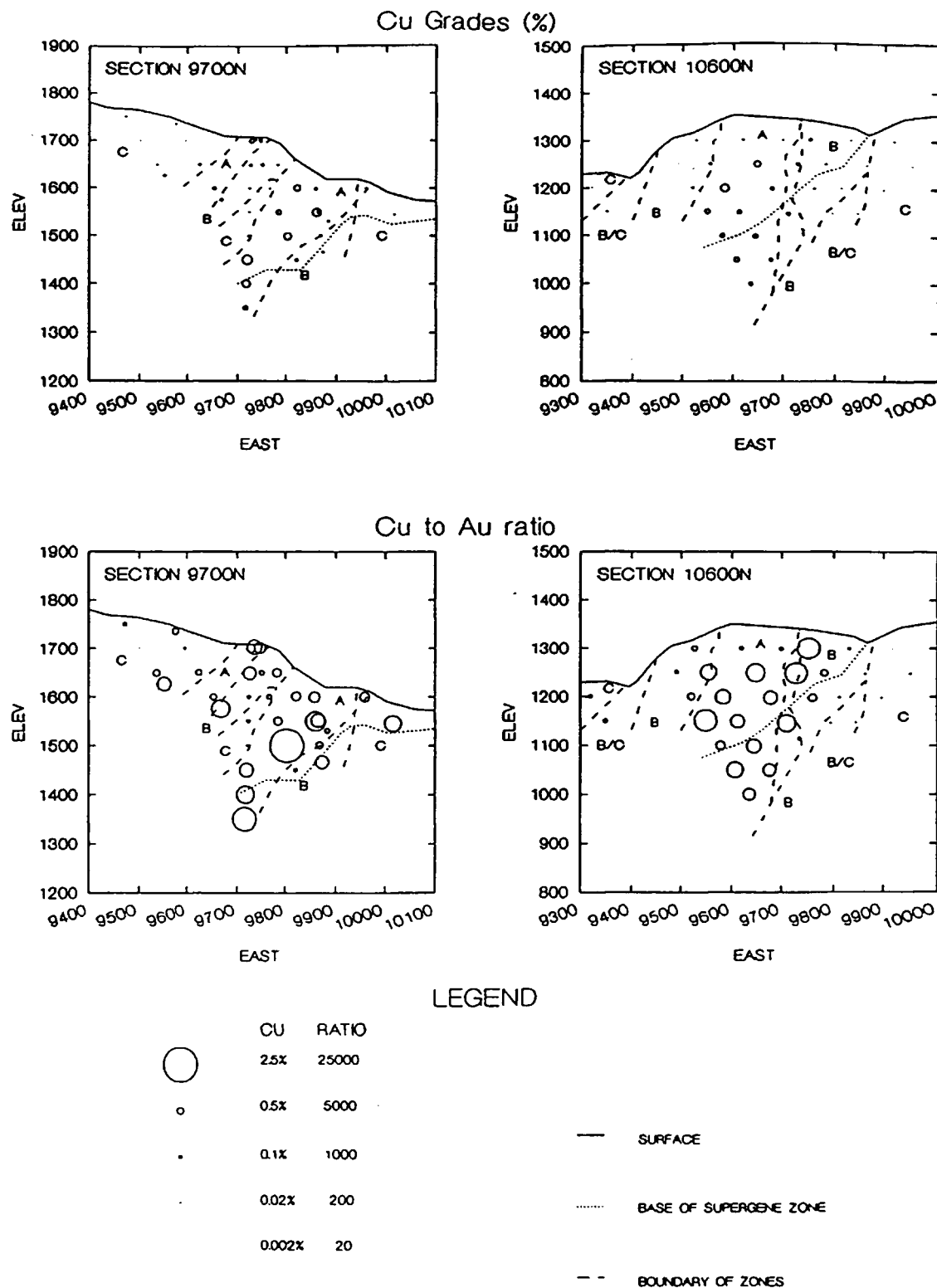


Figure 6.2. Copper and copper to gold ratios on sections 9700N and 10600N, Kerr deposit, northwestern British Columbia. Size of bubble is proportional to the arithmetic concentration of copper or the ratio of copper (%) and gold (%). Region A = core, region B = halo, region C = periphery alteration.

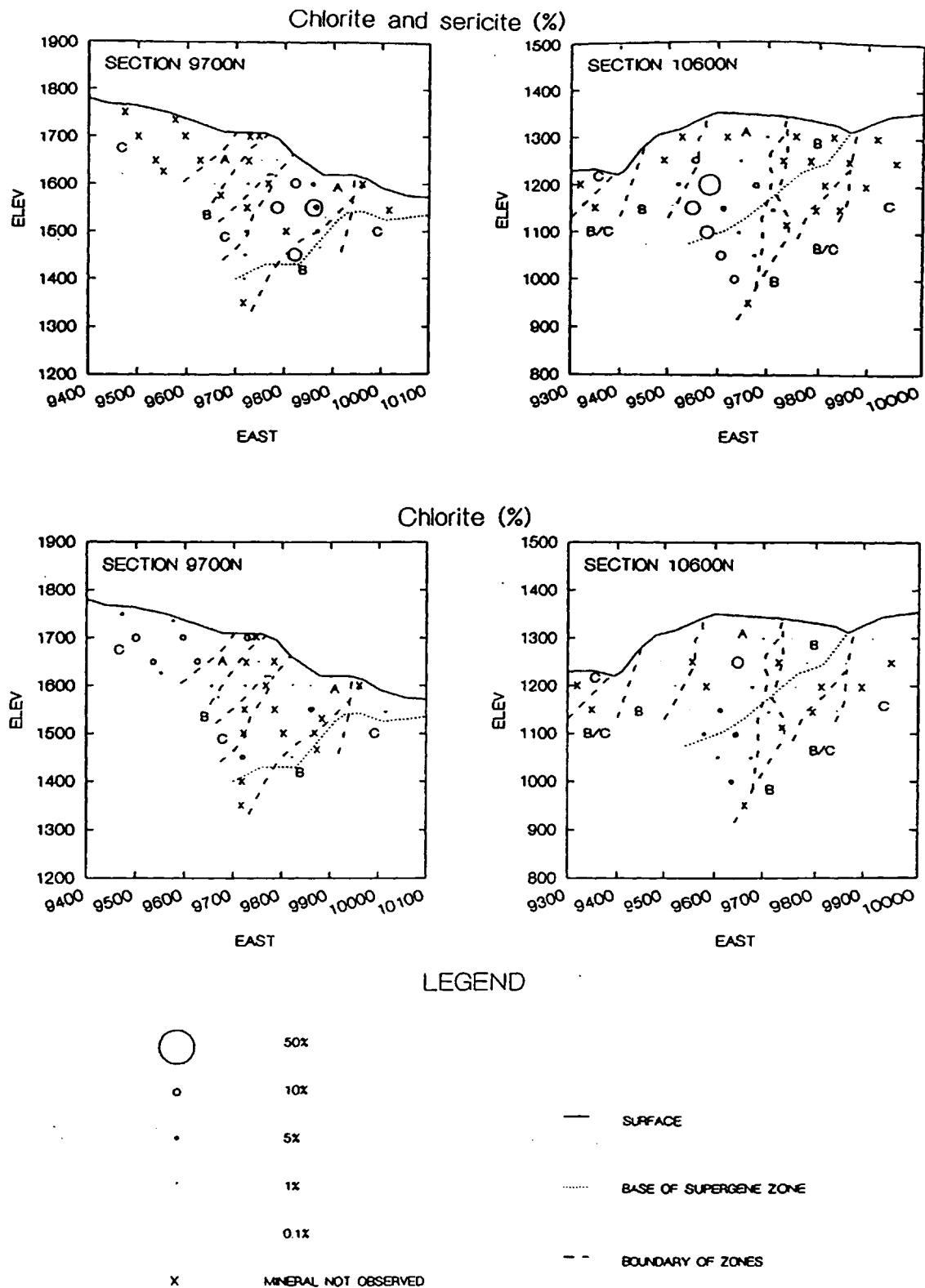


Figure 6.3. Distribution of visually estimated chlorite and sericite and chlorite on sections 9700N and 10600N, Kerr deposit, northwestern British Columbia. Size of bubble is proportional to the arithmetic amount of the mineral present. Region A = core, region B = halo, region C = periphery alteration.

X-ray diffraction patterns of water-separated phyllosilicate minerals indicate that the dominate chlorite is iron-rich chamosite  $[(\text{Fe}, \text{Al}, \text{Mg}, \text{Mn})_6(\text{Si}, \text{Al})_4\text{O}_{10}(\text{OH})_8]$  in the core alteration zone; the composition was confirmed by scanning electron microscopy (Appendix C). This chlorite occurs with grey sericite and disseminated anhydrite in weakly deformed rock; however, chlorite intergrown with anhydrite is Mg-rich. Anomalous blue interference colours of chlorite grains indicate that it varies from 50 to 80%  $\text{Fe}/(\text{Fe}+\text{Mg})$  based on the petrographic method of Albee (1962).

Scanning electron microscopy indicates that radiating chlorite grains in the centre of the core alteration zone contain minor potassium due to intergrowths with sericite (Fig. C.3, Appendix C). Rare chlorite clots in altered rock have brownish, higher relief centres containing disseminated 1-5 micron rutile inclusions. Analysis of the central grain yields consistent potassium peaks during analysis. The composition, disseminated rutile and high relief of these grains suggest that the original mineral was biotite.

Chlorite in the upper mineralized lens is magnesium rich where they occur with disseminated calcite, microcrystalline quartz and sericite.

Petrographic analysis of chlorite replacing amphiboles in massive tuff in the hanging wall of the deposit indicates that it is chamosite. Magnesium rich chlorite replaces the matrix of the tuff.

*Sericite* occurs as pervasive grey sericite throughout the Kerr deposit, or as blue sericite restricted to altered feldspars in syn-mineralization monzonite dykes (Fig. 6.4). The sericite exhibits second order birefringence, which is characteristic of ordered micas (Deer, Howie and Zussman, 1966). Scanning electron microscopy of grey sericite indicates minor iron and trace magnesium (Appendix C, Fig. C.6) in the mineral which defines it as phengite (Deer, Howie and Zussman, 1966). Electron microprobe analyses of blue sericite grains confirms that it is

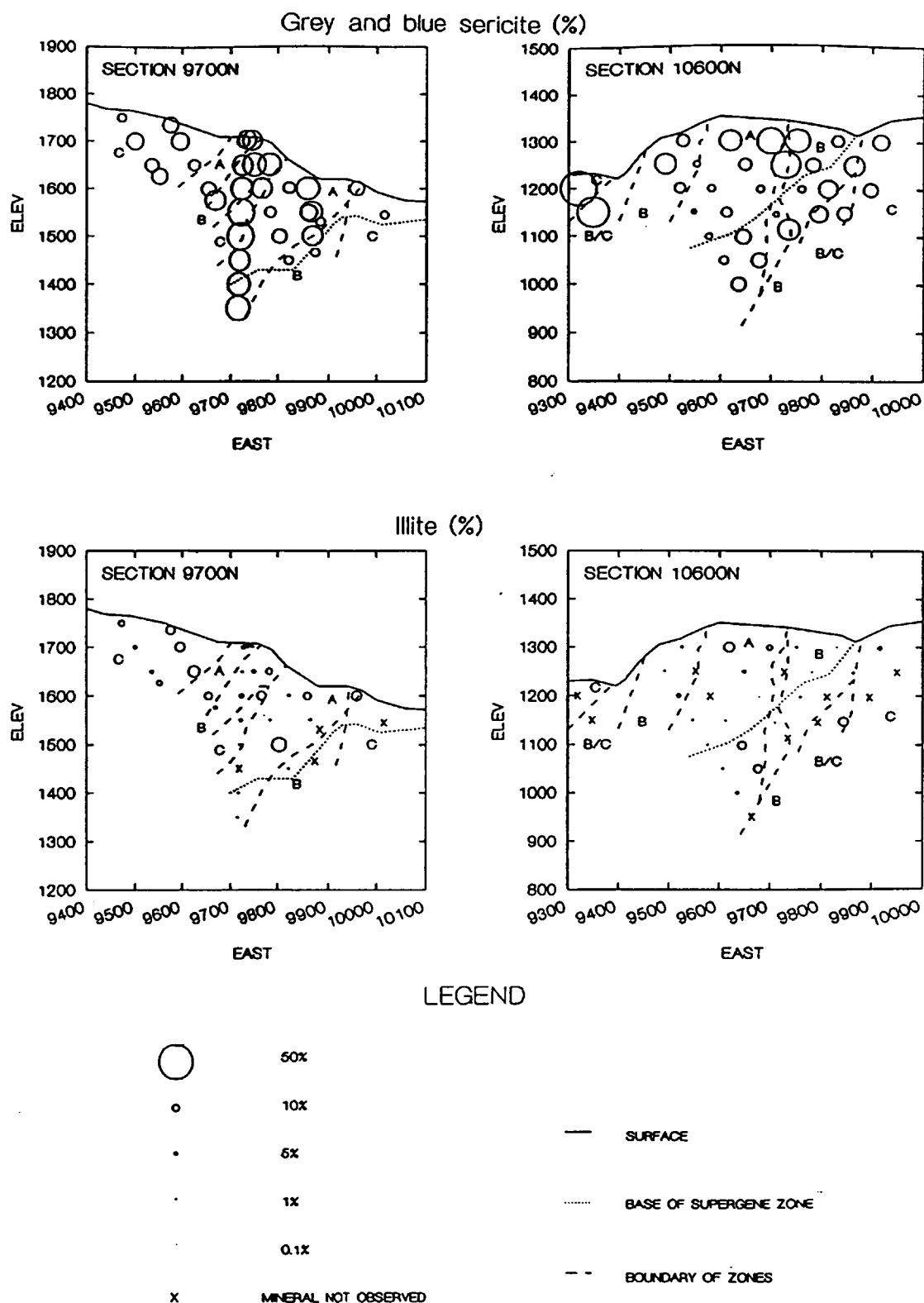


Figure 6.4. Distribution of visually estimated grey and blue sericite and illite on sections 9700N and 10600N, Kerr deposit, northwestern British Columbia. Size of bubble is proportional to the arithmetic of the amount of mineral present. Region A = core, region B = halo, region C = periphery alteration.

phengite. Highest concentrations of grey sericite (up to 40%) occur around the edges of the chlorite and intergrown chlorite and sericite in the core alteration zone in section 10600N.

Grey sericite also occurs intergrown with microcrystalline quartz in kidney shaped to oval masses in deformed core, halo and periphery alteration zones. At the top of drill hole KS-094 in the halo alteration, these masses grade into a K-feldspar flooded rock. The original texture of the rock was destroyed by the alteration. Portions of the K-feldspar flooded rock are cut by millimetre wide sericitic shear zones. Sericite flakes in these shear zones parallel the foliation in the rock.

Pervasive *yellow sericite* is always intergrown with grey sericite (phengite) and rutile. The concentration of yellow sericite is proportional to the amount of rutile in the rock. Highest concentrations of the yellow sericite occur immediately outward from the disappearance of intergrown chlorite and sericite, and it is least abundant in highly silicified areas (Fig. 6.5).

Yellow sericite can be distinguished from phengite by its first to second order interference colours, smaller grain size and association with rutile (Plate 6.2). Scanning electron microscopic analyses of yellow sericite indicates the possible presence of Ti in the mica (Appendix C, Fig. C.15). The intergrown rutile has yellow-brown internal reflections, which suggests that the colour of the yellow sericite is due to rutile.

In the halo alteration zone along the footwall of section 9700N, minor amounts of pale olive green sericite are intergrown with yellow sericite. Analyses of the rutile and sericite grains indicate the presence of moderate amounts of Cr and Fe, and trace amounts of Fe and Cr, respectively (Appendix C, Fig. C.16).

*Illite and other hydromicas* are relatively abundant immediately below surface on both cross - sections and in the halo and periphery alteration zones (Fig. 6.4). The highest

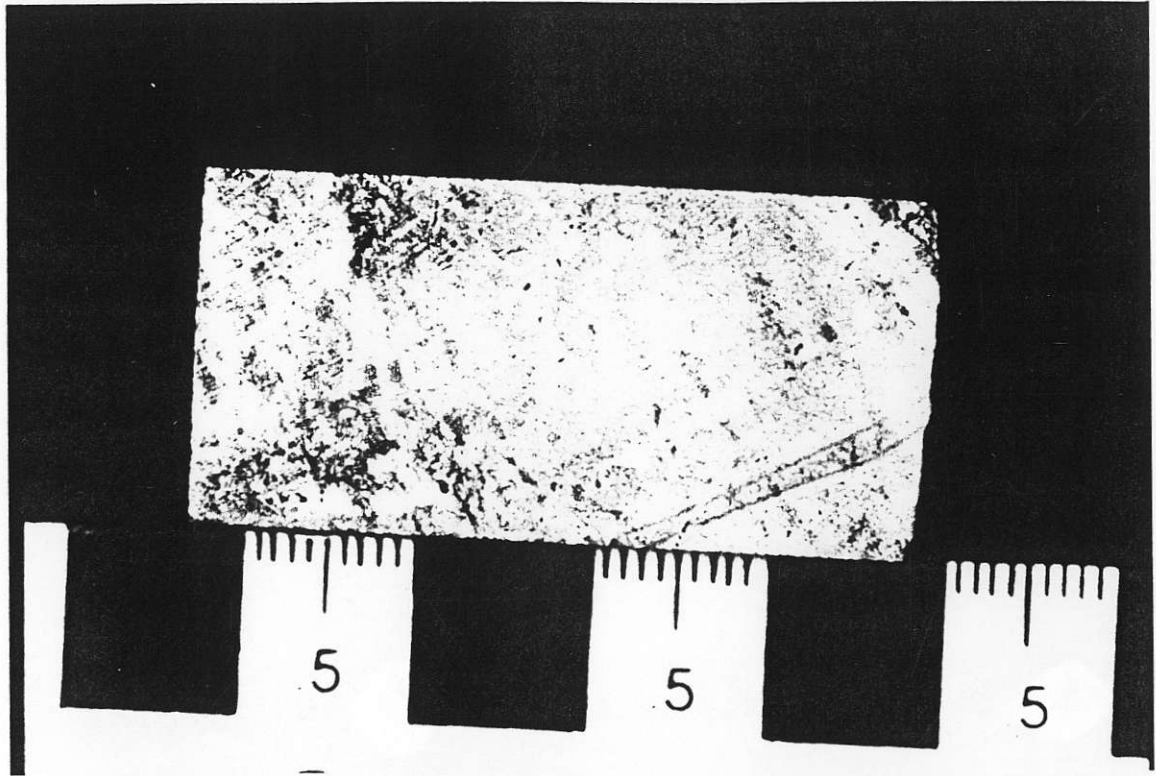


Plate 6.1. Sample from KS-94 40.8m, Figure 4.2, stained for K-feldspar (bright yellow patches). K-feldspar occurs as microcrystalline grains with minor sericite and quartz replacing it. Pale patches are aligned sericite flakes and minor quartz grains. White vuggy quartz veins are extensional veins with fibres parallel to the foliation.



Plate 6.2. Broken pyrite grains in a matrix of Fe - chlorite grains, quartz and minor sericite. Gold occurs with chalcopryite in fractures in pyrite. Sample is from KS-125 286.0 m, Figure 4.2. Field of view is 1.25 mm. Legend: Au - Gold, Cl - chlorite, Cp - chalcopryite, Py - pyrite, and Qz - quartz.

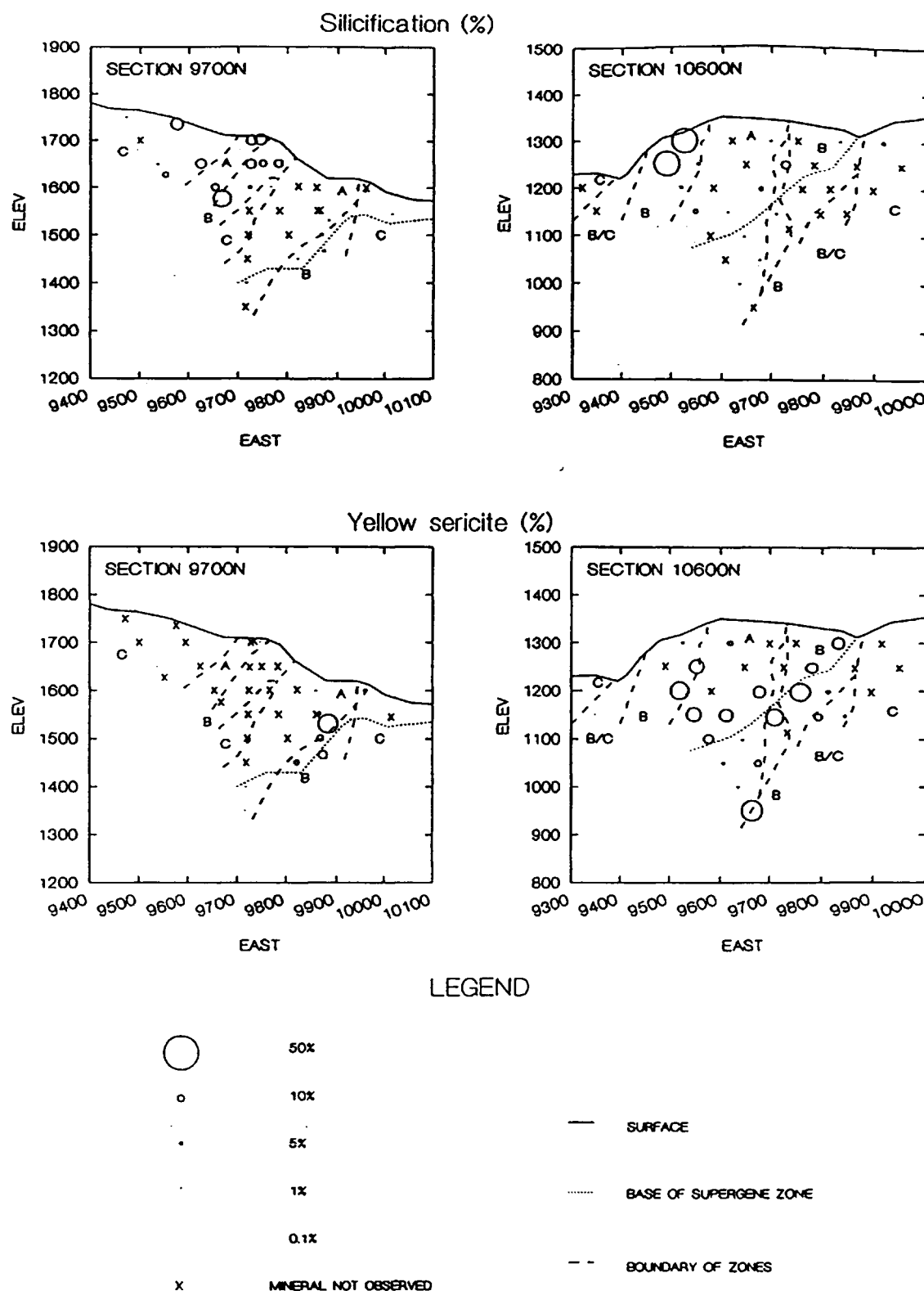


Figure 6.5. Distribution of visually estimated silicification and yellow sericite on sections 9700N and 10600N, Kerr deposit, northwestern British Columbia. Size of bubble is proportional to the arithmetic amount of the mineral present. Region A = chlorite core, region B = yellow sericite halo, region C = periphery alteration.

concentration of the clay minerals occurs in weakly deformed rock along the hanging wall of section 9700N where they replace the centres of plagioclase laths in syenodiorite and the matrix to the tuff. In other regions the clay minerals are intergrown with phengite in altered plagioclase laths; this makes them difficult to identify using X-ray diffraction.

Disseminated *clintonite* (Ca-trioctahedral bittle mica) was identified by petrography by its high relief and pale green pleochroism. It occurs throughout the halo and periphery alteration zones in the presence of disseminated calcite. In intensely deformed rock, clintonite forms flakes parallel to the foliation in the rock, or as aggregates of grains that are stretched and boudinaged parallel to the foliation. The mineral forms euhedral crystals in weakly deformed, sericite altered mudstone in the footwall of section 10600N.

Pervasive *silicification* is widespread within and around the core alteration zone. Highest concentrations of microcrystalline quartz are in fragmental rocks in the hanging wall of section 10600N and in breccia in the upper lens of core alteration on section 9700N. This quartz forms patches of interlocking grains with minor sericite in the rock. The contacts between the grains are sutured with rare stylolitic contacts parallel to the foliation in the rock. These patches of quartz differ from the primary quartz grains in having intergrown sericite. Primary quartz grains are generally free of phyllosilicates inclusions and occur as isolated neoblasts ringed by flakes of sericite parallel to the foliation.

Pervasive silicification also occurs in the footwall of section 10600N where it replaces the matrix and rims of clasts in the conglomerate. This silicification consists of very fine grained comb quartz with minor 0.5 mm to 2.0 mm patches of vuggy quartz in the centre of the silicified zones. This alteration, where noted along faults and fracture zones in the footwall of the deposit, has elevated Au grades (up to 2.2 ppm) and minor pyrite and trace chalcopyrite.



Disseminated *magnetite* occurs in the centre of the core alteration with chlorite and minor grey sericite. Disseminated magnetite also occurs in periphery alteration where it is partially replaces hornblende phenocrysts in syenodiorite. Disseminated magnetite in the core alteration only occurs where there is abundant magnetite and specular hematite veins. Scanning electron analysis of two magnetite grains showed that it has trace amounts of titanium. Hematite replaces magnetite in the outer fringes of the chlorite alteration zone; therefore, the distribution of total magnetite and specular hematite is shown in Figure 6.6 to show the original extent of magnetite. Disseminated hematite occurs in the core alteration at the top of the upper mineralized lens on section 9700N.

Disseminated *pyrite* varies in habit from ragged clusters of grains to rounded cubes in the core alteration zone. Most pyrite grains in intensely deformed rock are rounded and are flanked by pressure shadows filled with quartz and chlorite fibres. Fractures in these pyrite grains are filled with quartz fibres and chalcopyrite. Pyrite commonly hosts round inclusions of chalcopyrite and pyrrhotite, and rare inclusions of bornite, ilmenite, rutile and tetrahedrite (Appendix C, Fig. C.6). Pyrite in the centre of the core is dominated by 5 to 25 micron chalcopyrite inclusions. At the edge of the alteration zone, pyrite hosts either: (i) chalcopyrite, or (ii) chalcopyrite and pyrrhotite, or (iii) chalcopyrite and bornite inclusions. The inclusions are concentrated in the centre of the pyrite grains and are associated with rare rutile and sericite inclusions.

Disseminated pyrite, in the halo zone, forms ragged to euhedral grains with round, 1 to 5 micron inclusions of pyrrhotite, chalcopyrite, bornite, tetrahedrite and sphalerite. Ragged pyrite occurs in weakly deformed alteration. Euhedral pyrite occurs in rock with abundant sericite or in highly deformed rock. Chalcopyrite and trace amounts of tetrahedrite-tennantite fill fractures in pyrite grains. The concentration of pyrite in the halo zone is approximately equal to that in the chlorite core.

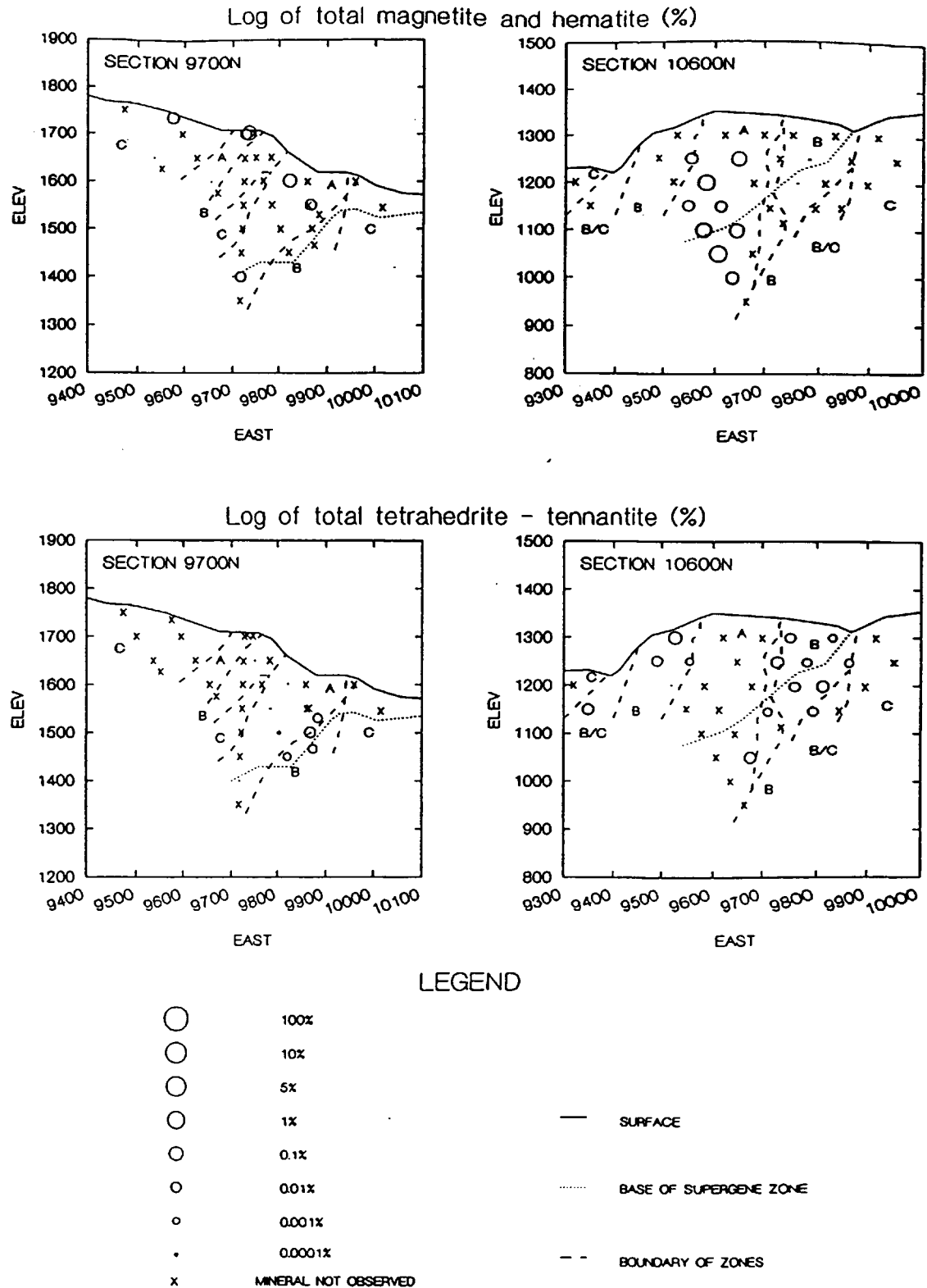


Figure 6.6. Distribution of visually estimated total magnetite and hematite and total tetrahedrite-tennantite on sections 9700N and 10600N, Kerr deposit, northwestern British Columbia. Size of bubble is proportional to the  $\log_{10}$  of the amount of mineral present. Region A = core, region B = halo, region C = periphery alteration

Disseminated *chalcopyrite* occurs as 1 to 5 micron inclusions in pyrite, 5 to 100 micron rims on pyrite, and 5 to 25 micron disseminated grains throughout the core alteration assemblage. The concentration of chalcopyrite exceeds pyrite when it is associated with magnetite, but usually the ratio of disseminated chalcopyrite to pyrite is about 1:20 in the core (Table 6.1). Chalcopyrite also occurs intergrown with radiating clusters of chlorite and sericite grains. These clusters also contain anhydrite, minor siderite and rare barite. Chalcopyrite fills broken pyrite grains and apatite grains in intensely deformed rock.

Chalcopyrite occurs as inclusions in disseminated pyrite and in trace amounts as free grains in sericite-quartz patches in the halo alteration. The chalcopyrite to pyrite ratio of 1:100 is less than in the core because of the lower concentrations of chalcopyrite (Table 6.1).

Disseminated chalcopyrite in periphery alteration occurs with pyrrhotite in the undeformed footwall of section 9700N.

Disseminated *tetrahedrite-tennantite* is As-rich in the footwall and Sb-rich in the hanging wall of the Kerr deposit based on scanning electron microprobe analysis (Appendix C, Figs. C.6 and C.10). These minerals are distributed in a halo around the core alteration (Fig 6.3). They occur as either 50 to 100 micron grains disseminated in the rock or in contact with pyrite; it also occurs as inclusions in disseminated pyrite.

*Anhydrite* occurs as equant, disseminated grains intergrown with chamosite and sericite in weakly deformed rock or as elongate grains intergrown with clinochlore parallel to the foliation in the core alteration zone. The elongate grains are possibly related to mineral growth during deformation. Near the base of the supergene zone anhydrite is replaced by gypsum. Anhydrite also occurs with calcite in sericite - quartz - pyrite altered monzonite dyke at the base of section 9700N.

*Calcite* occurs in fractures in bull and banded quartz veins in the core alteration zone. Disseminated calcite is found in all alteration zones except in the core alteration zone on section 10600N. Highest concentrations of calcite in the halo alteration are around type 6 veins. In the periphery, calcite is disseminated around sericite altered feldspar grains and intergrown with clinocllore. Calcite is disseminated in the upper mineralized lens on section 9700N.

*Siderite* occurs in fractures in type 1 and type 3 veins with anhydrite and chalcopryrite in the core alteration zone.

*Barite* occurs in trace amounts in quartz veins. It is also intergrown with radiating clusters of pervasive sericite and chlorite that recrystallized after deformation.

*Gold* with a low silver content (scanning electron microscope analysis, Appendix C, Fig. C.5e) was observed in one polished section. It occurs as a 20 micron grain in chalcopryrite that rims a fractured pyrite grain (Plate 6.2).

Disseminated *rutile* varies in composition from the core to halo alteration zones. It occurs as 1 to 5 micron grains with chlorite and sericite in the core alteration zone. Scanning electron microprobe analysis indicates that it does not have impurities. These grains have white internal reflections. Rutile occurring with yellow sericite has yellow-brown internal reflections and electron microprobe analysis indicates the presence of iron in the mineral. In intensely deformed rock, rutile is disseminated with sericite, but it is concentrated in bands, 10 microns wide, parallel to the foliation in the rock.

*Ilmenite* occurs in the core alteration intergrown with chamosite and sericite.

*Sphene* occurs in stylolites in periphery alteration in the hanging wall and footwall of section 9700N. The mineral only occurs where there is abundant calcite in the matrix to the tuffaceous rock.

*Epidote and clinozoisite* occur in the periphery alteration zone on section 9700N. They replace plagioclase in monzonite and in tuff.

*Carbonaceous material* occurs in stylolites in highly deformed rock. It also occurs with calcite - pyrite veins hosted by coarser beds of argillite along the footwall of section 10600N.

## 6.5 Description of Vein Assemblages

Seven distinct compositions of veins related to mineralization and two shear and extension vein assemblages have been recognized in the Kerr deposit. Their temporal order was determined from cross-cutting relationships among the veins and syn- and post-mineralization dykes.

Type 1 bull quartz with minor pyrite veins with rare chlorite envelopes are reddish and up to 20 mm thick. Where the veins are cut by magnetite veins, they are filled with minor amounts of magnetite. Thin, millimetre thick chlorite alteration envelopes occur along their margins.

Type 2 veins, magnetite and specular hematite with minor chalcopyrite, are concentrated in the core, especially where magnetite is disseminated in the matrix. The veins are 0.5 to 20 mm thick without distinctive alteration envelopes in the chlorite alteration zone,

but have chlorite alteration envelopes when they occur in sericite - quartz - pyrite alteration. Where deformed, the magnetite is rimmed by specular hematite. Where anhydrite veins cut magnetite veins, red hematite and minor pyrite replace magnetite. Chalcopyrite, up to 0.5% of the vein, occurs as 10 micron to sub-micron grains within the iron oxides.

Type 3 veins, banded quartz - pyrite, are concentrated above the monzonite dykes in the core and halo. They occur rarely in the periphery alteration. Relatively undeformed quartz veins are 0.2 to 25 mm thick and consist of 0.1 mm to 2 mm thick, parallel layers of coxcomb quartz crystals. Growth banding on each side of a vein can be matched with the other side. Where the vein is intensely deformed, this banding is generally destroyed. Minor amounts of 0.1 mm grains of pyrite occur as layers in the veins at the terminations of quartz crystals.

Type 4 veins, pyrite - chalcopyrite - quartz, are concentrated in the core alteration zone on section 10600N and in the halo on section 9700N (Fig. 6.5). The veins are dominantly pyrite with minor chalcopyrite. The veins range in thickness from 0.1 to 200 mm. Smaller veins are concentrated in the centre of the deposit where they have chlorite envelopes. Large veins in the halo alteration zone have sericite - quartz envelopes. Undeformed periphery alteration has rare sulphide veins with K-feldspar envelopes. The veins cut magnetite and banded quartz veins, and are hosted in the monzonite and syenodiorite dykes on section 9700N.

Type 5 veins, anhydrite - siderite - quartz - pyrite - chalcopyrite with trace tetrahedrite-tennantite and molybdenite, are concentrated in and around the margins of the monzonite

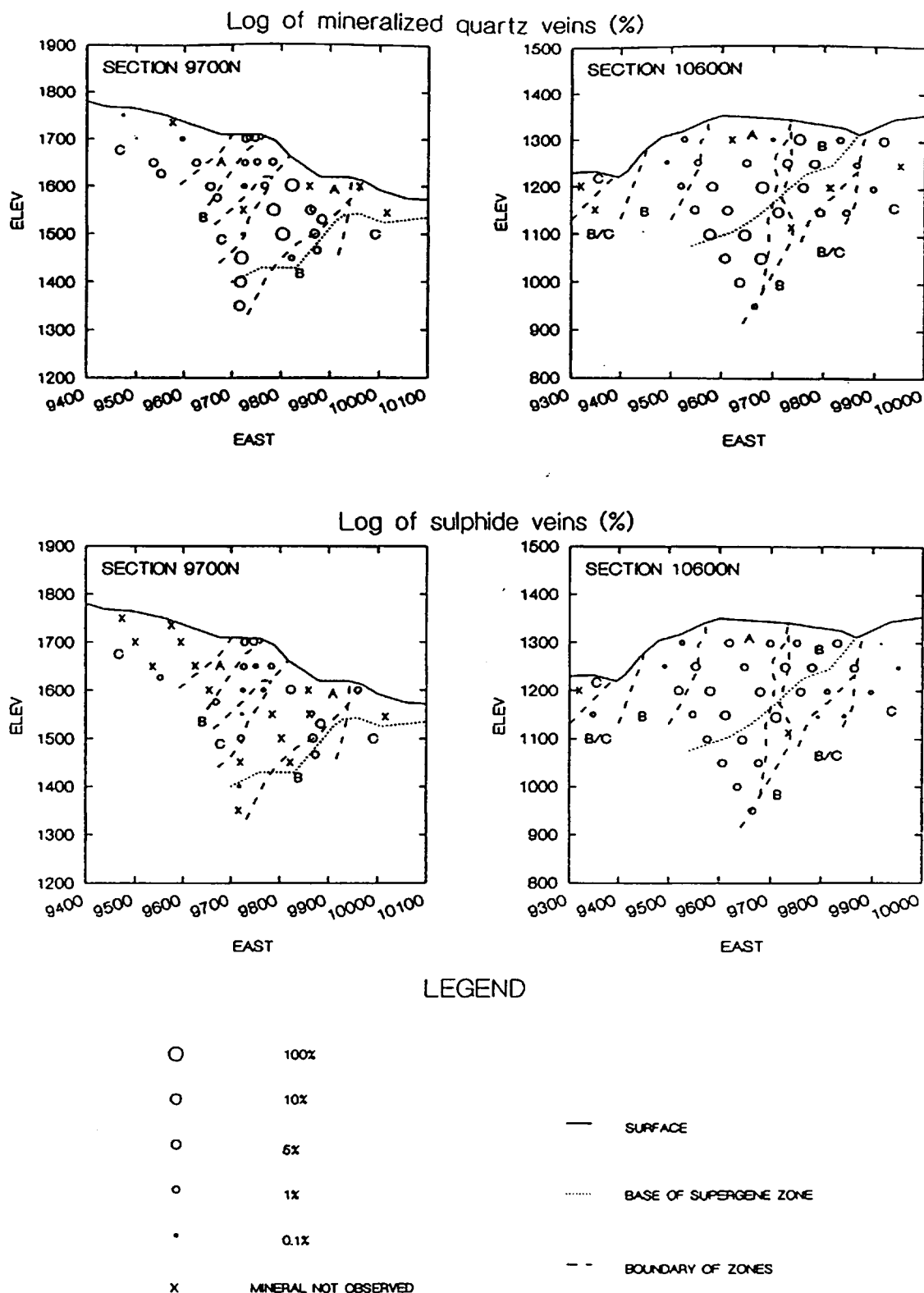


Figure 6.7. Distribution of measured mineralized quartz veins (type 1 and type 3) and sulphide veins (type 4) on sections 9700N and 10600N, Kerr deposit, northwestern British Columbia. Size of bubble is proportional to the  $\log_{10}$  of the amount of vein present. Region A = core, region B = halo, region C = periphery alteration.

dyke. Most minerals in Type 5 veins have been dissolved by groundwater above the base of the supergene zone. The veins consist of interlocking grains of anhydrite, siderite, quartz, minor pyrite and chalcopryite and rare specular hematite and tetrahedrite-tennantite. Vein thicknesses vary from 0.5 to 20 mm and they commonly have 0.5 mm chlorite envelopes. Scanning electron microscopy of siderite indicates trace amounts of Mn and Mg.

Type 6 veins, pink anhydrite with minor chalcopryite and molybdenite are 0.2 to 10 mm wide and have chlorite envelopes. Minor chalcopryite and trace molybdenite occurs on selvages with chlorite. These veins have been observed locally to branch off type 5 veins. This might indicate that some of the grey anhydrite veins reopened during subsequent fracturing and precipitation of sulphate continued.

Type 7 veins, carbonate - quartz - pyrite - tetrahedrite - galena - sphalerite, occur on either side of the chlorite core. They are concentrated in the halo and diminish in numbers in the periphery zone. They are 0.5 to 40 mm wide and have 0.5 to 2.0 mm thick sericite and quartz envelopes in yellow sericite alteration. These veins, with no alteration envelopes, have been recognized up to 1 km away from the chlorite core of the deposit.

The sulphide mineralogy in the carbonate veins is similar to that of the sulphate veins except that sphalerite and galena occurs in increasing quantities away from the core. Calcite is the dominant carbonate in the veins, and it has slightly higher concentrations of Mn and Mg than the siderite in the sulphate veins (Appendix C). In addition, scanning electron microscopy indicated trace amounts of Ba-Ca-Sr sulphates and barite in the veins (Appendix C).



## 6.6 Alteration of Late Syn- and Post-Mineralization Dykes

The alteration mineral assemblages in: (i) augite and hornblende porphyry dykes and (ii) feldspar megacrystic dykes record alteration due to very late stage mineralization and the affects of metamorphism and deformation of the Kerr deposit.

### 6.6.1 Alteration in augite and hornblende porphyry dykes

Augite and hornblende porphyry dykes occur in the halo and periphery alteration zones. Altered augite porphyry dykes in the periphery alteration zone have actinolite replacing augite phenocrysts and clay minerals (dominantly kaolinite) replacing plagioclase laths. The matrix is replaced by clay minerals and quartz. Augite porphyry dykes in the halo alteration zone have bluish clay minerals replacing the augite and phengite replacing the matrix and plagioclase laths. In these dykes the outlines of the grains can be readily distinguished.

Hornblende porphyry dykes in the halo alteration along section 9700N have epidote and clinozoisite replacing plagioclase in the cores of the dykes. Chlorite replaces hornblende laths. Ilmenite exsolution lamellae in magnetite and rutile are replaced by sphene. The matrix consists of intergrown calcite, chlorite, sericite and quartz grains. Edges of the dykes have phengite replacing plagioclase and hornblende altering to chlorite, sericite and leucoxene. Minor round grains of pyrite occur sporadically in the matrix.

### 6.6.2 Alteration in albite and K-Ba-feldspar megacrystic plagioclase hornblende porphyry dykes

The K-Ba-feldspar (hyalophane) megacrystic plagioclase hornblende porphyry dykes host type 7 veins where they cut the periphery alteration in the hanging wall of section 9700N. In the margins of these dykes, hyalophane and apatite is unaltered, but plagioclase and

hornblende is extensively altered to sericite and chlorite, respectively. The core of the dyke intersected in section 10600N has fresh plagioclase and hornblende grains. Euhedral pyrite is disseminated throughout the dyke.

Alteration mineral assemblages in the north-south trending, post-mineralization albite megacrystic dyke vary from core to margins. These dykes are interpreted to be post-mineralization because they are not cut by type 5 to 7 veins, which are related to the final stages of porphyry copper mineralization. The centre of the dyke contains saussuritized plagioclase and chlorite altered hornblende in a matrix of hematite, chlorite and calcite. Albite megacrysts are weakly altered to sericite. Margins of the dyke contain deformed chlorite and sericite altered hornblende and plagioclase laths. Minor disseminated pyrite (5%) occurs in the matrix of the deformed margin with chlorite, sericite and carbonate. This pyrite may have formed by the introduction of sulphur from the surrounding sericite - quartz - pyrite alteration. If this pyrite formed during crystallization of the dyke, it would be disseminated throughout the dyke, and not concentrated along its deformed margins.

## 6.7 Effects of Deformation and Metamorphism on the Distribution of Minerals in the Three Alteration Zones

### 6.7.1 Core alteration zone

The core alteration zone exhibits a less pronounced penetrative fabric than the surrounding sericite alteration. It also hosts fewer extension veins. Analysis of the habits of minerals in extension and shear veins and pressure shadows indicates that most of the silicates and sulphides except possibly pyrite have recrystallized during deformation.

Below the level of supergene oxidation, extension veins on section 10600N are composed of quartz, anhydrite, siderite with minor chalcopryrite and pyrite. Calcite and anhydrite extension veins on section 9700N are intimately related to shear veins in the sericite

- quartz - pyrite altered syn-mineralization monzonite dyke. No sulphate extension veins remain above the altered dyke due to dissolution of anhydrite. Extension veins in the upper lens of mineralization are composed of quartz, calcite and chlorite (Fig. 6.8). The mineralogy of the extension veins in the three regions is similar to that in pressure shadows around quartz and broken pyrite grains (Table 6.3).

Broken pyrite grains with round inclusions of chalcopyrite, bornite and rare pyrrhotite have quartz, chlorite and rare anhydrite and minor sericite fibres filling fractures. The mineral fibres around the pyrite grains suggest that pyrite formed before deformation; otherwise, there would not be pressure shadows. Chalcopyrite both rims and fills fractures in pyrite, and it occurs in the interstices of parallel flakes of chlorite and sericite as well as in extension veins. Chalcopyrite was therefore remobilized and re-precipitated during and immediately after deformation because it now resides in sites that were formed by deformation. Gold within a chalcopyrite rim around a broken pyrite grain (Plate 6.2) indicates that gold was also redistributed during deformation.

Quartz occurring as single grains in a matrix of chlorite and sericite shows undulose extinction, or rarely, is replaced by an aggregate of neocrysts. Quartz grains in massive and banded veins are sutured with stylolitic contacts; however, growth banding in the veins is preserved, which suggests that there has not been extensive translation of neocrysts during deformation. The sutured boundaries of the quartz grains indicate that the quartz was undergoing pressure solution during deformation. The dissolved quartz may have been re-precipitated in extension veins and pressure shadows around pyrite grains.

#### 6.7.2 Halo alteration zone

This alteration zone has the most pronounced penetrative fabric in the Kerr deposit. Highest intensity of the fabric is developed immediately surrounding the chlorite core and decreases outward on either side. This fabric is defined by sericite flakes and elongate quartz

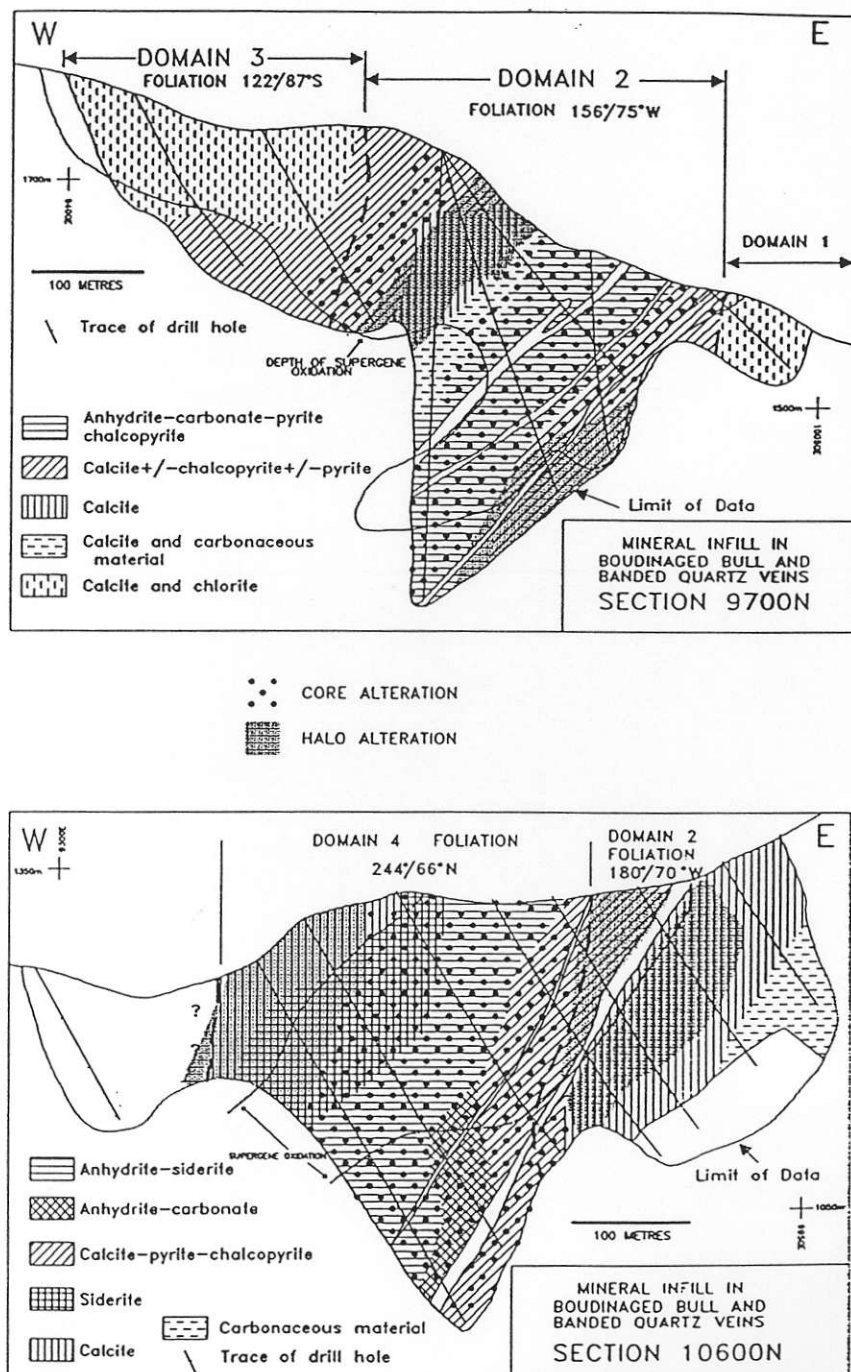


Figure 6.8. Distribution of minerals filling fractures and pressure shadows in bull and banded quartz veins (type 1 and type 3), Kerr deposit, northwestern British Columbia.

Table 6.3. Effect of deformation and metamorphism on minerals in the core alteration zone, Kerr deposit, northwestern British Columbia.

Mineral	Primary	Syn-deformation	Unknown	Recrystallized after deformation
Fe-chlorite		Flakes parallel to fabric in rock and fibres in pressure shadows		Radiating grains replacing ferromagnesian minerals
Phengite (sericite)		Flakes parallel to fabric in rock with chlorite infilling veins		Replaces K-feldspar grains
K-feldspar	Altered to quartz and sericite			
Quartz	Undulose extinction	Neocrysts replaces strained grains; sutured grains in quartz veins		Replaces K-feldspar grains
Siderite			Anhedral grains	
Anhydrite		Filling fractures in quartz veins	Anhedral grains in contact with siderite and chlorite.	
Barite			Anhedral grains	
Pyrite	Broken grains with primary cp, po and tt inclusions. Quartz fibres in pressure shadows suggest that the pyrite is pre-deformation.			Possible overgrowths on pyrite grains
Chalcopyrite				Overgrowths on broken pyrite grains, intergrown with recrystallized chlorite and sericite
Magnetite and specular hematite	Deformed veins		Anhedral grains in matrix of chlorite	

grains in altered tuffaceous rocks. Siliceous regions in this alteration have abundant extensional quartz - calcite veins that are perpendicular to the deformation fabric. These areas grade into pervasive K-feldspar flooding at the top of drill hole KS-094 on section 9700N. Extensional quartz veins along the footwall of section 9700N contain minor tennantite.

Fractures in mineralized bull quartz and banded quartz veins along the footwall contact with the core alteration zone are filled by calcite with minor pyrite and chalcopyrite (Fig. 6.8). Fractured veins along the weakly deformed, sericite altered footwall and central sericite lens on section 9700N are filled only with calcite.

The grey sericite flakes in this alteration zone are parallel to the fabric, but minor patches of recrystallized radiating grains replace clots of sericite and remnants of K-feldspar. Yellow sericite and rutile form an anastomosing pattern around sericite flakes. All quartz grains exhibit either undulose extinction or neocrysts replacing them. Pressure shadows around pyrite grains are filled with quartz fibres and minor sericite; rare calcite occurs along their contacts (Table 6.4). Pyrite grains are broken and filled with minor quantities of chalcopyrite, tetrahedrite-tennantite, calcite and quartz.

### 6.7.3 Periphery alteration zone

Intensity of deformation of the periphery alteration varies from undeformed along the footwall of section 9700N to a weak penetrative fabric along the hanging wall and footwall of section 10600N. Weakly deformed regions have abundant quartz, calcite and chlorite extensional veins in areas of propylitic alteration in tuffaceous rocks and post-mineralization dykes (Table 6.5, Fig. 6.8). Calcite and carbonaceous material in shear and extension veins are concentrated in the argillite and siltstone units (section 10600N) and in the central conglomerate lens.

Table 6.4. Effect of deformation and metamorphism on minerals in the halo alteration zone, Kerr deposit, northwestern British Columbia.

Mineral	Primary	Syn-deformation	Unknown	Recrystallized after deformation
Phengite (sericite)		Flakes parallel to fabric in rock		Radiating clusters replacing K-feldspar and strained grains
Quartz		Undulose extinction; neocrysts replacing strained grains; pressure shadows occur around pyrite		
K-feldspar	K-feldspar in weakly deformed rock; primary phenocrysts are broken			Replaced by radiating sericite and clots of quartz
Yellow sericite			Clusters of flakes with rutile	
Apatite	Broken and stretched grains			
Clintonite			Euhedral grains in weakly deformed rock	
Pyrite	Broken grains with pressure shadows			
Chalcopyrite			Anhedral grains	Clots with sericite clots
Tetrahedrite-tennantite	Inclusions in pyrite		Anhedral grains	

Table 6.5. Effect of deformation and metamorphism on minerals in the peripheral alteration zone, Kerr deposit, northwestern British Columbia.

Mineral	Primary	Syn-deformation	Unknown	Recrystallized after deformation
Plagioclase	Replaced by sericite flakes parallel to fabric in rock			
Orthoclase	Broken grains with sericite and calcite along fractures			
Hornblende	Replaced by chlorite flakes			
Augite	Replaced by chlorite and actinolite			
Quartz		Undulose extinction; shear and extension veins		Recrystallization of K-feldspar
Phengite (sericite)	Replaces plagioclase	Flakes parallel to fabric in the rock		Replaces minor chlorite in altered hornblende grains
Chlorite		Flakes parallel to fabric in the rock		
Calcite	Deformed calcite veins	Neocrysts in calcite veins; fibres in shear and extensional veins	Anhedral grains	
Pyrite	Aggregates and euhedral grains			
Chalcopyrite			Anhedral grains	
Sphalerite			Anhedral grains	



### **6.8 Alteration of Tertiary Dykes**

Kersantite dykes occur along steeply dipping faults, and they exhibit the least amount of alteration in the Kerr deposit. They contain calcite filled vesicles and a pervasive chlorite alteration of the ferromagnesian minerals. Plagioclase exhibits minor sericite alteration throughout the dyke, and magnetite is altered to hematite along margins of dykes. Rare calcite veins cut the dyke. Margins of these dykes contain rare xenoliths of highly altered host rock and blebs of pyrite and chalcopyrite.

### **6.9 Late Gypsum Veins**

White gypsum veins, up to 2 millimetres thick, are concentrated in the core. These veins cut all earlier veins and penetrative fabric, but they do not occur in the post-mineralization dykes that cut the core. In regions of pronounced foliation, the veins form a stockwork parallel to the foliation with up to 100 veins per metre of drill core. In these areas there is extensive replacement of disseminated anhydrite by gypsum. The gypsum veins are composed of fibres perpendicular to the veins walls and their selvages are striated.

Gypsum veins in less deformed rock have a random orientation but are planar. Their orientation appears to be controlled by the variation in alignment of silicate minerals, micro-faults and quartz veins.

Scanning electron microprobe analysis of gypsum from a vein indicates no significant amounts of other elements. No sulphide minerals or alteration envelopes have been identified with these veinlets.

### **6.10 Magmatic and Hydrothermal Alteration of the Kerr Deposit**

K-feldspar alteration preserved at the top of a drill hole in the centre of section 9700N and along the undeformed footwall suggests that the Kerr deposit had an early stage of K-

feldspar flooding that was subsequently altered to grey sericite and quartz. This K-feldspar flooding is also exposed along the undeformed footwall where it interfingers with propylitically altered plagioclase augite diorite and tuff. Pervasive chlorite with traces of biotite and related magnetite, specular hematite and bull quartz veins are located in the centre of the Kerr deposit as depicted in Figure 6.9. Figure 6.9 is an idealized cross - section 10600N showing the early alteration zonation prior to intrusion of the syn-mineralization monzonite dyke. The remains of biotite and K-feldspar flooding are diagnostic of potassic alteration in porphyry copper deposits in the southwest United States and the Philippines (Beane, 1982; Sillitoe and Gappe, 1984).

Intrusion of the syn-mineralization monzonite dyke was followed by intense phyllic alteration first around banded quartz veins and later around sulphide veinlets (Fig. 6.10). Figure 6.10 shows that the distribution of the quartz and sulphide veins is superimposed upon the trace of the monzonite dyke. This dyke is intensely altered to sericite - quartz - pyrite, but the outlines of plagioclase phenocrysts are still visible. Thus, these veins introduced more fluid into the deposit partially altering the potassic assemblage to chlorite, sericite and possibly clay minerals. The composition of the envelopes around the sulphide veins generally mimic host alteration suggesting that vein fluids are the same as those that caused the widespread retrograde alteration. Similar alteration occurs in overprinted plagioclase hornblende monzonite to diorite porphyry copper deposits in the Philippines and Chile (Sillitoe and Gappe, 1984; Vila and Sillitoe, 1991).

Timing of the growth of the inclusion filled pyrite grains is unknown, but they probably formed during widespread retrograde alteration of the original potassic alteration. The inclusions formed during growth of the pyrite when the hydrothermal solutions were supersaturated with respect to the sulphides (Walshe and Solomon, 1981). Inclusions in pyrite in the pervasive chlorite alteration are dominantly chalcopryite, but in the yellow sericite alteration halo inclusions are pyrrhotite, chalcopryite, bornite and minor tetrahedrite-tennantite. Further out in weak yellow sericite alteration, there are galena and sphalerite

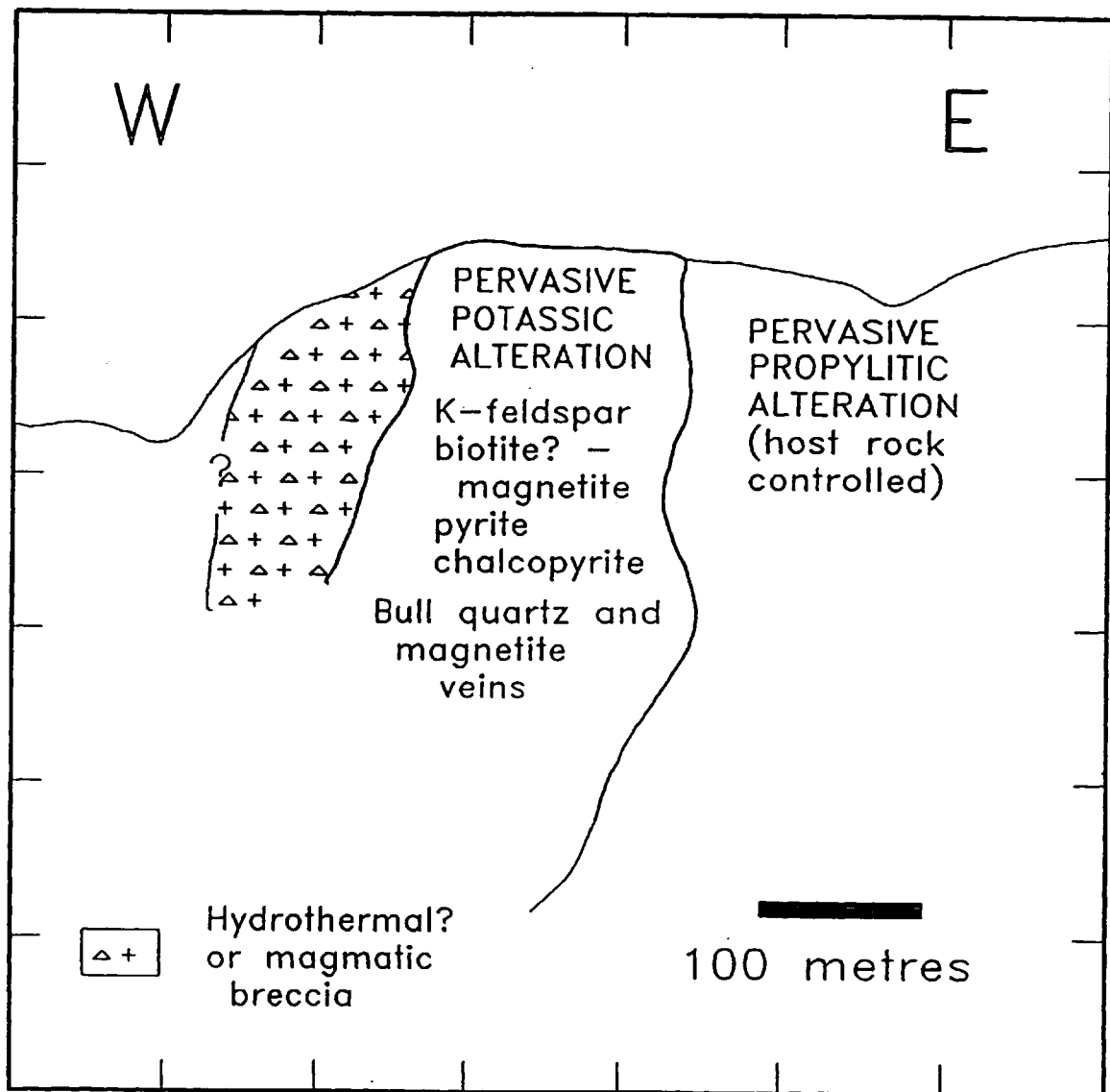


Figure 6.9. Distribution of early pervasive potassic and propylitic alteration across an idealized cross - section 10600N, Kerr deposit, northwestern British Columbia.

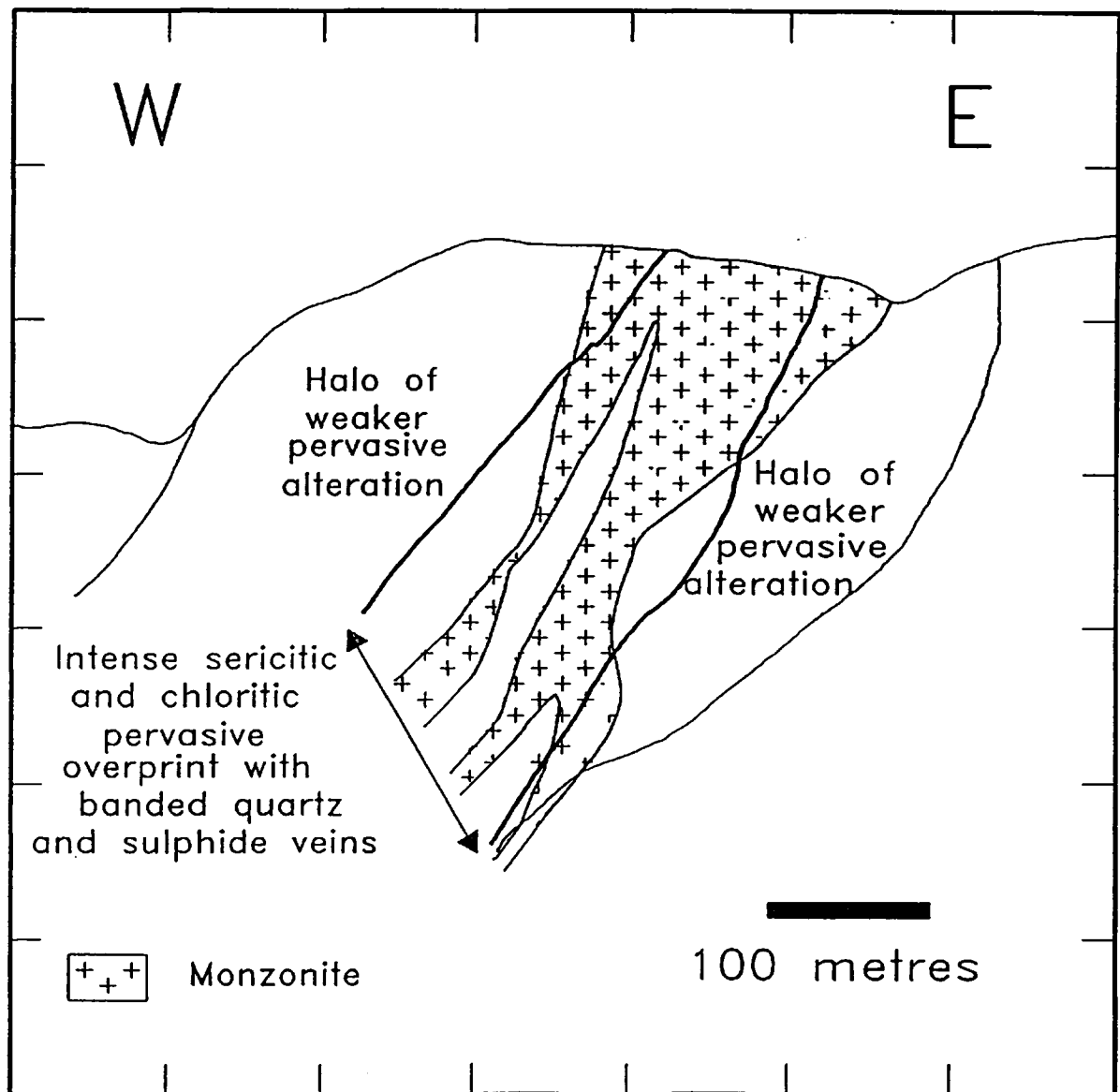


Figure 6.10. Distribution of pervasive phyllic alteration and syn-mineralization monzonite dyke across an idealized cross - section 10600N, Kerr deposit, northwestern British Columbia.

inclusions plus minor chalcopryrite and bornite. The variation in the composition of the sulphide inclusions from copper sulphides in the core to galena and sphalerite in the periphery are similar to the base metal zoning common to most porphyry copper deposits.

Following the phyllic alteration, sulphate and carbonate veins precipitated from fluids flowing through the Kerr deposit. The sulphate veins are restricted to the outline of the early potassic alteration (Fig. 6.11). The composition of the sulphides in the sulphate veins mimic the base metal zonation in the Kerr deposit.

### **6.11 Discussion of the Effects of Deformation on the Mineralogy of the Kerr Deposit**

Aldrick and Britton (1988) estimated that the metamorphic grade in the Sulphurets gold camp is lower greenschist. At this metamorphic grade, volcanic and sedimentary rocks are partially replaced by chlorite, epidote, calcite and minor albite by reaction of primary minerals with salty, dilute CO<sub>2</sub> rich aqueous fluids derived from dehydration of clay and zeolite minerals (Vernon, 1976). For this assemblage to form, the temperature and pressure should be between 250°C to 400°C and 2 to 6 Kb, respectively. These temperature and pressure conditions are above the stability field for clay and mixed layer clay minerals in NaCl fluids (Aja et al., 1991). Biotite can crystallize in sandstone at temperatures above 325°C in chloride rich brines in equilibrium with hematite, pyrite and chalcopryrite in the Broadlands hydrothermal system (McDowell and Elders, 1980). Thus, the replacement of biotite by chlorite in the Kerr deposit suggests that peak metamorphic temperatures during deformation of the deposit was less than 325°C but greater than 250°C. These temperature conditions are the same temperature of intermediate argillic alteration in porphyry deposits, but at much higher pressures than in porphyry deposits (Vila and Sillitoe, 1991; Vila et al., 1991).

The highly deformed core and yellow sericite alterations zones are composed of recrystallized phyllosilicate and copper sulphide minerals. Growth of fabric-parallel grains requires a fluid to transport ions from highly strained sites to lower pressure areas (Vernon,

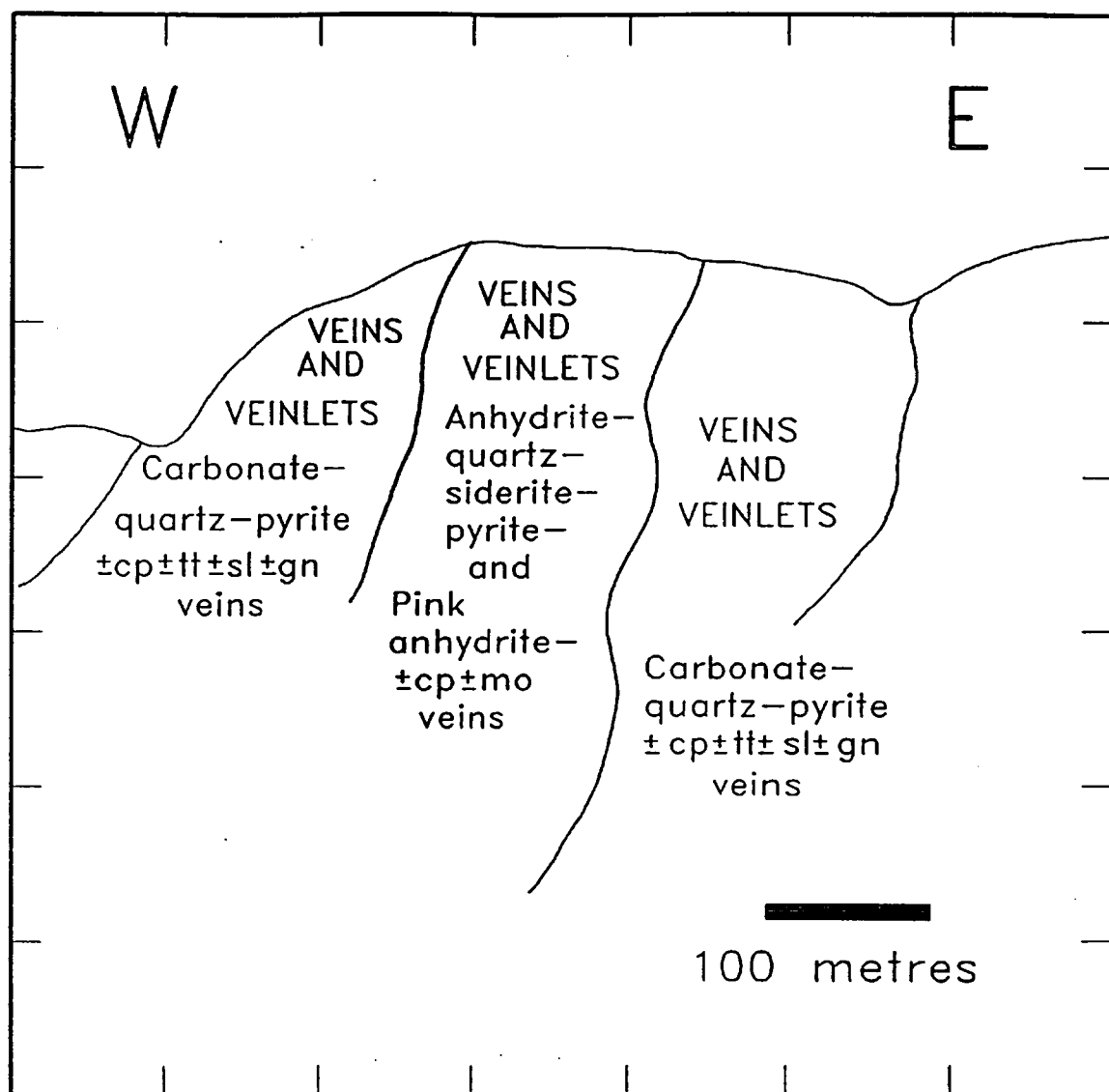


Figure 6.11. Distribution of sulphate and carbonate veins across an idealized cross - section 10600N, Kerr deposit, northwestern British Columbia.

1976). Additional evidence for this fluid in the Kerr deposit during deformation is the precipitation of minerals in extensional and shear veins. The composition of the minerals in these veins mimics the minerals in pressure shadows and in fractured quartz veins. This similarity in mineral assemblages suggests that the composition of the fluid was controlled by the host rock. Trace amounts of chalcopyrite in extensional quartz veins in an albite megacrystic plagioclase hornblende porphyry dyke indicate that migration of ions in this fluid is on the order of metres.

Mineral habits of phengite and chamosite that grew during deformation indicate that the two minerals were in geochemical equilibrium. The high Mg and Fe contents of the sericite are due to ion exchange with the chlorite during deformation (Mather, 1970; Hendry, 1981). This substitution of Mg and Fe into phengite increases the stability field of chlorite and prevents chlorite from altering to biotite at lower greenschist metamorphic conditions. Conversely, it increases the tendency of biotite to retrograde to chlorite at higher temperatures (up to 350°C). Remnants of pervasive biotite altering to chlorite are preserved in the centre of the chlorite alteration zone on section 10600N.

Deformation induced breakdown of K-feldspar to quartz and sericite along the top of drill hole KS-094 at the edge of the intensely deformed zone, releases  $K^+$  ions by the reaction:



assuming that Al is not mobile and electroneutrality of the reaction. In the core and halo alteration zones intergrowths of sericite and quartz replace K-feldspar. Potassium ions from breakdown of K-feldspar may react with clay minerals in the original hydrothermal alteration and alter them to sericite during deformation because the temperature and pressure conditions favour the formation of sericite instead of clay minerals. This process may account for the absence of clay minerals in the mineralized deformed zone.

The lower greenschist metamorphism temperature and fluid conditions are similar to that of phyllic alteration in a porphyry copper deposit so that alteration mineral assemblages in the

Kerr deposit probably reflect two periods of phyllic alteration. Thus, the mineral assemblages in the deposit reflect the original overprint assemblages in the Early Jurassic porphyry copper deposit. All sulphides and sulphates in the deformed region except for pyrite and magnetite have either recrystallized in place or have been remobilized and precipitated in fractures and pressure shadows.

There is no evidence to suggest that fluids moving through the deposit transported copper from the lower grade halo to the core; thus the distribution of copper likely reflects the grade in the original deposit before deformation. There is however evidence for S complex ions in the fluid because pyrite is disseminated in the margins of the post-mineralization albite megacrystic dyke. Breakdown of K-feldspar in micro-shear zones indicates that  $K^+$  ions were also in the fluid.

## 6.12 Discussion of Hydrothermal Alteration After Deformation

Alteration of the kersantite dyke suggests that there was fluid causing alteration of the ferromagnesian minerals and plagioclase after emplacement of the dyke in the Eocene. This alteration is not recognized away from the dyke because it forms the same minerals that define the penetrative fabric in the deposit. Alteration of the plagioclase and ferromagnesium minerals is most likely due to  $H^+$  metasomatism (Beane, 1982). Calcite infilling the vesicles is probably from  $Ca^{++}$  ions either from the breakdown of the anorthite component of plagioclase and/or from fluid circulating through the surrounding sericite - carbonate - quartz alteration.

The gypsum filled fractures in the core alteration zone have growth fibres perpendicular to their walls, indicative of precipitation from a fluid (Cox and Etheridge, 1983). Solubility data of anhydrite and gypsum in sulphate solutions show that gypsum does not precipitate from a fluid hotter than  $70^{\circ}C$  (Barnes, 1979). These data also indicates that anhydrite has retrograde solubility with decreasing temperature. Simple cooling of a fluid at constant pressure in contact with anhydrite will cause the anhydrite to be altered to gypsum when the



gypsum stability field is intersected (Blount and Dickson, 1973). Therefore, a fluid (probably groundwater) percolating through the deposit will alter anhydrite to gypsum and precipitate gypsum in fractures. The decrease with depth in the number of fractures hosting gypsum is possibly due to the increasingly restricted groundwater flow downward into the anhydrite stockwork.

## 7.0 DESCRIPTION OF SUPERGENE ALTERATION IN THE KERR DEPOSIT

### 7.1 Introduction

Supergene alteration of the Kerr deposit is concentrated in a 'rubble zone' consisting of poker chip shaped pieces of rock. The rubble zone, up to 250 meters deep, is restricted to the central chlorite alteration and minor yellow sericite immediately surrounding the chlorite. This zone grades downward successively to gypsum filled fractures and to anhydrite veins. The 'rubble zone' formed by dissolution of the sulphate and minor carbonate veins by rainwater percolating down through the deposit. This process was modelled with the water - rock reaction geochemical computer program PCPATH (Perkins, 1980) in order to determine constraints, such as the pH of the groundwater, variation in the amount of dissolved copper and gold, and solubility of gypsum in the host rock. Springs draining the rubble zone on the north and south sides of the deposit are precipitating iron oxides that cement overburden and form a ferricrete blanket.

Percentages of supergene limonite, chalcocite and covellite, wad, clay minerals and the zeolite offretite  $[(K,Ca,Mg)_3Al_5Si_3O_6 \cdot 14H_2O]$  in Table 7.1 are from estimates over twenty metre intervals on cross - sections 9700N and 10600N. Figure 7.1 shows their distribution across the deposit. The black line in Figure 7.1 marks the top of the region where sulphates and calcite are not dissolved. Figure 7.2 shows the same data, but displays the rubble zone and unweathered rock beneath it. The profile has been split into four regions distinguished, from top to bottom as: (A) leached Cu and Au, (B) abundant chalcocite and covellite coatings on chalcopyrite, (C) fresh chalcopyrite and pyrite but no gypsum, and (D) competent rock with abundant gypsum veins.

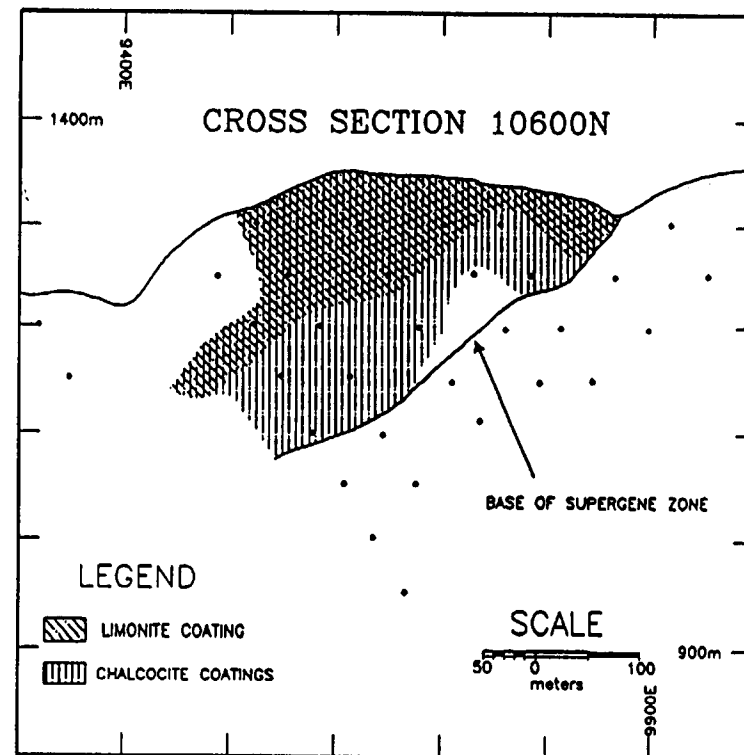
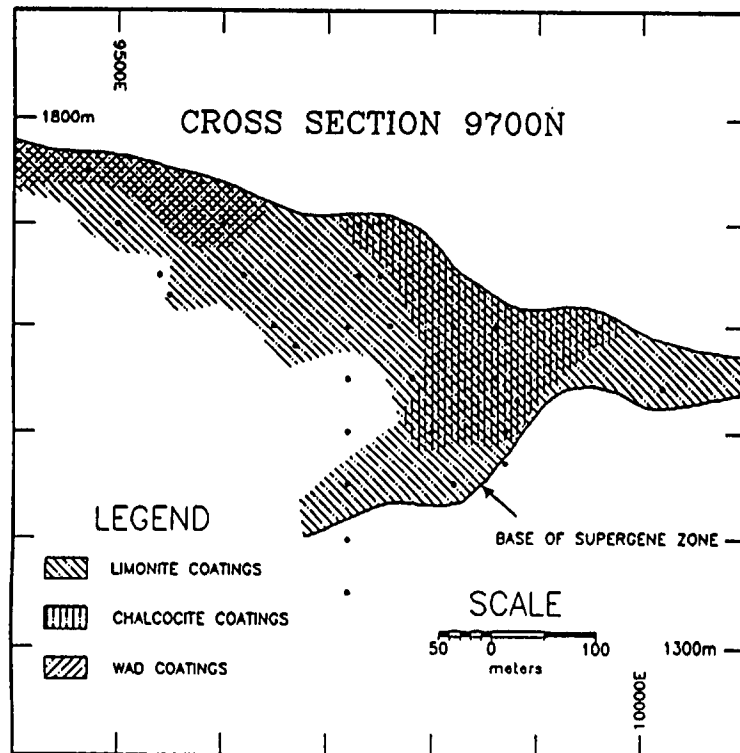


Figure 7.1. Distribution of supergene minerals on sections 9700N and 10600N, Kerr deposit, northwestern British Columbia.

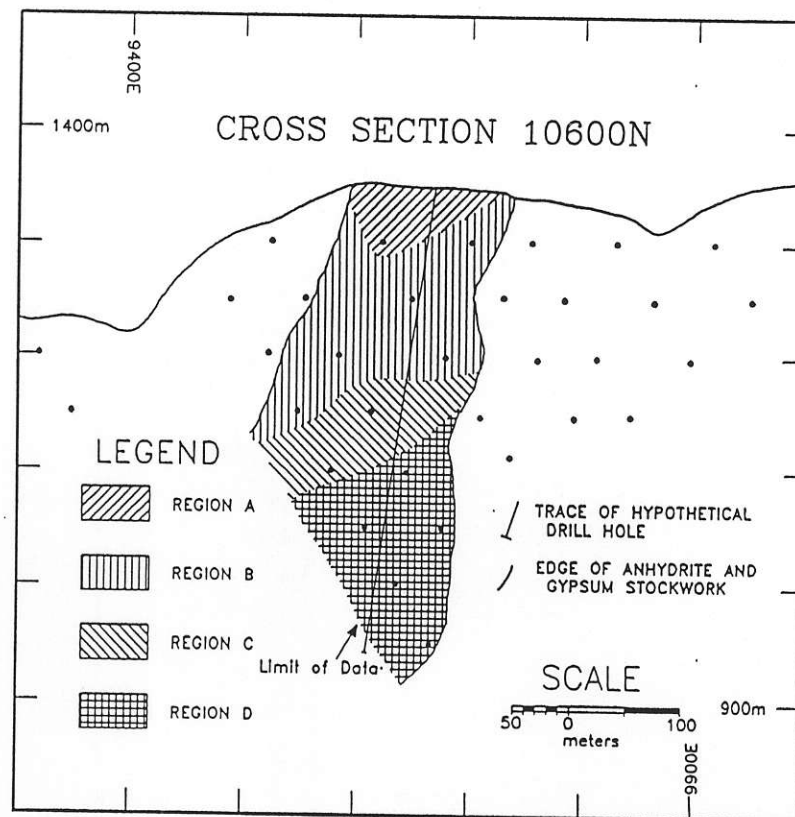
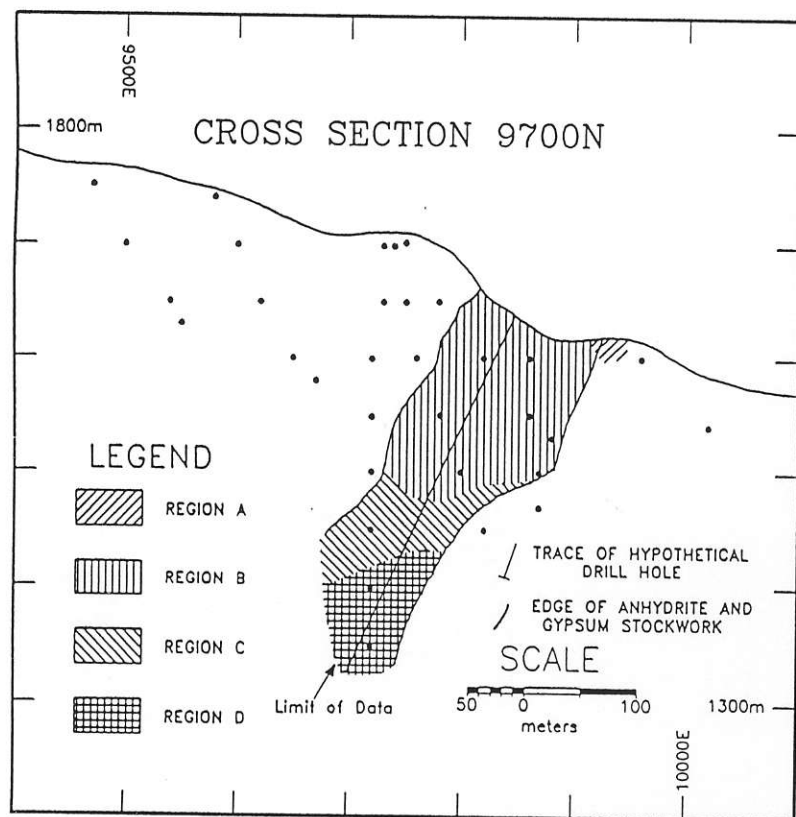


Figure 7.2. Four supergene regions A to D in the pervasive chlorite alteration zone on sections 9700N and 10600N, Kerr deposit, northwestern British Columbia.

## 7.2 Supergene Mineralogy

*Limonite* varies in composition from a bright yellow jarosite in the leached region (A) of section 10600N to pale red hematite coating pyrite grains with chalcocite in region B (Fig. 7.2). In the rubble zone, limonite coats pyrite grains or fills boxwork after pyrite. In competent rock within 50 metres of the surface, limonite coats fracture surfaces, and especially, chalcopyrite and pyrite along sulphide veinlets.

Sericite altered plagioclase grains exposed on surface are stained red from adsorbed iron oxides. Where the calcite is only partially dissolved in veins and extensional quartz veins, the cavities are coated with limonite. Locally these cavities contain yellow-brown, transparent Fe-Ca-Zn carbonates. Their composition was identified by using scanning electron microscopic analysis.

*Chalcocite and covellite* coats chalcopyrite and to a lesser extent pyrite below the leached areas on sections 9700N and 10600N (Fig. 7.2). The transition from limonite coated chalcopyrite and pyrite to copper sulphide coatings occurs within a metre. The apparent strong correlation between chalcocite and covellite, and limonite on Figure 7.1 is spurious, because the minerals do not occur together, but appear to do so when averaged over 20 m intervals.

*Native copper and cuprite* occur in trace quantities on poker chip rock pieces at the top of region B above chalcocite bearing material, or along fractures in green andesite dykes up to 200 metres below surface. The minerals appear to be restricted to regions of high permeability either near surface or in fault zones.

*Wad*, hydrous manganese oxides, forms coatings on fractures up to 50 metres from the surface on the hanging wall of section 9700N. It also occurs in trace amounts on poker chip pieces of pervasive chlorite altered rock on section 10600N immediately below the leached region. The manganese is derived from manganiferous siderite in type 5 sulphate veins and from the weathering of ferromagnesian minerals.

*Zeolite*, offretite  $[(K,Ca,Mg)_3Al_5Si_3O_6 \cdot 14H_2O]$ , is cream coloured, but locally stained pale blue where it occurs with chalcocite (region B). It cements poker chip shaped

Table 7.1. Percentages of alteration and supergene minerals intersected by a hypothetical flow path through the Kerr deposit, northwestern British Columbia.

POSITION ALONG DRILL HOLE (metres)	REGION	COPPER (wt%)	GOLD (ppm)	TOTAL MAGNETITE AND HEMATITE (%)	TOTAL PYRITE (%)	TOTAL LIMONITE (%)	TOTAL CHALCOPYRITE (%)	CHALCOHITE AND COVELLITE (%)
10	A & B	0.4	0.27	SECTION 9700N 0	4.7	3.1	0	0.74
50	B	0.54	0.42	0.32	9.7	0.33	0.51	0.27
115	B	0.8	0.49	0	8.4	0.003	1.66	0.00049
285	D	1.23	0.56	0.05	14.7	0	2.3	0
5	A	0.065	0.13	SECTION 10600N 0	8	0.078	0	0.05
95	B	0.72	0.31	1	5.6	0.006	0.55	0.27
225	C & D	0.61	0.31	0.6	8	0	1.43	0
320	D	0.61	0.31	2.8	7.8	0	1.25	0
POSITION ALONG DRILL HOLE (metres)	REGION	TOTAL CARBONATE (%)	PYROLUSITE (%)	TOTAL ANHYDRITE AND GYPSUM (%)	TOTAL CHLORITE (%)	OFFERITE (%)	TOTAL CLAY MINERALS (%)	TOTAL SERICITE (%)
10	A & B	0	0	SECTION 9700N 0	0.17	0.36	10.4	32.4
50	B	0.26	0	0	1	0.00014	5.9	24.6
115	B	1.47	0	0	0.49	0.001	6.9	16.6
285	D	0.79	0	1.4	3.3	0	0.72	33.3
5	A	0	0	SECTION 10600N 0	0.77	0.23	7.9	39.8
95	B	0.12	0.0063	0	11.6	0.74	2.7	26.6
225	C & D	0.48	0	5.2	6.7	0	6.1	32.9
320	D	0.31	0	5	4.7	0	2.3	31.1

rock chips in the core alteration zone up to a depth of 100 metres (mainly in regions A to C). This mineral also fills voids left by dissolved calcite in extensional quartz - carbonate veins in post-mineral dikes that cut the core alteration zone.

*Clay* minerals were rarely observed on poker chip shaped pieces of pervasive chlorite altered rock. However, weathered samples of yellow sericite - quartz - pyrite alteration have a strong earthy smell when wetted. The sericite was coated with a dusty white clay, possibly kaolinite. Trace amounts of gibbsite were identified using X-ray diffraction of weakly weathered flakes of sericite - quartz - pyrite rock.

### 7.3 Geochemical Modelling

Percentages of supergene and hypogene minerals along a possible groundwater flow path are in Table 7.1. The groundwater flow path is marked by the trace of a hypothetical drill hole on cross - sections 9700N and 10600N (Fig. 7.2). The flow path was restricted to the central core alteration zone because this zone contains sulphates, which after their dissolution becomes rubble that is very permeable compared to the intact rock on either side. Evidence for its permeable nature is that the core recovery from the rubble zone is poor due to the loss of water from the drill bit.

The drill hole on section 9700N is 300 m south and 20 m below the crest of the ridge hosting the deposit. Groundwater, in mountainous terrain, flows vertically downward at the ridge crest and outward along either side of the ridge (Freeze and Cherry, 1979). Thus groundwater will flow downward beneath the ridge below Kerr Peak before flowing toward the south below the collar of the hypothetical drill hole in section 9700N. Thus, groundwater will flow parallel to the north facing slope on section 10600N. The composition of the alteration assemblages to the south of section 10600N are the same as this section; therefore, the fluid was assumed to have the same composition as if the groundwater had flowed

Table 7.2. Starting and equilibrium solutions for geochemical modeling of supergene process in the Kerr deposit, northwestern British Columbia.

	Starting solution	Equilibrium solution
	ACTIVITY	ACTIVITY
O <sub>2</sub> (gas)	0.2	3.7 x 10 <sup>-66</sup>
CO <sub>2</sub> (gas)	0.003	0.114
pH	5.6	6.3
Ca <sup>2+</sup>	2.42 x 10 <sup>-5</sup> m *	1.6 x 10 <sup>-2</sup> m
K <sup>+</sup>	6.6 x 10 <sup>-6</sup> m *	2.2 x 10 <sup>-3</sup> m
Cl <sup>-</sup>	4.7 x 10 <sup>-5</sup> m *	3.1 x 10 <sup>-5</sup> m
SO <sub>4</sub> <sup>2-</sup>	1.25 x 10 <sup>-5</sup> m *	6.2 x 10 <sup>-3</sup> m
H <sub>3</sub> SiO <sub>4</sub> <sup>-</sup>	1.0 x 10 <sup>-10</sup> m *	2.3 x 10 <sup>-8</sup> m
Fe <sup>2+</sup>	2.0 x 10 <sup>-30</sup> m \$	1.5 x 10 <sup>-6</sup> m
Mn <sup>2+</sup>	1.0 x 10 <sup>-30</sup> m \$	2.4 x 10 <sup>-4</sup> m
Cu <sup>2+</sup>	1.3 x 10 <sup>-30</sup> m \$	1.2 x 10 <sup>-20</sup> m
Au <sup>+</sup>	1.0 x 10 <sup>-30</sup> m \$	5.3 x 10 <sup>-31</sup> m
Al <sup>3+</sup>	2.0 x 10 <sup>-30</sup> m \$	7.2 x 10 <sup>-12</sup> m

(\*) Values from Kwong (1987)

(\$) Values set to very low numbers are constrained by precipitation of hematite, gibbsite, native gold and pyrolusite.



vertically. Drill holes on the slope below section 10600N, which intersect the rubble zone, act as artesian wells. Water from these holes precipitate iron oxides.

### 7.3.1 PCPATH computer program

The computer program, PCPATH, calculates the distribution of aqueous species in 1.0 kg of water after dissolving an increment of a stipulated mineral assemblage (Helgeson et al., 1970; Perkins, 1980). The 1.0 kg of water contains a concentration of ions specified to the reacting solution. The amount of the each increment of dissolved minerals is proportional to the progress of the reaction variable XI. The distribution of aqueous species is calculated by balancing two independent matrices for the total moles in the system of each component and total ionic charges for each species. Electroneutrality of the chemical reactions is maintained by having an excess of one ion (Cl in this model) balance the charges. The program then calculates log Q values from the ionic species and compares them to log K values of minerals composed of the components. If the log Q value exceeds log K, the mineral precipitates and it is added to the product side of the reaction for the next increment.

The next increment recalculates the distribution of species with a larger amount of mineral assemblage but the program adds the new product to the list of ionic species in the matrices. If the log Q value becomes less than the log K, the new mineral is added to the reactant side of the equation and the mineral dissolves. The solution is in equilibrium once all of the reacting minerals stabilize in the solution.

### 7.3.2 Assumptions required for modelling the reactions between host rock and fluid

Several key simplifying assumptions had to be made in order to use the PCPATH computer program, and to apply the results to the development of the rubble zone in the Kerr deposit: (a) temperature and pressure of the fluids was held constantly at 25°C and 1 bar fluid

pressure during the run of the computer model; (b) chemical reactions between ionic species and host rock were assumed to be instantaneous and at equilibrium for each increment of dissolution (log XI); (c) The reactions between dissolving minerals in 1.0 kg of water was applied to the flow of groundwater from surface to a depth of 250 m; (d) no Fe-rich chlorite was allowed to react with the groundwater in the rubble zone, and the sericite was assumed to be muscovite instead of phengite. The reacting mineral assemblage consisted of quartz, muscovite, hematite, pyrite, chalcopryite, carbonate (95% siderite and 5% rhodocrosite) and native gold.

Assumption (a), above, is required because the geochemical data set used in this model has only standard room temperature and pressure conditions for certain Fe-sulphate minerals. Kinetic controlled reactions are not calculated by the program so minor temperature differences should not affect the results. However, the grain size of the dissolving grains is known to control the extent of fluid rock interaction to such an extent that the precipitation of goethite, hematite and jarosite is affected (Bladh, 1978). The depth of the water table along the hypothetical drill hole is not known, but the presence of a small lake 50 m north of the eastern edge of section 9700N suggests that the water table is close to surface. A creek runs along the edge of the rubble zone intersected by section 10600N. The water table is apparently close to the surface otherwise the stream would flow underground.

Assumption (b), above, is known to be a gross simplification of the behaviour of chemical reactions (Lasaga, 1989); however, the results can still be applied to the Kerr deposit (see assumption (c)).

Assumption (c), above, is valid considering the downward flow of one droplet of fluid through the permeable rubble zone. Initially the droplet would encounter and react with a small fraction of the host rock: namely muscovite, pyrite, chalcopryite, siderite, rhodocrosite, native gold and gypsum. As the droplet proceeded downward, it would continue to react and precipitate minerals as it encountered more rock; therefore, the proportion of (dissolved) rock

to fluid increases as the droplet proceeds downward. This increase in rock to fluid ratio describes the progress variable log XI of the PCPATH program.

Assuming that Fe-chlorite does not react with the rain water and later groundwater is based upon the observation that the chlorite exposed on surface at the Kerr deposit is not supergene altered. The thermodynamic properties of pure chamosite (Fe-chlorite) suggests that it is a stable mineral at surface conditions. Substitution of phengite by muscovite was done due to the lack of thermodynamic data for phengite. The Fe and Mg substitution in phengite increases the stability of the mineral at low temperatures; therefore, replacing phengite by muscovite may over estimate the importance of a phyllosilicate in the model.

### 7.3.3 Geochemical model results

Modified rainwater (Table 7.2) was reacted with quartz, gypsum, muscovite, hematite, carbonate (95% siderite and 5% rhodocrosite), pyrite, chalcopyrite and gold in order to describe the variation in solution chemistry in the rubble zone. The mineral assemblage reflects the dominant minerals in the chlorite alteration zone. Absolute amounts of individual minerals in the assemblage appeared not to reflect a change in the solution chemistry in the model.

The starting solution has very low  $\text{Fe}^{2+}$  and  $\text{Cu}^{2+}$  ion concentrations compared to the concentration of sulphate and silica in rain water, otherwise the PCPATH program would immediately supersaturate with hematite and the model would not proceed.

The sequence of minerals precipitating from the reactions are in Table 7.3. Figures 7.3 and 7.4 show the variation in the solution chemistry during the run.

Hematite precipitates first from dissolution of the reacting assemblage (reaction 1, Table 7.3). Continuous precipitation of hematite occurs until all of the dissolved  $\text{O}_2(\text{aq})$  in solution is consumed (reaction 7). After this point, hematite either slowly precipitates in an

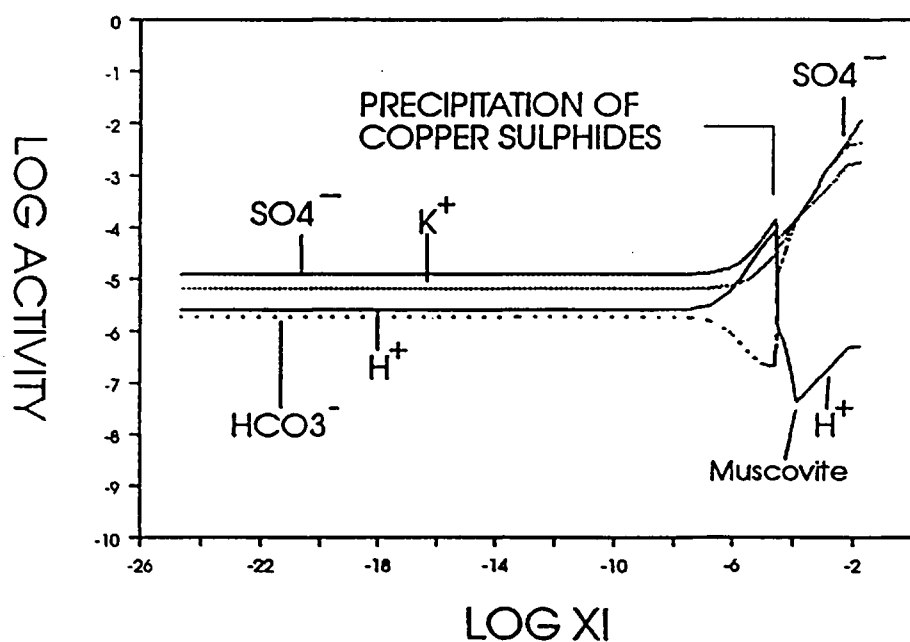
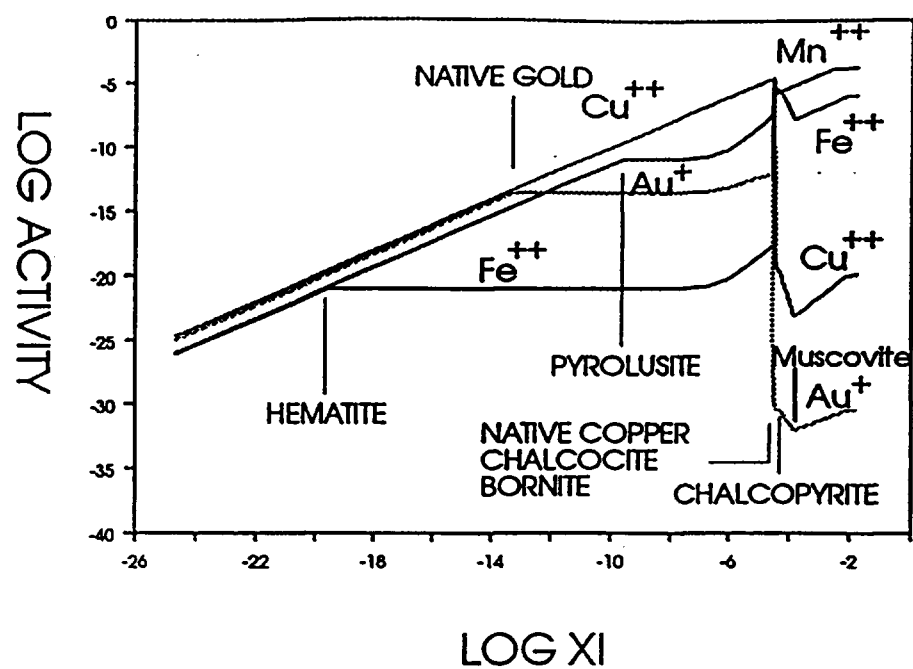


Figure 7.3. a) Variation of log molality of  $\text{Cu}^{2+}$ ,  $\text{Fe}^{2+}$ ,  $\text{Mn}^{+}$ ,  $\text{Au}^{+}$  ions versus Log XI.  
 b) Variation of log molality of  $\text{H}^{+}$ ,  $\text{HCO}_3^{-}$ ,  $\text{Ca}^{2+}$  and  $\text{SO}_4^{2-}$  versus Log XI.

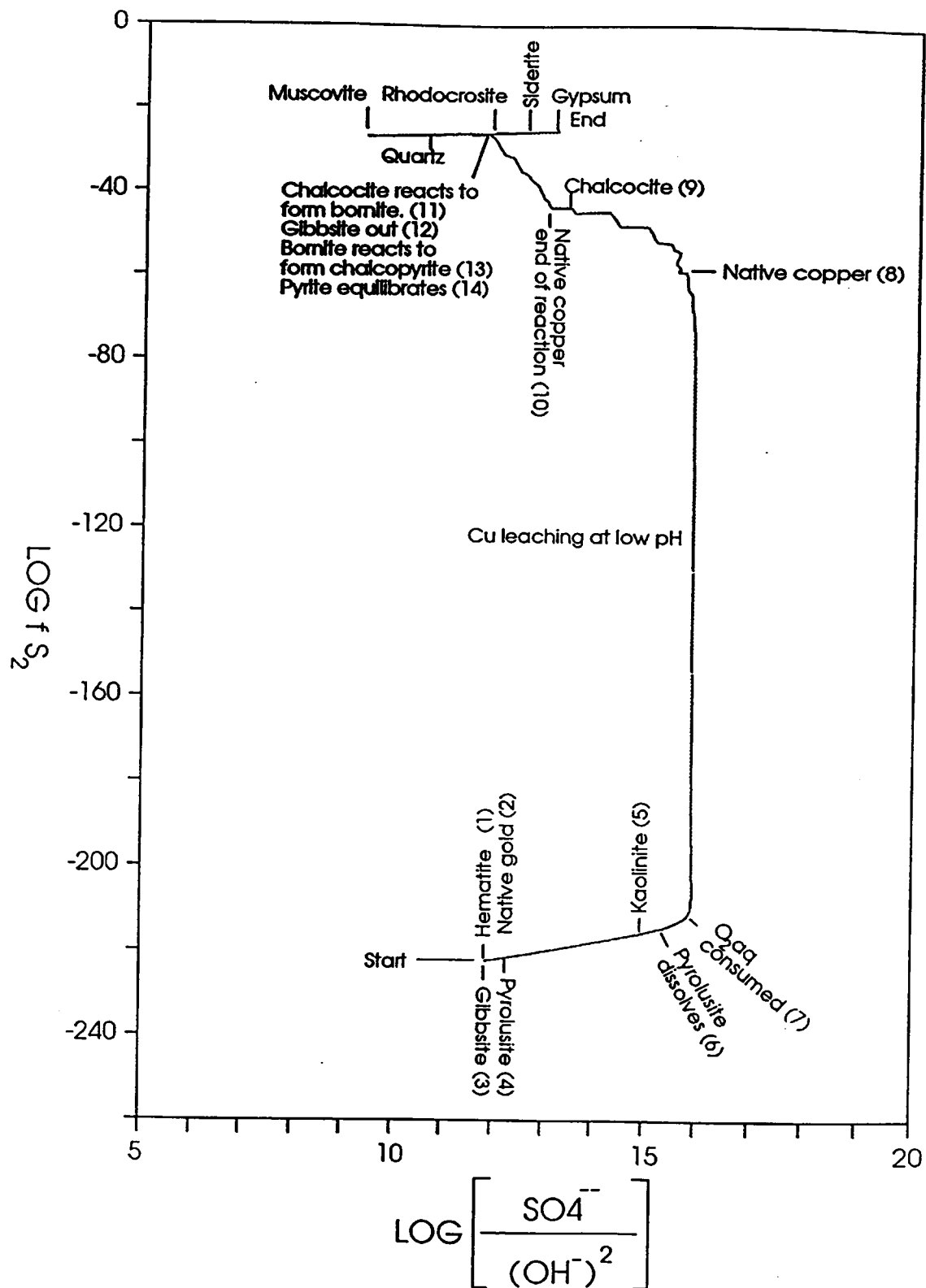


Figure 7.4. Variation in  $\log f(S_2)$  and  $\log [SO_4^{2-}/(OH^-)^2]$  during the PCPATH model.

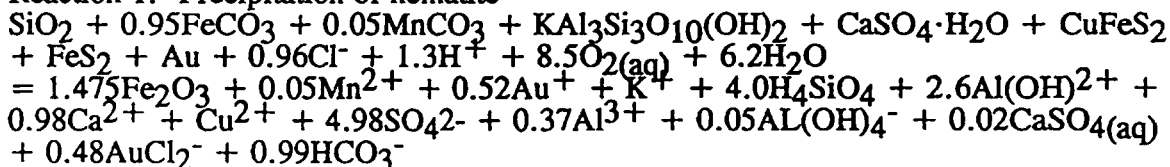
Table 7.3. List of chemical reactions for supergene processes on the Kerr deposit, northwestern British Columbia. (Specified reactions are referred to in text and on figures).

Disolution of rock consisting of: quartz, muscovite, gypsum, 0.95 siderite and 0.05 rhodocrosite, pyrite, chalcopyrite and gold.

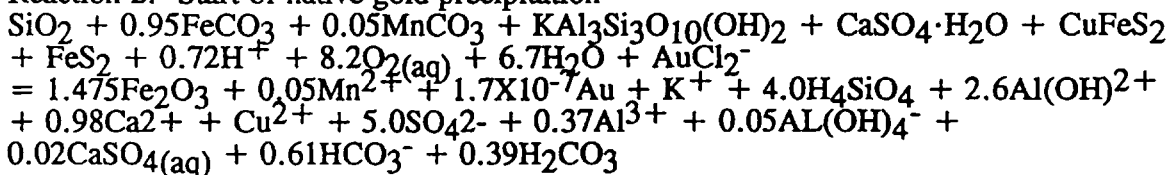
#### ABBREVIATIONS AND CHEMICAL FORMULAS

Quartz	$\text{SiO}_2$
Muscovite	$\text{KAl}_3\text{Si}_3\text{O}_{10}(\text{OH})_2$
Gibbsite	$\text{Al}(\text{OH})_3$
Kaolinite	$\text{Al}_4\text{Si}_4\text{O}_{10}(\text{OH})_8$
Chalcopyrite	$\text{CuFeS}_2$
Bornite	$\text{Cu}_5\text{FeS}_4$
Chalcocite	$\text{Cu}_2\text{S}$
Native copper	$\text{Cu}$
Pyrite	$\text{FeS}_2$
Hematite	$\text{Fe}_2\text{O}_3$
Rhodocrosite	$\text{MnCO}_3$
Pyrolusite	$\text{MnO}_2$
Siderite	$\text{FeCO}_3$
Native gold	$\text{Au}$
Gypsum	$\text{CaSO}_4 \cdot \text{H}_2\text{O}$

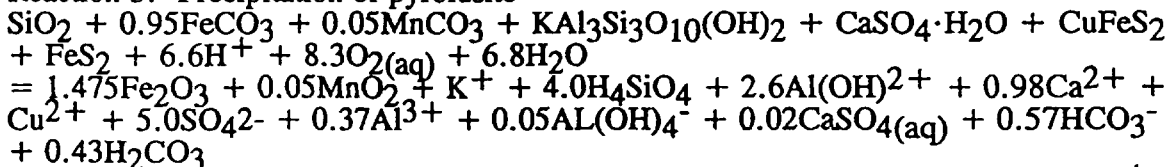
#### Reaction 1: Precipitation of hematite



#### Reaction 2: Start of native gold precipitation



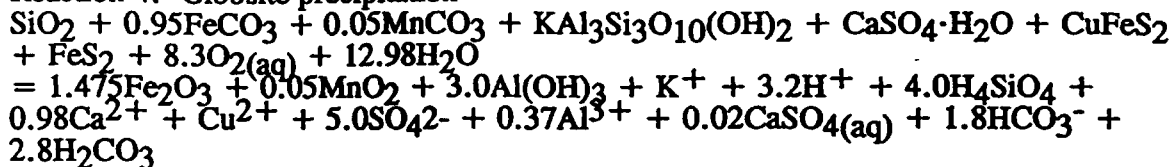
#### Reaction 3: Precipitation of pyrolusite



Replacement of rhodocrosite by pyrolusite in an oxidizing fluid which consuming  $\text{H}^+$ .  
Trace amounts of native gold precipitate.

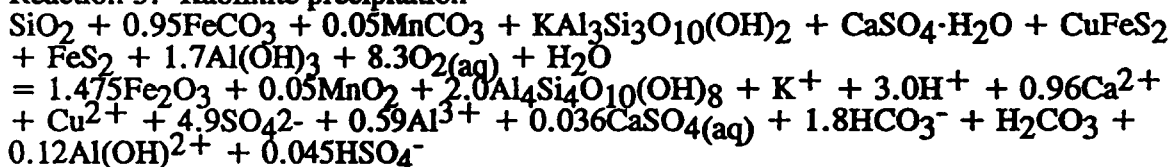
Table 7.3. cont'd

## Reaction 4: Gibbsite precipitation



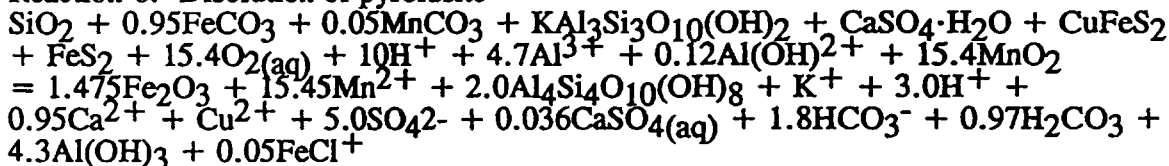
Gibbsite precipitates as fluid consumes more  $\text{O}_{2(\text{aq})}$ . Trace amounts of native gold dissolves as remaining solution acidifies.

## Reaction 5: Kaolinite precipitation



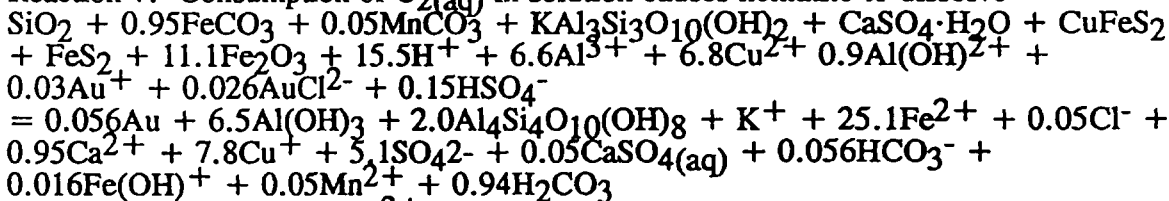
Gibbsite reacts with an acidic solution to precipitate kaolinite and more gold dissolves.

## Reaction 6: Disolution of pyrolusite



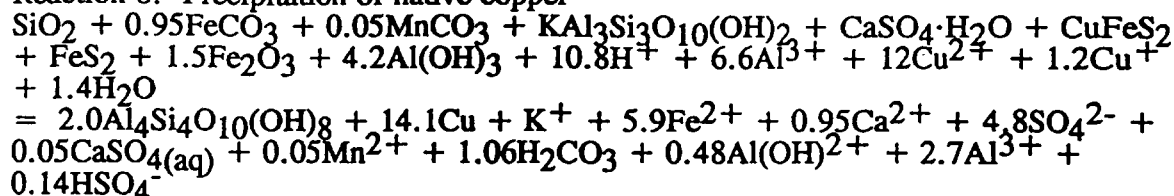
Disolution of pyrolusite is followed by trace amounts of native gold precipitating.

Disolution reactions consume more  $\text{O}_{2(\text{aq})}$  and  $\text{H}^+$  in solution.

Reaction 7: Consumption of  $\text{O}_{2(\text{aq})}$  in solution causes hematite to dissolve

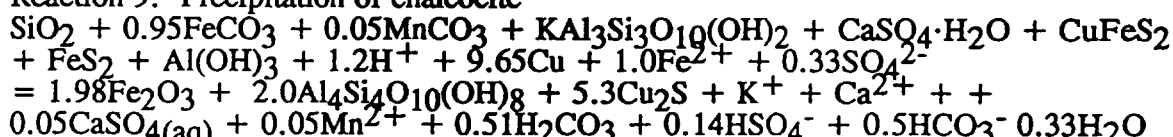
Reducing solution causes  $\text{Cu}^{2+}$  to be reduced and most of gold in solution to be precipitated.

## Reaction 8: Precipitation of native copper



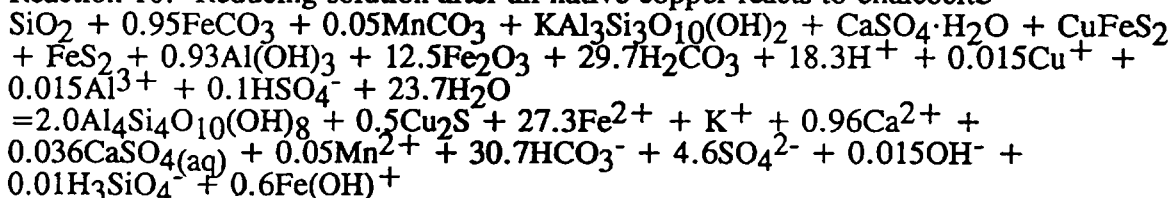
Hematite dissolves and acid is consumed while native copper precipitates in reducing solution and gibbsite reacts to kaolinite.

## Reaction 9: Precipitation of chalcocite



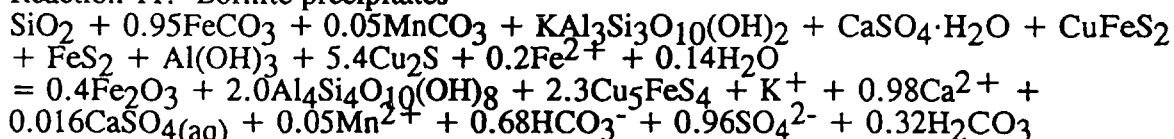
Consumption of native copper in an oxidizing solution is coupled with precipitation of chalcocite and hematite.

## Reaction 10: Reducing solution after all native copper reacts to chalcocite



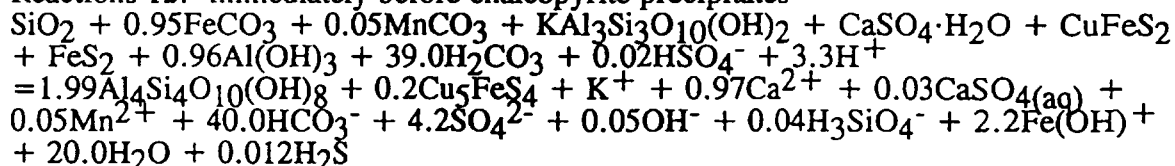
Chalcocite and kaolinite precipitates while hematite and gibbsite dissolves in reducing solution.

## Reaction 11: Bornite precipitates



Chalcocite reacts with bornite and minor hematite precipitates.

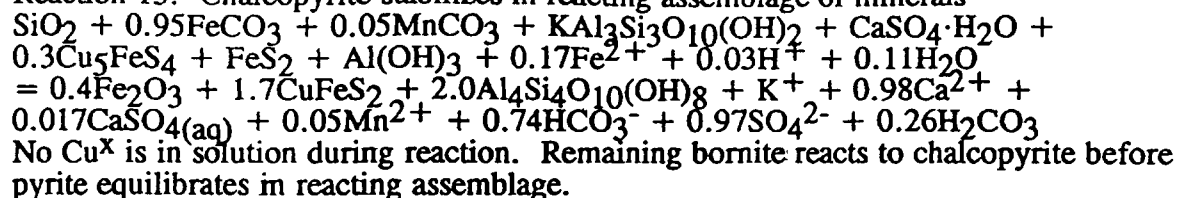
## Reactions 12: immediately before chalcopyrite precipitates



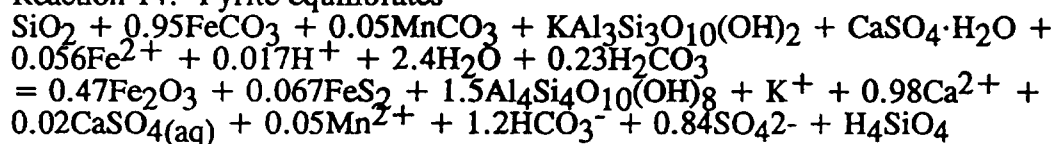
Hematite dissolve and gibbsite reacts to kaolinite.



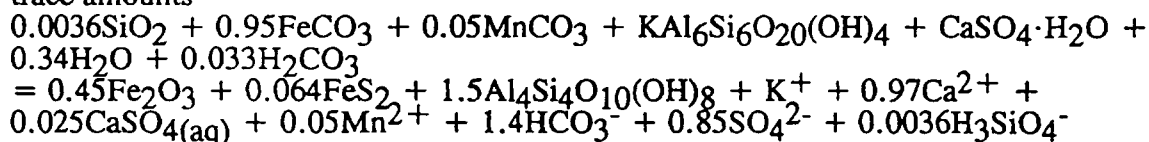
Reaction 13: Chalcopyrite stabilizes in reacting assemblage of minerals



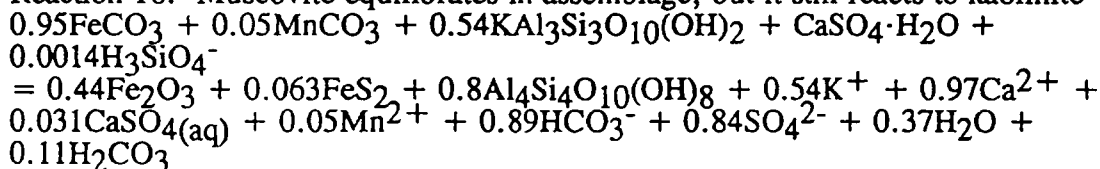
Reaction 14: Pyrite equilibrates



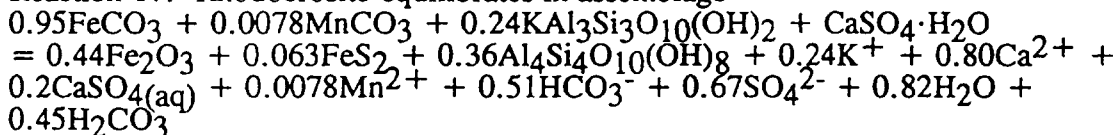
Reaction 15: Quartz equilibrates in assemblage, but it still dissolves into solution in trace amounts



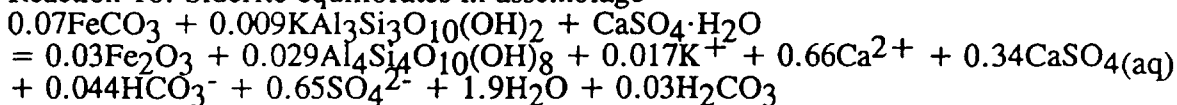
Reaction 16: Muscovite equilibrates in assemblage, but it still reacts to kaolinite



Reaction 17: Rhodocrosite equilibrates in assemblage



Reaction 18: Siderite equilibrates in assemblage



Gypsum equilibrates

oxidizing fluid or dissolves in a reducing one. Hematite is reduced to  $\text{Fe}^{2+}$  when native copper precipitates or when chalcopyrite is replaced by chalcocite (reaction 10).

Native gold precipitates once the activity of  $\text{Au}^+$  increases to approximately  $10^{-14}$ . It subsequently dissolves once the solution becomes more acidic when kaolinite precipitates. The highest concentration of gold in solution occurs immediately before pyrolusite dissolves (reaction 6). The dissolved gold precipitates in trace amounts until chalcopyrite stabilizes in the host rock. The highest concentration of  $\text{Au}^+$  in solution is roughly  $10^{-7}$  ppm.

Gibbsite precipitates as more muscovite dissolves and reacts with aqueous oxygen (reaction 3). Minor amounts of gibbsite are later replaced by kaolinite (reaction 5). Gibbsite does not completely convert to kaolinite until the solution stabilizes muscovite, pyrite and chalcopyrite.

When the amount of  $\text{O}_2(\text{aq})$  suddenly decreases in activity, the solution changes from oxidizing to reducing. At this point,  $\text{Cu}^{2+}$  ions are reduced to  $\text{Cu}^+$ , hematite dissolves and most of the gold in solution precipitates (reaction 7). The sudden decrease in  $\text{O}_2(\text{aq})$  in solution represents the water table boundary in the model. Reactions in an oxygen rich environment represent those that take place above the water table in the capillary zone.

Native copper precipitates when the  $\log(f\text{S}_2)$  is more than -60 by the reduction of  $\text{Cu}^{2+}$  and  $\text{Cu}^+$  in solution and there is a minor component of chalcopyrite. This reducing solution also causes hematite to dissolve and the acidity of the fluid to decrease.

Chalcocite initially replaces native copper in an oxidizing solution (reaction 9) that subsequently turns into a reducing one once all the native copper is consumed (reaction 10). The pH of the reducing solution increases during the reaction causing most of the remaining Cu in solution to precipitate as chalcocite; however, nearly 99% of the Cu for chalcocite is derived from chalcopyrite. Hematite and gibbsite dissolve during the reaction, while more kaolinite precipitates. The amount of sulphate in solution decreases with this reaction by the reduction of sulphate to sulphide.

Bornite replaces chalcocite with minor amounts of hematite precipitating and gibbsite reacting to form kaolinite. After all chalcocite is consumed, chalcopyrite alters to bornite in a reducing fluid which also alters pyrite to  $\text{Fe}(\text{OH})^+$ . When chalcopyrite is in equilibrium with the fluid, the remaining bornite reacts to chalcopyrite removing  $\text{Fe}^{2+}$  from solution. The  $\text{Cu}^{2+}$  ion activity has dropped from roughly  $10^{-5}$  to  $10^{-20}$  during the precipitation of the native copper and copper sulphides, whereas the  $\text{Fe}^{2+}$  has increased from roughly  $10^{-19}$  to  $10^{-7}$ . The increase in activity of  $\text{Fe}^{2+}$  is due to the precipitation of chalcocite in a reducing fluid that reduced hematite to  $\text{Fe}^{2+}$  (reaction 10).

Pyrite followed by quartz, muscovite, rhodocrosite and siderite stabilize in the solution before the gypsum equilibrates. Pyrite and hematite still precipitate in all reactions until siderite is in equilibrium with the fluid.

Once equilibrium between the solution and the starting mineral assemblage has been obtained, the solution has higher molalities of all ions than the rainwater except for  $\text{Au}^+$  and  $\text{H}^+$ . The pH of the equilibrium solution is at 6.3 when it started at 5.6. Only gypsum is very soluble in the solution. Its components are concentrated as  $\text{Ca}^{2+}$ ,  $\text{SO}_4^{2-}$  and  $\text{CaSO}_4(\text{aq})$  ions at 623, 1432 and 977 ppm respectively.

#### 7.4 Application of Model Results to the Formation of the 'Rubble Zone' in the Kerr deposit

In general, the PCPATH modeling of the supergene alteration describes the processes active in the Kerr deposit; however, there are several limitations. Average mean temperature of the deposit is less than  $25^\circ\text{C}$  so that chemical reactions will be slower than the model. This may cause the supergene alteration to miss some of the reactions specified in Table 7.3 and produce false reaction fronts: for example bornite was not observed in the Kerr deposit, but the model indicates that it exists. The mineral reactions in Table 7.3 do not predict that some of the sulphides and silicates will react completely; whereas, the field observations indicate the pyrite remains in several of the regions where it is unstable. This pyrite will react with groundwater flowing through the deposit, but the products of the reaction will be different than the model because all of the reacting minerals are not present. Therefore, application of the PCPATH model results to the supergene processes in the Kerr deposit in areas where one reacting mineral dominates others is not justified. The reacting minerals in the supergene alteration zone (region D) are evenly distributed such that one mineral does not dominate the assemblage.

The major minerals observed in intervals along the hypothetical flow paths through the Kerr deposit show that region A, located at the top of both sections, has lower Cu and Au assays than the intervals beneath them. The apparent lowering of Cu and Au assays at the top of section 10600N is possibly due to the rock not containing abundant mineralization prior to supergene alteration. The total chlorite and total magnetite and hematite indicate that this interval is not completely within the central chlorite core (Table 7.3). The rock in region A is leached; abundant clay replaces sericite; there are trace amounts of chalcocite. Reactions 1 to 7 describe the processes active in this region.

Region B is dominated by pyrite and chalcocite with minor chalcopyrite and abundant pyrite remaining. The copper grade of this region on section 10600N is slightly elevated with respect to the unweathered mineralization below it (Table 7.3). Rare blebs of native copper were identified at the top of the region. The rare occurrence of native copper is supported by the observation that the small leached zones above the region were not extensively mineralized. Thus, the groundwater is not transporting abundant Cu in solution to region B. The top part of the region on both sections has alternating hematite and chalcocite patches along sulphide veinlets. Lower in the region, chalcocite patches are larger and dominate the supergene assemblage. Reaction 9 describes the possible association of hematite and chalcocite; reaction 10 explains the predominance of chalcocite over hematite. The PCPATH model does not predict the presence of covellite in the supergene assemblage. This problem may be due to the fact that the precipitation of covellite rims on chalcopyrite is controlled by different processes than what is described in the model. Trace amounts of wad (pyrolusite) occur in the top portion of region B on section 10600N. In this area, partially leached siderite in extension and quartz veins may be the source of Mn for the pyrolusite. The absence of pyrolusite from the remainder of the region is because pyrolusite is not stable because of reaction 6.

Region C varies in thickness from 10 to 60 metres. The region is characterized by chalcopyrite and pyrite on flakes of altered rock. The grade of the mineralization is the same as unweathered rock. The PCPATH model indicates that only a trace amount of Cu is in solution with moderate amounts of Fe and abundant sulphate. The groundwater in equilibrium with gypsum in fractures contains up to 19 mg of dissolved gypsum per 1.0 kg of water. The high solubility of the gypsum would allow the dissolution front to propagate quickly into the adjacent wall rock if there were abundant gypsum filled fractures. Therefore, the depth and extent of the supergene alteration in the Kerr deposit is controlled by the presence and subsequent dissolution of gypsum in the rock. Below the line of gypsum dissolution, gypsum replaces anhydrite in the rock.

## 7.5 Discussion of Supergene Alteration

Computer modeling of gypsum dissolution in a rock containing muscovite, quartz, hematite, pyrite, chalcopyrite, siderite and rhodocrosite reflects the observations that the depth of supergene weathering in the Kerr deposit is controlled by the presence of gypsum filled fractures. When the gypsum dissolves, the rock increases in permeability. This allows more groundwater to flow into the deposit and dissolve more gypsum. Above the dissolution front, chalcopyrite is in equilibrium with the fluid and the total dissolved Cu is very low compared to Fe. This dissolved Fe is transported towards springs that drain the rubble zone where it reacts with  $O_2(aq)$  in the surface water and atmospheric  $O_2$  to precipitate iron oxides that form the ferricrete below the springs on the deposit.

The chalcocite and covellite blanket in the Kerr deposit results from alteration of chalcopyrite to chalcocite and covellite below the water table. Only a small proportion of the chalcocite is due to dissolved Cu from leached regions above the water table. The mineralogy of the region is the same as in enriched blankets of other porphyry Cu deposits in the southwestern United States (Guilbert and Park, 1986).

Rock on either side of the rubble zone is not weathered as deeply except along fractures and faults. These features have limonite stains with minor amounts of calcite being dissolved. Except for the faults and fractures, the rock has very low permeability where compared to the rubble zone; therefore, relatively little groundwater can pass through the rock compared to the rubble zone. Thus, supergene alteration outside of the rubble zone is generally restricted to a 50 m thick layer below surface.

## 8.0 SUMMARY AND CONCLUSIONS

The Kerr deposit is a deformed Early Jurassic copper - gold porphyry deposit hosted by a steeply dipping sequence of Late Triassic Stuhini Group sediments and volcanoclastic rocks. The porphyry deposit is part of a volcanoplutonic arc along the western edge of the Stikine terrane. Magmatic and hydrothermal activity in the deposit is related to intermediate calc-alkaline dykes related to the Early Jurassic Texas Creek plutonic suite.

Early alteration recognizable in the high grade core of the Kerr deposit is pervasive, texturally destructive potassic alteration. This alteration consists of biotite with disseminated chalcopyrite and minor magnetite forming envelopes around magnetite and bull quartz veins. Pervasive K-feldspar flooding forms a halo to these regions with minor chalcopyrite. Early alteration in the halo consists of patchy, pervasive K-feldspar flooding which grades outward to propylitic alteration. This sequence of early alteration from a potassic core surrounded by propylitic alteration is typical of early, high temperature alteration surrounding monzonite to quartz monzonite porphyry intrusions in the southwest United States and Philippines (Beane, 1982; Sillitoe and Gappe, 1984).

Monzonite dykes intruded the early potassic and propylitic alteration. These dykes were subsequently altered in the core and halo alteration zones to sericite - quartz - pyrite. Alteration of the dykes occurred during fracturing of the potassic alteration and precipitation of banded quartz followed by sulphide veins. These veins are concentrated around the margins of the dykes which suggests that the dykes were a focus for the fluids. Chlorite envelopes around the sulphide veins in the core alteration suggest that the fluids forming the sulphide veins also altered the early potassic alteration. During the sulphide veinlet phase of mineralization, the Kerr deposit was intruded by syenodiorite dykes ( $197 \pm 3.0$  Ma) related to the earlier monzonite. Anhydrite - quartz - siderite - pyrite - chalcopyrite veins with chlorite selvages

and subsequent pink anhydrite - chalcopyrite - molybdenite veins overprinted the retrograded potassic assemblage in the core alteration zone. Carbonate - quartz - pyrite - tetrahedrite - sphalerite - galena veins formed in the halo and peripheral alteration zones.

Syn-mineralization augite to hornblende porphyry dykes intruded the deposit parallel to the dip of the mineralization. These dykes have a different modal mineralogy, which suggests that they were derived from a different igneous source than the earlier monzonite dykes.

K-Ba-feldspar megacrystic plagioclase hornblende porphyry dykes ( $195 \pm 1.5$  Ma) intruded the peripheral and halo alteration zones of the Kerr deposit before the carbonate veins ceased to form. All copper - gold mineralization was cut subsequently by a north striking, west dipping, albite megacrystic plagioclase hornblende porphyry dyke. This dyke has a similar rare earth element signature as the K-Ba-feldspar megacrystic dyke, but it contains albite megacrysts and interstitial quartz instead of K-Ba feldspar megacrysts and reabsorbed quartz phenocrysts.

Tholeiitic aphanitic intermediate dykes were emplaced in the deposit along east-west striking fractures that cut all previous dykes. These dykes are possibly related to crustal extension possibly during the Early Jurassic in the Sulphurets gold camp.

Deformation of the Kerr deposit occurred during southwesterly directed shortening and southeasterly directed extension in the Late Jurassic to Early Tertiary. This major period of deformation possibly formed the southeasterly vergent Sulphurets thrust fault and the McTagg anticlinorium. The deformation coincided with lower greenschist metamorphism of the Sulphurets gold camp. The temperatures of this metamorphism are the same as experienced by the Kerr deposit during retrograde alteration but at a higher lithostatic and hydrostatic pressure. The prominent foliation in the Kerr deposit is due to extensive recrystallization of phyllosilicate minerals during deformation. Pyrite remained relatively undeformed whereas tetrahedrite-tennantite, chalcopyrite and gold underwent pressure solution and precipitated in pressure shadows around broken pyrite grains. Copper and gold mineralization was

extensively remobilized into local pressure shadows, but was only weakly concentrated in quartz extension veins.

The extensive recrystallization during Late Jurassic to Early Tertiary deformation did not destroy the original alteration zoning in the Kerr deposit. Therefore, the relative abundance of alteration minerals estimated along intervals of drill holes through the deposit reflect the extent of magmatic and hydrothermal alteration (Fig. 8.1). This has allowed the recognition of alteration zoning in an intensely deformed deposit.

Supergene alteration of the Kerr deposit was focused on the anhydrite stockwork in the elongate core of the deposit. Hydration of the disseminated and vein anhydrite to gypsum caused the foliated rock to swell and fracture along foliation planes. Saturated sulphate solutions precipitated gypsum in these fractures. The downward propagating hydration front was followed by a gypsum dissolution front. Rapid dissolution of gypsum by groundwater left a fractured, rubbly rock that allowed rapid oxidation of the contained sulphide minerals.

Three supergene alteration zones developed in the region of dissolved gypsum filled fractures: (i) leached hematite/jarosite, (ii) minor native copper and coatings of chalcocite and covellite, and (iii) stable chalcopyrite and pyrite without gypsum or anhydrite. Computer modelling of irreversible chemical reactions between minerals and aqueous species using the program PCPATH indicated that copper from the leached zone precipitated in the chalcocite zone below the water table. The minor amounts of chalcocite coating chalcopyrite in the chalcocite zone could be due to oxidation of the chalcopyrite rather than addition of copper from above. The region of stable chalcopyrite and pyrite, but no gypsum, is due to the high sulphate content of groundwater, which also had a high  $f(S_2)$ .



# Porphyry Stage Alteration

(Modified by: Deformation, Regional Metamorphism, and Supergene Alteration)

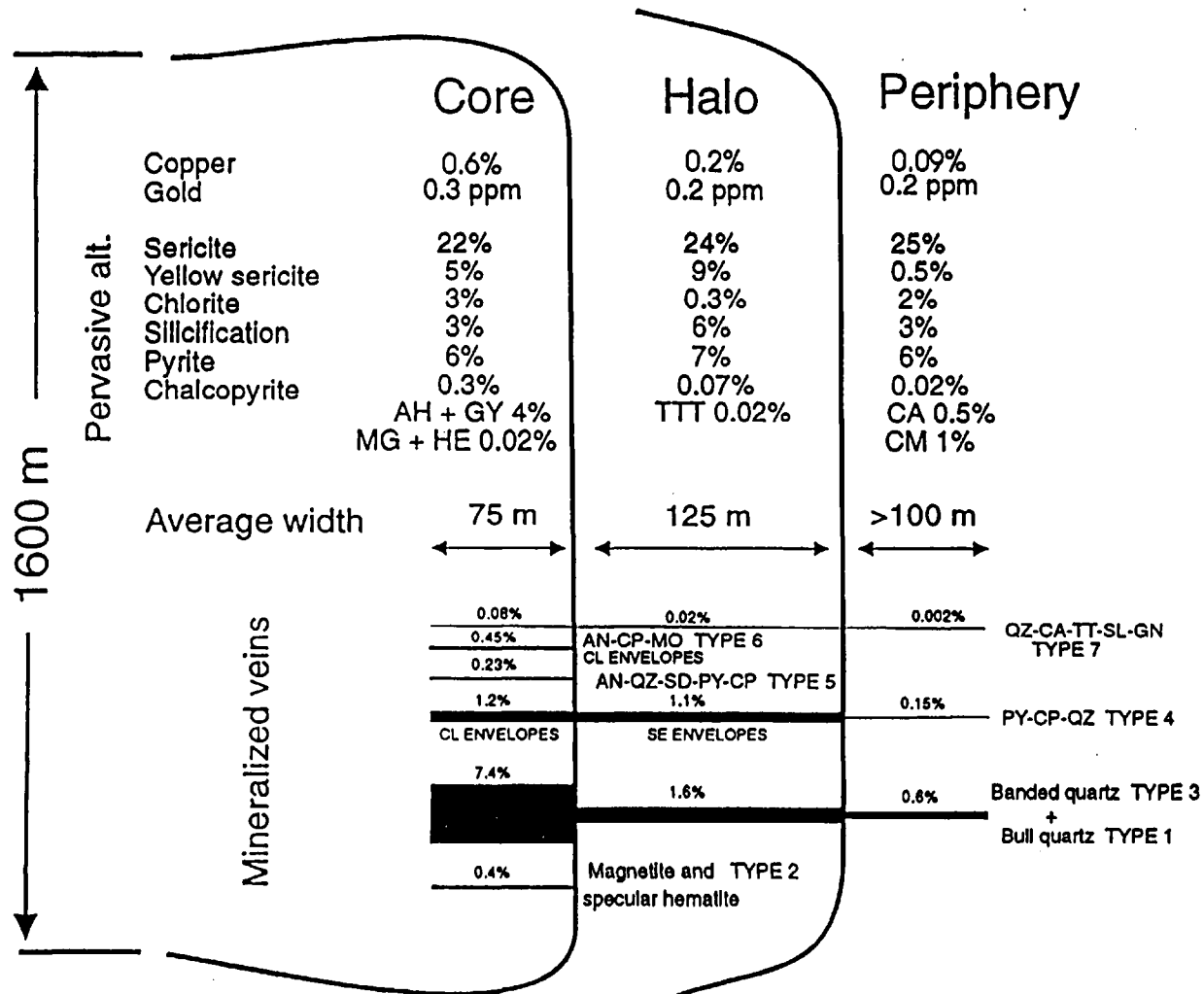


Figure 8.1 Major alteration zones in the Kerr deposit, northwestern British Columbia. Data is from Tables 6.1 and 6.2.

## 9.0 REFERENCES

- Aja, S.U., Rosenberg, P.E. and Kittrick, J.A., 1991. Illite equilibria in solutions: I. Phase relationships in the system  $K_2O-Al_2O_3-SiO_2-H_2O$  between 25 and 250°C; *Geochimica et Cosmochimica Acta*, 55, pp 1353-1364.
- Albee, A.L., 1962. Relationships between the mineral association, chemical composition and physical properties of the chlorite series; *American Mineralogist*, 47, pp 851-870.
- Alldrick, D.J. 1989. Volcanic centres in the Stewart Complex (103P and 104A,B); *in* Geological Fieldwork 1988, B.C. Ministry of Energy, Mines and Petroleum Resources, Paper 1989-1, pp 233-240.
- Alldrick, D.J., and Britton, J.M., 1988. Geology and mineral deposits of the Sulphurets area; B.C. Ministry of Energy, Mines and Petroleum Resources, Open File Map 1988-4.
- Alldrick, D.J., and Britton, J.M., 1991. Sulphurets area geology; B.C. Ministry of Energy, Mines and Petroleum Resources, Open File 1991-21.
- Anderson, R.G., 1989. A stratigraphic, plutonic, and structural framework for the Iskut River map area northwestern British Columbia; *in* Current Research, Part E, Geological Survey of Canada, Paper 89-1E, pp 145-154.
- Anderson, R.G., and Bevier, M.L., 1990. A note on Mesozoic and Tertiary K-Ar geochronometry of plutonic suites, Iskut River map area, northwestern British Columbia; *in* Current Research, Part E, Geological Survey of Canada, Paper 90-1E, pp 141-147.
- Anderson, R.G. and Thorkelson, D.J., 1991. Mesozoic stratigraphy and setting for some mineral deposits in Iskut River Map Area, northwestern British Columbia; *in* Current Research, Part E, Geological Survey of Canada, Paper 90-1E, pp 131-139.
- Anderson, R.G., 1993. A Mesozoic stratigraphy and plutonic framework for northwestern Stikinia (Iskut River area), northwestern British Columbia, Canada; *in* Dunne, G. and McDougall, K., eds, Mesozoic Paleogeography of the Western United States -- II, Pacific Section SEPM, 71, pp 477-494.
- Barnes, H.L., 1979. *Geochemistry of Hydrothermal Ore Deposits* 2nd Edition, John Wiley & Sons, New York, 798p.
- Bartsch, R., 1993. Volcanic Straigraphy and Lithogeochemistry of the Lower Jurassic Hazelton Group, Host to the Eskay Creek Precious and Base Metal Volcanogenic Deposit; Unpublished MSc thesis, University of British Columbia, 178p.
- Bladh, K.W., 1978. The weathering of sulfide-bearing rocks associated with porphyry - type copper deposit; Unpublished PhD, 98 p.

- Blount, C.W. and Dickson, F.W., 1973. Gypsum - anhydrite equilibria in systems  $\text{CaSO}_4\text{-H}_2\text{O}$  and  $\text{CaSO}_4\text{-NaCl-H}_2\text{O}$ ; *American Mineralogist*, 58, pp 323-331.
- Bridge, D.J. and Godwin, C.I., 1992. Preliminary geology of the Kerr copper-(gold) deposit, northwestern British Columbia; in *Geological Fieldwork 1991*, B.C. Ministry of Energy, Mines and Petroleum Resources, Paper 1992-1, pp 513-516.
- Britton, J.M. and Alldrick, D.J., 1988. Sulphurets Map Area (104A/05W, 12W; 104B/08E, 09/E); in *Geological Fieldwork 1987*, B.C. Ministry of Energy, Mines and Petroleum Resources, Paper 1988-1, pp 199-209.
- Brown, D., 1987. Geological setting of the volcanic-hosted Silbak Premier Mine, northwestern British Columbia (104 A/4, B1); unpublished MSc thesis, University of British Columbia, 216p.
- Cline, J.S. and Bodnar, R.J. 1991. Can economic porphyry copper mineralization be generated by a typical calc-alkaline melt?; *Journal of Geophysical Research*, v 96, pp 8113-8126.
- Cox, S.F. and Etheridge, M.A., 1983. Crack-seal fibre growth mechanisms and their significance in the development of oriented layer silicate microstructures; *Tectonophysics*, 92, pp 147-170.
- Deer, W.A., Howie, R.A. and Zussman, J., 1966. *An Introduction to the Rock Forming Minerals*, Longman House, Burnt Mill, 528p.
- Dunlap, W.J., Teyssier, C., McDougall, I. and Baldwin, S., 1991. Ages of deformation from K/Ar and  $^{40}\text{Ar}/^{39}\text{Ar}$  dating of white mica, *Geology*, 19, pp 1213-1216.
- Epp, W.R. 1985. Geochemical, geological, trenching and diamond drilling report on the Kerr claims, Skeena Mining Division; Brinco Limited, Unpublished assessment report 14p.
- Evenchick, C.A., 1991. Structural relationships of the Skeena Fold Belt west of the Bowser Basin, northwest British Columbia; *Canadian Journal of Earth Sciences*, 28, pp 973-983.
- Fletcher, W.K., 1981. Analytical methods in geochemical prospecting; G.J.S. Govett (editor), *Handbook of Exploration Geochemistry*, 1, 255p.
- Freeze, R.A. and Cherry, J.A., 1979. *Groundwater*, Prentice-Hall Inc., New Jersey, 604p.
- Grove, E.W., 1986. Geology and mineral deposits of the Unuk River - Salmon River - Anyox area, B.C. Ministry of Energy, Mines and Petroleum Resources, Bulletin 63, 152p.
- Guilbert, J.M. and Park, C.F., 1986. *The Geology of Ore Deposits*, Freeman, New York, 985p.
- Gy, P.M., 1979. Sample preparation; *Computer Methods for the 80's*, pp 163-169.
- Helgeson, H.C., Brown, T.H., Nigrini, A. and Jones, T.A., 1970. Calculation of mass transfer in geochemical processes involving aqueous solutions; *Geochimica et Cosmochimica Acta*, 34, pp 569-592.

- Henderson, J.R., Kirkham, R.V., Henderson, M.N., Payne, J.G., Wright, T.O., Wright, R.L., 1992. Stratigraphy and structure of the Sulphurets area, British Columbia; in Current Research, Part A, Geological Survey of Canada, Paper 92-1A, pp 323-332.
- Irvine, T.N. and Baragar, W.R.A., 1971. A guide to the chemical classification of the common rocks; Canadian Journal of Earth Sciences, 8, pp 523-548.
- Kamb, W.B., 1959. Petrofabric observations from Blue Glacier, Washington, in relation to theory and experiment; Journal of Geophysical Research, 64, pp 1908-1909.
- Kirkham, R.V., 1963. The geology and mineral deposits in the vicinity of the Mitchell and Sulphurets glaciers, northwestern British Columbia; unpublished M.Sc. thesis, The University of British Columbia, 122p.
- Kirkham, R.V., 1991. Provisional geology of the Mitchell - Sulphurets region, northwestern British Columbia (104B/8, 9); Geological Survey of Canada, Open File 2416 (1:20 000).
- Kowalchuk, J.M. and Jerema, M. 1987. A geological, geochemical, geophysical and drilling report on the Kerr project, NTS 104 B/8, Skeena Mining Division; Western Canadian Mining Corporation, Unpublished assessment report 28p.
- Kwong, Y.T.J., 1987. Evolution of the Iron Mask Batholith and its associated copper mineralization, Bulletin 77, B.C. Ministry of Energy, Mines and Petroleum Resources, 55p.
- Lasaga, A.C., 1989. Fluid flow and chemical reaction kinetics in metamorphic systems: a new simple model; Earth and Planetary Science Letters, 94, pp 417-424.
- McDowell, S.D. and Elders, W.A., 1980. Authigenic layer silicate minerals in borehole Elmore 1, Saltson Sea Geothermal Field, California, USA; Contributions to Mineralogy and Petrology, 74, pp 293-310.
- Margolis, 1992. Unpublished geological map of the geology between Mitchell and Sulphurets glaciers.
- Marsh, J.S., 1985. On the distribution and separation of crystals in convecting magma; Journal of Volcanology and Geothermal Research, 24, pp 95-150.
- Mather, J.D., 1970. The biotite isograd and the lower greenschist facies in the Dalradian rock of Scotland; Journal of Petrology, 11, pp 253-275.
- Monger, J.W.H., 1990. Unpublished report on terranes in British Columbia, 10p.
- Payne, J., 1989. Unpublished report on the geology of the Kerr deposit, northwestern British Columbia.
- Pearce, J.A., 1982. Trace element characteristics of lavas from destructive plate boundaries; in Thorpe, R.S. (Editor), Andesites: Orogenic Andesites and Related Rocks, John Wiley & Sons, pp 525-548.
- Perkins, E., 1980. A reinvestigation of the theoretical basis for the calculation of isothermal-isobaric mass transfer in geochemical systems involving an aqueous phase; Unpublished MSc thesis, University of British Columbia, 149p.

- Ramsay J.G. and Huber M.I., 1983. The techniques of modern structural geology, Volume I: Strain analysis; Academic Press, London, 307p.
- Roach, S. and Macdonald, A.J., 1992. Silver-gold vein mineralization, West zone, Brucejack Lake, northwestern British Columbia (104B/8E); in Geological Fieldwork 1991, B.C. Ministry of Energy, Mines and Petroleum Resources, Paper 1992-1, pp 503-511.
- Rock, N.M.S., 1987. The nature and origin of lamprophyres; in Fritton, J.G. and Upton, B.G. (Editors) Alkaline Igneous Rocks, Geological Society Special Publication, 30, pp 191-226.
- Sillitoe, R.H. and Gappe, I.M., 1984. Philippine porphyry copper deposits: Geologic setting and characteristics; United Nations ESCAP, CCOP Tech. Pub., 14.
- Sinclair, A.J., 1976. Applications of probability graphs in mineral exploration; The Association of Exploration Geochemists, Special Volume 4, 95p.
- Stanley, C.R., 1988. PROBLOT: An interactive computer program to fit mixtures of normal (or lognormal) distributions with maximum likelihood procedures; Association of Exploration Geochemists, Special Volume 14, 40p.
- Streckeisen, A., 1979. Classification and nomenclature of volcanic rocks, lamprophyres, carbonatites, and melilitic rocks: Recommendations and suggestions of the IUGS Subcommittee on the Systematics of Igneous rocks; Geology, 7, pp 331-335.
- Veron, R.H., 1976. Metamorphic Processes; London, Thomas Murby, 247p.
- Vila, T. and Sillitoe, R.H., 1991. Gold-rich porphyry systems in the Maricunga Belt, northern Chile; Economic Geology, 86, pp 1238-1260.
- Vila, T., Sillitoe, R.H., Betzhold, J. and Viteri, E., 1991. The porphyry gold deposit at Marte, northern Chile; Economic Geology, 86, pp 1271-1286.
- Walshe, J.L. and Solomon, M., 1981. An investigation into the environment of formation of the volcanic-hosted Mt. Lyell copper deposits using geology, mineralogy, stable isotopes, and a six-component chlorite solid solution model; Economic Geology, 76, pp 246-284.
- Wilson, M., 1989. Igneous petrogenesis; Unwin Hyman, London, 466p

## **A.0 APPENDIX GEOLOG DATABASE**

### **A.1 Introduction**

This appendix describes the methodology used to identify the alteration mineral assemblages and determine their spatial variation in the Kerr deposit. Drill core from cross sections 9700N and 10600N was logged in detail over twenty metre sections on fifty metre bench intervals. Detailed core logging consisted of recording the percentages of alteration minerals and vein types with respect to assay intervals. To determine the spatial variation of the alteration facies, percentages of alteration minerals were first analyzed using probability plots to identify distinct populations in each. Regions of distinct alteration mineral assemblages were then apparent once the populations were plotted on the cross sections.

### **A.2 Methodology of Collecting Data From the Drill Core**

Pearcing points were calculated at each point where the fifty metre bench interval intersected the drill hole on the cross section. Ten metres above and below these pearcing points was selected for detailed core logging. This length was modified to fit the start (to) and end (from) of assay intervals so that percentages of alteration minerals and veins could be compared to copper and gold grades. Placer Dome geologists used a 3.0 metre assay interval where there were no changes in alteration mineralogy, rock type and recovery of drill core. Assay intervals are shorter when they stop at a change in rock type or alteration. Assay intervals are longer then 3.0 metres - up to 10.0 metres, where there was insufficient recovery of the drill core.

Detailed core logging over seven, three metre assay intervals covers roughly 42% of the drill hole. This percentage of the total length of the drill hole allows less time to be spent core logging the whole hole, but still provides detailed coverage across the whole cross

section. This method is based upon two assumptions: (i) alteration mineral assemblages and copper and gold grades do not vary rapidly over 10 metres, and (ii) the whole deposit and hydrothermal system has a true thickness greater than 60 metres. The first point is affected by post-mineral dikes because they have a different alteration mineral assemblage and significantly different copper and gold grades. Therefore, the data from post-mineral dikes were removed from those intervals that were intersected. The remaining data was then averaged over the new shortened total length. The deposit has to have thickness greater than 60 metres perpendicular to the drill holes when the 50 metre bench interval is used otherwise the intervals will sample it once - either in the center or periphery. Cross sections 9700N and 10600N show thickness perpendicular to the trend of the drill holes to be 225 and 175 metres respectively.

#### A.2.1 Methodology for collection of alteration minerals and veins.

The data from the detailed core logging was recorded on forms using a modified GEOLOG format developed by C. Godwin. The purpose of recording the alteration mineralogy on these forms is that the data collection is kept consistent through the project. Each assay interval was characterized under seven separate headings (fields): location, rock unit, short description, structural data including fabric and vein orientations, pervasive and vein mineralogy, and measured percentages of different vein types.

Location of the assay interval is described by the number of metres from the collar of the drill hole. The rock unit is assigned a four letter code. A short description includes any observations that are not included in the GEOLOG form, such as, percentages of different alteration minerals, variation in the deformation style or vein densities, or notes on timing of veins and alteration.

Structural data fields were split into two sub-fields: (i) measurements of the fabric in the drill core with respect to the core axis, and (ii) the number of veins measured with respect

Table A.1. Table of minerals recorded during detail core logging of the Kerr deposit, northwestern British Columbia.

Symbol	Diagnostic Properties and occurrence
QZR	Pervasive, texturally destructive silicification characterized by a kidney texture. Two types of silicification have been combined: original quartz flood and pervasive K-feldspar which has been retrograded to quartz and sericite.
QZV	Total of all quartz in veins. The quartz ranges in colour from milky white to dark blue grey and texture from massive, fibrous to banded, comb quartz
SER	Pervasive, pale grey sericite distinguished by its colour and weak, earthy smell when wet. The amount of pale blue sericite replacing feldspar in syn-mineral dikes was included in this sub-field.
SEV	Grey sericite envelopes to sulphide veins.
YSR	Pervasive, texturally destructive yellow sericite consisting of illite 1M and phengite.
YSV	Yellow sericite envelopes.
GSR	Pervasive, texturally destructive inter-mixed chamosite (Fe-chlorite) and grey sericite.
GSV	Envelopes to sulphide veinlets.
CLR	Pervasive, texturally destructive chamosite and selective chlorite (clinochlore and chamosite) alteration. The selective chlorite replaces hornblende and augite in the footwall, hanging wall and post-mineral dikes in the Kerr deposit.
CLV	Envelopes and selvages to sulphide and sulphate veins and as masses in extensional quartz-carbonate veins where they occur in pervasively chlorite altered post-mineral dikes.
KAR	Selective illite alteration of feldspars and matrix to volcaniclastic rocks. Readily identified by its earthy smell when wet. The clay alteration also forms a whitish coating to the selvages of gypsum veins when the gypsum dissolves exposed to rain water.



Table A.1 cont'd

---

KAV	Cream white to pale blue clay infilling of weathered fractures in the sulphate stockwork was indentified by XRD as offerite ( zeolite).
CBR	Pervasive calcite alteration is readily identified by its reaction to cool, dilute 0.1M HCl.
CBV	Total calcite occurring in veins.
ANR	Total pervasive carbonate alteration: siderite, ankerite, dolomite not including calcite.
ANV	Total vein carbonate; composition of the carbonate was recorded in the short description.
AHR	Percentage of disseminated anhydrite was determined by the abundance of weathered pits on weathered intact drill core from below the supergene alteration.
AHV	Transparent, grey to milky white vein anhydrite.
GHR	Percentage of disseminated gypsum was not recorded.
GHV	Pink gypsum veins were readily distinguished from anhydrite because they could be scratched by a copper penny.
MHR	Disseminated magnetite.
MHV	Magnetite veins are readily distinguished from specular hematite by the remaining magnetism.
HER	Disseminated hematite was distinguished from magnetite because it was not magnetic and it produced a red to purple colour to the drill core.
HEV	Specular hematite veins are characterized by their blue to grey metallic luster and red streak.
RUR	Disseminated carbonaceous material characterized by its black to steel blue colour with grey sericite.
RUV	Veinlets of carbonaceous material.

Table A.1 cont'd

---

PYR	Disseminated pyrite ranges from euhedral cubes in the sericite - quartz schist to ragid aggregates in the less deformed and altered rocks.
PYV	Ragid pyrite in sulphide veins and coarse aggregates in sulphate and carbonate veins.
CPR	Disseminated ragid grains of chalcopyrite. Visual inspection under estimated the percentage of chalcopyrite in pervasive, chlorite altered rock because it was very fine grained and was surrounded by chlorite.
CPV	Ragid aggregates in sulphide veins.
TTR	Steel black with greenish luster tetrahedrite - tennantite blebs.
TTV	Blebs and masses of tetrahedrite - tennantite in carbonate and sulphate veins.
BOV	Bornite in fractured banded, grey quartz veins
MOV	Steel grey molybdenite on selvages to pink gypsum veinlets.
SLV	Reddish brown, resinous sphalerite blebs and masses in carbonate veins. Red sphalerite is disseminated in footwall mudstones and tuffaceous rocks.
CCC	Chalcocite coatings on chalcopyrite and pyrite in the supergene alteration zone. Chalcocite was distinguished from magnetite by its lack of magnetism and black, sooty streak.
JAC	Limonite coatings on weathered veins and disseminated pyrite grains in the supergene alteration zone.
WDC	Wad (manganese hydrous oxides) was identified by its dendritic pattern on weathered fractures.
GYV	White gypsum filling fractures below the supergene zone.

---

to the most prominent fabric in the assay interval. The orientation of each vein type was calculated from several measurements on the same type of veins. If the orientation of the vein type was random, it was recorded as a stockwork. The number of veins was averaged over the assay interval, so that the number of veins could be compared to the percentage of each in one metre.

The visually estimated percentages of pervasive and vein mineralogies were recorded separately. Mineralogy of vein envelopes was put in the vein fields because none of the veins were composed completely of alteration silicate minerals. Published concentration charts were used as a check on the estimation of the alteration mineralogy, which was later compared to the amount observed in thin section. Table A.1 lists the various minerals regularly recorded on the GEOLOG form.

Percentages of the various vein types were calculated from measurements of the thickness of veins along the centerline of the drill core. The total thickness over the assay interval was divided by the length of the remaining drill core. Veins that were parallel the core axis, but never intersected it, were included in the percentage by measuring the true thickness at intervals along their strike length depending upon drill core thickness. If the drill core recovery was below 60% and no pieces were longer than 4 centimetres, the percentage of vein material was estimated from the amount of vein pieces remaining in the interval. This results in an over - estimation of the amount of quartz vein in the interval because the softer sericitic alteration could have been ground to fine sand and washed away by the drilling mud.

### **10.3 Analysis of Visually Estimated Mineral Data**

A weighted average of each visually estimated minerals was calculated for each bench interval after the post-mineral dikes were subtracted from it. This was done so that the variability in the amounts of minerals in the 20 metre interval could be reduced. This variability is due to minor variations in the rock type, composition and intensity of alteration.

Once the data is averaged, the general variation in the percentages of alteration minerals can be observed across the whole deposit. This model is now less dependent upon the variability of the rock type and due more to gradual trends in alteration mineralogy. In order to separate the distinct mineral assemblage populations in the averaged data set, log normal probability plots were constructed using the computer program by C. Stanley (1988). The methodology for calculating the plots is outlined in Sinclair (1976). The data was divided into mineral populations, and then plotted onto cross sections with symbols representing the various populations. Selection of the regions of distinct mineral populations was done visually by comparing the frequency each population in a specific region characterized by a distinct mineral (see below).

#### A.3.1 Probability plots

Eight minerals, elements and ratios were selected for detailed analysis. They are: copper (%), total chalcopyrite to pyrite ratio, intergrown chlorite and sericite, chlorite envelopes, sericite envelopes, total tetrahedrite-tennantite, total magnetite and hematite, total gypsum and anhydrite, and total carbonaceous material. Each was chosen to represent a distinct alteration assemblage in the deposit so that other alteration minerals could be correlated with it. Visual inspection of drill core in the bench intervals helped to define relationships among the various alteration minerals.

#### A.3.2 Discussion of probability plots

Use of probability plots to determine populations of data assumes that the individual populations follow either a normal or a log normal distribution (Sinclair, 1976). Comparison of the calculated populations in a variable to ideal log normal curves help to establish whether or not this assumption is valid. Log normal curves also show where the raw data diverges from ideal distributions.

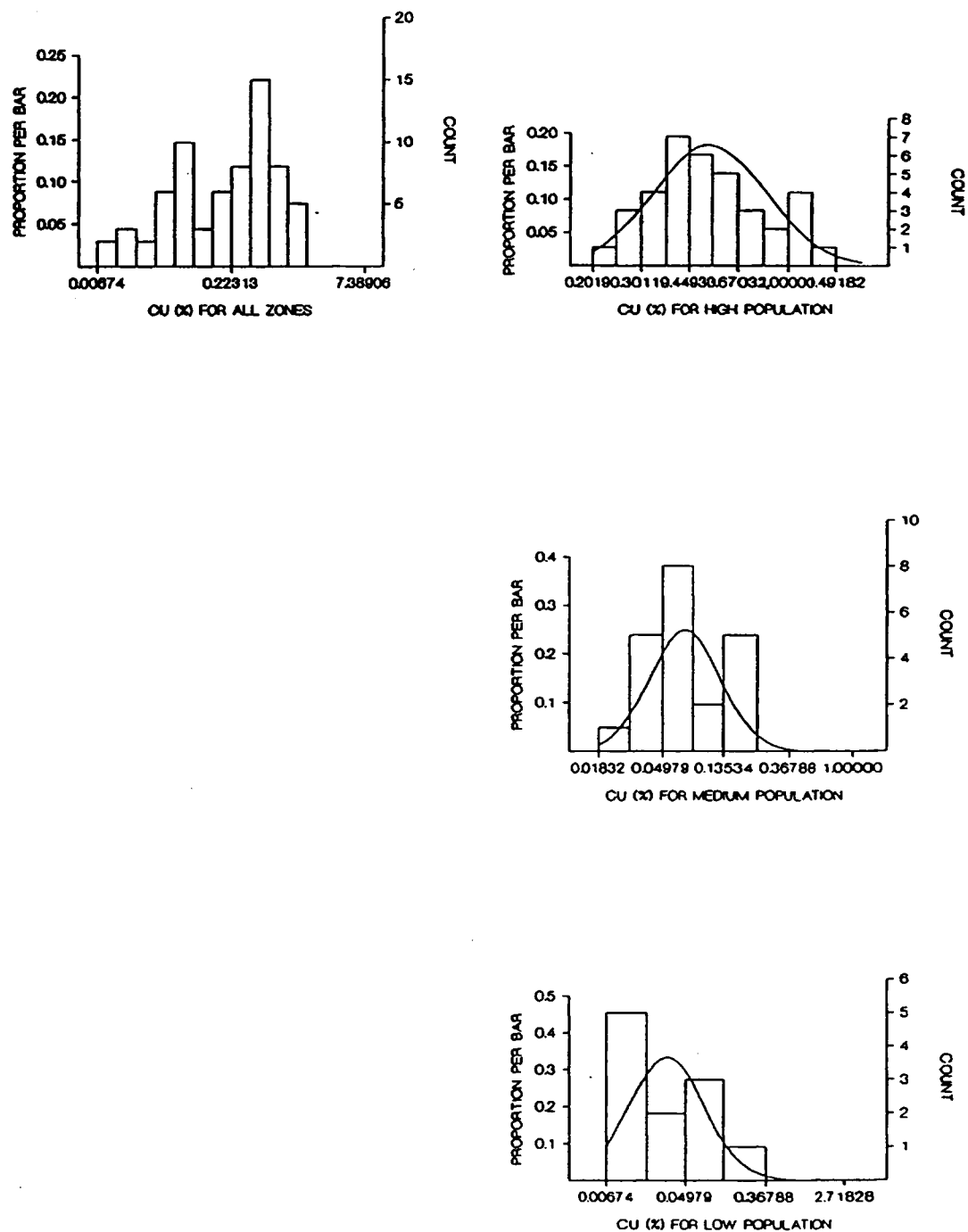


Figure A.1. Log histograms of averaged Cu (%) from intervals on cross - sections 9700N and 10600N in the Kerr deposit, northwestern British Columbia.

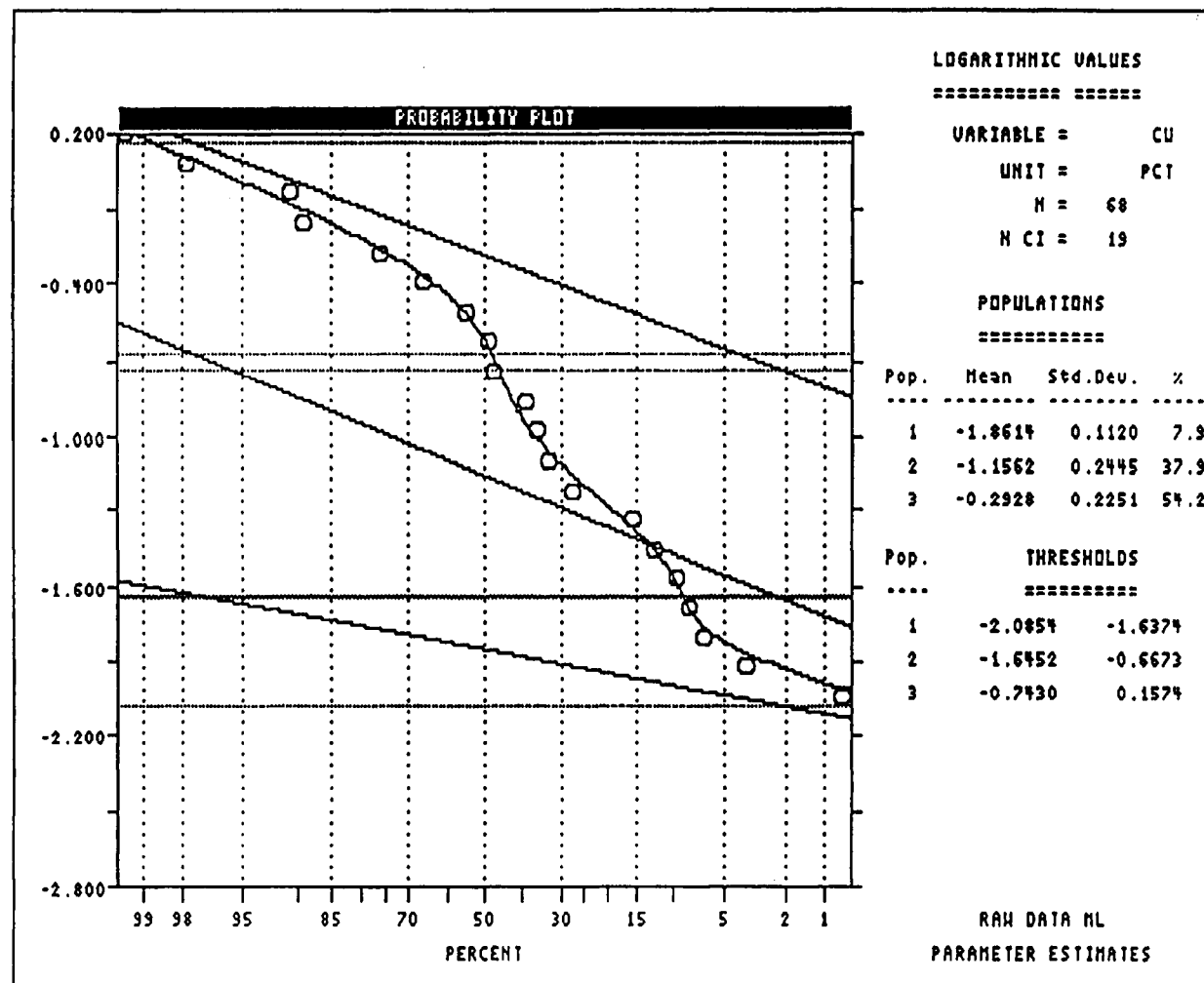


Figure A.2. Log probability plot of averaged Cu (%) from intervals on cross - sections 9700N and 10600N in the Kerr deposit, northwestern British Columbia. Plot shows three populations in the data and the thresholds separating them.

Figures A.1 and A.2 show the probability plot and histograms for Cu (wt%) in the averaged bench intervals on sections 9700N and 10600N. Three populations in the data can be identified in a log normal histogram. The thin lines on the histogram for each population is the trace of an ideal log normal population. The copper probability plot shows the three populations. The log histogram of the low population for copper indicates that the lower portion of the data may be affected by the 0.005 ppm detection limit. Both poor precision and the recording of Cu assays as multiples of 0.005 close to the detection limit may have caused the last bar to diverge from the ideal log normal distribution.

The log normal histogram of total chalcopyrite to pyrite ratio (Fig A.3) shows that there are only two populations in the data. This is confirmed by the log probability plot (Fig A.4). Thresholds calculated split the data into two distinct groups which can be seen in the raw data log histogram.

The lower portion of the log probability plot of chlorite and sericite shows two populations (Fig. A.5). Comparison of each of the populations to a log normal curve shows a good fit to the upper population, but a poor fit to the lower one which is skewed to higher values (Fig. A.6). The lower population is affected by one very low value, which was truncated from the data. This graph shows two populations in the data, a high one that has a small standard deviation and a low population which overlaps the high one (Fig. A.7).

Two overlapping populations can be identified in the chlorite envelope data (Fig. A.8). Most of the data is in the upper log normal population which approximates an ideal log normal distribution (Fig. A.9).

Two distinct populations can be identified in the sericite envelope data (Fig. A.10). This is confirmed by a log histogram of all of the data and inspection of the raw averaged data (Fig. A.11). An anomalous high value in the data set plots above the fitted curve in the probability plot, however, this value fits the ideal log normal distribution.

Table A.2 Table of thresholds and means of mineral populations.

MINERAL (NUMBER OF DATA ABOVE 0.0001)	TRANSFORM	POPULATION	MEAN (x, top std., bottom std.)	PERCENTAGE OF POPULATION	TOP THRESHOLD	BOTTOM THRESHOLD	THRESHOLD USED IN ANALYSIS	NUMBER OF DATA POINTS
COPPER 68	LOG	H (HIGH)	0.510,0.856,0.303	54.2	1.437	0.181	0.215	34
		MH					0.181	0
		M (MODERATE)	0.070,0.123,0.040	37.9	0.215	0.023	0.023	20
		L (LOW)	0.014,0.018,0.011	7.9	0.023	0.008		11
TOTAL CP/ TOTAL PY 45	LOG	H	0.069,0.159,0.03	86.4	0.365	0.013	0.01	38
		L	0.002,0.004,0.001	13.6	0.008	0		12
CHLORITE SERICITE 31	LOG	H	5.716,15.385,2.124	79	24.08	0.573	1.89	15
		LH					0.573	0
		L	0.074,0.296,0.019	21	1.89	0.005		16
CHLORITE ENVELOPES 43	LOG	H	0.379,0.822,0.175	86.1	1.781	0.081	0.307	31
		LH					0.081	0
		L	0.002,0.025,0.00017	13.9	0.307	0.0000137		6
SERICITE ENVELOPES 32	LOG	H	0.284,1.109,0.073	90.4	4.325	0.019	0.01	32
		L	0.00015,0.0009,0.000025	9.6	0.005	0.000004		
TOTAL TETRAHEDRITE 27	LOG	H	0.06,0.157,0.023	77.7	0.41	0.009	0.005	18
		L	0.00019,0.0007,0.000053	22.3	0.003	0.000015		6
MAGNETITE AND HEMATITE 18	LOG	H	0.509,1.988,0.13	82.3	7.766	0.033	0.01	16
		L	0.00016,0.00022,0.00012	17.7	0.0003	0.00009		4
CARBONACEOUS MATERIAL 4		H	no plot					6
		L	insufficient data					1



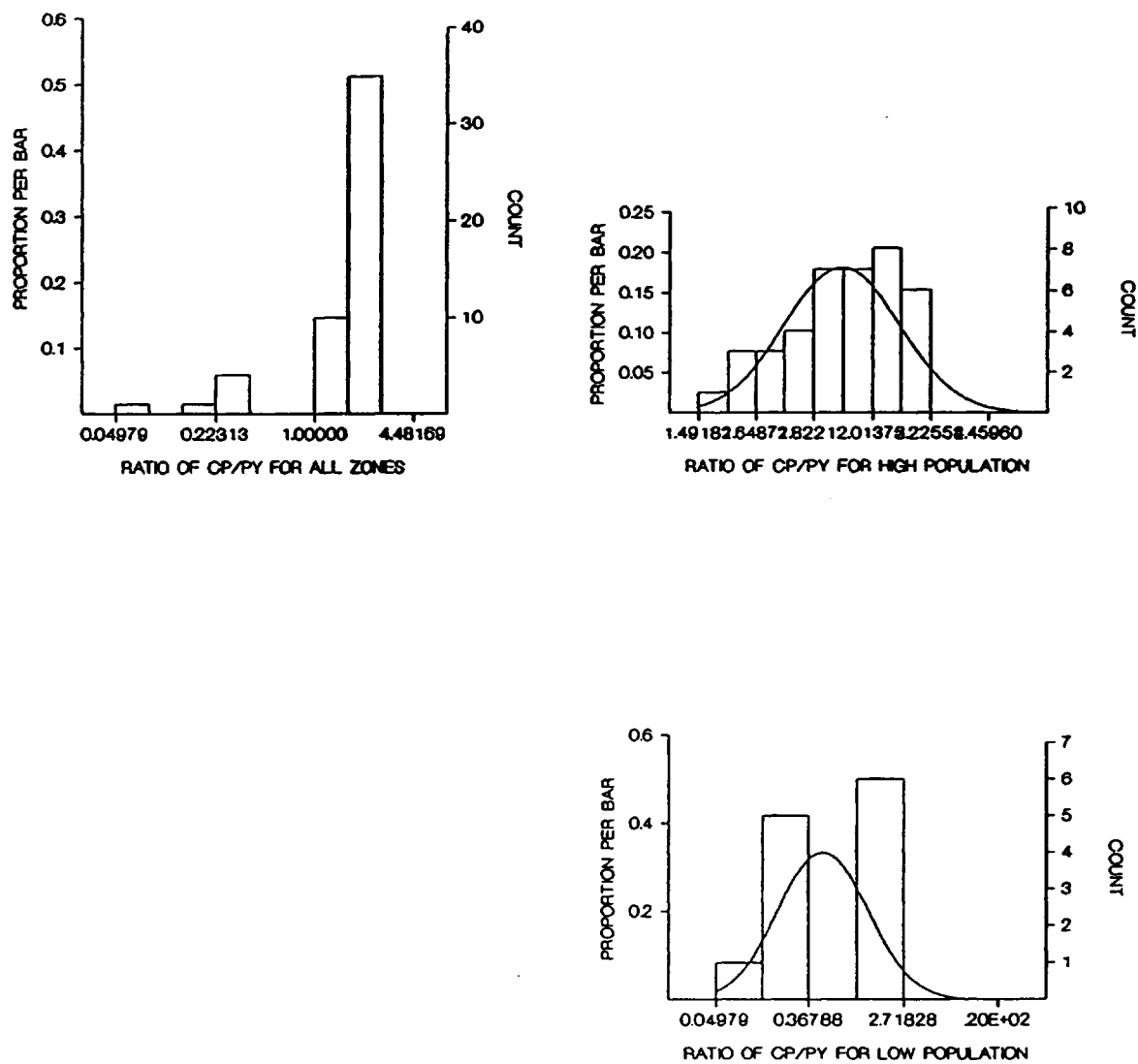


Figure A.3. Log histograms of averaged ratio of total chalcopyrite to pyrite (CP/PY) over intervals on cross - sections 9700N and 10600N in the Kerr deposit, northwestern British Columbia.

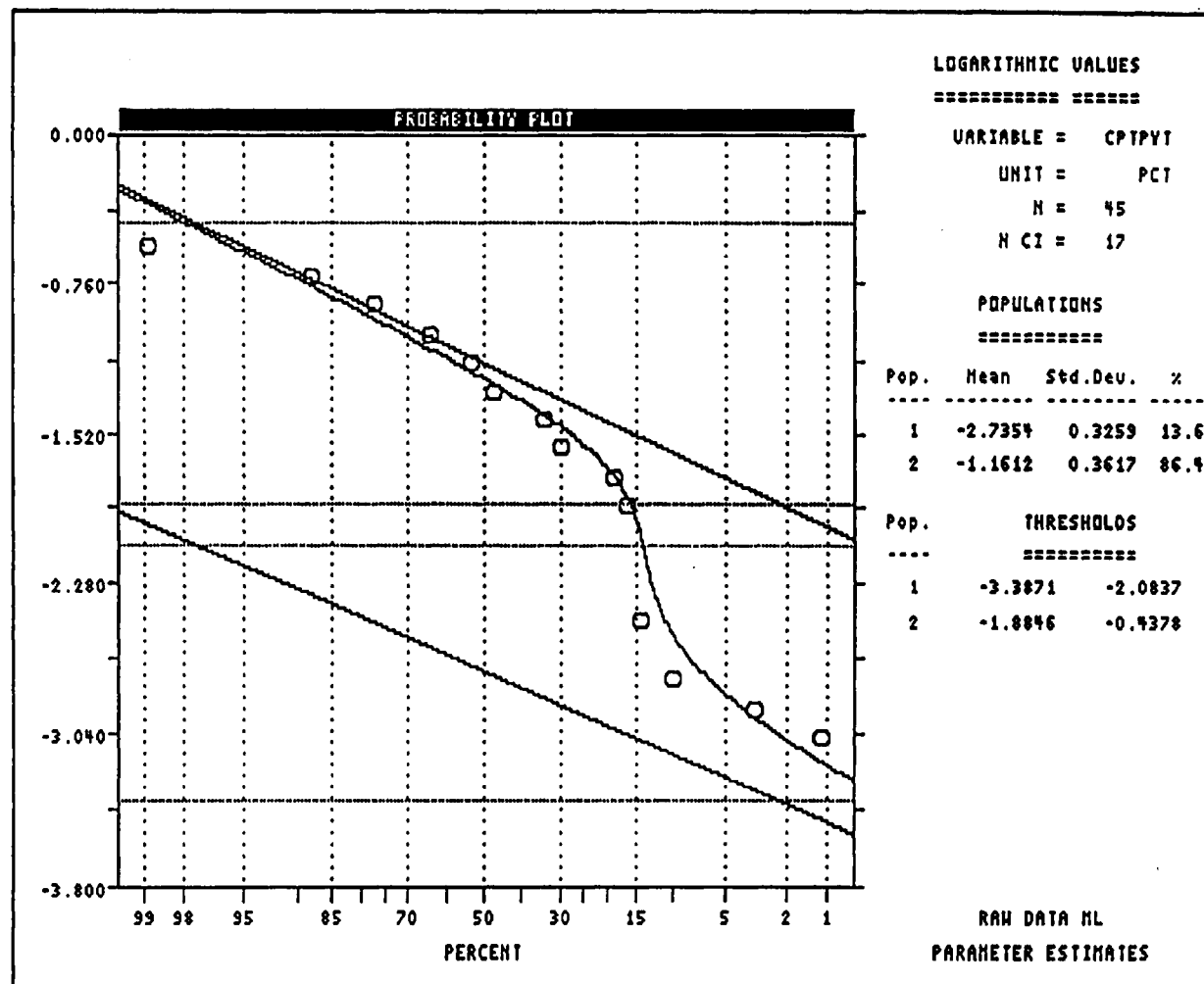


Figure A.4. Log probability plot of averaged ratio of total chalcopryite to pyrite over intervals on cross - sections 9700N and 10600N in the Kerr deposit, northwestern British Columbia. Plot shows two populations in the data and the thresholds separating them.

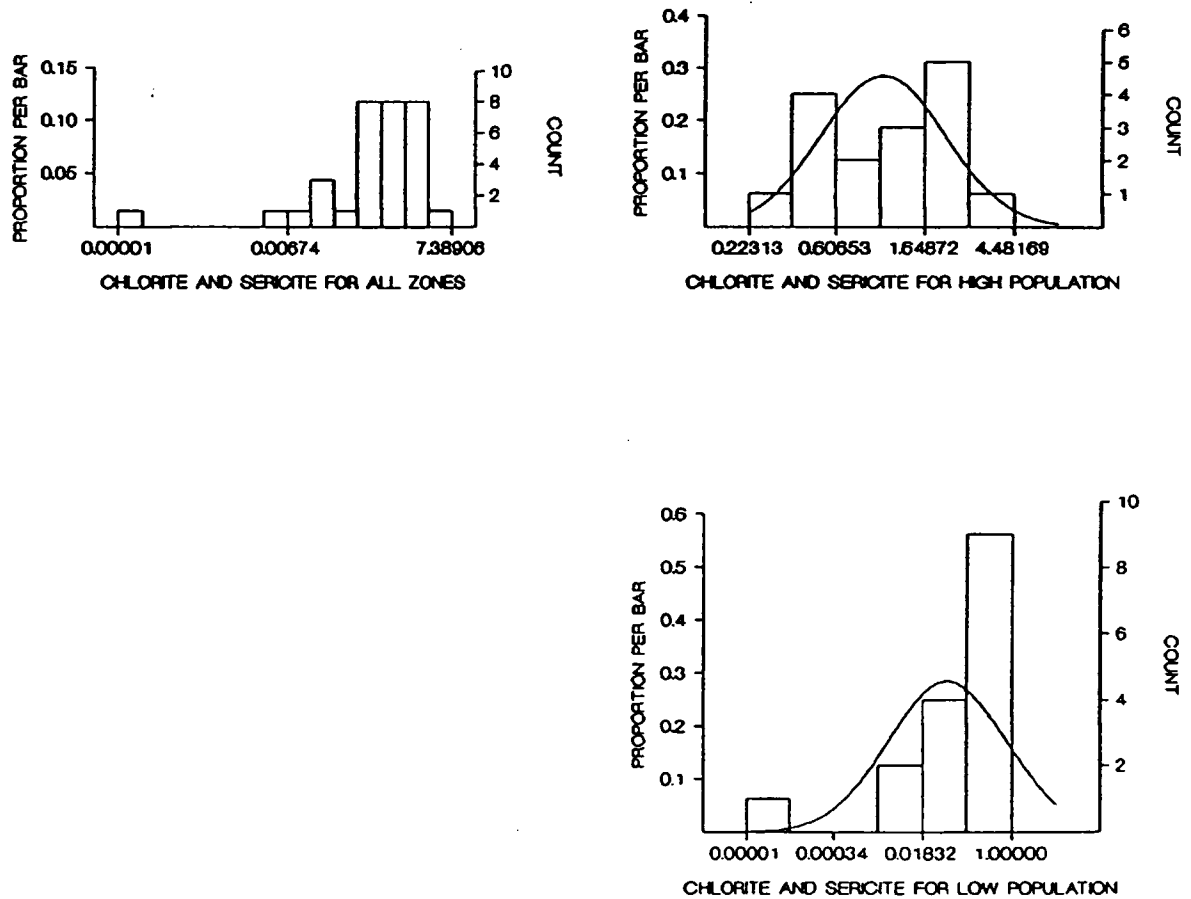


Figure A.5. Log histograms of averaged intergrown chlorite and sericite over intervals on cross - sections 9700N and 10600N in the Kerr deposit, northwestern British Columbia.

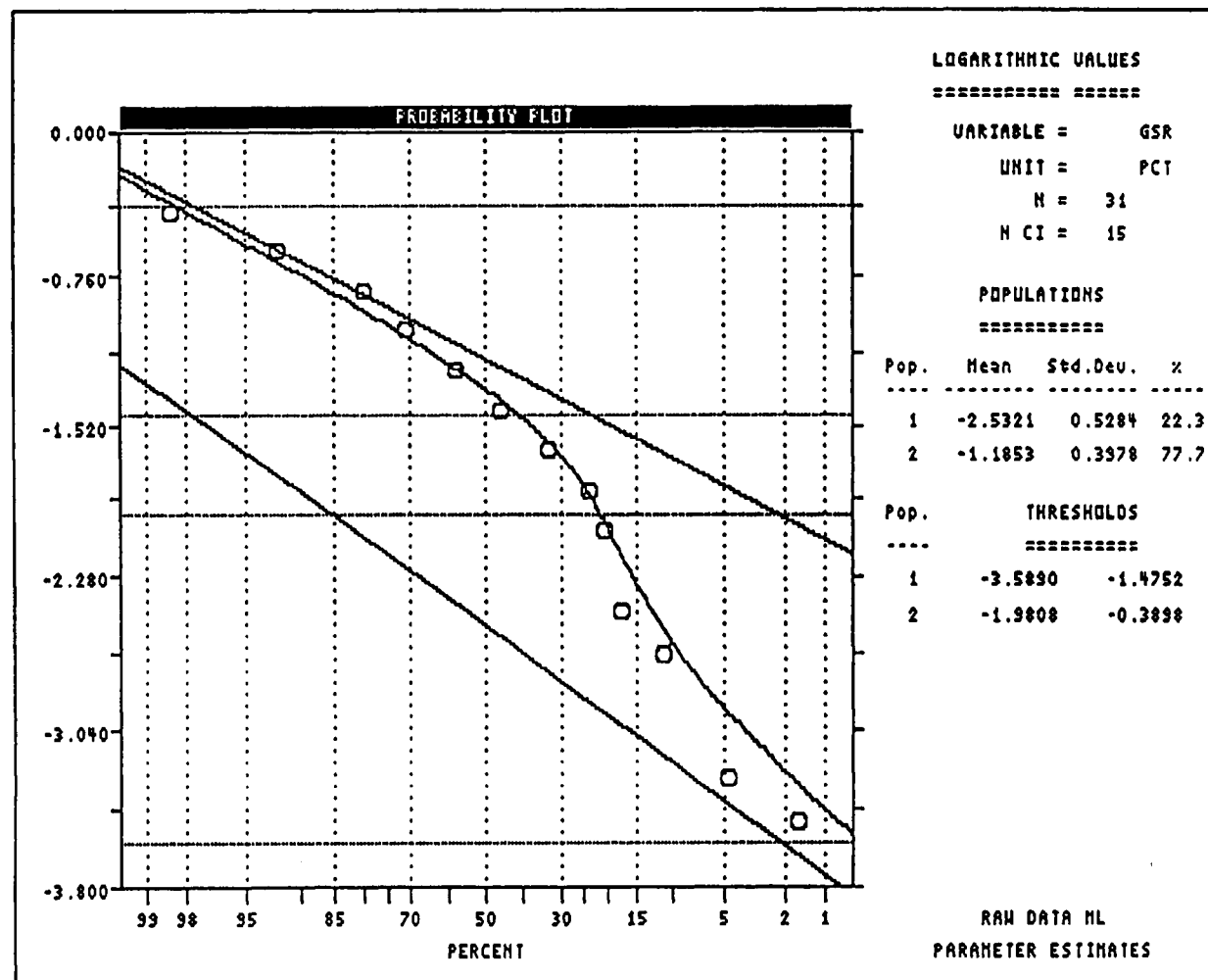


Figure A.6. Log probability plot of averaged intergrown chlorite and sericite over intervals on cross - sections 9700N and 10600N in the Kerr deposit, northwestern British Columbia. Plot shows two populations in the data and the thresholds separating them.

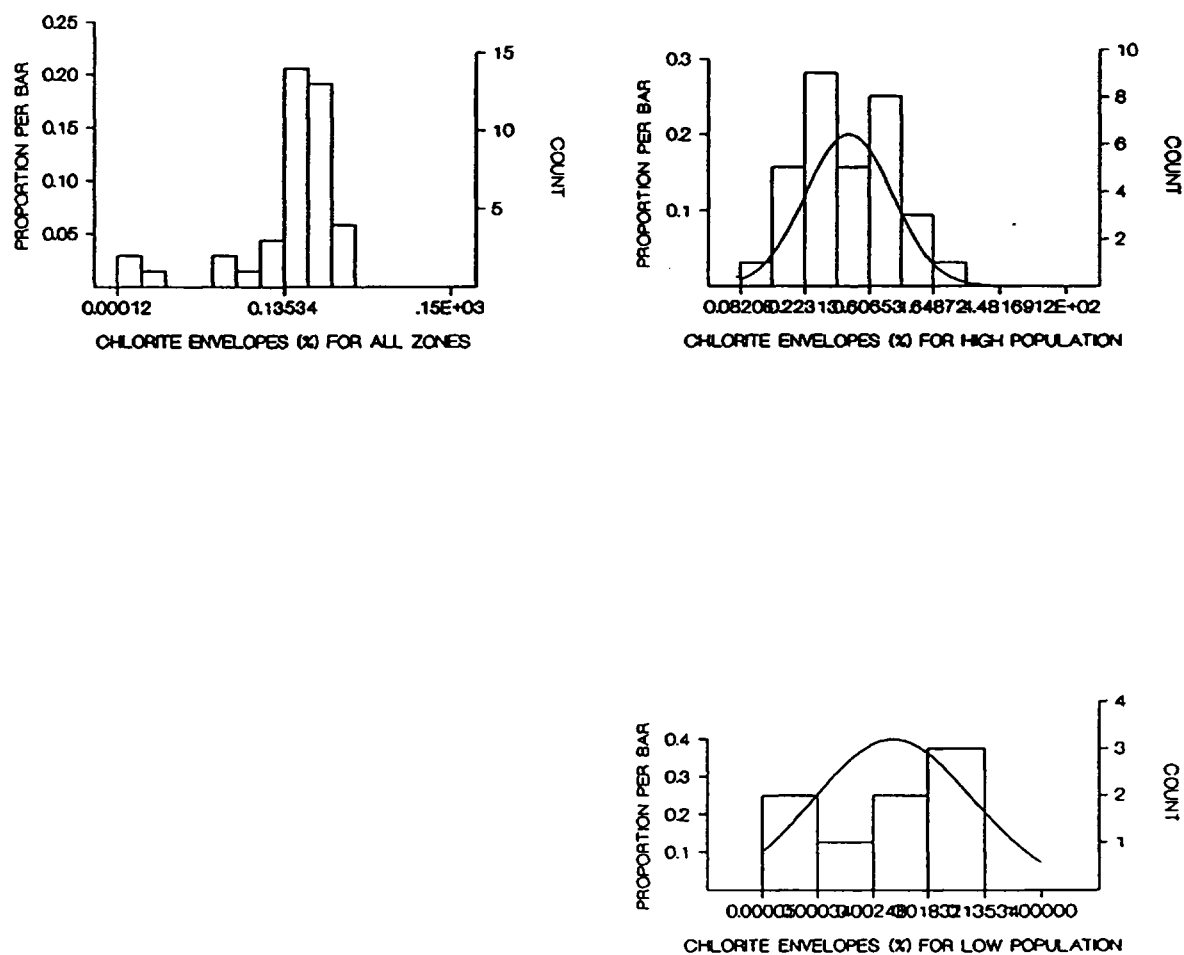


Figure A.7. Log histograms of averaged chlorite envelopes to sulphide and sulphate veins over intervals on cross - sections 9700N and 10600N in the Kerr deposit, northwestern British Columbia.

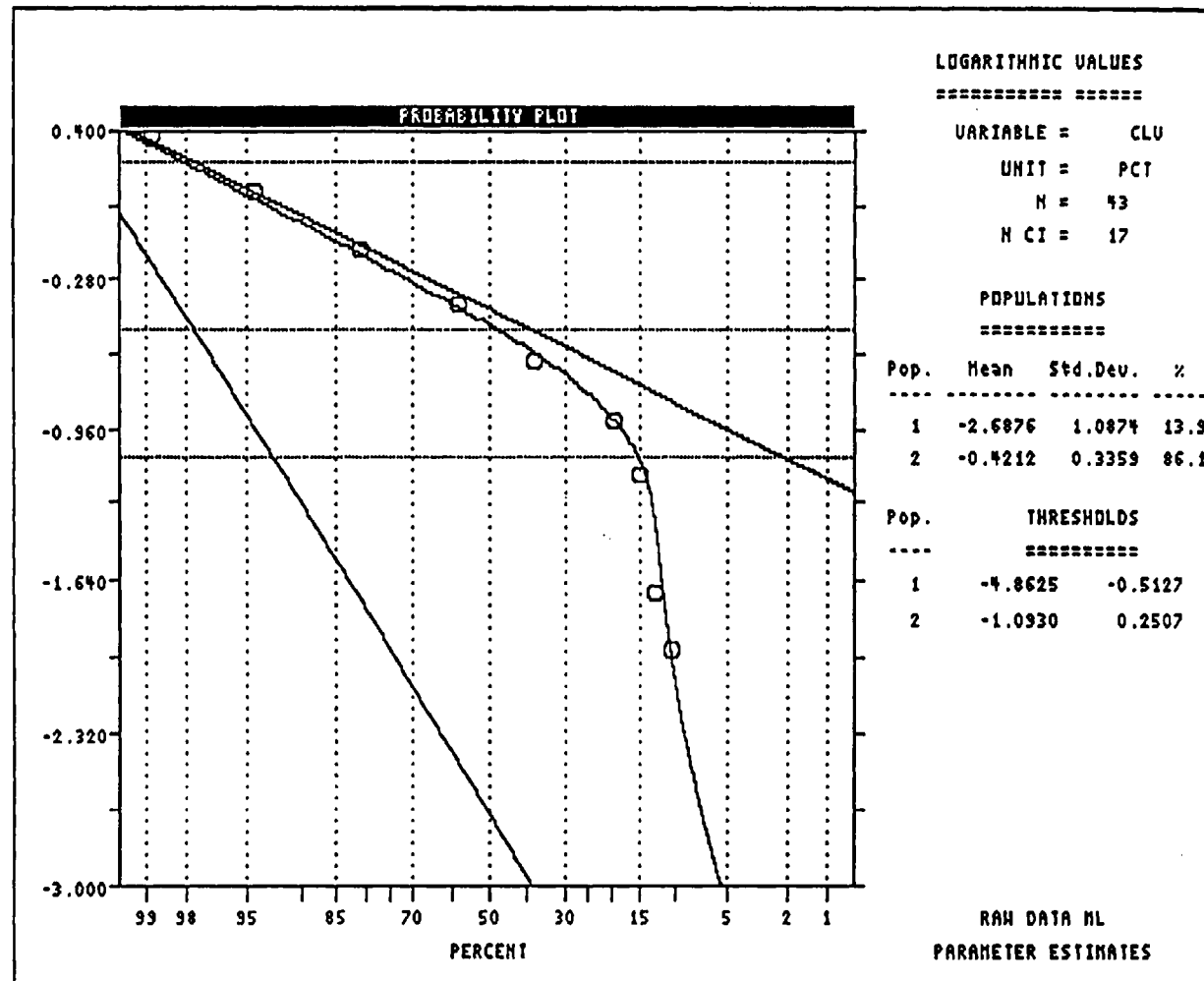


Figure A.8. Log probability plot of averaged chlorite envelopes to sulphide and sulphate veins over intervals on cross - sections 9700N and 10600N in the Kerr deposit, northwestern British Columbia. Plot shows two populations in the data and the thresholds separating them.

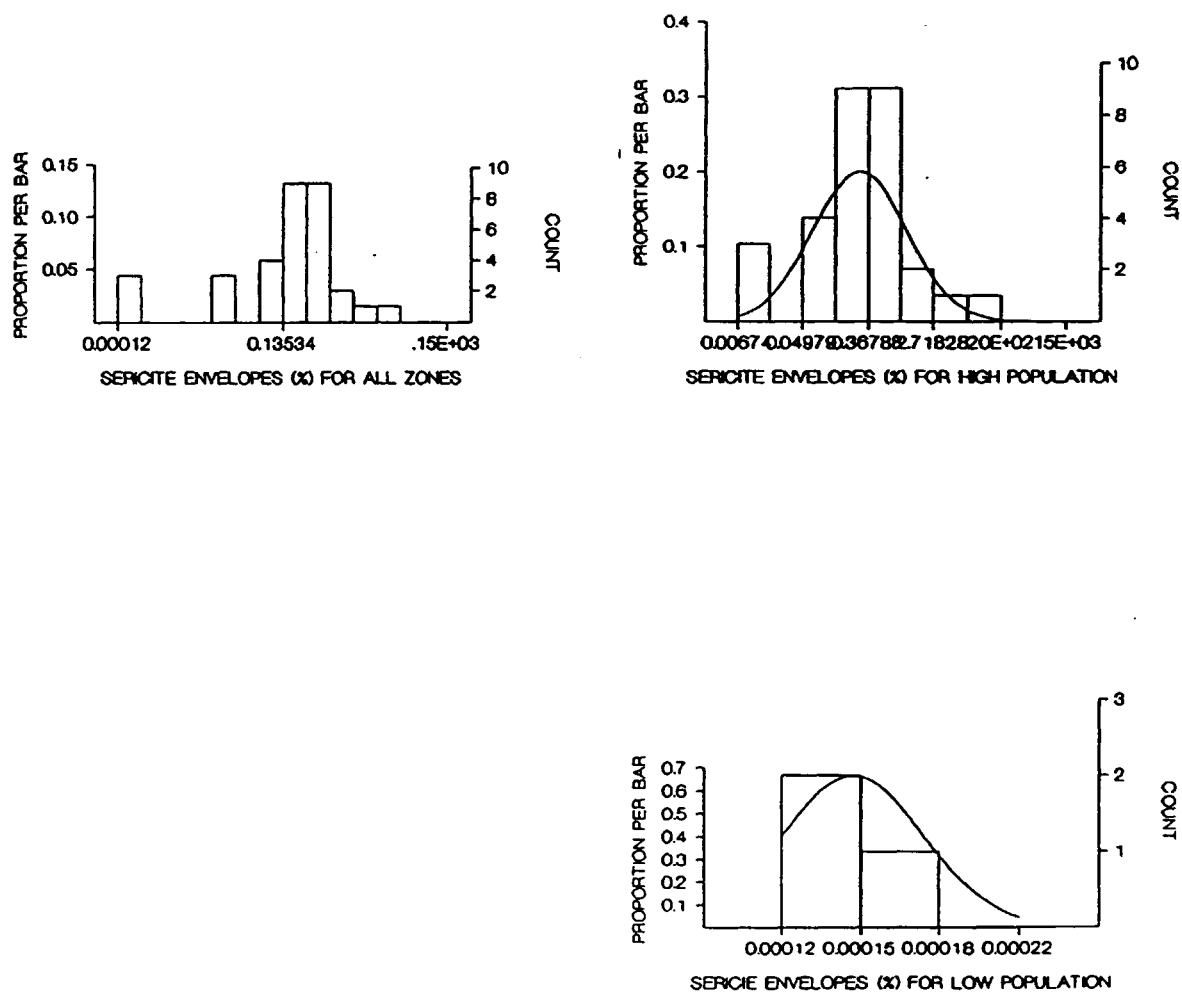


Figure A.9. Log histograms of averaged sericite envelopes to sulphide veins over intervals on cross - sections 9700N and 10600N in the Kerr deposit, northwestern British Columbia.

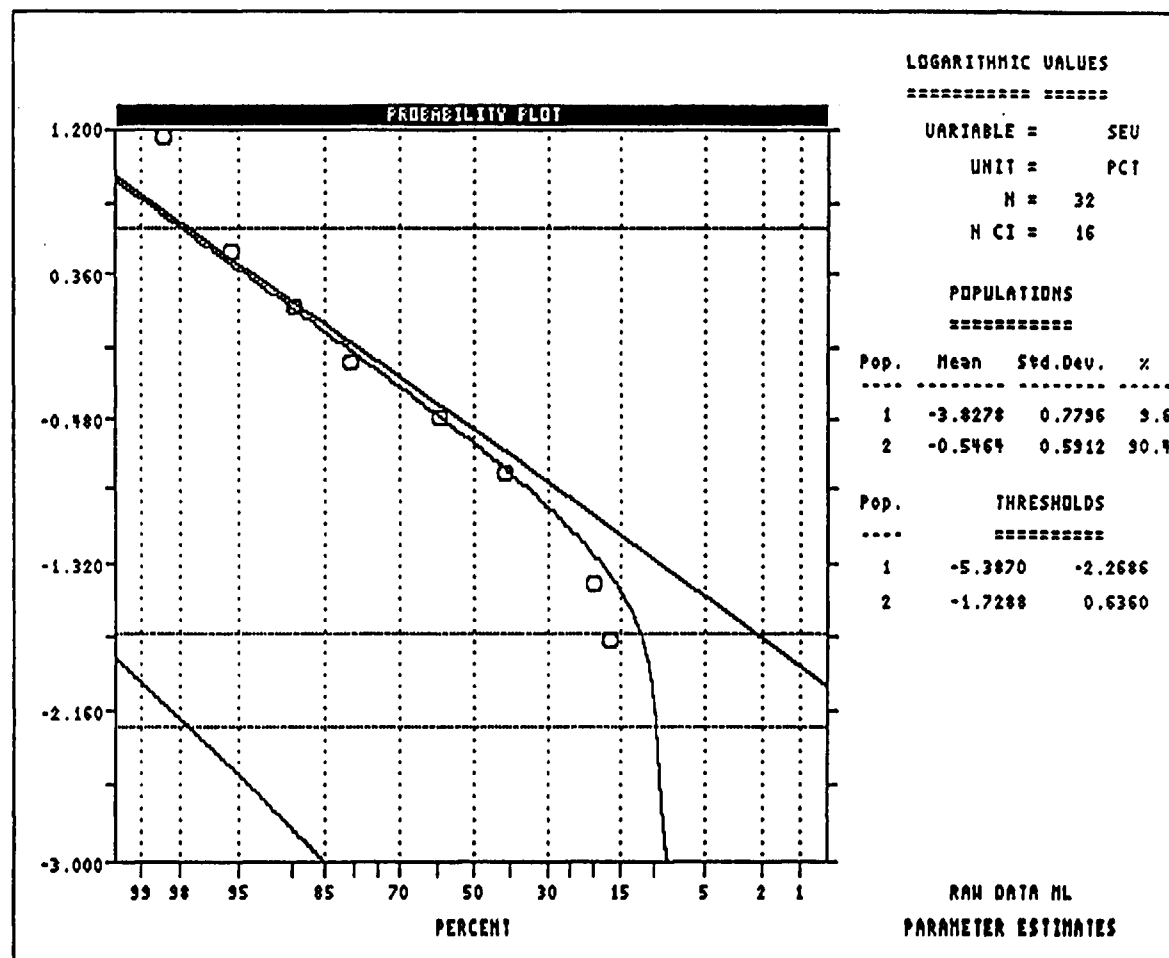


Figure A.10. Log probability plot of averaged sericite envelopes to sulphide veins over intervals on cross - sections 9700N and 10600N in the Kerr deposit, northwestern British Columbia. Plot shows two populations in the data and the thresholds separating them.



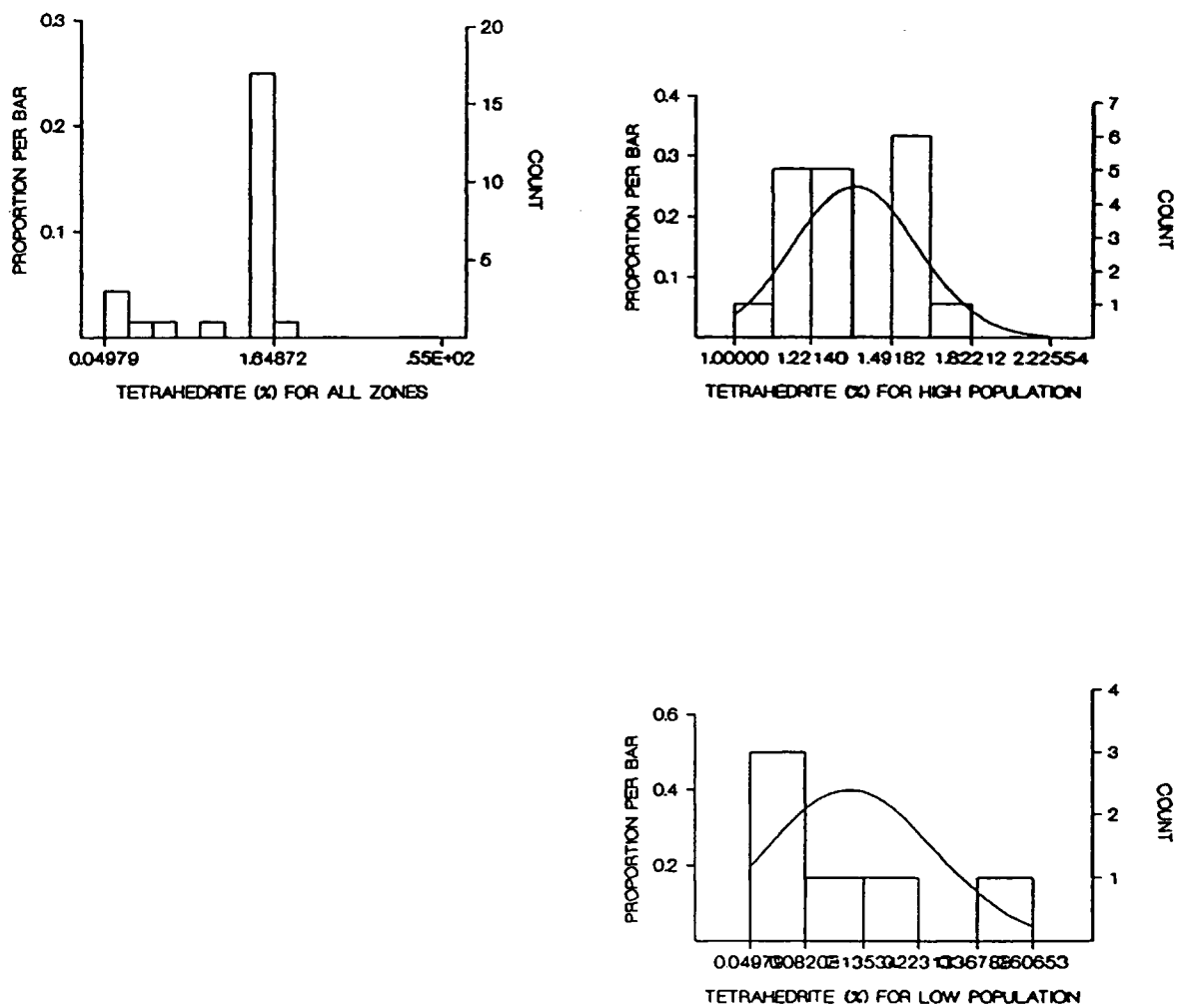


Figure A.11. Log histograms of averaged total tetrahedrite - tennantite over intervals on cross - sections 9700N and 10600N in the Kerr deposit, northwestern British Columbia.

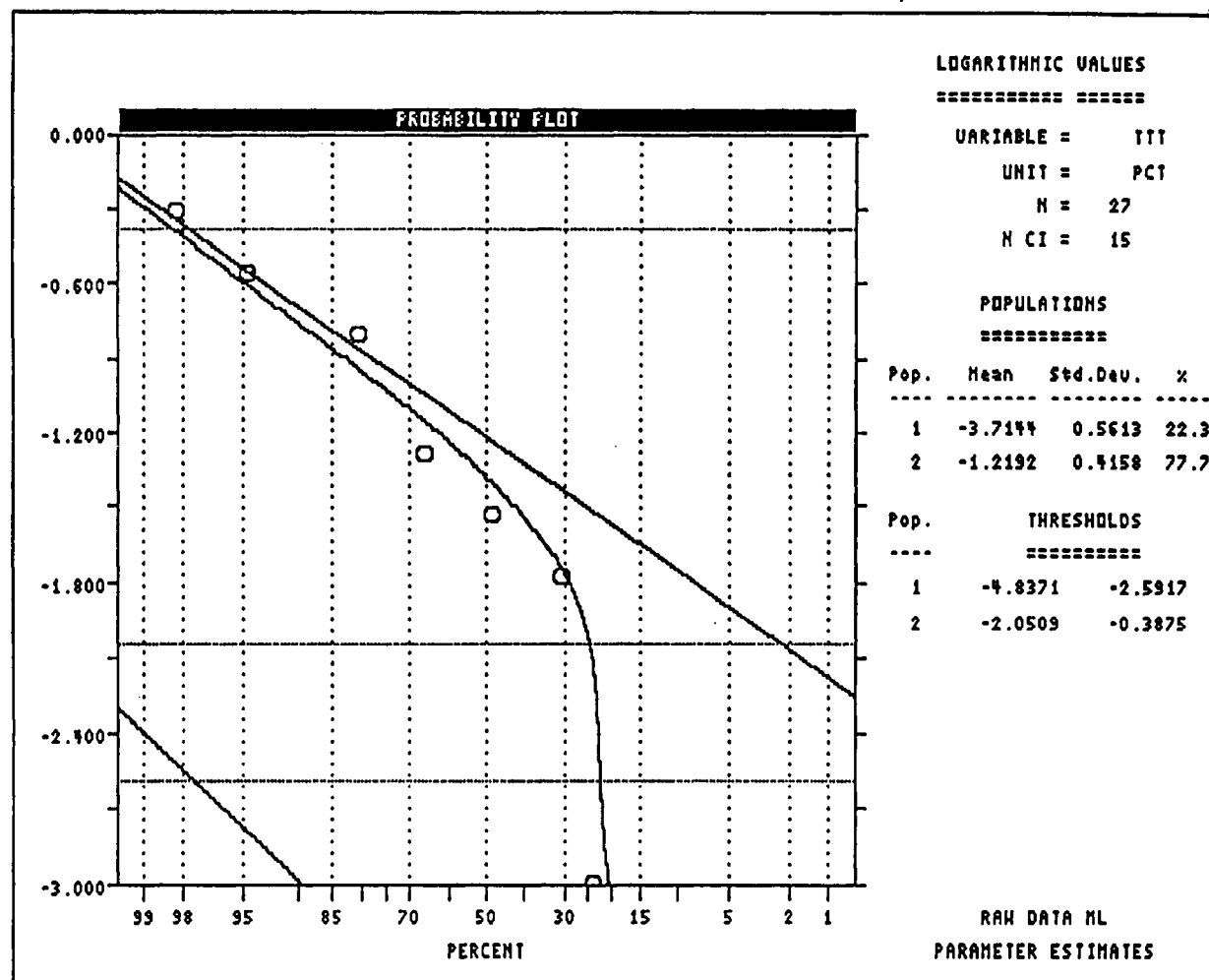


Figure A.12. Log probability plot of averaged tetrahedrite - tennantite over intervals on cross - sections 9700N and 10600N in the Kerr deposit, northwestern British Columbia. Plot shows two populations in the data and the thresholds separating them.

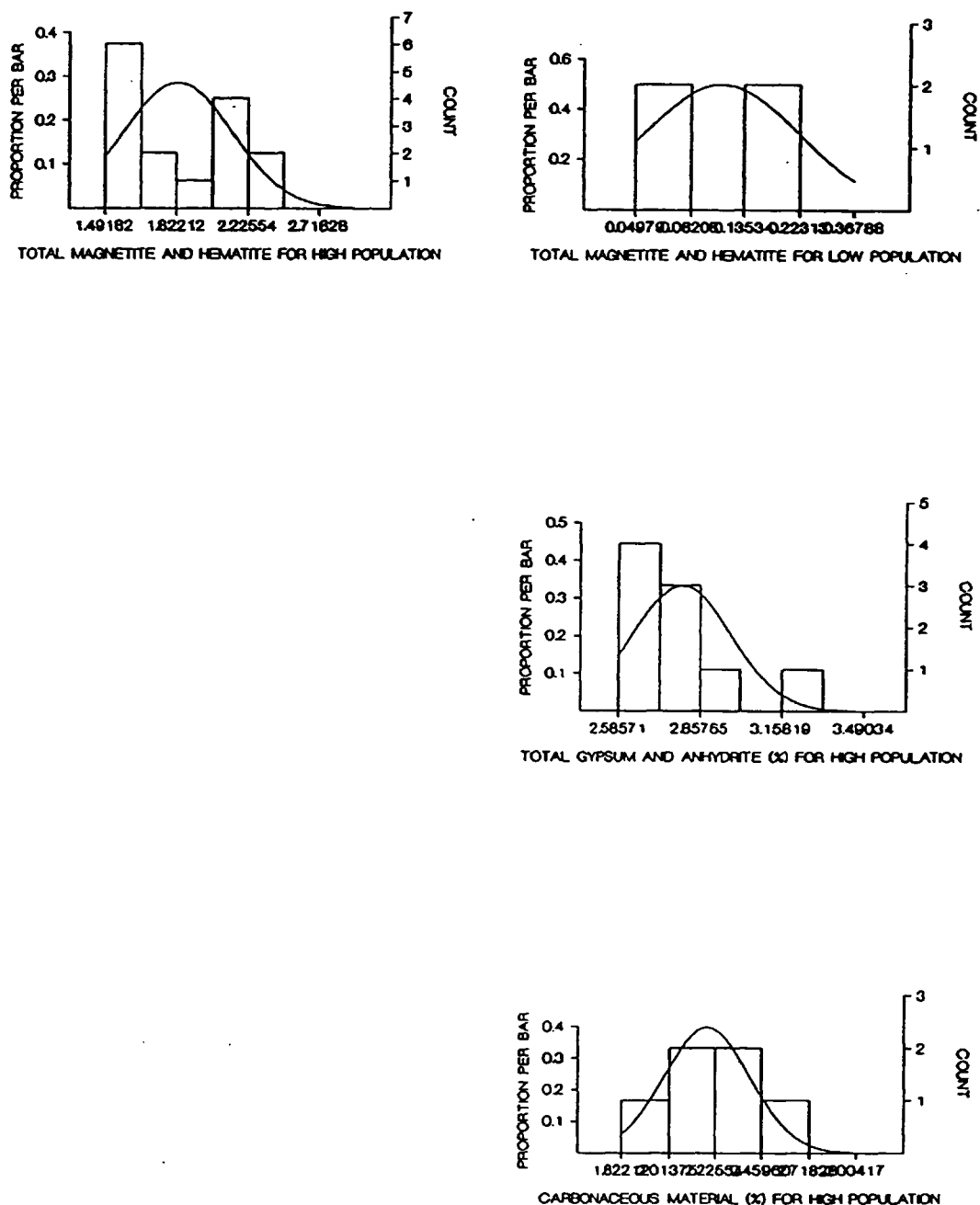


Figure A.13. Log histograms of averaged total magnetite and hematite, total gypsum and anhydrite and carbonaceous material over intervals on cross - sections 9700N and 10600N in the Kerr deposit, northwestern British Columbia.

A probability plot of total tetrahedrite-tennantite shows two populations (Fig A.12). The upper population is distinct from the lower one. It occurs as an isolated peak on the log histogram (Fig. A.13).

Total magnetite and hematite data plot in either an upper population or a lower one (Figs. A.13 and A.14).

Log histograms of total gypsum and anhydrite and total carbonaceous material show that they consist of only one population of data. Percentages of carbonaceous material approximate an ideal log normal distribution, while the sulphates have a truncated distribution.

### A.3.3 Plots of mineral populations

Data for each mineral, ratio or element were subdivided into populations, and it was plotted on cross sections. Using these diagrams three regions were outlined using the occurrence of alteration minerals, intensity of alteration and copper mineralization to characterize region.

The central chlorite core is dominated by: high copper population, high total chalcopryrite to pyrite, high chlorite selvages and envelopes, low to absent tetrahedrite-tennantite, and gypsum and anhydrite below supergene alteration zone. The top portion of the chlorite core on section 10600N is affected by the supergene oxidation of chalcopryrite. In this area the copper and chalcopryrite to pyrite ratios plot in the medium and absent populations respectively. The area was assigned to the chlorite core because the area as chlorite and sericite alteration and high magnetite and hematite contents.

The phyllic region is characterized by: medium copper population, high and low chalcopryrite to pyrite ratio, high sericite selvages and envelopes, high total tetrahedrite-tennantite and no magnetite and hematite veins.

The peripheral region has: low to medium copper, low to zero chalcopryrite to pyrite ratio and high carbonaceous material.

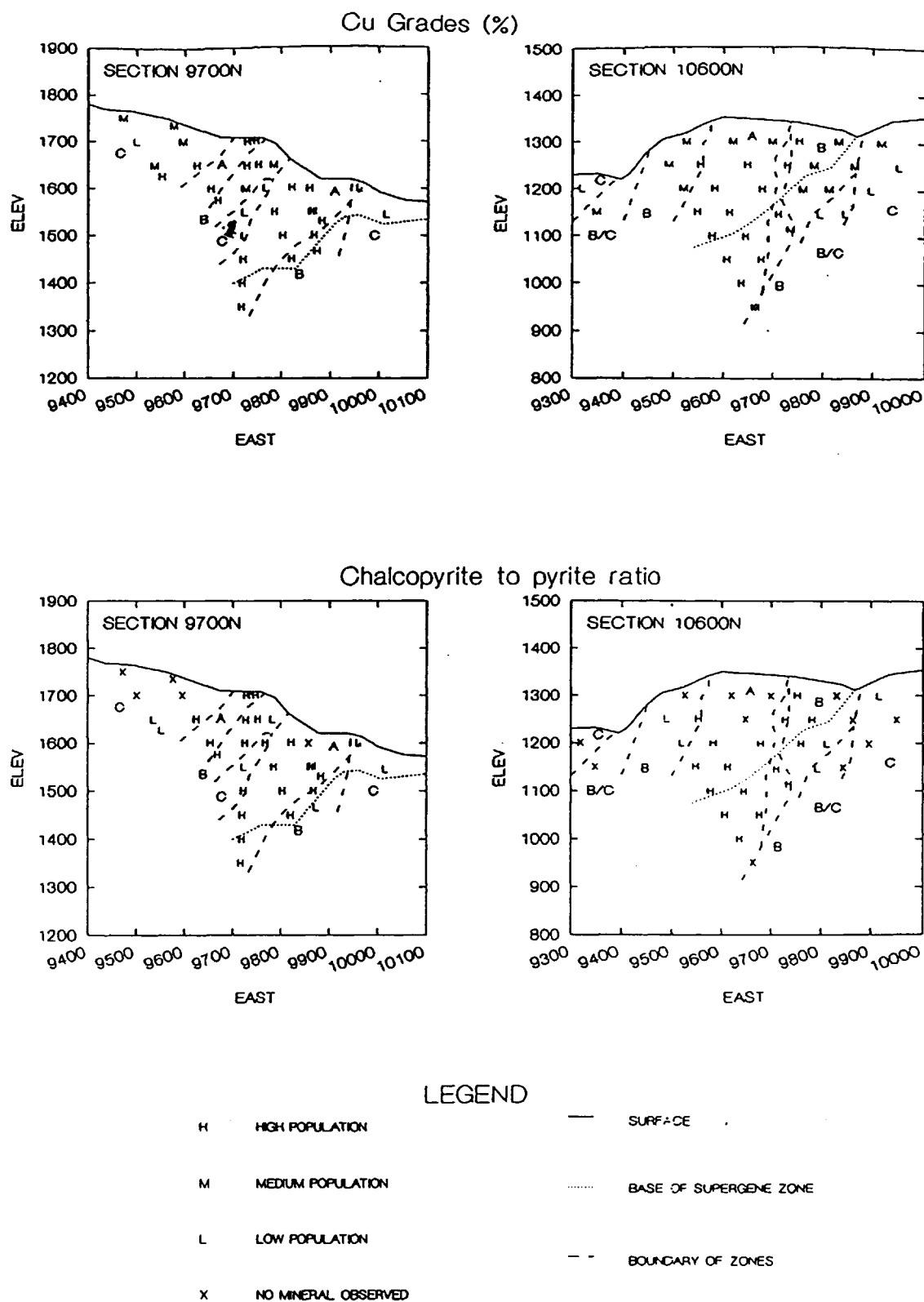


Figure A.14. Cross - sections 9700N and 10600N showing the distribution of the high, medium and low populations in averaged Cu (%) and total chalcopyrite to pyrite ratio. Region A = core, B = halo, C = periphery alteration zones.

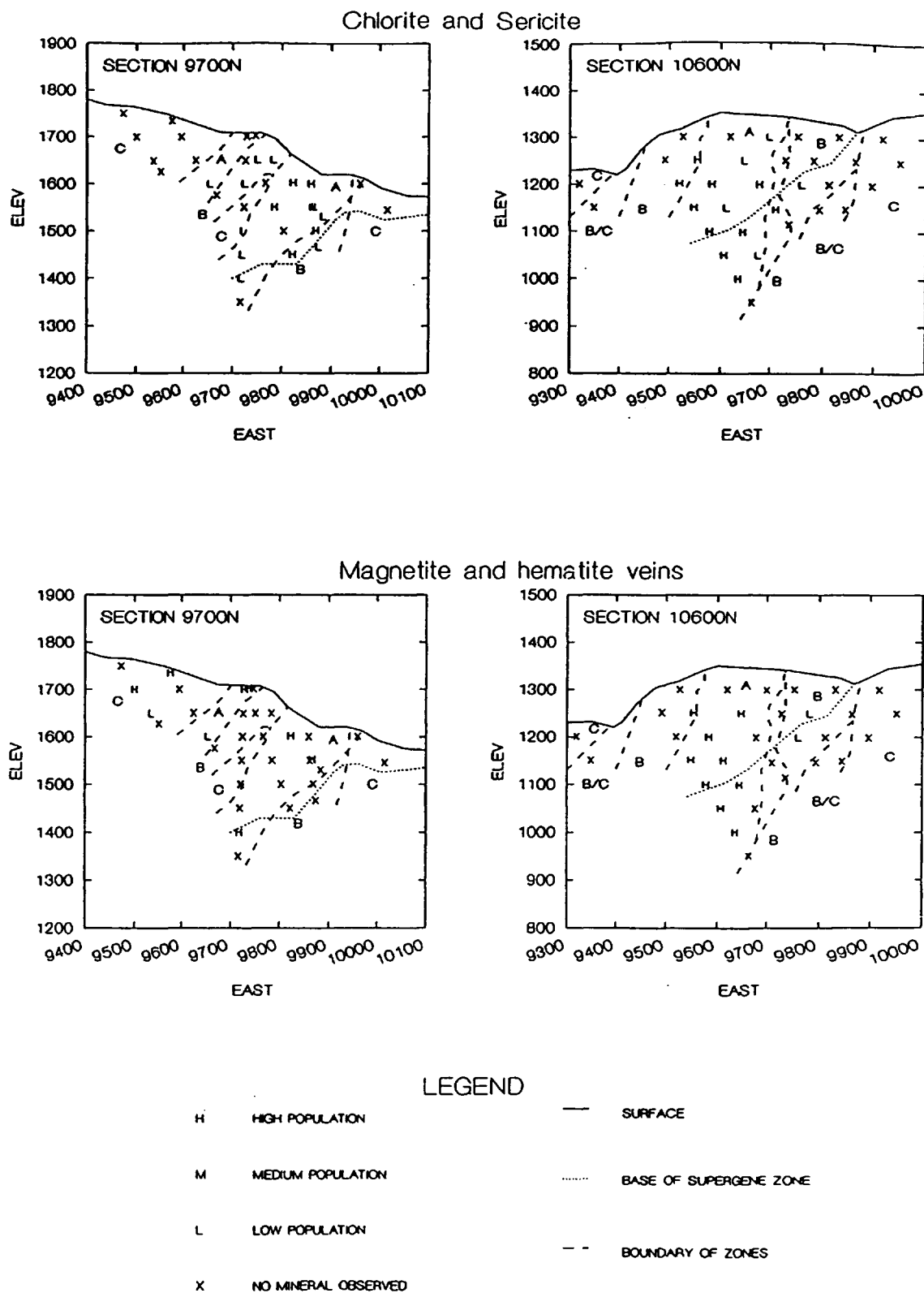


Figure A.15. Cross - sections 9700N and 10600N showing the distribution of the high, medium and low populations in averaged intergrown chlorite and sericite and total magnetite and hematite. Region A = core, B = halo, C = periphery alteration zones.

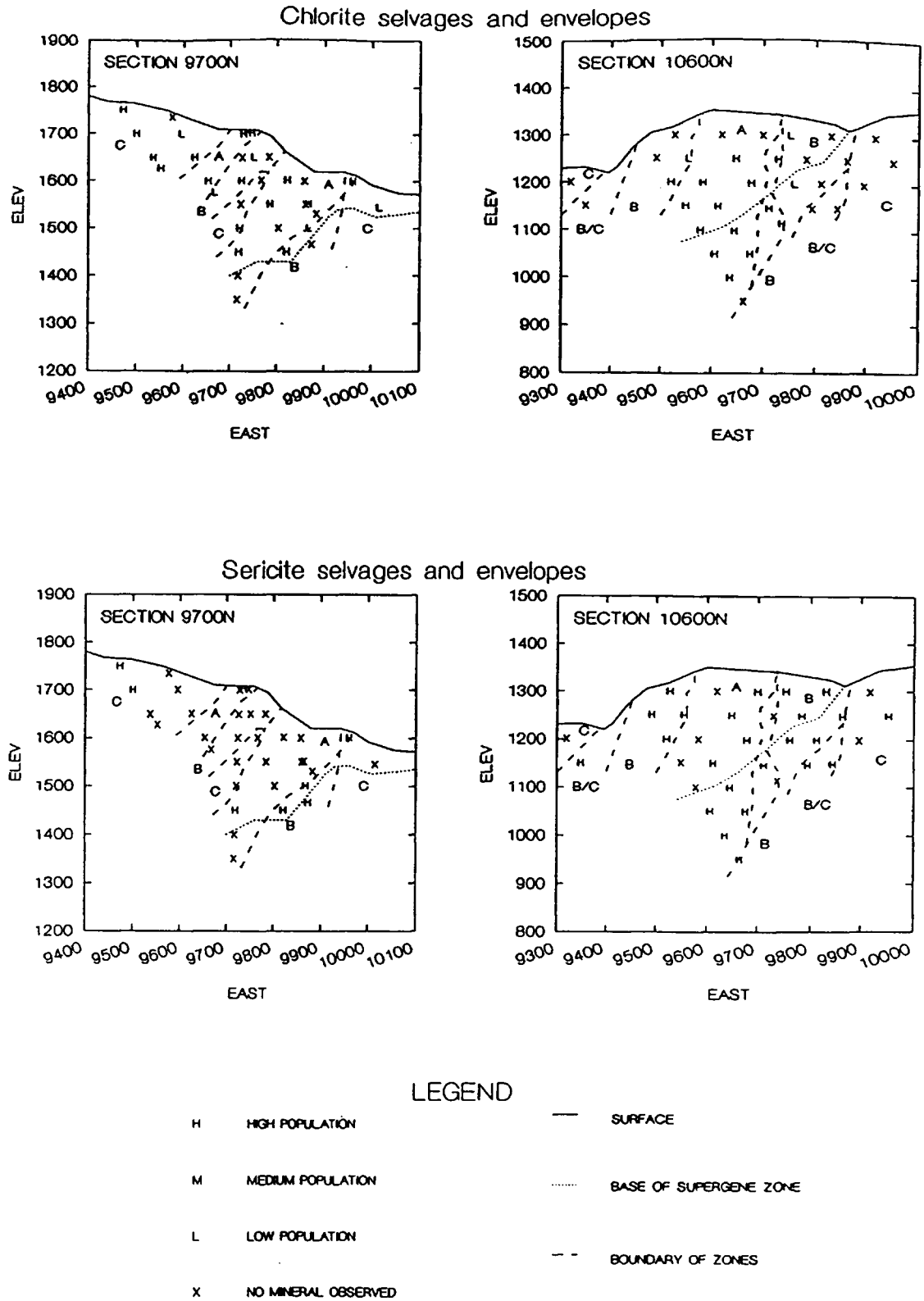


Figure A.16. Cross - sections 9700N and 10600N showing the distribution of the high, medium and low populations in averaged chlorite envelopes and sericite envelopes. Region A = core, B = halo, C = periphery alteration zones.

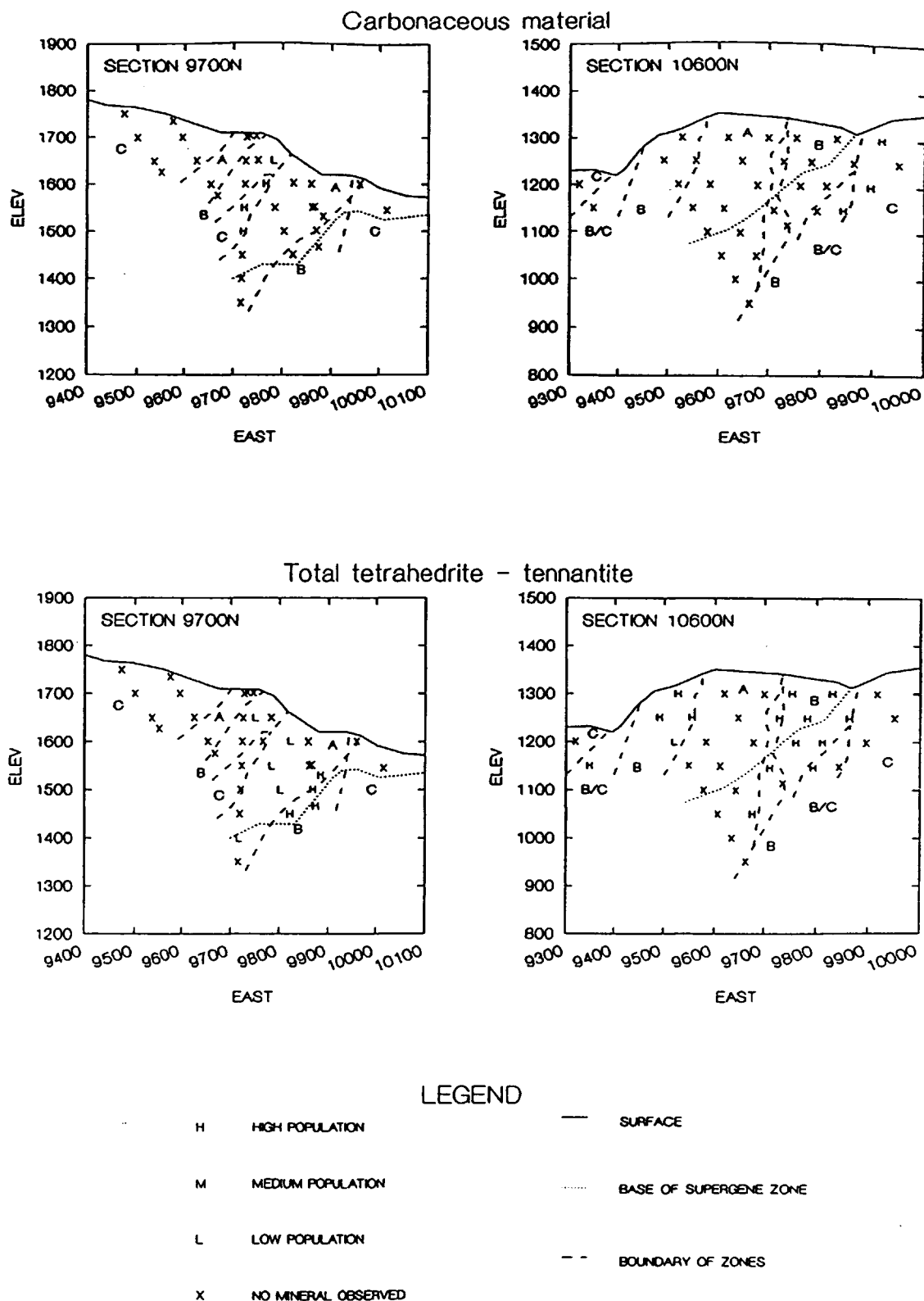


Figure A.17. Cross - sections 9700N and 10600N showing the distribution of the high, medium and low populations in averaged carbonaceous material and total tetrahedrite - tennantite. Region A = core, B = halo, C = periphery alteration zones.



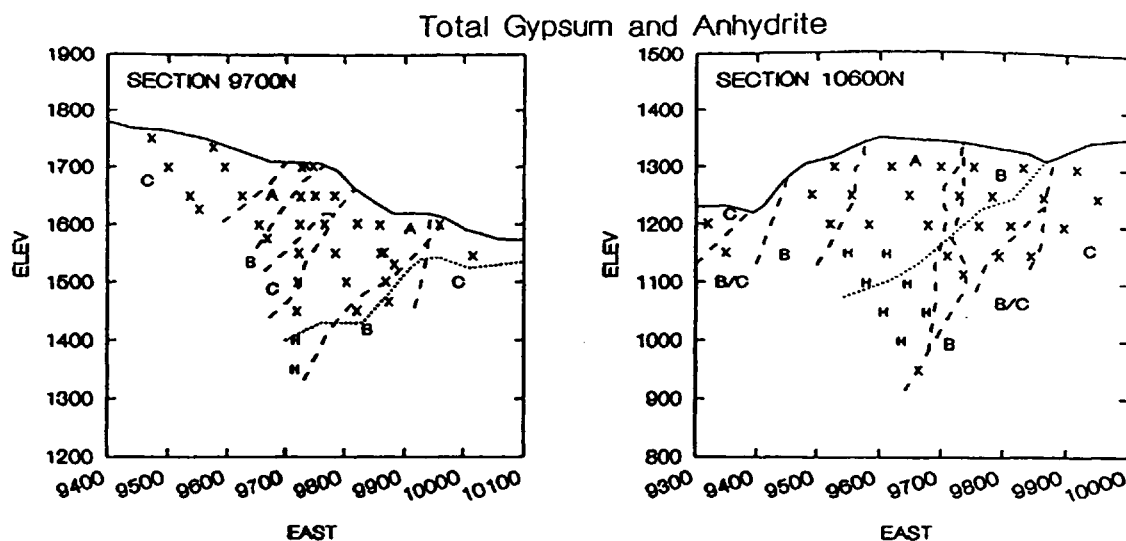


Figure A.18. Cross - sections 9700N and 10600N showing the distribution of the high, medium and low populations in averaged total gypsum and anhydrite. Region A = core, B = halo, C = periphery alteration zones.

## APPENDIX B SAMPLE PREPARATION AND ANALYSIS OF ROCK SAMPLES

### B.1 Sample Preparation

Ten samples of least altered intrusive rocks exposed on the Kerr deposit were analyzed for their trace and major elements. Each sample was selected so that it was free of surface oxidation due to weathering, hematite and was filled fractures and any obvious contamination due to paint markings or organic material.

The size of each sample crushed was determined from the grain size distribution using the method outlined by Gy (1979). The weight of crushed samples ranged in size from 100 grams of fine grained green andesite to ten kilograms of feldspar megacrystic dykes. The large samples of the megacrystic dykes were pulverized to diminish the nugget effect of 30 mm albite and hyalophane crystal in a matrix of 4 mm plagioclase and hornblende grains.

The samples were first crushed using a steel jaw crusher followed by a steel disc mill and finally by a tungsten carbide ring mill. The crushing equipment was brushed and blown clean and the ring mill was washed after each sample. Final subsample selection for analysis and collection of duplicates was accomplished by splitting the sample using a whiffle separator.

Possible contamination from the wear of the equipment consists of Fe, Co, Cr, Cu, Mo, Mn, Ni and V from the disc mill and jaw crusher and Co, Ti and W from the ring mill (Fletcher, 1981). Only Ti contamination from the equipment will effect the results presented in this thesis. It is possibly less than the 5% analytical precision for the element because the contamination is strongly dependent upon the toughness of the rock sample. Most samples contain 40% phyllosilicate minerals so they were readily crushed, and no chips were observed on the rings in the ring mill between samples (Toma, personal comm. 1992).

## **B.2 Sample Analysis**

Ten grams subsamples of each of the rock samples, duplicates and standards were analyzed by X-ray Assay Laboratories (XRAL) in Don Mills, Ontario for trace and major elements. Table B.1 indicates the methodology for each of the 67 elements.

## **B.3 Precision and Accuracy of Results from XRAL**

Precision control graphs were constructed using the duplicates inserted into the analyzed sample suite (figs. B.1 - B.9). The methodology used to construct the diagrams is from Thompson and Howarth (1978). Estimates of the precision for each element are included in Table B.2. The range of average values and absolute values were included in the table because the precision estimation was noted to be dependent upon how close the average was to the detection limit and if the absolute value was a single multiple of it.

Precision estimates of the elements in graphs range from 1 to 30%. The low concentrations of HRE elements are strongly affected by their precision of 10 to 20% on the lower portion of the log spider diagram. Precision estimates for the LIL elements range from 1 to 20%.

Accuracy of results was monitored by three internal standards which were mineralogy similar to the samples submitted for analysis. Tables B.3 to B.5 show the results of the analyses. Accuracy of the results plotted in graphs has less of an effect on them than the precision of the duplicate samples.

Table B.1. Methodology for sample digestions use for analysis by X-ray Assay Labs, (Levin, personal communication 1992)

ANALYTICAL	ELEMENTS	PROCEDURE
Inductive coupled plasma	Co, Sc, Ni, Cu, Zn, Y, Ag, Mo, Pb	
Inductive coupled plasma mass spectrometry	La, Ce, Pr, Nd, Sm, Eu, Gd, Tb, Dy, Ho, Er, Tm, Yb, Lu, Tl	"A half gram sample is weighed into a Teflon dish. 5ml H <sub>2</sub> O, 10ml HF and 10ml of HClO <sub>4</sub> are added and the sample is digested on a hot plate to copious white fumes. The volume should be reduced to about 2-3 ml. Remove from hot plate and add 20 ml of 10% HCl. Re-heat the solution to boiling and then allow to cool. Transfer to a volumetric and make up to 50 ml."
Neutron Activation	Cr, As, Sb, U, W, Th, Cs	
Atomic Absorption	Cd	
G, Flame Atomic Absorption	Se	
Direct-Current Plasma emission spectrometer	B, Ge, V	"(A) 0.05 (gm) sample and 3KOH pellets are added in a Ni crucible. The crucible is placed in a furnace at 500 degrees Celsius for 15 minutes, then cooled and dissolved in 50 ml of 5% HCl. The resulting solution is run on a Spectrametrics Direct-current Plasma emission spectrometer. In house standards, previously analyzed samples or standard reference materials and blanks are used to calibrate and monitor the fusion procedure. Calibration standards contain an identical concentration of KOH as the samples."
Atomic Absorption	Te	"A 0.25 gram sample is digested with 10 ml HF and 2 ml aqua regia to dryness; cooled, and repeated with 5 ml HF and 1 ml aqua regia to dryness. The residue is dissolved in HCl and taken to volume. An aliquot is diluted with

Table B.1. cont'd

		50% HCl, MIBK added, the sample agitate, and the MIBK fraction injected into the graphite furnace of an A.A.S. The sample result is read on a chart recorder and quantified verses a standard curve of Te standards."
Fire Assay Direct Current Spectrometry	Au, Pt, Pd	
X-ray fluoresce	SiO <sub>2</sub> , Al <sub>2</sub> O <sub>3</sub> , K <sub>2</sub> O, Na <sub>2</sub> O, CaO, Fe <sub>2</sub> O <sub>3</sub> , MgO, TiO <sub>2</sub> , MnO, P <sub>2</sub> O <sub>5</sub>	Fused pellets
X-ray fluoresce	Sr, Ba, Cl, Rb, Zr, Nb	Fused pellets
Coulometric	CO <sub>2</sub>	Coulometric procedure
Wet chemistry	H <sub>2</sub> O	"H <sub>2</sub> O is determined when the sample is dried, and heated in a pyrex test tube with either sodium tungstate (Na <sub>2</sub> WO <sub>4</sub> .2H <sub>2</sub> O) or lead oxide (PbO)."

Table B.2 Precision control graph data from duplicates submitted to X-ray Assay Lab.

## PRECISION CONTROL GRAPH DATA FROM DUPLICATES SUBMITTED TO X-RAY ASSAY LAB

ELEMENT	PRECISION (%)	DATA POINT PLOTTED	TOTAL POINTS	DETECTION LIMIT	RANGE OF AVERAGE VALUES		RANGE OF ABSOLUTE DIFFERENCE	
					MAXIMUM	MINIMUM	MAXIMUM	MINIMUM
XRF whole rock major elements				(wt %)				
SiO2	1	8	8	0.01	77.2	44.25	1.4	0.1
Al2O3	1	6	8	0.01	17.85	11.3	0.4	0.1
K2O	1	7	8	0.01	6.785	0.495	0.08	0.01
Na2O	1	8	8	0.01	5.44	0.115	0.14	0.01
CaO	1	6	8	0.01	4.715	1.745	0.13	0.02
Fe2O3	1	7	8	0.01	12.25	1.045	0.77	0.01
MgO	5	8	8	0.01	6.57	0.365	0.08	0.01
TiO2	5	6	8	0.01	1.56	0.0785	0.042	0.001
MnO	5	3	8	0.01	0.615	0.01	0.02	0.01
P2O5	5	2	8	0.01	0.495	0.02	0.02	0.01
XRF whole rock trace elements				(ppm)				
Sr	5	7	7	10	631.5	65	16	2
Ba	5	7	7	10		357	150	4
Cl	5	3	7	100	302	119.5	17	2
Rb	10	7	8	10	152.5	19	12	1
Zr	5	8	8	1	323	44.5	14	1
Nb	20	6	8	2	26.5	4	3	1
Neutron Activation								
Cr	>5	3	7	2	250	9	20	2
As	>5	7	7	0.1	28	2.25	1.1	0.2
Sb	5	5	7	0.1	9.9	0.2	0.2	0.1
U	20	7	7	0.1	8.35	0.05	0.5	0.1
W	10	1	7	1	6.5	1	1	1
Th	5	5	7	0.5	10	1.15	0.6	0.1
Cs	no plot	0	7	1	4	2	2	1
DCP								
B	30	6	7	10	39.5	19	16	4
Ge	no plot	0	4	10	<10			
V	5	5	7	2	288	3.5	22	1
FADCP				(ppb)				
Au	>50	6	6	1	82	6	156	2
Pd	20	2	6	1	4.5	2.5	1	1
Pt	no plot	0	4	10	<10			
Wet								
Hg	20	7	7	5	105	10.5	11	1

Table B.2 cont'd

ELEMENT	PRECISION (%)	DATA POINT PLOTTED	TOTAL POINTS	DETECTION LIMIT	RANGE OF AVERAGE VALUES		RANGE OF ABSOLUTE DIFFERENCE	
					MAXIMUM	MINIMUM	MAXIMUM	MINIMUM
LECO				(wt %)				
S	10	6	6	0.005	0.165	0.013	0.025	0.001
ICP				(ppm)				
Co	20	4	7	1	35.5	3.5	1	1
Ni	10	3	6	1	72.5	1.5	3	1
Cu	5	5	7	0.5	338	2.75	6	0.1
Zn	10	7	7	0.5	174.5	7.05	8	3
Y	10	5	7	1	79	11.5	10	1
Sc	20	7	7	0.05	42.2	0.665	1.4	0.1
Ag	no plot	0	7	0.1	1	0.4	0	
Mo	no plot	0	4	1	<1			
Pb	no plot	2	4	2	38.5	6	2	1
ICPMS								
La	20	7	7	0.1	31.5	4.35	6.3	0.2
Ce	10	5	7	0.1	62	10.9	11.2	0.9
Pr	10	5	7	0.1	8.4	1.9	1.5	0.1
Nd	10	6	7	0.1	32	8.65	6.3	0.5
Sm	10	7	7	0.1	8.6	2.15	0.9	0.1
Eu	10	6	7	0.05	1.635	0.145	0.27	0.01
Gd	10	7	7	0.1	8.1	2.7	1.3	0.2
Tb	20	6	7	0.1	1.6	0.5	0.3	0.1
Dy	10	6	7	0.1	11.2	2.85	2.2	0.1
Ho	20	7	7	0.05	2.45	0.51	0.64	0.01
Er	20	6	7	0.1	7.4	1.9	1.6	0.1
Tm	20	3	7	0.1	1	0.2	0.2	0.1
Yb	20	5	7	0.1	6.9	1.4	1.4	0.1
Lu	30	6	7	0.05	1.015	0.215	0.43	0.01
Tl	50	5	7	0.1	3.15	0.7	0.7	0.1
Bi	no plot	0	7					

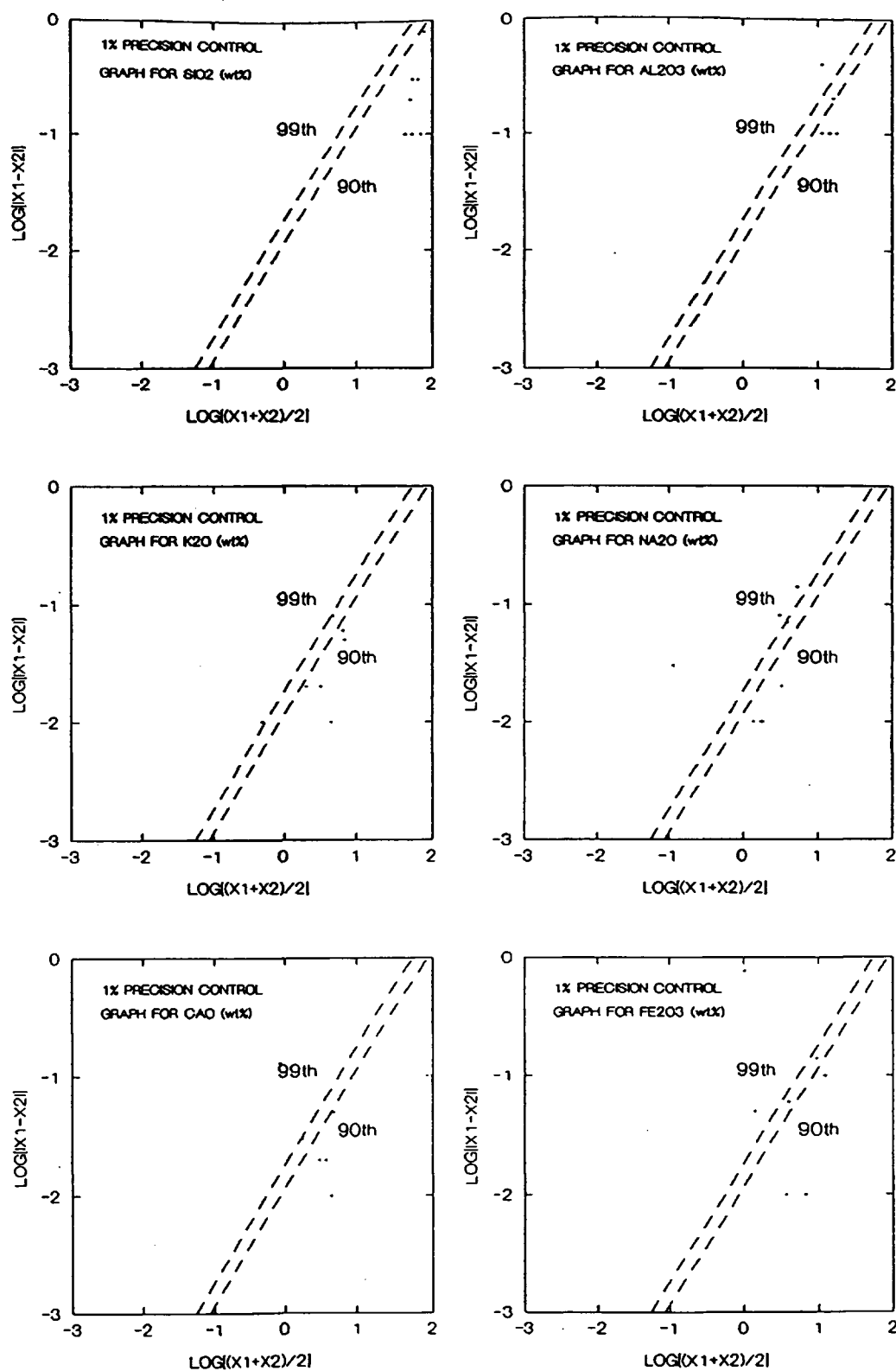


Figure B.1 Precision control graphs for:  $\text{SiO}_2$ ,  $\text{Al}_2\text{O}_3$ ,  $\text{K}_2\text{O}$ ,  $\text{Na}_2\text{O}$ ,  $\text{CaO}$  and  $\text{Fe}_2\text{O}_3$  (wt%).



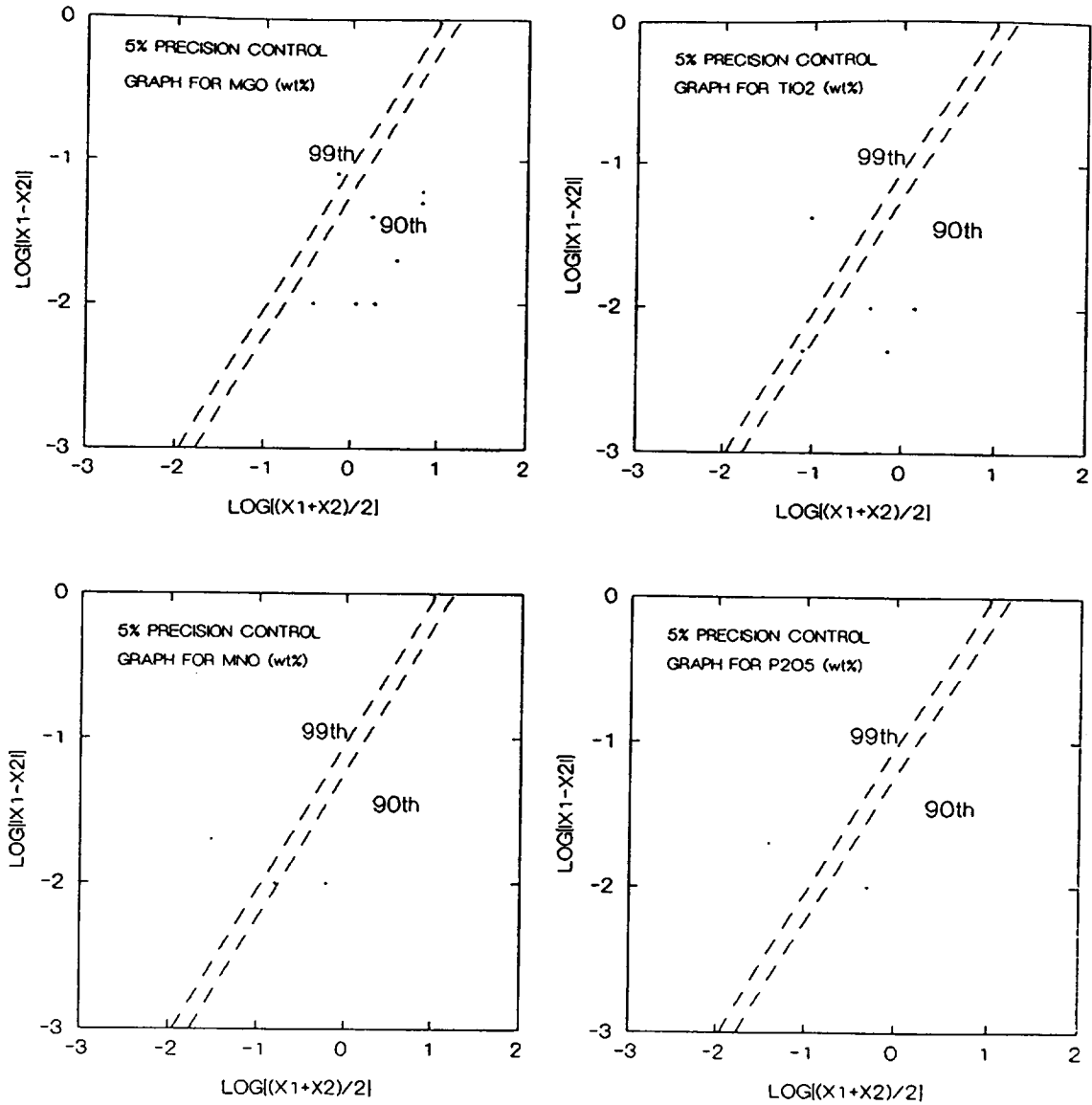


Figure B.2. Precision control graphs for: MgO, TiO<sub>2</sub>, MnO and P<sub>2</sub>O<sub>5</sub> (wt%).

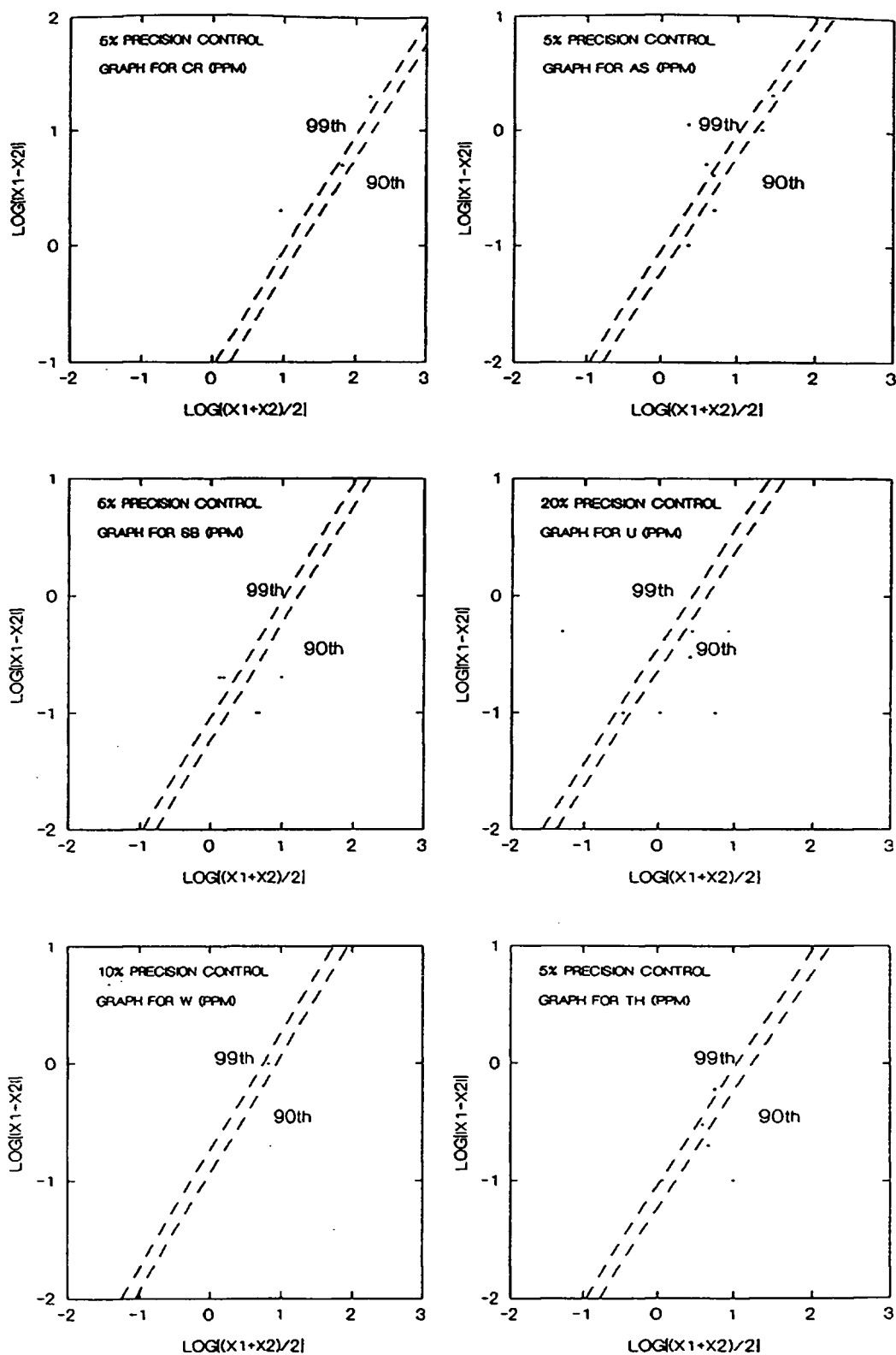


Figure B.3. Precision control graphs for: Cr, As, Sb, U, W and Th (ppm).

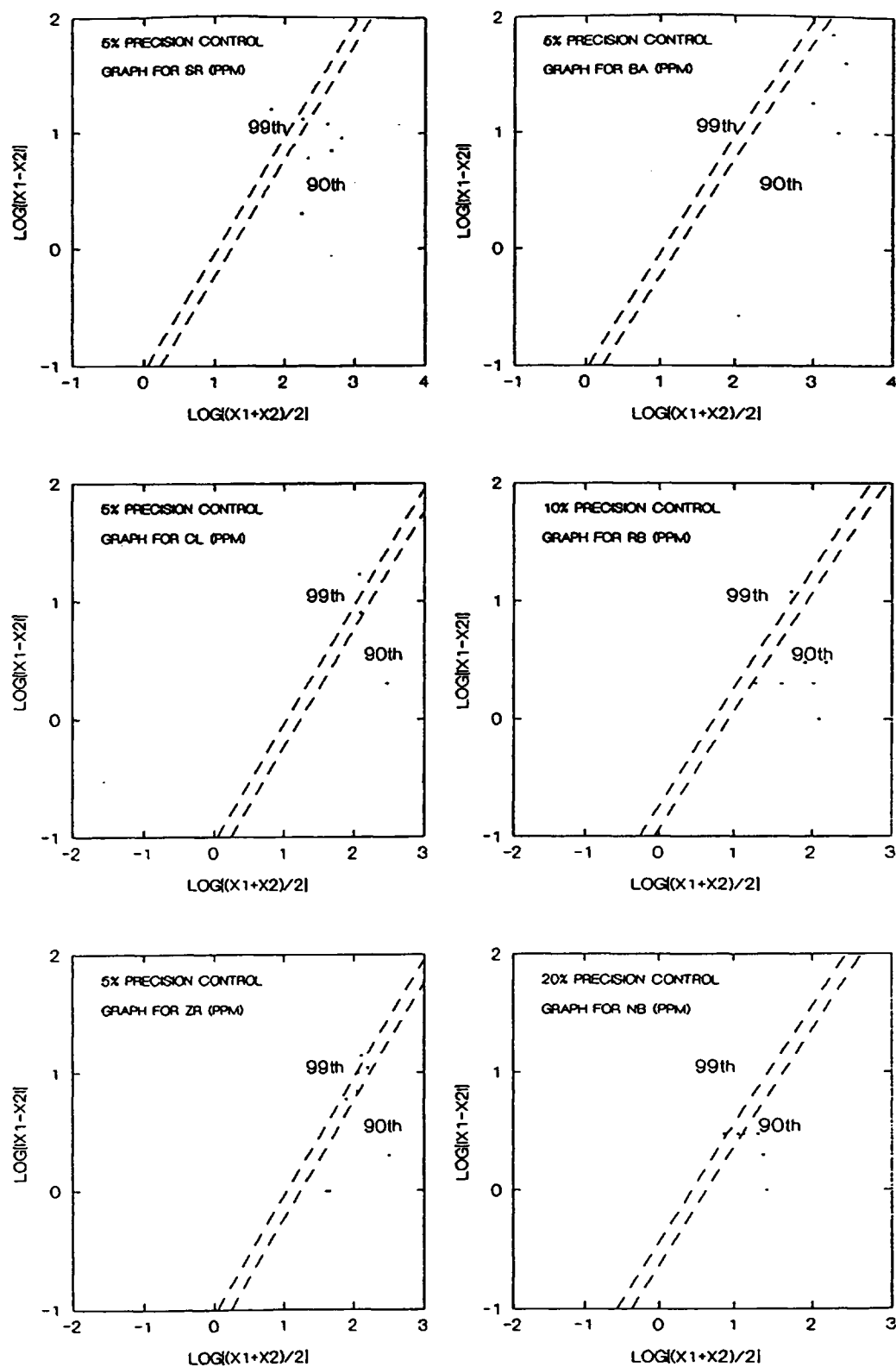


Figure B.4. Precision control graphs for: Sr, Ba, Cl, Rb, Zr and Nb (ppm).

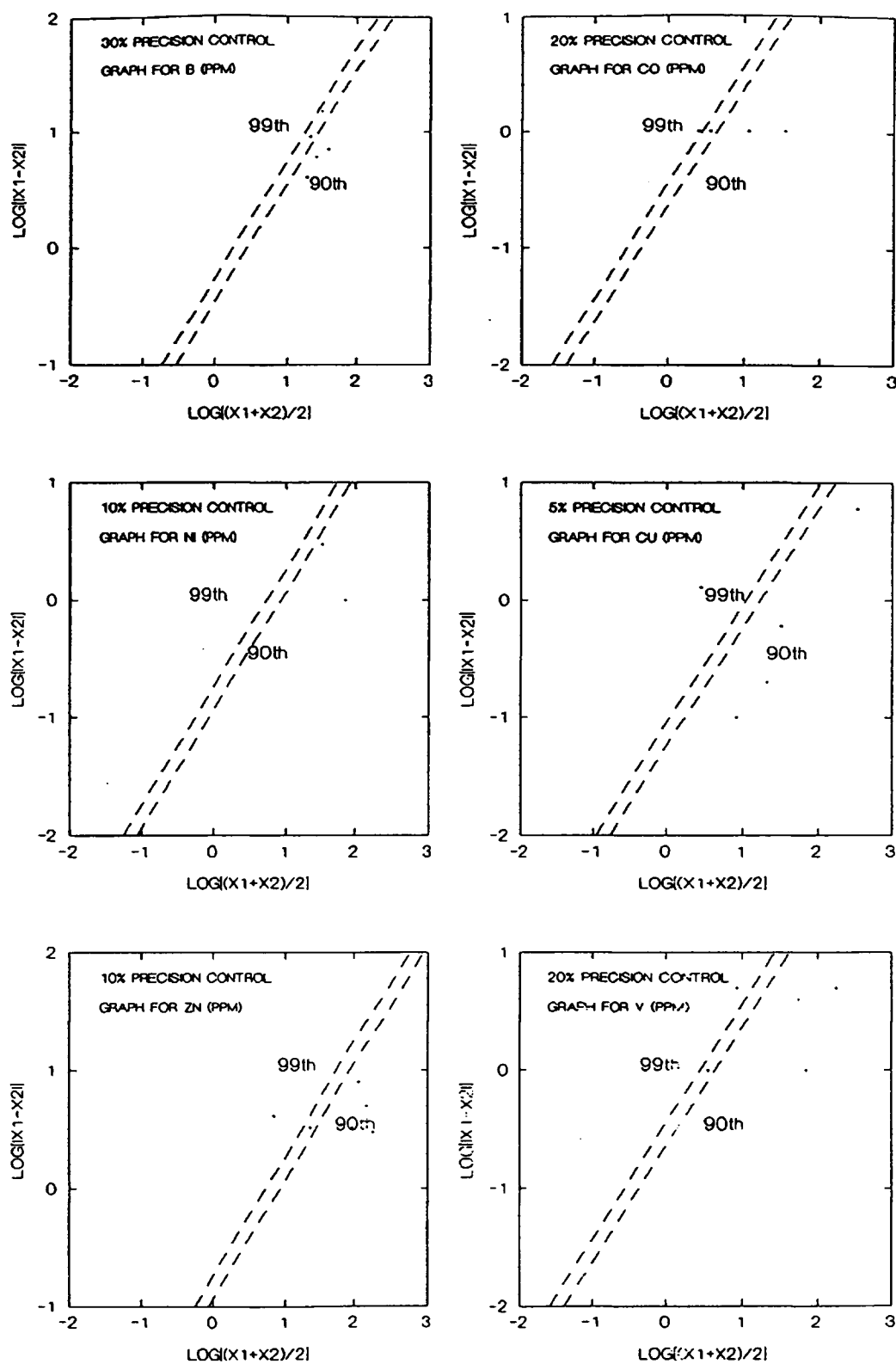


Figure B.5. Precision control graphs for: B, Co, Ni, Cu, Zn and V (ppm).

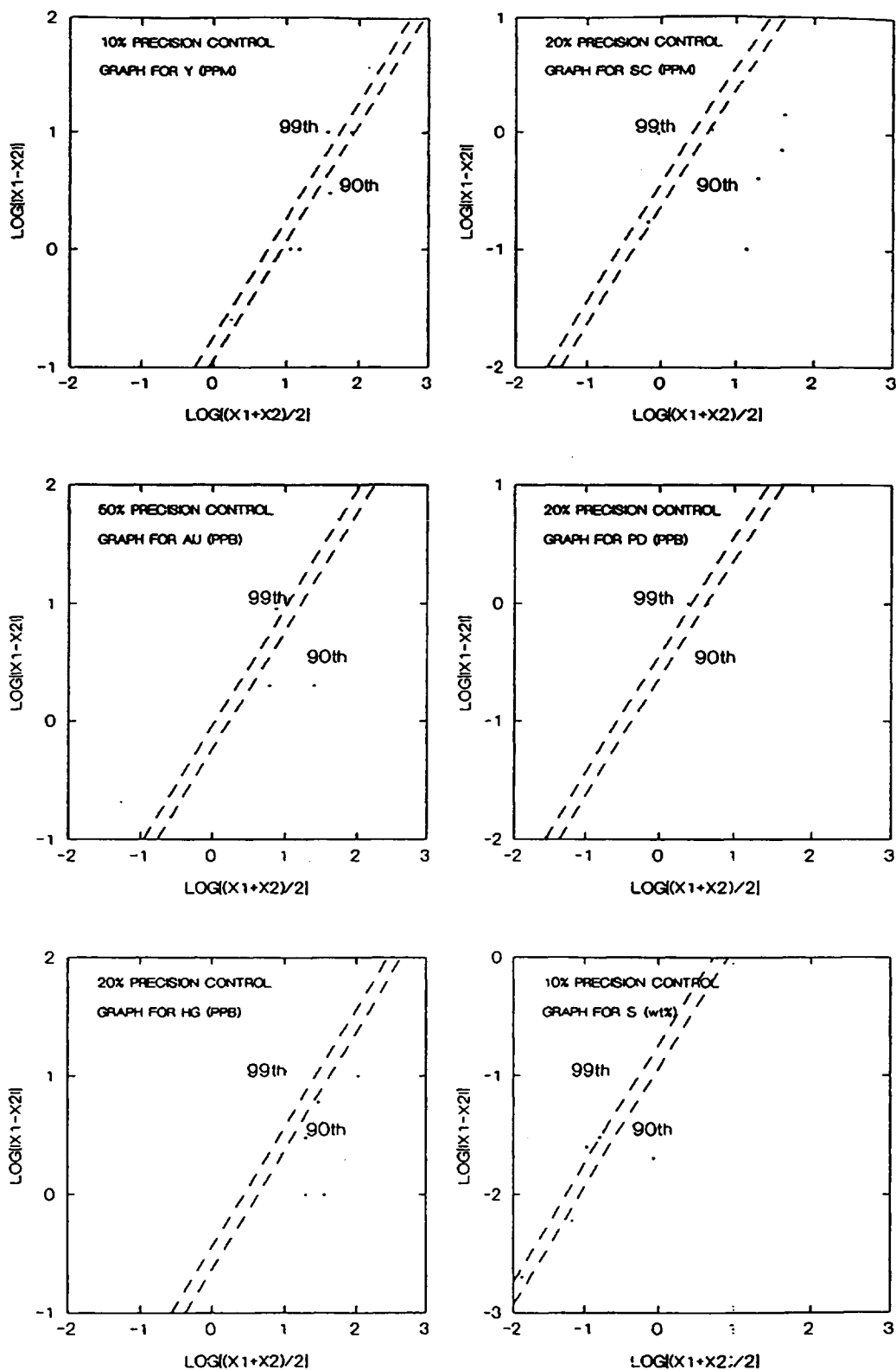


Figure B.6. Precision control graphs for: Y (ppm), Sc (ppm), Au (ppb), Pd (ppb), Hg (ppb) and S (wt%).

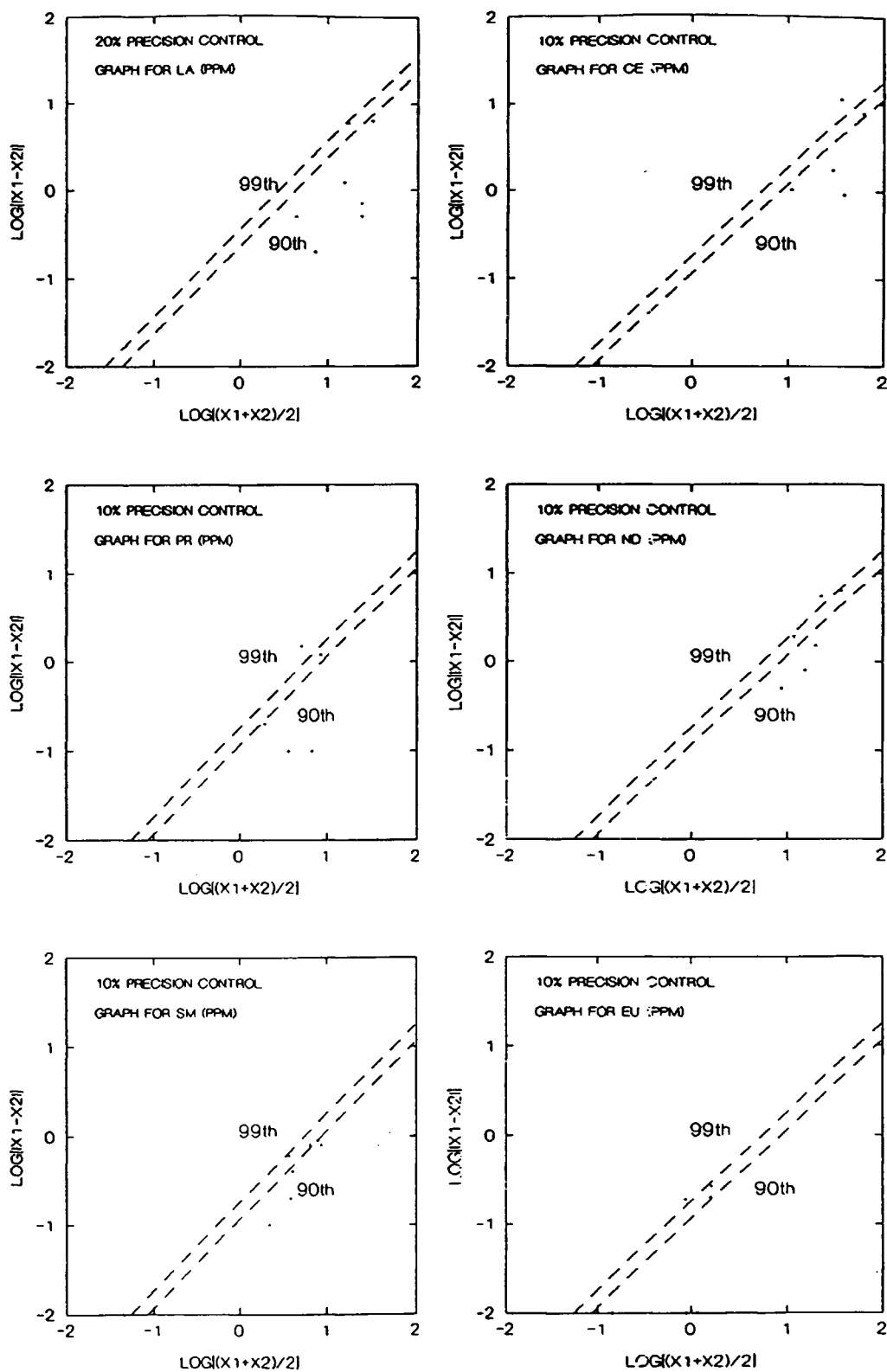


Figure B.7. Precision control graphs for: La, Ce, Pr, Nd, Sm and Eu (ppm).

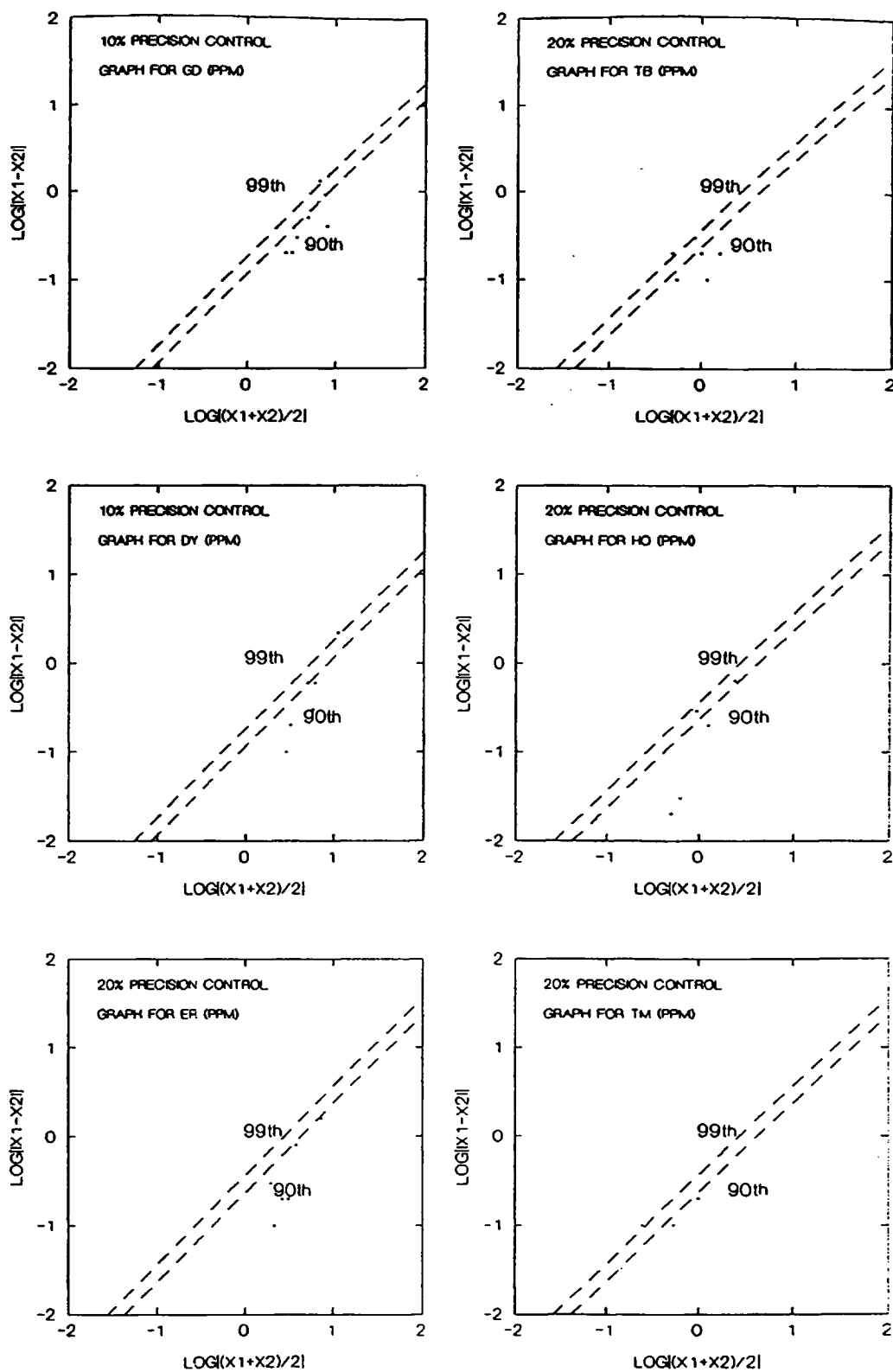


Figure B.8. Precision control graphs for: Gd, Tb, Dy, Ho, Er and Tm (ppm).

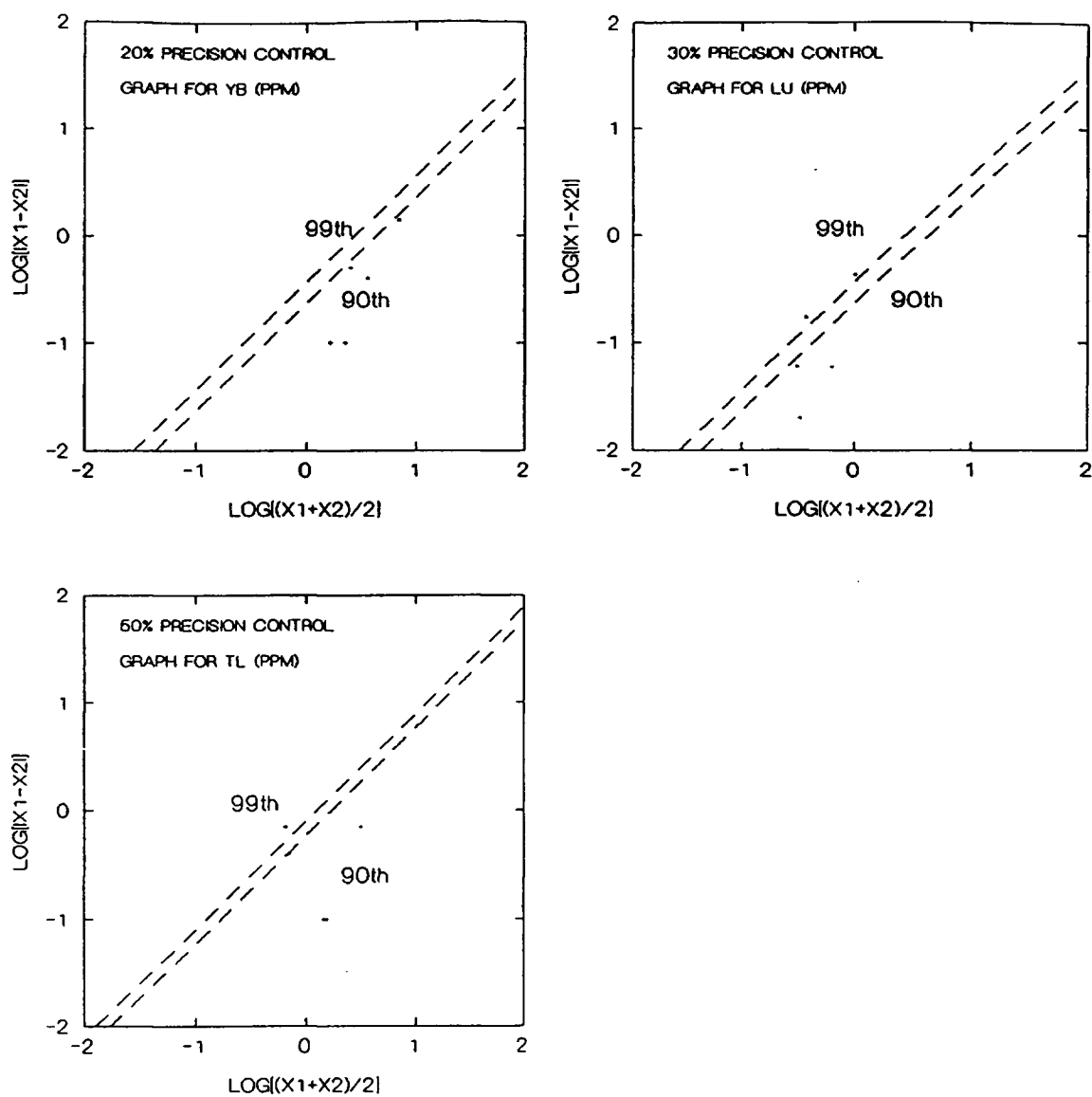


Figure B.9. Precision control graphs for: Yb, Lu and Tl (ppm).



#### **B.4 Precision of Cu and Au Assays Analyzed by Placer Dome Inc.**

Precision of the Cu assays used for plots of Cu across the two cross sections was calculated using the method of Thompson and Howarth (1978) for over fifty duplicates to be

$$P_c = 0.133/c + 1.57$$

where  $c$  is the concentration of Cu (wt%) and  $P_c$  is the precision (fig B.10). Gold duplicates have a 5 % precision using the method of Thompson and Howarth (1978) for less than fifty duplicates. These precision estimates have little effect to the size of the bubbles on Figure 6.2 and on the thresholds used to determine the separate mineral assemblage populations.

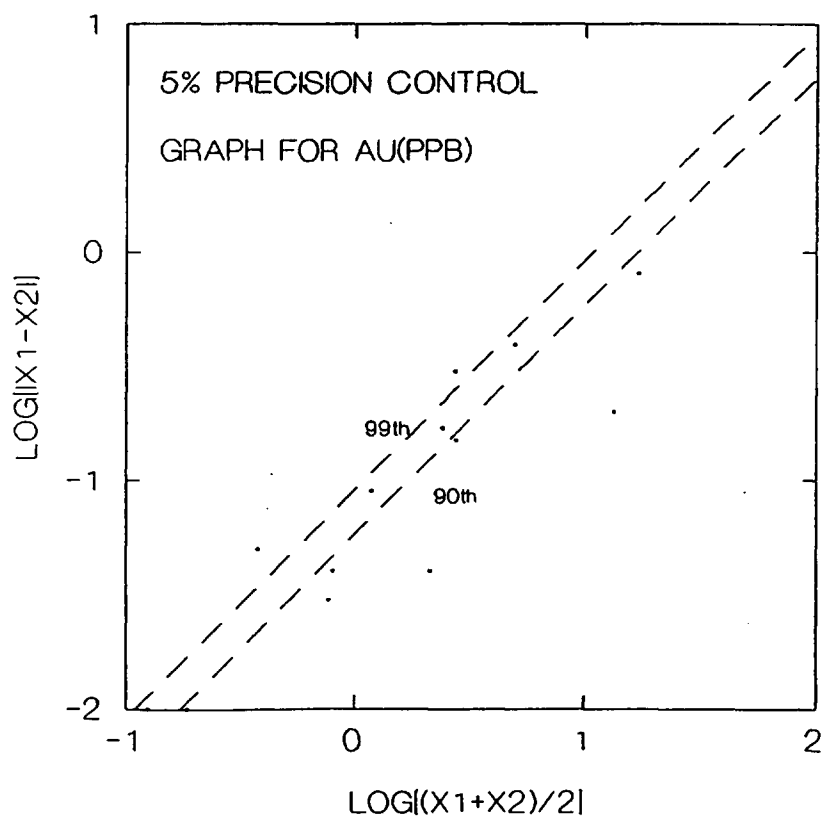
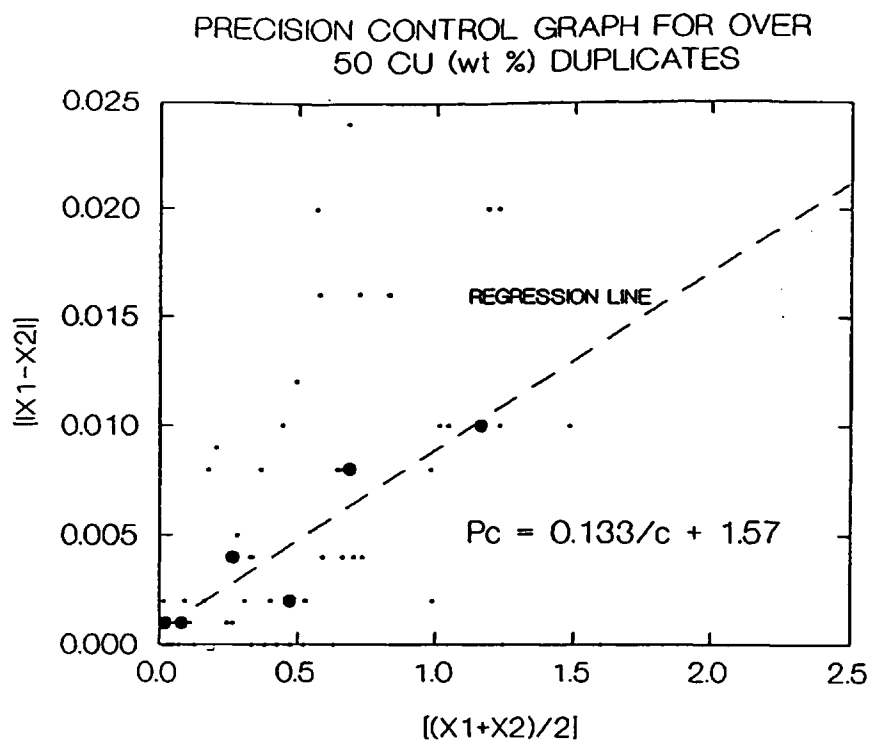


Figure B.10. Precision control graphs for assayed Cu (wt %) and Au (ppb) for intervals on cross - sections 9700N and 10600N in the Kerr deposit, northwestern British Columbia.

Table B.3 Table of geochemistry for an internal standard WP1. NC = not calculated

STANDARD WP1						
	ELEMENT	UNITS	AVG	STD	NUMBER OF SAMPLES	FIRST BATCH
						SECOND BATCH
XRF whole rock major elements						
	SiO <sub>2</sub>	%	64.080	0.449	5	64.2
	Al <sub>2</sub> O <sub>3</sub>	%	16.500	0.063	5	16.5
	CaO	%	5.156	0.022	5	5.12
	MgO	%	2.694	0.045	5	2.64
	Na <sub>2</sub> O	%	4.368	0.050	5	4.32
	K <sub>2</sub> O	%	1.530	0.041	5	1.51
	Fe <sub>2</sub> O <sub>3</sub>	%	4.408	0.045	5	4.42
	MnO	%	0.090	0.000	5	0.09
	TiO <sub>2</sub>	%	0.519	0.005	5	0.522
	P <sub>2</sub> O <sub>5</sub>	%	0.180	0.000	5	0.18
	LOI	%	0.256	0.096	5	0.31
	SUM	%	99.929	0.475	5	100.016
XRF whole rock trace elements						
	RB	PPM	23.600	1.625	5	22
	SR	PPM	851.600	64.519	5	888
	BA	PPM	685.750	20.945	5	707
	Y	PPM	16.600	5.571	5	26
	ZR	PPM	123.600	5.389	5	123
	NB	PPM	NC	NC	5	4
	CL	PPM	211.400	38.134	5	220
Neutron Activation						
	CR	PPM	66.600	4.841	5	65
	AS	PPM	0.540	0.136	5	0.7
	SB	PPM	0.860	1.471	5	0.1
	TH	PPM	1.960	0.102	5	2.1
	U	PPM	0.760	0.185	5	0.8
	W	PPM	NC	NC	5	2
	CS	PPM	NC	NC	5	<1
DCP						
	B	PPM	25.000	9.230	5	24
	GE	PPM	NC	NC	5	16
	V	PPM	81.200	8.183	5	74
FADCP						
	AU	PPB	NC	NC	5	2
	PD	PPB	NC	NC	5	<1
	PT	PPB	<10	0.000	5	<10
Wet						
	HG	PPB	47.250	51.608	5	22
	H <sub>2</sub> O +	%	0.280	0.040	5	0.3
	CO <sub>2</sub>	%	NC	NC	5	0.03
LECO						
	S	PPM	NC	NC	5	110
						70

Table B.3 cont'd

	ELEMENT	UNITS	AVG	STD	NUMBER OF SAMPLES	FIRST BATCH	SECOND BATCH
ICP	CO	PPM	9.400	2.871	5	9	8
	NI	PPM	40.200	1.720	5	41	43
	CU	PPM	15.800	1.359	5	14.3	15
	ZN	PPM	57.540	3.331	5	56.6	60.1
	SC	PPM	9.018	0.338	5	8.45	9.48
	MO	PPM	NC	NC	5	1	<1
	SE	PPM	<.5	0.000	5	<.5	<.5
	AG	PPM	NC	NC	5	<.1	0.4
	CD	PPM	<.2	0.000	5	<.2	<.2
	PB	PPM	<2	0.000	5	<2	<2
	TE	PPM	0.040	0.000	5	<.02	<.02
ICPMS	LA	PPM	14.040	0.628	5	14.9	14.7
	CE	PPM	29.240	1.353	5	29.9	31.3
	PR	PPM	3.740	0.361	5	4.2	4.1
	ND	PPM	16.420	1.450	5	18	18.1
	SM	PPM	3.120	0.402	5	3.6	3.5
	EU	PPM	0.900	0.105	5	1.09	0.89
	GD	PPM	2.780	0.366	5	3.1	3.1
	TB	PPM	0.420	0.075	5	0.5	0.5
	DY	PPM	2.480	0.223	5	2.8	2.7
	HO	PPM	0.448	0.010	5	0.45	0.45
	ER	PPM	1.540	0.206	5	1.9	1.5
	TM	PPM	0.220	0.040	5	0.2	0.2
	YB	PPM	1.440	0.102	5	1.6	1.4
	LU	PPM	0.230	0.032	5	0.28	0.22
	TL	PPM	NC	NC	5	<.1	0.1
	BI	PPM	<1	0.000	5	<1	<1

Table B.4. Table of geochemistry for an internal standard P1. NC = not calculated

STANDARD P1					NUMBER OF SAMPLES	FIRST BATCH	SECOND BATCH
ELEMENT	UNITS	AVG	STD				
XRF whole rock major elements							
SiO <sub>2</sub>	%	70.060	0.215	5	70	69.8	
Al <sub>2</sub> O <sub>3</sub>	%	14.380	0.098	5	14.5	14.2	
CaO	%	3.614	0.033	5	3.6	3.67	
MgO	%	1.130	0.022	5	1.13	1.15	
Na <sub>2</sub> O	%	4.032	0.049	5	3.95	4.07	
K <sub>2</sub> O	%	1.968	0.039	5	1.92	2	
Fe <sub>2</sub> O <sub>3</sub>	%	3.796	0.036	5	3.84	3.78	
MnO	%	0.090	0.000	5	0.09	0.09	
TiO <sub>2</sub>	%	0.403	0.009	5	0.411	0.414	
P <sub>2</sub> O <sub>5</sub>	%	0.090	0.000	5	0.09	0.09	
LOI	%	0.454	0.102	5	0.47	0.4	
SUM	%	100.150	0.198	5	100.158	99.791	
XRF whole rock trace elements							
RB	PPM	46.800	0.980	5	47	48	
SR	PPM	267.400	21.086	5	282	288	
BA	PPM	883.200	25.631	5	903	833	
Y	PPM	22.000	4.940	5	27	18	
ZR	PPM	124.200	12.057	5	147	115	
NB	PPM	NC	NC	5	3	12	
CL	PPM	NC	NC	5	<100	111	
Neutron Activation							
CR	PPM	130.000	6.325	5	130	140	
AS	PPM	NC	NC	5	1	1	
SB	PPM	0.800	1.101	5	0.2	0.3	
TH	PPM	4.080	0.147	5	3.9	4	
U	PPM	1.540	0.080	5	1.6	1.6	
W	PPM	NC	NC	5	2	3	
CS	PPM	1.000	0.000	5	1	1	
DCP							
B	PPM	27.200	7.884	5	32	32	
GE	PPM	4.400	5.426	5	<10	<10	
V	PPM	60.600	6.406	5	55	61	
FADCP							
AU	PPB	NC	NC	5	<1	6	
PD	PPB	NC	NC	5	<1	1	
PT	PPB	0.000	0.000	5	<10	<10	
Wet							
HG	PPB	NC	NC	5	5	<5	
H <sub>2</sub> O +	%	0.500	0.000	5	0.5	0.5	
CO <sub>2</sub>	%	NC	NC	5	0.03	0.71	
LECO							
S	PPM	NC	NC	5	140	70	

Table B.4. cont'd

	ELEMENT	UNITS	AVG	STD	NUMBER OF SAMPLES	FIRST BATCH	SECOND BATCH
ICP	CO	PPM	5.800	2.227	5	5	4
	NI	PPM	NC	NC	5	<1	3
	CU	PPM	9.060	1.686	5	7	8.3
	ZN	PPM	43.360	1.322	5	43.7	45.2
	SC	PPM	10.264	0.282	5	10.7	10.3
	MO	PPM	NC	NC	5	1	<1
	SE	PPM	0.000	0.000	5	<.5	<.5
	AG	PPM	<.1	0.000	5	<.1	<.1
	CD	PPM	<.2	0.000	5	<.2	<.2
	PB	PPM	<2	0.000	5	<2	<2
	TE	PPM	NC	NC	5	<.02	<.02
ICPMS	LA	PPM	13.360	0.432	5	12.7	13.6
	CE	PPM	25.860	0.731	5	25.1	25.6
	PR	PPM	3.140	0.162	5	3.4	3.1
	ND	PPM	13.580	0.983	5	15.4	13.1
	SM	PPM	2.940	0.196	5	3	3.2
	EU	PPM	0.820	0.076	5	0.92	0.73
	GD	PPM	2.860	0.450	5	3	3.5
	TB	PPM	0.460	0.080	5	0.5	0.5
	DY	PPM	3.100	0.141	5	3.3	3
	HO	PPM	0.644	0.033	5	0.66	0.7
	ER	PPM	2.120	0.133	5	2.2	2.3
	TM	PPM	0.340	0.049	5	0.3	0.4
	YB	PPM	2.140	0.150	5	2.2	2.1
	LU	PPM	0.332	0.021	5	0.34	0.35
	TL	PPM	0.340	0.120	5	0.2	0.4
	BI	PPM	<1	0.000	5	<1	<1

## **APPENDIX C.0 SCANNING ELECTRON AND MICROPROBE ANALYZES**

### **C.1 Introduction**

Scanning electron microscopy with energy dispersal spectrometry (EDS) was used to identify sulphide inclusions, oxides, carbonates and silicate minerals in drill core samples from the three alteration zones in the Kerr deposit. Three feldspar and three sericite grains were analyzed by K. Wilks using a Cameca SX-50 electron microprobe. The three feldspars were from different dykes that intruded the Kerr deposit during and immediately after mineralization. Their chemistry may reflect the variations in magma chemistry during evolution of the porphyry copper-gold deposit. Analysis of the sericite grains was to determine the ratio of Si:Al in their tetrahedral layers and the presence of impurities. Pure muscovite has a 3:1 ratio and phengite is an impure muscovite with a ratio  $> 3:1$  (Deer, Howie and Zussman, 1966).

### **C.2 Preparation of Samples**

Each sample was mounted onto glass slide 2.5 cm in diameter by Y. Douma then ground down to 0.03mm and polished with diamond grit. The slides were then placed in ethanol on a vibersonic plate for 10 to 15 seconds. Sites selected for analysis were marked with permanent ink. Samples for the electron microprobe were coated with a 250 Å thick layer of sputtered carbon and the scanning electron samples a 500 Å layer. Slides for the scanning electron microscope were mounted on aluminium mounts and graphite paint was used to connect the carbon coating to the aluminium mount.

### **C.3 Analysis of Electron Microprobe Results**

Geochemical analysis traverses across three different feldspar grains were completed. Three sericite grains were analyzed so that the Si:Al ratio could be determined in order to

identify the sericite as a muscovite  $\text{Si:Al} = 3:1$  or as a phengite with  $\text{Si:Al} > 3:1$ . No pronounced geochemical zoning in the center of the feldspars was identified. This confirmed the observed absence of geochemical zoning using the petrographic microscope. Results from impurities such as albite and quartz grains in the feldspars were removed before the results were averaged (Table C.1).

The average composition of the each feldspar grain was calculated by assuming 8 oxygen per formula (Deer Howie and Zussman, 1966). Atomic percents of K, Na, Ba, Ca and Sr added together assuming that the variations in charges are balance by small changes in the Al to Si ratio. The percentage of atomic O in the samples closely match that of the ideal feldspar. The proportion of each component feldspar was calculated by dividing the actual atomic percent by the ideal percent. Summation of the individual components was close to 100% for each one.

Geochemical analysis of sericite grains were averaged over each one (Table C.2). The low weight percent totals are due to the missing H atoms that were not detected by the electron microprobe. In order to determine the Si:Al ratio in the sericite, the percentage of Al substitution in the octrahedral site needed to be calculated. In pure muscovite with no impurities, the octrahedral site contains 4 Al atoms for 24 (O, OH, F, Cl) atoms (Deer, Howie and Zussman, 1966) otherwise the site is partially filled with Mg, Fe, Mn, Cr and Ti atoms. In the analyzed samples, atomic percents of Al, Mg, Fe, Mn, Cr and Ti were added together and the ideal proportion of the octrahedral site was subtracted. The remainder is the percentage available for the tetrahedral site. The ratio of Si:Al was calculated by dividing the total Si by the remaining Al. The first sample (Muscovite) has a ratio very close to the ideal muscovite, and the remaining samples have ratios greater than 3.



Table C.1. Table of calculated composition of K-feldspars analyzed by electron microprobe from three different dykes

K-feldspar from Plagioclase hornblende Monzonite		Hyalophane megacryst from K-Ba-feldspar megacrystic plagioclase hornblende porphyry		Albite megacryst from Albite megacrystic plagioclase hornblende porphyry
Number of analyzes	8	Feldspar 19	Perthite 2	22
	wt%	wt%	wt%	wt%
Na <sub>2</sub> O	1.5	1.1	11.3	11.3
K <sub>2</sub> O	12.4	12.1	0.14	0.31
FeO	0.089	0.082	0.026	0.11
CaO	0.19	0.14	0.50	0.20
MgO	0.006	0.0013	0.0058	0.014
SrO	0	0	0	0.038
BaO	4.6	7.1	0.039	0.055
Al <sub>2</sub> O <sub>3</sub>	19.2	19.9	20.2	20.1
SiO <sub>2</sub>	61.4	58.8	67.9	67.8
Total	99.4	99.3	100	99.9
Number of atoms in mineral balanced on 8 oxygen				
Na	0.13	0.11	0.96	0.96
K	0.75	0.75	0.008	0.017
Fe	0.0035	0.0033	0.0010	0.0039
Ca	0.0096	0.0070	0.024	0.0093
Mg	0.0004	0.00009	0.0004	0.0010
Sr	0	0	0	0.0010
Ba	0.087	0.13	0.0007	0.0010
Al	1.1	1.1	1.0	1.0
Si	2.9	2.9	3.0	3.0
O	8.0	8.0	8.0	8.0
Percentage of each component of feldspar				
KAlSi <sub>3</sub> O <sub>8</sub>	75	75	96	2
NaAlSi <sub>3</sub> O <sub>8</sub>	13	11	1	96
CaAl <sub>2</sub> Si <sub>2</sub> O <sub>8</sub>	1	1	2	1
BaAl <sub>2</sub> Si <sub>2</sub> O <sub>8</sub>	9	13		0.1
SRAL <sub>2</sub> Si <sub>2</sub> O <sub>8</sub>				0.1
TOTAL (%)	98	100	99	99

Table C.2. Table of calculated composition of sericite analyzed by electron microprobe from three samples.

Three sericite grains from sericite - quartz - pyrite altered monzonite			
Number of analyzes	3	3	3
	wt%	wt%	wt%
Na <sub>2</sub> O	0.42	0.40	0.18
K <sub>2</sub> O	10.2	10.5	10.9
CaO	0.029	0.027	0.0063
FeO	2.0	1.8	1.1
TiO <sub>2</sub>	0.060	0.21	0.13
Cr <sub>2</sub> O <sub>3</sub>	0.0023	0.0026	0.0044
MgO	0.99	1.2	1.9
MnO	0.0039	0.013	0.015
Al <sub>2</sub> O <sub>3</sub>	33.4	32.8	32.1
SiO <sub>2</sub>	45.8	47.0	48.2
F <sub>2</sub> O	0.12	0.24	0.18
Cl <sub>2</sub> O	0.014	0.013	0.0012
Total	93.1	94.4	94.7
Number of atoms in mineral balanced on 24 (O,F,Cl,OH)			
Na	0.12	0.11	0.050
K	1.9	1.9	2.0
Ca	0.0046	0.0040	0.0010
Fe	0.24	0.22	0.14
Ti	0.0065	0.023	0.014
Cr	0.0003	0.0003	0.0006
Mg	0.21	0.26	0.39
Mn	0.0006	0.0017	0.0017
Al	4.3	4.2	4.1
Al in tet. site	1.4	1.3	1.2
Si	6.6	6.7	6.8
F	0.039	0.075	0.058
Cl	0.0029	0.0026	0.0004
O	23.2	23.2	23.2
Si:Al ratio in tetrahedral layer			
	4.7	5.1	5.7

#### **C.4 Analysis of Scanning Electron Microprobe Results**

Samples chosen for scanning electron microprobe analysis are representative of each of the alteration mineral and vein assemblages in the Kerr deposit. Samples from the central chlorite alteration zone are discussed first followed by the yellow sericite and finally by ones from the peripheral alteration zone.

The scanning electron microscope does not detect elements with atomic numbers less than 11 (H, He, Li, Be, B, C, N, O, F, Ne). The peaks on the EDS graphs are proportional to the concentration of the element in the mineral. The peaks represent the excitation of Ka and Kb shells for elements between Na and Zn, La and Lb shells for atoms between As and Cd, La, Lb, Lc and Ld for atoms In to Hg and Ma for Pb. The major source of contamination to the EDS graph of individual minerals is due to radiation from surrounding minerals. Bright minerals on scanning electron photographs have an higher average atomic mass than minerals that are grey or black; thus, barite appears as a bright mineral while calcite will be dark grey.

##### **C.4.1 Core alteration zone**

###### **Sample KS-125 190.6m (Extensional anhydrite - siderite - quartz vein)**

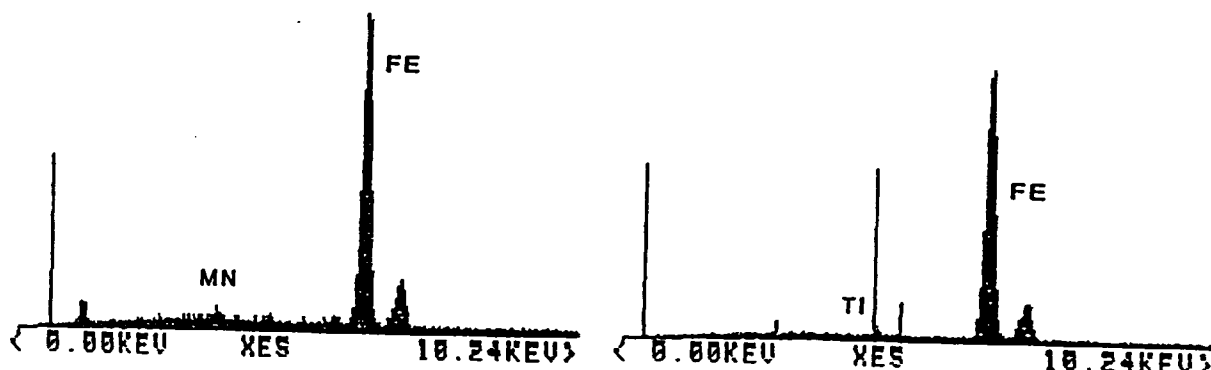
The vein consists of interlocking anhedral anhydrite, siderite and quartz grains with anhydrite and minor barite filled fractures in quartz. Analysis of the siderite indicates trace amounts of Mn in the grain (Fig. C.1a). No impurities were found in the anhydrite or barite.

**Sample KS-125 191.6m (Texturally destructive chlorite alteration with disseminated magnetite, chalcopyrite and pyrite cross cut by a anhydrite - quartz - siderite vein with chlorite selvages)**

Fifty micron grains of disseminated magnetite have trace amounts of Ti in them (Fig. C.b). EDS spectra from a chlorite grain along the margin of the anhydrite - quartz - siderite vein was contaminated by Ca and S from a neighbouring anhydrite (Fig. C.1c). The siderite in the vein also was contaminated by Ca and S from anhydrite (Fig. C.1d). The extra Mg and

a  
KS-125 190.6 SIDER LK Z=26 FE  
PR= S 15SEC 0 INT  
U=2048 H=10KEV 1.1H AQ=10KEV 1H

b  
KS-125 191.6 SITE 1 LK Z=22 TI  
PR= S 5SEC 0 INT  
U=2048 H=10KEV 1.1H AQ=10KEV 1H



c  
KS-125 191.6 SITE 1 LK Z=26 FE  
PR= S 15SEC 0 INT  
U=2048 H=10KEV 1.1H AQ=10KEV 1H

d  
KS-125 191.6 SITE 1 LK Z=26 FE  
PR= S 15SEC 0 INT  
U=2048 H=10KEV 1.1H AQ=10KEV 1H

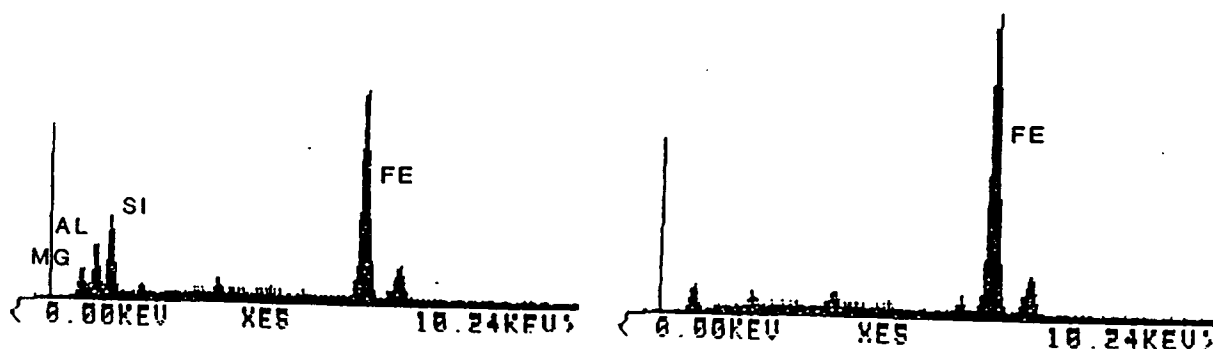


Figure C.1. Energy dispersive spectrometry (EDS) spectra for a) siderite in sample KS-125 190.6m, b) disseminated magnetite, c) chlorite and d) siderite. Spectra b to d are from sample KS-125 191.6m.

Mn peaks in the siderite spectra are thought to be from the mineral because if the Mg was from neighbouring chlorite there would also be Al and Si peaks on the graph. The Mn peak is similar to that from siderite in sample KS-125 190.6m.

**Sample KS-125 197.5m** (Pervasive chlorite and sericite envelope to anhydrite vein and cross cutting gypsum veinlets)

The chlorite analysis showed a prominent Fe peak and the presence of Ca and S from neighbouring anhydrite (Fig. C.2a). Intergrown sericite has peaks in order of intensity  $Si > K > Al > Fe > Mg$  (Fig. C.2b). The presence of Fe and Mg in the grain indicates that the sericite is probably phengite because the ions substitute for Al in the octahedral layer (Deer, Howie and Zussman, 1966). Anhydrite intergrown with the silicates is pure. The gypsum in the veinlet is thought to be pure because the small Si, Al and Fe peaks on the graph are probably from surrounding chlorite (Fig. C.2d).

**Sample KS-125 252.7m** (Pervasive chlorite and sericite alteration with clots of chlorite replacing biotite? and disseminated pyrite, chalcopyrite, anhydrite, barite and molybdenite)

Several sites with a number of minerals were analyzed on the section. Site 1 has intergrown grains of chlorite, chalcopyrite, sericite and minor barite. The chlorite, at point 1, neighbouring chalcopyrite has trace amounts of K in it that may be due to phengite intergrown with the flakes (Fig. C.3 a,b), but the individual phengite flakes can not be identified under high power using either the scanning electron or petrographic microscope. Other well developed chlorite grains in contact with chalcopyrite do not have K peaks, but they have higher Fe peaks that may indicate these grains have more Fe (Figs. C.3c,d). The higher Fe analysis is not due to the neighbouring chalcopyrite grains because they would have S or Cu

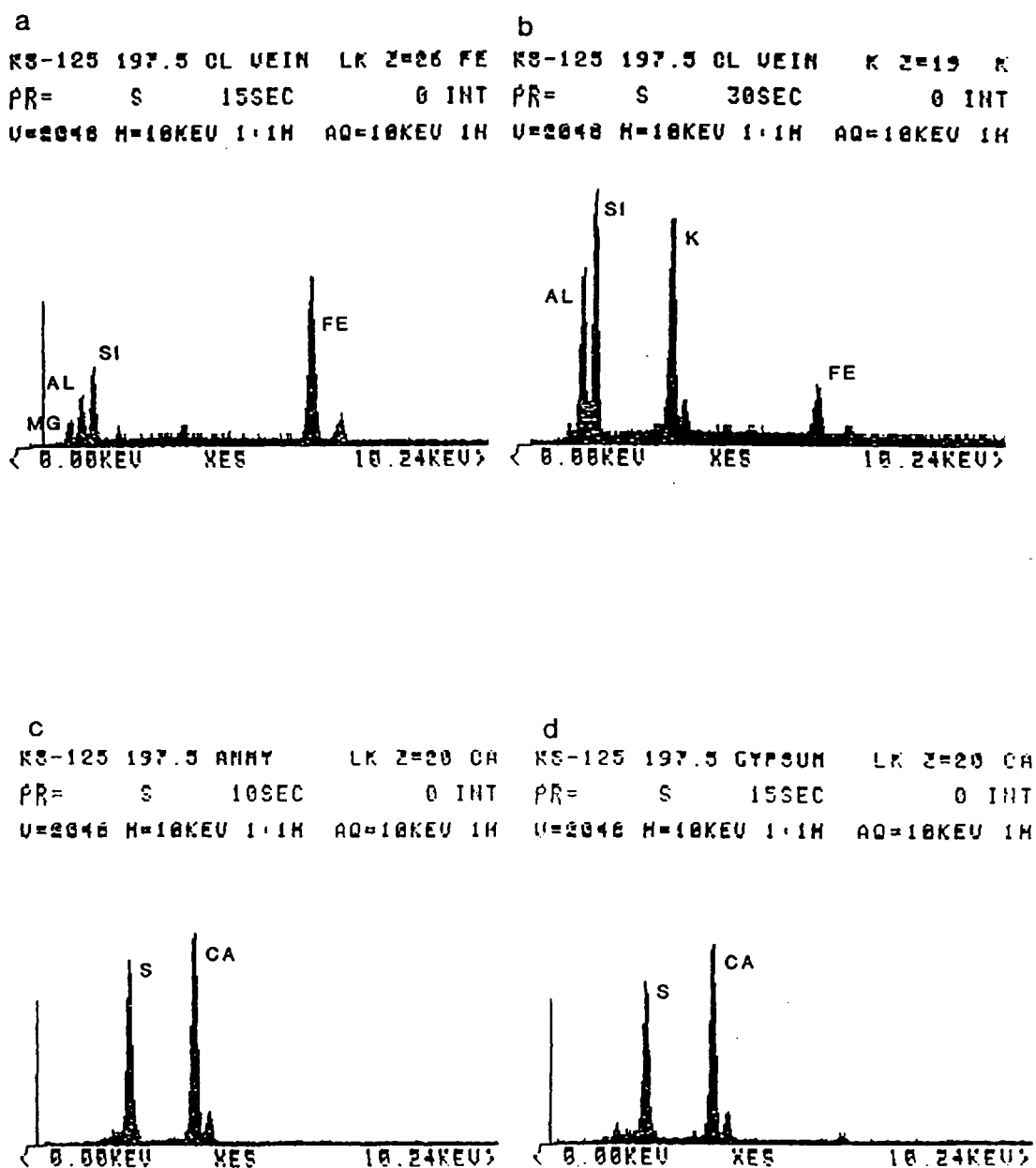


Figure C.2. EDS spectra for a) chlorite neighbouring anhydrite, b) sericite, c) anhydrite and d) gypsum in veinlet. Spectra a to d are from sample KS-125 197.5m.

contamination as well. Barite occurs in contact with chlorite (Fig. C.3e) and molybdenite grains were observed to be broken and filled by sericite.

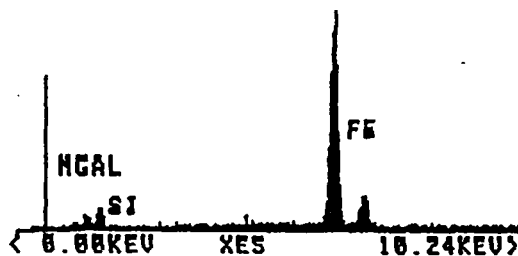
Site 2 is of a moderate relief grain replaced by rutile and chlorite. These grains appear as dark green chlorite spots in pervasive pale chlorite and sericite. Point B shows peaks typical of chlorite as in site 1. It also has a Ti peak from minute rutile grains in the grain (Fig. C.4a). Points C and D show that the chlorite replacing and surrounding the grains are Fe rich (Figs. C.4b,c). Analysis further down the grain indicates the presence of K in it and no Ti phases (Fig. C.4d). The presence of K and inclusions of rutile in the high relief grain strongly suggest that it was originally biotite or another K-bearing mafic phase. Ti is usually liberated from biotites (2 to 4 wt%  $\text{TiO}_2$ ) when they alter to chlorite because it accommodates less Ti ( $< 1$  wt%  $\text{TiO}_2$ ) (Deer, Howie and Zussman, 1966). Sericite in the matrix surrounding the grain at point G has a Fe peak higher than an Al peak (Fig. C.4e). This indicates that the sericite has minor amounts of Fe in it.

**Sample KS-125 286m** (Patches of chlorite and grey sericite - quartz alteration with disseminated pyrite, anhydrite, chalcopyrite, ilmenite, rutile and trace native gold)

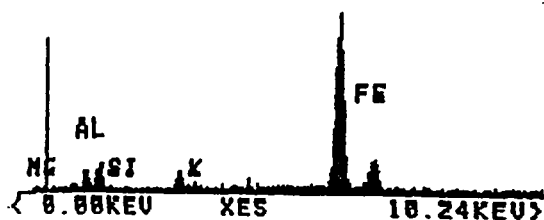
Disseminated chalcopyrite occurs with chlorite and ilmenite in the sample. The chlorite has a K peak and analysis of intergrown ilmenite shows contamination from neighbouring chlorite grains (Figs. C.5a,b). Sericite analyzed near the chlorite has the same intensity of peaks as phengite in sample KS-125 197.5m (Fig. C.5c). Ilmenite in contact with the sericite has a similar composition as that with chlorite (Fig. C.5d).

Native gold occurs as a 20 micron grain with chalcopyrite in broken pyrite. The gold has a trace amount of Ag with it (Fig. C.5e). The Fe peak on the graph is due to contamination by the surrounding pyrite grain.

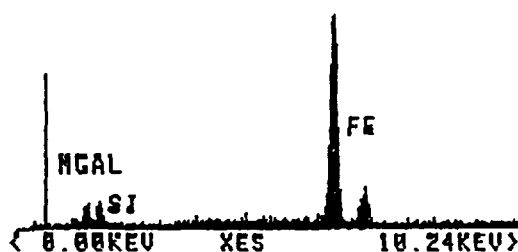
a  
K9-125 252.7 CHL 5 LK Z=26 FE  
PR= S 100SEC 0 INT  
U 1024 H=10KEV 1.1H AQ=10KEV 1H



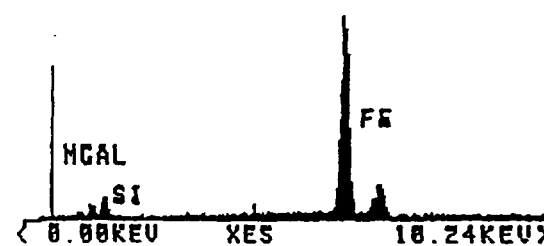
b  
K9-125 252.7 FE-K 1 LK Z=26 FE  
PR= S 100SEC 0 INT  
U 1024 H=10KEV 1.1H AQ=10KEV 1H



c  
K9-125 252.7 CHL 3 LK Z=26 FE  
PR= S 60SEC 0 INT  
U 512 H=10KEV 1.1H AQ=10KEV 1H



d  
K9-125 252.7 CHL 4 LK Z=26 FE  
PR= S 100SEC 0 INT  
U 1024 H=10KEV 1.1H AQ=10KEV 1H



e  
K9-125 252.7 ST2 BA1 HL Z=56 BA  
PR= S 50SEC 0 INT  
U 1024 H=10KEV 1.1H AQ=10KEV 1H

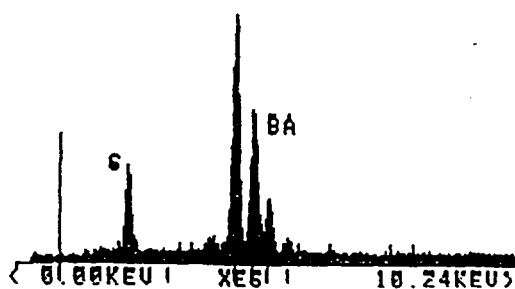
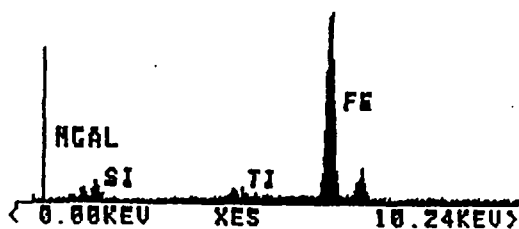


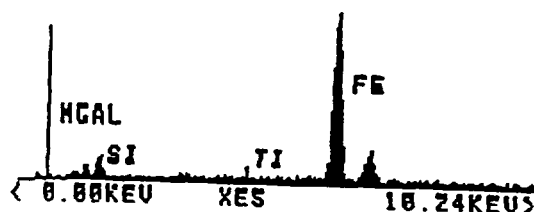
Figure C.3. EDS spectra for a) chlorite intergrown with chalcopyrite and sericite, b) same chlorite as a but with minor K, c) chlorite intergrown with chalcopyrite, d) same as c but with Fe contamination, and e) barite in contact with chlorite. Spectra a to e are from sample KS-125 252.7m.



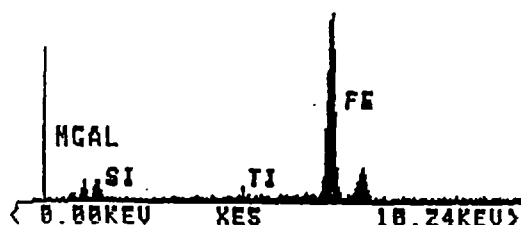
a  
KS-125 252.7 CHL B LK Z=26 FE  
PR= S 100SEC 0 INT  
U 1024 H=10KEV 1.1H AQ=10KEV 1H



b  
KS-125 252.7 CHL C LK Z=26 FE  
PR= S 100SEC 0 INT  
U 1024 H=10KEV 1.1H AQ=10KEV 1H



c  
KS-125 252.7 CHL D LK Z=26 FE  
PR= S 100SEC 0 INT  
U=1024 H=10KEV 1.1H AQ=10KEV 1H



d  
KS-125 252.7 CHL E LK Z=26 FE  
PR= S 100SEC 0 INT  
U=1024 H=10KEV 1.1H AQ=10KEV 1H



e  
KS-125 252.7 SITE G K Z=19 K  
PR= S 100SEC 0 INT  
U=512 H=10KEV 1.1H AQ=10KEV 1H

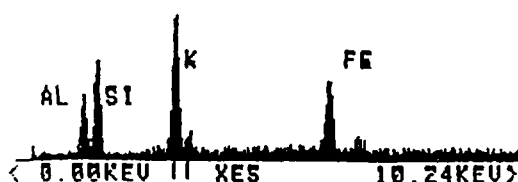


Figure C.4. EDS spectra for a) point B on a chlorite grain with minor intergrown rutile, b) point C on the chlorite grain, c) point D on the chlorite grain showing minor K in it, and e) sericite in the matrix surrounding the chlorite grain. Spectra a to e are from sample KS-125 252.7m

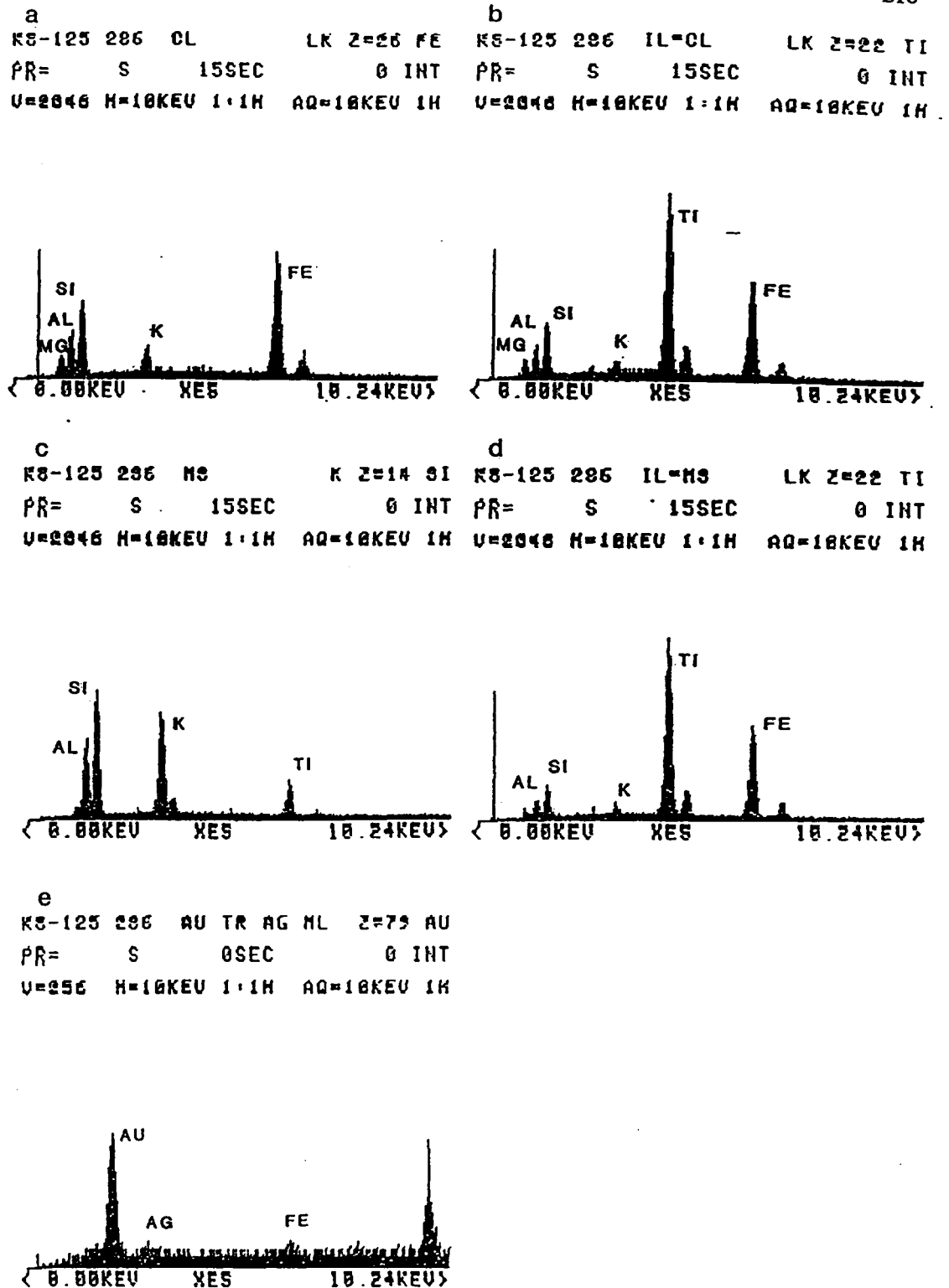


Figure C.5. EDS spectra for a) chlorite intergrown with ilmenite, b) ilmenite intergrown with a, c) sericite intergrown with ilmenite, d) ilmenite intergrown with c, and e) gold with a minor silver content intergrown with chalcopyrite. Spectra a to e are from sample KS-125 286m.

#### C.4.2 Halo alteration zone

**Sample KS-125 16.0m** (Sericite - quartz - pyrite altered monzonite with minor disseminated and vein tetrahedrite - tennantite)

Analysis of tetrahedrite - tennantite in quartz veins indicates the presence of Sb and As in the mineral with minor Fe and trace Zn (Fig. C.6a). The ratio of As and Sb cannot be determined in this sample so the correct mineral name cannot be assigned to it.

**Sample KS-125 72.9m** Yellow sericite - quartz - pyrite alteration with quartz - chlorite extension veins.

Rings of inclusions of Ti phases and pyrrhotite with chalcopyrite occur occasionally in pyrite grains. The Ti phases cannot be properly identified because of the contamination by the surrounding pyrite (Fig. C.6b) Pyrrhotite (pale pinkish brown in reflected light) occurs as a half moon with chalcopyrite in a 10 micro inclusion. The chalcopyrite side can be easily identified but the pyrrhotite shows the same Fe and S peaks as the surrounding pyrite (Figs. C.6 c,d).

An analyzed yellow sericite grain in the sample has peak heights  $Si > Al = K > > Ti = Fe$  (Fig. C.6e). Radiating chlorite clusters in an extensional quartz vein have trace amounts of K in them (12.6f).

**Sample KS-102 151.2m** (Partially recrystallized pyrite - carbonate vein in yellow sericite altered mudstone with minor chlorite - pyrite veins.

Pale brown calcite near the edge of a broken pyrite grain has trace amounts of Mn in it (Fig. C.7a). Calcite fibres surrounding the pyrite grain have slightly more Mn (Fig. C.7b). There is minor S contamination to the EDS spectra from the pyrite grain. Analysis of the

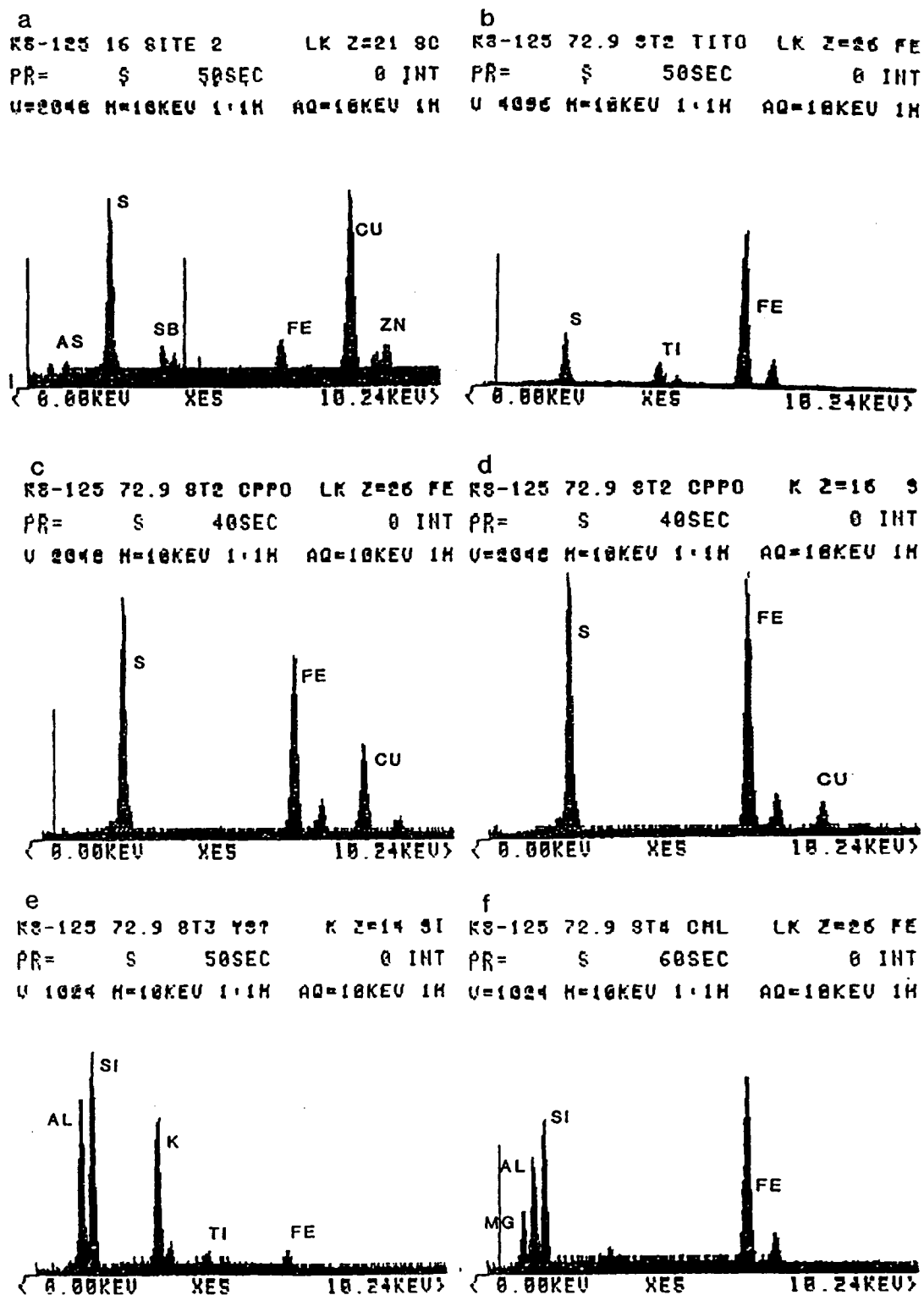


Figure C.6. EDS spectra for a) tetrahedrite - tennantite grain in quartz vein in sample KS-125 16 m, b) Ti phase inclusions in pyrite, c) chalcopyrite inclusion intergrown with pyrrhotite in pyrite, d) pyrrhotite with c, e) yellow sericite grain, and f) radiating chlorite in extensional quartz vein. Spectra b to f are from sample KS-125 72.9m.

calcite fibres away from the pale brown calcite show very little Mn present and no S contamination (Fig. C.7c). Chlorite was identified along a 2 mm pyrite veinlet. The spectra shows Fe, and Mg and more intense Al and Si typical of chlorite. There is also a Ca peak which may be due to intergrown calcite (Fig. C.7d).

**Sample KS-104 153.95m** (Partially recrystallized polymetallic carbonate - sulphate veins in yellow sericite altered mudstone)

Scanning electron microprobe analysis of sulphides along the edges of pyrite grains in recrystallized calcite indicated the presence of the sphalerite, tennantite, pure barite, Ba-Sr-carbonates and Ba-Sr-sulphates (Figs. C.8a to d). The analysis of the tennantite was contaminated by Ca from surrounding calcite. The Ca peak has probably covered the Sb peak of the mineral. The recrystallized calcite does not have any detectable impurities (Fig. C.8e)

**Collar of drill hole KS-101** (Yellow sericite altered mudstone)

Subhedral, hexagonal plates of clintonite, sericite, a Zn phase and apatite were analyzed. A 20 micron clintonite grain was analyzed in its center to minimize contamination from the surrounding phases. The EDS graph has strong Si and Al peaks with less Fe, Ca, Mg and Ti (Fig. C.9a). The presence of Ca and the other elements without K and the mineral's hexagonal habit confirms that this mineral is clintonite. The bright grain in contact with it has very high Zn Ka and Kb peaks with minor Si and Ca (Fig. C.9b). The grain is most likely zincite (ZnO) or smithsonite ( $\text{ZnCO}_2$ ) with minor Si and Ca contamination from neighbouring minerals. Analysis of a sericite lath in the sample shows equal peaks heights of K and Si, lesser Al and small Fe and S peaks that may be contamination from surrounding pyrite grains (Fig. C.9c).

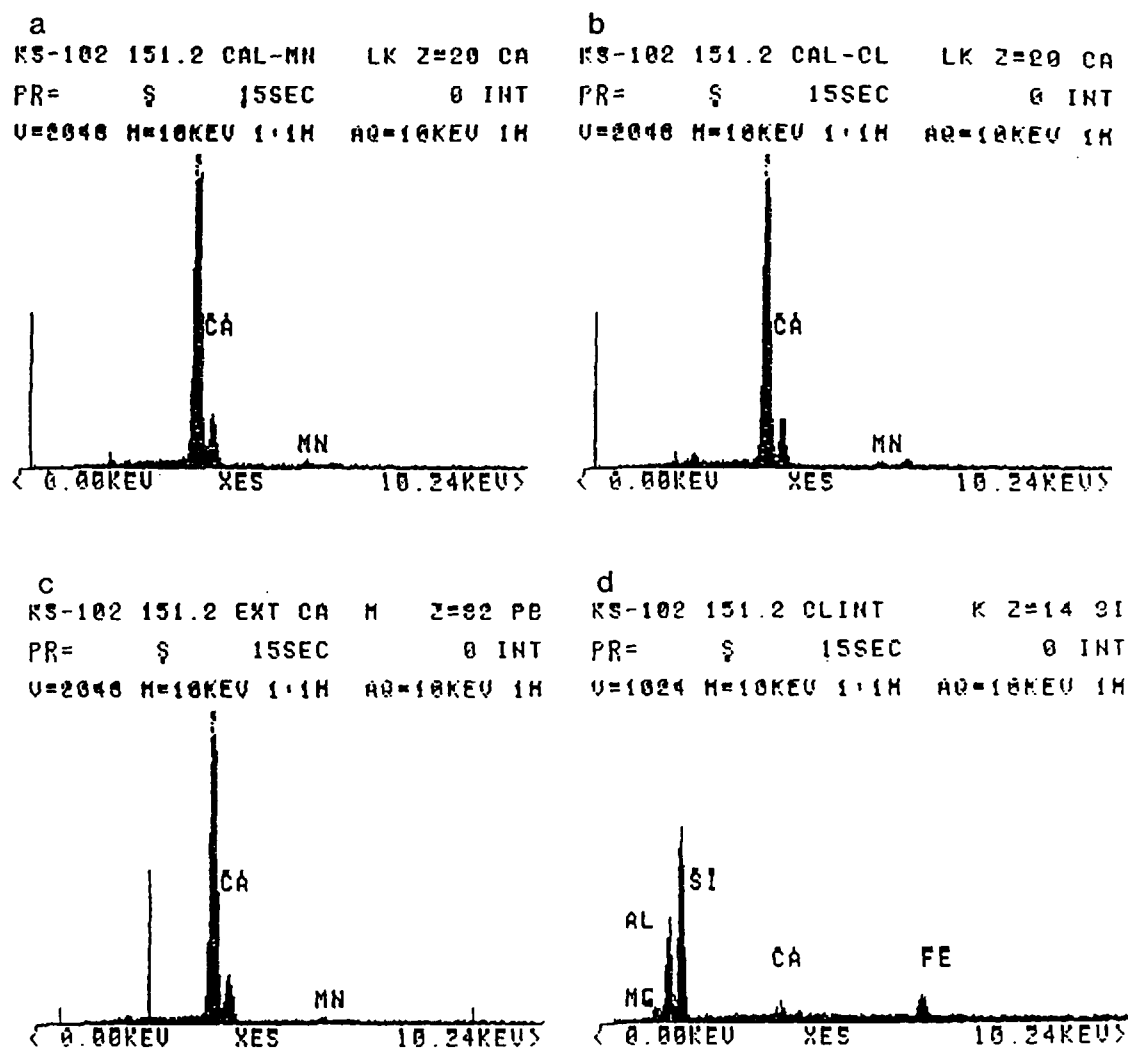
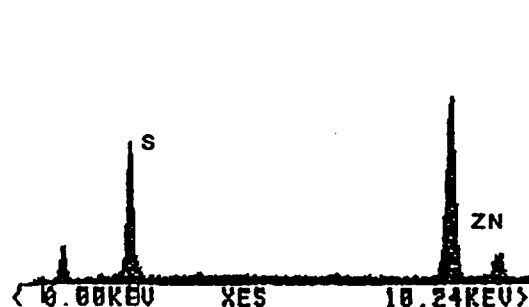
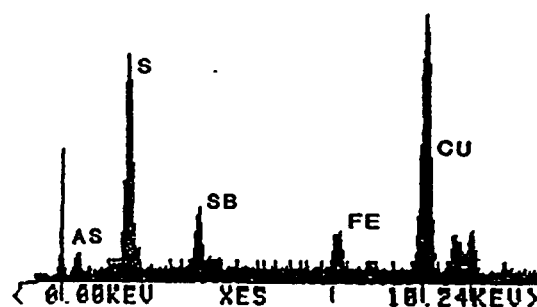


Figure C.7. EDS spectra for a) pale brown calcite with trace Mn b) calcite fibres near a, c) calcite fibres away from a with no Mn peak, and d) chlorite along pyrite veinlet. Spectra are from sample KS-104 151.2m.

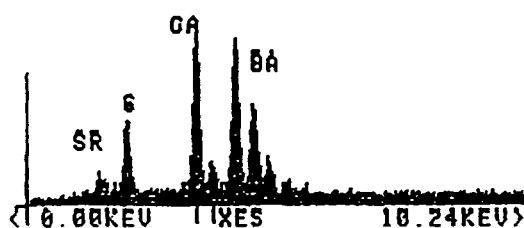
a  
KS-104 153.95 SL2 K Z=16 S  
PR= S 15SEC 0 INT  
U=2046 H=10KEV 1.1H AQ=10KEV 1H



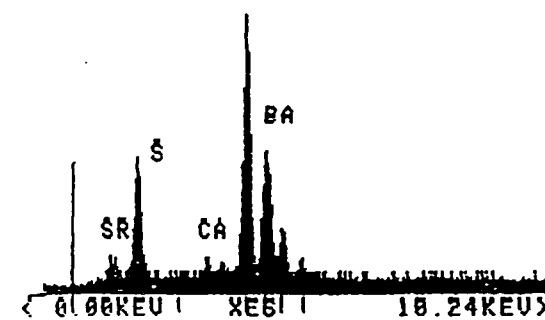
b  
KS-104 153.95 TT LK Z=29 CU  
PR= S 15SEC 0 INT  
U=1024 H=10KEV 1.1H AQ=10KEV 1H



c  
KS-104 153.95 BA9RCA LK Z=20 CA  
PR= S 15SEC 0 INT  
U=1024 H=10KEV 1.1H AQ=10KEV 1H



d  
KS-104 153.95 BA9R ML Z=56 BA  
PR= S 15SEC 0 INT  
U=1024 H=10KEV 1.1H AQ=10KEV 1H



e  
KS-104 153.95 CA LK Z=20 CA  
PR= S 15SEC 0 INT  
U=4096 H=10KEV 1.1H AQ=10KEV 1H

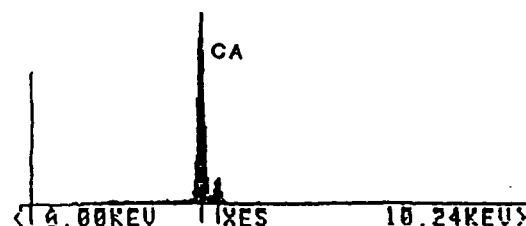
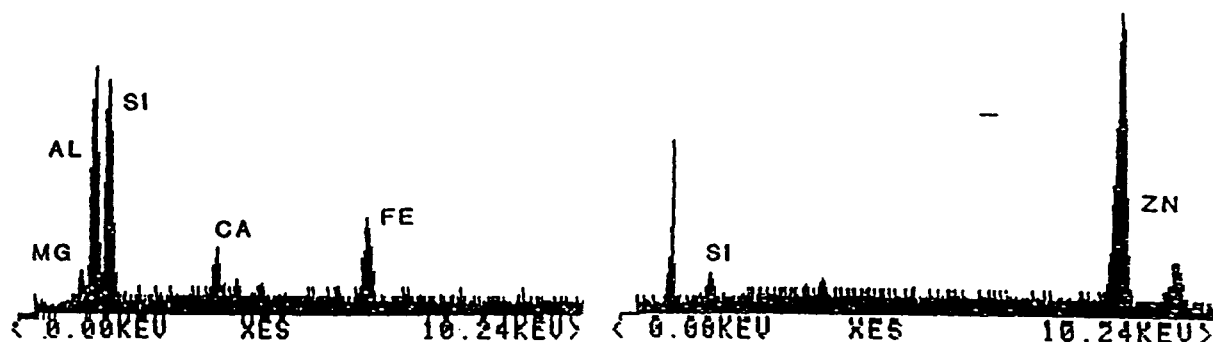


Figure C.8. EDS spectra for a) sphalerite in carbonate vein, b) tennantite with a, c) Br-Sr-Ca sulphate mineral with a, d) Ba-Sr-sulphate mineral with a, and e) recrystallized calcite in the carbonate vein. Spectra are from sample KS-104 153.95.

a  
 CAFE NICA SAMPLE SL K Z=14 SI ZN OXIDE SAMPLE SL LK Z=30 ZN  
 PR= S 30SEC 0 INT PR= S 20SEC 0 INT  
 U=512 H=10KEV 1:1H AQ=10KEV 1H U=512 H=10KEV 1:1H AQ=10KEV 1H



c  
 MUSCOVITE SAMPLE SL K Z=19 K  
 PR= S 30SEC 0 INT  
 U 1024 H=10KEV 1:1H AQ=10KEV 1H

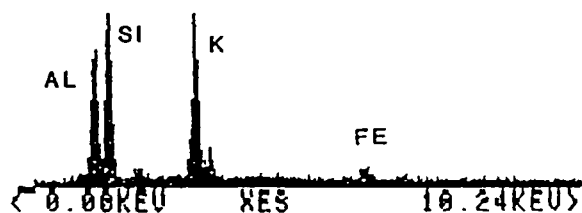


Figure C.9. EDS spectra for a) clintonite in yellow sericite altered mudstone, b) Zn mineral in rock which may be zincite or smithsonite, and c) sericite in the matrix. Spectra are from a sample from the collar of drill hole KS-101.



**Sample KS-66 128.5m** (Disseminated pyrite, tennantite in yellow sericite altered rock with polymetallic quartz - carbonate veins).

Pyrite has 2 to 10 micron bornite and chalcopyrite inclusions in it, and it is in contact with tennantite blebs. EDS analysis of the chalcopyrite shows smaller Cu peaks than the separate bornite inclusions (C.10a,b). The chalcopyrite spectra is typical of pure chalcopyrite while the Cu peaks on the bornite graph are lower than normal. This may be due to extra Fe and S radiation from the surrounding pyrite grain. Analysis of tennantite shows that it has trace amounts of Sb and less Zn and Fe than samples from KS-104 and KS-125 (Fig. C.10c).

Analysis of yellow sericite intergrown with rutile shows peak heights  $Si > Al = K > > Ti$  (Fig. C.10d) whereas grey sericite flakes indicate similar peaks (Fig. C.10e), but the ratio of Si to Al or K is lower and there is Fe instead of Ti. The Ti peak may be due radiation from intergrown rutile.

**Sample KS-66 176.2** (Olive green and yellow sericite - quartz - pyrite - rutile alteration)

EDS analysis of olive green sericite indicated that it had minor amounts of Cr and Fe in it (Fig. C.11a). Rutile near the analyzed grain was composed of Ti with trace amounts of Cr (Fig. C.11b). Radiation from the rutile grain could not have caused the Cr peak in the sericite because there would be a larger Ti peak as well.

**Sample KS-125 358.6m** (Yellow sericite-quartz-pyrite-rutile alteration)

EDS analysis of yellow sericite intergrown with rutile indicated that it has minor amounts of Fe and Mg in it (Fig. C.12a). The small Ti peak in the EDS spectra is probably due to the intergrown rutile. This rutile has trace amounts of Fe in it (Fig. C.12b); however, the Al, Si and K peaks in the spectra suggest that the Fe peak may be due to radiation from neighbouring yellow sericite grains.

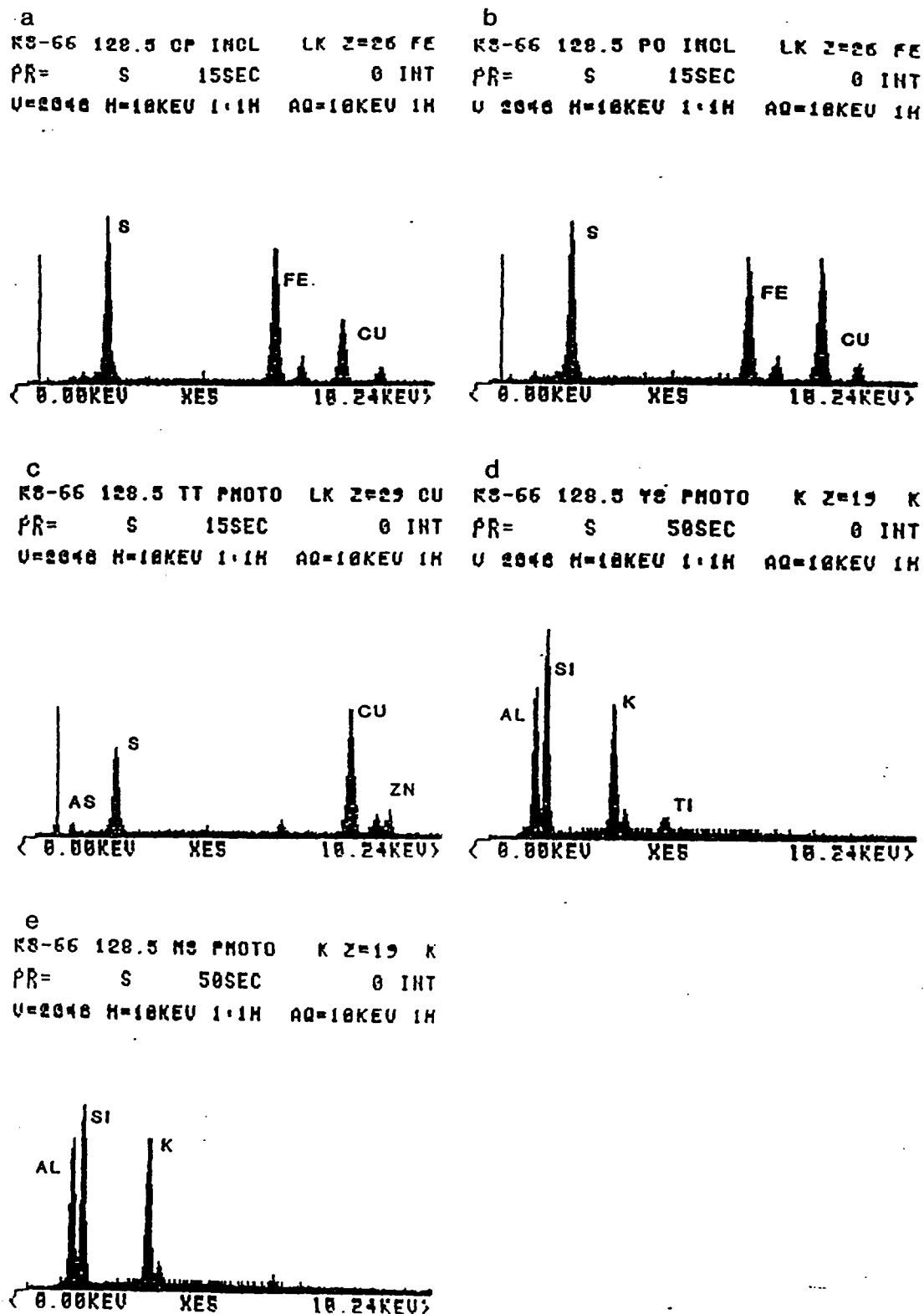


Figure C.10. EDS spectra for a) chalcopyrite inclusion in pyrite, b) bornite inclusion in pyrite grain in a, c) disseminated tennantite, d) yellow sericite grain and e) grey sericite grain. Spectra are from KS-66 128.5m.

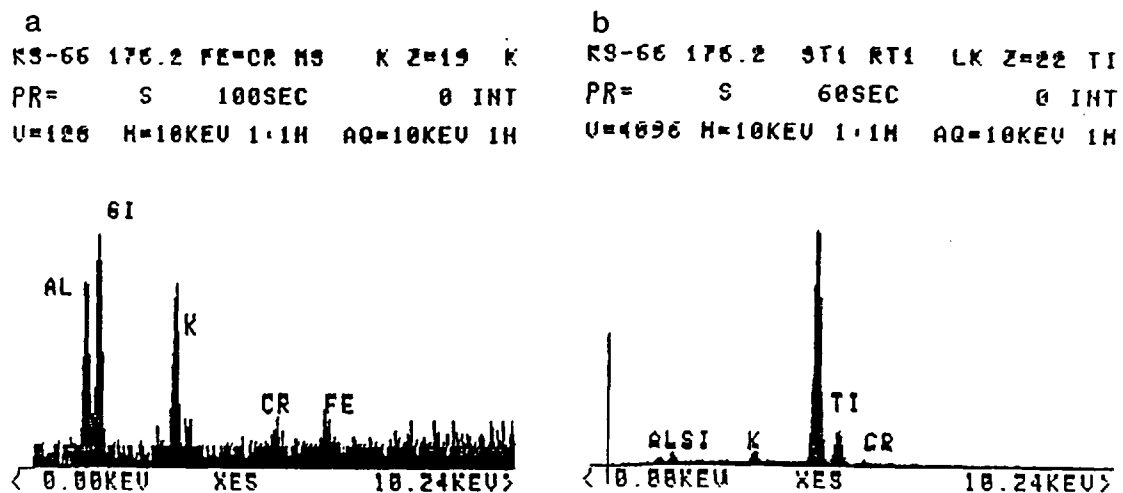
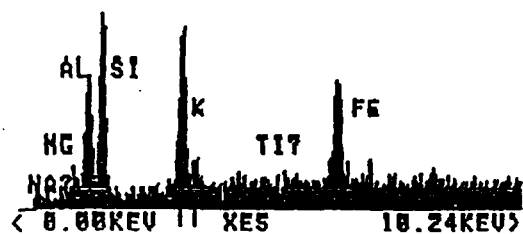


Figure C.11. EDS spectra for a) olive green sericite intergrown with rutile and b) rutile intergrown with a). Spectra are from KS-66 176.2m.

a  
 SAMPLE DG SITE 1 H3 K Z=19 K  
 PR= S 100SEC 0 INT  
 V=256 H=10KEV 1:1H AQ=10KEV 1H



b  
 SAMPLE DG SITE 2 RT LK Z=22 TI  
 PR= S 60SEC 0 INT  
 V=1024 H=10KEV 1:1H AQ=10KEV 1H

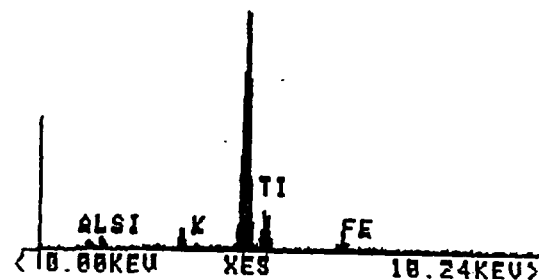


Figure C.12. EDS spectra for a) yellow sericite intergrown with rutile and b) rutile intergrown with a). Spectra are from KS-125 358.6m.

# APPENDIX D.0 LIST OF VISUALLY ESTIMATED AMOUNTS OF ALTERATION MINERALS AND MEASURED AMOUNTS OF VEINS

## D.1 List of Abbreviations

Abbreviation:	Explanation:
INTRVAL	interval
CU	copper
AU	gold
ZN	zinc
PB	lead
AG	silver
RECOV	recovery
ROCK\$	rock unit
ANDY	Kersantite
ANPP	Albite megacrystic plagioclase hornblende porphyry
BNDK	Hornblende porphyry
BRXX	Breccia
CONG	Conglomerate
FRAG	Fragmental rock
LAAP	Aphanitic intermediate dyke
LAPP	Syenodiorite
PHFG	Fine grained tuffaceous rock
PHMG	Monzonite
PHPP	Fine grained tuffaceous or intrusive rock
SACO	Sandstone and conglomerate
SAND	Sandstone
SEDM	Sedimentary rock
TFAH	Well bedded mudstone
TFCO	Tuffaceous conglomerate
TFLP	Fragmental/conglomerate
TRAC	Tractytic plagioclase porphyry
TUFF	Tuff
TURB	Argillite
VLCO	Volcanic conglomerate
XCOR	Missing core
BX	Angle between bedding and core axis
FB	Angle between bedding and foliation
FX	Angle between foliation and core axis
VF	Angle between foliation and vein
QZR	Silicification
QZV	Quartz veins
QZT	Total silicification and quartz veins
AHR	Disseminated anhydrite
AHV	Anhydrite veins
AHT	Total anhydrite

GYR	Disseminated gypsum
GYV	Gypsum veins
GYT	Total gypsum
AHGYT	Total anhydrite and gypsum
SER	Disseminated sericite
SEV	Sericite in veins
SET	Total sericite
YSR	Disseminated yellow sericite
YSV	Yellow sericite in veins
YST	Total yellow sericite
GSR	Disseminated intergrown chlorite and sericite
GSV	Intergrown chlorite and sericite in veins
GST	Total intergrown chlorite and sericite
SYGST	Total sericite, yellow sericite and intergrown sericite and chlorite
KAR	Disseminated clay minerals
KAV	Offrerite in veins
KAT	Total offerite and clay minerals
CLR	Disseminated chlorite
CLV	Chlorite in veins
CLT	Total chlorite
CAR	Disseminated calcite
CAV	Calcite in veins
CAT	Total calcite
AKR	Disseminated siderite
AKV	Siderite in veins
AKT	Total siderite
MGR	Disseminated magnetite
MGV	Magnetite in veins
MGT	Total magnetite
HER	Disseminated specular hematite
HEV	Specular hematite veins
HET	Total specular hematite
RUR	Disseminated carbonaceous material
RUV	Carbonaceous material in veins
RUT	Total carbonaceous material
PYR	Disseminated pyrite
PYV	Pyrite in veins
PYT	Total pyrite
CPR	Disseminated chalcopyrite
CPV	Chalcopyrite in veins
CPT	Total chalcopyrite
TTR	Disseminated tetrahedrite-tennantite
TTV	Tetrahedrite-tennantite in veins
TTT	Total tetrahedrite-tennantite
BOV	Bornite in veins
MOV	Molybdenite in veins
SLV	Sphalerite in veins
GLV	Galena in veins
WDC	Wad coatings
JAC	Jarosite coatings
CCC	Chalocite and covellite
GYLV	Gypsum veinlets

V1	Type 1 and 3 veins
V2	Type 5 veins
V3	Type 4 veins
V4	Type 7 veins
X1	Type 6 veins
X2	Extensional quartz carbonate veins
X3	Extensional quartz veins
CLEAV	Estimate of deformation

DDHS	FROM metres	TO metres	INTRVAL	CU (%)	AU (ppm)	ZN (ppm)	PB (ppm)	AG (ppm)	RECOV (%)	ROCKS	BX
KS-062	19.00	21.34	2.34	0.083	0.16	97	15	3.5	100	TFAH	25
KS-062	21.34	24.00	2.66	0.099	0.15	110	9	1.9	75	LAPP	
KS-062	24.00	28.30	4.30	0.073	0.06	86	8	2.0	93	TFAH	35
KS-062	28.30	29.20	0.90	0.068	0.10	100	6	1.7	100	LAPP	
KS-062	29.20	31.30	2.10	0.041	0.10	81	13	0.9	76	LAPP	
KS-062	31.30	36.15	4.85	0.039	0.13	118	6	0.4	66	LAPP	
KS-062	36.15	38.90	2.75	0.033	0.05	103	8	0.4	90	LAPP	
KS-062	38.90	42.07	3.77	0.017	0.10	87	27	0.5	73	LAPP	
KS-062	74.80	78.80	4.00	0.023	0.49	71	12	0.5	100	LAPP	
KS-062	78.80	81.99	3.19	0.002	0.06	42	5	0.1	100	LAPP	
KS-062	81.99	85.04	3.05	0.001	0.13	48	8	0.1	100	LAPP	
KS-062	85.04	86.25	1.21	0.001	0.18	40	8	0.2	100	LAPP	
KS-062	86.25	89.40	3.15	0.005	0.19	73	20	0.2	97	LAPP	
KS-062	89.40	92.40	3.00	0.014	0.12	65	11	0.2	100	LAPP	
KS-062	92.40	95.40	3.00	0.016	1.17	73	13	0.4	88	LAPP	
KS-062	95.40	97.84	2.44	0.014	0.05	72	13	0.2	88	LAPP	
KS-062	138.85	140.25	1.40	0.092	0.10	38	9	0.4	100	PHFG	
KS-062	140.25	141.85	1.60	0.092	0.10	38	9	0.4	100	PHFG	
KS-062	141.85	144.85	3.00	0.113	0.11	50	7	0.4	100	PHFG	
KS-062	144.85	147.15	2.30	0.031	0.09	54	10	0.2	90	PHFG	
KS-062	147.15	150.85	3.70	0.018	0.05	80	5	0.2	83	TUFF	
KS-062	150.85	153.85	3.00	0.264	0.34	92	18	5.0	100	PHFG	
KS-062	153.85	155.25	1.40	0.174	0.19	80	13	1.2	100	PHFG	
KS-062	155.25	156.85	1.60	0.174	0.19	80	13	1.2	100	PHFG	
KS-062	156.85	159.85	3.00	0.194	0.09	148	43	1.1	100	PHFG	
KS-062	159.85	162.85	3.00	0.239	0.17	88	19	1.5	100	PHFG	
KS-062	171.85	174.85	3.00	0.296	0.30	214	54	1.4	100	BRXX	
KS-062	174.85	177.85	3.00	0.384	0.11	153	14	2.0	100	BRXX	
KS-062	177.85	182.00	4.15	0.400	0.14	124	23	1.7	80	BRXX	
KS-062	182.00	182.85	0.85	0.033	0.04	57	5	0.2	98	LAPP	
KS-063	6.10	7.00	0.90	0.033	0.09	90	24	0.9	67	LAPP	25
KS-063	7.00	10.00	3.00	0.105	0.15	50	9	0.5	100	LAPP	
KS-063	10.00	13.00	3.00	0.112	0.07	12	7	0.5	100	SEDM	
KS-063	13.00	15.70	2.70	0.039	0.03	9	6	0.2	100	SEDM	
KS-063	45.10	46.68	1.58	0.026	0.05	57	3	0.2	100	LAPP	
KS-063	46.68	50.00	3.32	0.029	0.17	75	6	0.5	60	LAPP	
KS-063	50.00	53.00	3.00	0.019	0.08	65	6	0.1	67	LAPP	
KS-063	53.00	56.00	3.00	0.023	0.08	64	8	0.2	100	LAPP	
KS-063	56.00	59.30	3.30	0.059	0.16	84	7	0.3	100	LAPP	
KS-063	59.30	59.90	0.60	0.212	0.23	190	9	0.8	100	PHPP	
KS-063	96.00	99.00	3.00	0.214	0.13	137	14	0.7	100	BRXX	
KS-063	99.00	100.00	1.00	0.138	0.05	110	12	0.4	93	BRXX	
KS-063	100.00	101.55	1.55	0.138	0.05	110	12	0.4	100	LAPP	
KS-063	101.55	102.00	0.45	0.138	0.05	110	12	0.4	100	BRXX	
KS-063	102.00	105.00	3.00	0.260	0.14	150	20	1.0	100	BRXX	
KS-063	105.00	108.00	3.00	0.348	1.10	940	12	3.0	91	BRXX	
KS-063	108.00	109.70	1.70	0.031	0.19	236	16	0.2	82	LAPP	
KS-063	109.70	113.00	3.30	0.267	0.35	68	8	2.8	85	BRXX	
KS-063	113.00	116.00	3.00	0.568	0.37	480	8	2.8	100	BRXX	
KS-063	116.00	119.00	3.00	0.524	0.53	1250	84	5.0	97	BRXX	



DDHS	FROM metres	TO metres	FB	FX	VF	QZR (%)	QZV (%)	QZT (%)	AHR (%)	AHV (%)	AHT (%)
KS-062	19.00	21.34				0	1	1	0	0	0
KS-062	21.34	24.00				0.01	0	0.01	0	0	0
KS-062	24.00	28.30				1	1	2	0	0	0
KS-062	28.30	29.20				0	0	0	0	0	0
KS-062	29.20	31.30				0	0	0	0	0	0
KS-062	31.30	36.15				0	1	1	0	0	0
KS-062	36.15	38.90				0	1	1	0	0	0
KS-062	38.90	42.67				1	0	1	0	0	0
KS-062	74.80	78.80				0	1	1	0	0	0
KS-062	78.80	81.99				0	2.5	2.5	0	0	0
KS-062	81.99	85.04				0	1	1	0	0	0
KS-062	85.04	86.25				0	1	1	0	0	0
KS-062	86.25	89.40				0	2.5	2.5	0	0	0
KS-062	89.40	92.40				0	1	1	0	0	0
KS-062	92.40	95.40				0	1	1	0	0	0
KS-062	95.40	97.84				0	1	1	0	0	0
KS-062	138.85	140.25				5	20	25	0	0	0
KS-062	140.25	141.85				1	1	2	0	0	0
KS-062	141.85	144.85		70		1	1	2	0	0	0
KS-062	144.85	147.15		30		1	1	2	0	0	0
KS-062	147.15	150.85		30		1	1	2	0	0	0
KS-062	150.85	153.85		70		1	20	21	0	0	0
KS-062	153.85	155.25		50		2.5	20	22.5	0	0	0
KS-062	155.25	156.85		60		1	1	2	0	0	0
KS-062	156.85	159.85		80		1	1	2	0	0	0
KS-062	159.85	162.85		35		1	5	6	0	0	0
KS-062	171.85	174.85		45		5	1	6	0	0	0
KS-062	174.85	177.85		60		10	2.5	12.5	0	0	0
KS-062	177.85	182.00		60		10	2.5	12.5	0	0	0
KS-062	182.00	182.85		60		0	0	0	0	0	0
KS-063	6.10	7.00				0	0	0	0	0	0
KS-063	7.00	10.00		50		0	1	1	0	0	0
KS-063	10.00	13.00				30	0	30	0	0	0
KS-063	13.00	15.70				30	0	30	0	0	0
KS-063	45.10	46.68		45		0	1	1	0	0	0
KS-063	46.68	50.00				0	1	1	0	0	0
KS-063	50.00	53.00		45		0	0.001	0.001	0	0	0
KS-063	53.00	56.00				0	0	0	0	0	0
KS-063	56.00	59.30				0	0	0	0	0	0
KS-063	59.30	59.90		60		2.5	2.5	5	0	0	0
KS-063	96.00	99.00		50		10	1	11	0	0	0
KS-063	99.00	100.00		60		20	1	21	0	0	0
KS-063	100.00	101.55		60		0	1	1	0	0	0
KS-063	101.55	102.00		60		20	1	21	0	0	0
KS-063	102.00	105.00		60		20	2.5	22.5	0	0	0
KS-063	105.00	108.00		70		10	1	11	0	0	0
KS-063	108.00	109.70				0	0	0	0	0	0
KS-063	109.70	113.00		70		20	1	21	0	0	0
KS-063	113.00	116.00		70		20	2.5	22.5	0	0	0
KS-063	116.00	119.00				20	1	21	0	0	0

DDHS	FROM metres	TO metres	GYR (%)	GYV (%)	GYT (%)	AHGYT (%)	SER (%)	SEV (%)	SET (%)	YSR (%)	YSV (%)
KS-062	19.00	21.34	0	0	0	0	2.5	0	2.5	0	0
KS-062	21.34	24.00	0	0	0	0	10	0	10	0	0
KS-062	24.00	28.30	0	0	0	0	2.5	0.001	2.501	0	0
KS-062	28.30	29.20	0	0	0	0	2.5	0	2.5	0	0
KS-062	29.20	31.30	0	0	0	0	10	0	10	0	0
KS-062	31.30	36.15	0	0	0	0	20	0	20	0	0
KS-062	36.15	38.90	0	0	0	0	20	0	20	0	0
KS-062	38.90	42.67	0	0	0	0	20	0	20	0	0
KS-062	74.80	78.80	0	0	0	0	20	0	20	0	0
KS-062	78.80	81.99	0	0	0	0	30	0	30	0	0
KS-062	81.99	85.04	0	0	0	0	30	0	30	0	0
KS-062	85.04	86.25	0	0	0	0	30	0	30	0	0
KS-062	86.25	89.40	0	0	0	0	20	0.001	20.001	0	0
KS-062	89.40	92.40	0	0	0	0	30	0	30	0	0
KS-062	92.40	95.40	0	0	0	0	20	0	20	0	0
KS-062	95.40	97.84	0	0	0	0	20	0	20	0	0
KS-062	138.85	140.25	0	0	0	0	40	0	40	5	0
KS-062	140.25	141.85	0	0	0	0	20	0	20	0	0
KS-062	141.85	144.85	0	0	0	0	20	0	20	0	0
KS-062	144.85	147.15	0	0	0	0	20	0	20	0	0
KS-062	147.15	150.85	0	0	0	0	5	0	5	0	0
KS-062	150.85	153.85	0	0	0	0	20	0	20	0	0
KS-062	153.85	155.25	0	0	0	0	20	0	20	0	0
KS-062	155.25	156.85	0	0	0	0	2	0	2	0	0
KS-062	156.85	159.85	0	0	0	0	30	0	30	0	0
KS-062	159.85	162.85	0	0	0	0	30	0	30	0	0
KS-062	171.85	174.85	0	0	0	0	30	0	30	0	0
KS-062	174.85	177.85	0	0	0	0	20	0	20	0	0
KS-062	177.85	182.00	0	0	0	0	20	0	20	0	0
KS-062	182.00	182.85	0	0	0	0	30	0	30	0	0
KS-063	6.10	7.00	0	0	0	0	20	0	20	0	0
KS-063	7.00	10.00	0	0	0	0	30	0	30	0	0
KS-063	10.00	13.00	0	0	0	0	20	0	20	0	0
KS-063	13.00	15.70	0	0	0	0	20	0	20	0	0
KS-063	45.10	46.68	0	0	0	0	30	0	30	0	0
KS-063	46.68	50.00	0	0	0	0	30	0	30	0	0
KS-063	50.00	53.00	0	0	0	0	30	0	30	0	0
KS-063	53.00	56.00	0	0	0	0	20	0	20	0	0
KS-063	56.00	59.30	0	0	0	0	20	0	20	0	0
KS-063	59.30	59.90	0	0	0	0	20	0	20	0	0
KS-063	96.00	99.00	0	0	0	0	20	0	20	0	0
KS-063	99.00	100.00	0	0	0	0	20	0	20	0	0
KS-063	100.00	101.55	0	0	0	0	10	0	10	0	0
KS-063	101.55	102.00	0	0	0	0	0	0	0	0	0
KS-063	102.00	105.00	0	0	0	0	10	0	10	0	0
KS-063	105.00	108.00	0	0	0	0	20	0	20	0	0
KS-063	108.00	109.70	0	0	0	0	20	0	20	0	0
KS-063	109.70	113.00	0	0	0	0	20	0	20	0	0
KS-063	113.00	116.00	0	0	0	0	20	0	20	0	0
KS-063	116.00	119.00	0	0	0	0	10	0	10	0	0

DDHS	FROM metres	TO metres	YST (%)	GSR (%)	GSV (%)	GST (%)	SYGST (%)	KAR (%)	KAV (%)	KAT (%)	CLR (%)
KS-062	19.00	21.34	0	0	0	0	2.5	2.5	0	2.5	1
KS-062	21.34	24.00	0	0	0	0	10	10	0	10	2.5
KS-062	24.00	28.30	0	0	0	0	2.501	10	0	10	0
KS-062	28.30	29.20	0	0	0	0	2.5	10	0	10	2.5
KS-062	29.20	31.30	0	0	0	0	10	10	0	10	5
KS-062	31.30	36.15	0	0	0	0	20	10	0	10	10
KS-062	36.15	38.90	0	0	0	0	20	10	0	10	5
KS-062	38.90	42.67	0	0	0	0	20	5	0	5	2.5
KS-062	74.80	78.80	0	0	0	0	20	2.5	0	2.5	10
KS-062	78.80	81.99	0	0	0	0	30	1	0	1	20
KS-062	81.99	85.04	0	0	0	0	30	1	0	1	20
KS-062	85.04	86.25	0	0	0	0	30	2.5	0	2.5	2.5
KS-062	86.25	89.40	0	0	0	0	20.001	10	0	10	5
KS-062	89.40	92.40	0	0	0	0	30	2.5	0	2.5	10
KS-062	92.40	95.40	0	0	0	0	20	10	0	10	5
KS-062	95.40	97.84	0	0	0	0	20	10	0	10	5
KS-062	138.85	140.25	5	0	0	0	45	0	0	0	0
KS-062	140.25	141.85	0	0	0	0	20	10	0	10	2.5
KS-062	141.85	144.85	0	0	0	0	20	10	0	10	2.5
KS-062	144.85	147.15	0	0	0	0	20	10	0	10	1
KS-062	147.15	150.85	0	0	0	0	5	0	0	0	20
KS-062	150.85	153.85	0	0	0	0	20	2.5	0	2.5	20
KS-062	153.85	155.25	0	0	0	0	20	10	0	10	10
KS-062	155.25	156.85	0	0	0	0	2	10	0	10	10
KS-062	156.85	159.85	0	0	0	0	30	0	0	0	0
KS-062	159.85	162.85	0	0	0	0	30	0	0	0	0
KS-062	171.85	174.85	0	0	0	0	30	10	0	10	0
KS-062	174.85	177.85	0	0	0	0	20	2.5	0	2.5	5
KS-062	177.85	182.00	0	0	0	0	20	10	0	10	2.5
KS-062	182.00	182.85	0	0	0	0	30	2.5	0	2.5	2.5
KS-063	6.10	7.00	0	0	0	0	20	2.5	0	2.5	5
KS-063	7.00	10.00	0	0	0	0	30	2.5	0	2.5	5
KS-063	10.00	13.00	0	0	0	0	20	20	0	20	0.001
KS-063	13.00	15.70	0	0	0	0	20	20	0	20	0.001
KS-063	45.10	46.68	0	0	0	0	30	0.001	0	0.001	5
KS-063	46.68	50.00	0	0	0	0	30	2.5	0	2.5	2.5
KS-063	50.00	53.00	0	0	0	0	30	20	0	20	10
KS-063	53.00	56.00	0	0	0	0	20	20	0	20	10
KS-063	56.00	59.30	0	0	0	0	20	20	0	20	10
KS-063	59.30	59.90	0	0	0	0	20	10	0	10	2.5
KS-063	96.00	99.00	0	0	0	0	20	20	0	20	5
KS-063	99.00	100.00	0	0	0	0	20	20	0	20	5
KS-063	100.00	101.55	0	0	0	0	10	10	0	10	20
KS-063	101.55	102.00	0	0	0	0	0	20	0	20	5
KS-063	102.00	105.00	0	0	0	0	10	20	0	20	20
KS-063	105.00	108.00	0	0	0	0	20	20	0	20	2.5
KS-063	108.00	109.70	0	0	0	0	20	10	0	10	10
KS-063	109.70	113.00	0	0	0	0	20	10	0	10	5
KS-063	113.00	116.00	0	0	0	0	20	10	0	10	5
KS-063	116.00	119.00	0	0	0	0	10	20	0	20	5

DDHS	FROM metres	TO metres	CLV (%)	CLT (%)	CAR (%)	CAV (%)	CAT (%)	AKR (%)	AKV (%)	AKT (%)	MGR (%)
KS-062	19.00	21.34	1	2	0.001	2.5	2.501	0	0	0	0
KS-062	21.34	24.00	0	2.5	5	0	5	0	0	0	0
KS-062	24.00	28.30	0	0	2.5	1	3.5	0	0	0	0
KS-062	28.30	29.20	0	2.5	0	0	0	0	0	0	0
KS-062	29.20	31.30	2.5	7.5	0	0	0	0	0	0	0
KS-062	31.30	36.15	0	10	0	1	1	0	0	0	0
KS-062	36.15	38.90	0	5	0.001	1	1.001	0	0	0	0
KS-062	38.90	42.67	0	2.5	0.001	1	1.001	0	0	0	0
KS-062	74.80	78.80	1	11	5	1	6	0	0	0	0
KS-062	78.80	81.99	1	21	5	2.5	7.5	0	0	0	0
KS-062	81.99	85.04	1	21	1	1	2	0	0	0	0
KS-062	85.04	86.25	0.001	2.501	5	1	6	0	0	0	0
KS-062	86.25	89.40	0.001	5.001	1	2.5	3.5	0	0	0	1
KS-062	89.40	92.40	0.001	10.001	5	1	6	0	0	0	1
KS-062	92.40	95.40	0.001	5.001	2.5	1	3.5	0	0	0	0
KS-062	95.40	97.84	0.001	5.001	2.5	1	3.5	0	0	0	0
KS-062	138.85	140.25	1	1	0.001	1	1.001	1	2.5	3.5	0
KS-062	140.25	141.85	2.5	5	0.001	0.001	0.002	0	0	0	0
KS-062	141.85	144.85	2.5	5	0	0.001	0.001	0	0	0	0
KS-062	144.85	147.15	1	2	0	0.001	0.001	0	0	0	0
KS-062	147.15	150.85	1	21	2.5	1	3.5	0	0	0	0
KS-062	150.85	153.85	1	21	5	2.5	7.5	0	0	0	0
KS-062	153.85	155.25	2.5	12.5	0.001	5	5.001	0	0	0	0
KS-062	155.25	156.85	0.001	10.001	0	1	1	0	0	0	0
KS-062	156.85	159.85	0	0	0	1	1	0	0.001	0.001	0
KS-062	159.85	162.85	0.001	0.001	0	0.001	0.001	0	0.001	0.001	0
KS-062	171.85	174.85	0	0	0	0.001	0.001	0	0	0	0
KS-062	174.85	177.85	0	5	0.001	0	0.001	0	0	0	0
KS-062	177.85	182.00	2.5	5	0.001	1	1.001	0	0	0	0
KS-062	182.00	182.85	0	2.5	1	0.001	1.001	0	0	0	0
KS-063	6.10	7.00	0	5	0	0	0	0	0	0	0
KS-063	7.00	10.00	0	5	1	1	2	0	0	0	0
KS-063	10.00	13.00	0	0.001	0	0	0	0	0	0	0
KS-063	13.00	15.70	0	0.001	0	0	0	0	0	0	0
KS-063	45.10	46.68	1	6	0	1	1	0	0	0	0
KS-063	46.68	50.00	0	2.5	1	1	2	0	0	0	0
KS-063	50.00	53.00	0	10	0	0	0	0	0	0	0
KS-063	53.00	56.00	0	10	0	0	0	0	0	0	0
KS-063	56.00	59.30	0	10	0	0	0	0	0	0	0
KS-063	59.30	59.90	0	2.5	0	0	0	0	0	0	0
KS-063	96.00	99.00	5	10	1	0	1	0	0	0	0
KS-063	99.00	100.00	0	5	0.001	0	0.001	0	0	0	0
KS-063	100.00	101.55	0	20	0	0	0	0	0	0	0
KS-063	101.55	102.00	0	5	0.001	0	0.001	0	0	0	0
KS-063	102.00	105.00	0	20	1	0	1	0	0	0	0
KS-063	105.00	108.00	0	2.5	0	0	0	0	0	0	0
KS-063	108.00	109.70	0	10	2.5	1	3.5	0	0	0	0
KS-063	109.70	113.00	0	5	0	1	1	0	1	1	0
KS-063	113.00	116.00	0	5	0	0.001	0.001	0	0	0	0
KS-063	116.00	119.00	1	6	0	0.001	0.001	0	0	0	0



DDHS	FROM metres	TO metres	PYV (%)	PYT (%)	CPR (%)	CPV (%)	CPT (%)	TTR (%)	TTV (%)	TTT (%)	BOV (%)
KS-062	19.00	21.34	1	2	0	0	0	0	0	0	0
KS-062	21.34	24.00	0	10	0	0	0	0	0	0	0
KS-062	24.00	28.30	0	5	0	0	0	0	0	0	0
KS-062	28.30	29.20	0	2.5	0	0	0	0	0	0	0
KS-062	29.20	31.30	0	2.5	0	0	0	0	0	0	0
KS-062	31.30	36.15	0	1	0	0	0	0	0	0	0
KS-062	36.15	38.90	0.001	2.501	0	0	0	0	0	0	0
KS-062	38.90	42.67	0	2.5	0	0	0	0	0	0	0
KS-062	74.80	78.80	0	2.5	0	0	0	0	0	0	0
KS-062	78.80	81.99	0	2.5	0	0	0	0	0	0	0
KS-062	81.99	85.04	0	5	0	0	0	0	0	0	0
KS-062	85.04	86.25	0	2.5	0	0	0	0	0	0	0
KS-062	86.25	89.40	0	1	0	0	0	0	0	0	0
KS-062	89.40	92.40	0	5	0	0	0	0	0	0	0
KS-062	92.40	95.40	0	5	0	0	0	0	0	0	0
KS-062	95.40	97.84	0	2.5	0	0	0	0	0	0	0
KS-062	138.85	140.25	0.001	5.001	0	0.001	0.001	0	0	0	0
KS-062	140.25	141.85	5	25	0	0.001	0.001	0	0	0	0
KS-062	141.85	144.85	2.5	22.5	0	0.001	0.001	0	0	0	0
KS-062	144.85	147.15	1	11	0	0	0	0	0	0	0
KS-062	147.15	150.85	0	1	0.001	0	0.001	0	0	0	0
KS-062	150.85	153.85	2.5	22.5	0	0.1	0.1	0	0	0	0.001
KS-062	153.85	155.25	2.5	22.5	0.001	0	0.001	0	0	0	0
KS-062	155.25	156.85	1	6	0.001	0.001	0.002	0	0	0	0
KS-062	156.85	159.85	0	10	0	0.001	0.001	0	0	0	0
KS-062	159.85	162.85	1	11	0.001	0.001	0.002	0	0	0	0
KS-062	171.85	174.85	1	11	0	0	0	0	0	0	0
KS-062	174.85	177.85	1	6	0	0.001	0.001	0	0	0	0
KS-062	177.85	182.00	1	11	0	0	0	0	0	0	0
KS-062	182.00	182.85	0	10	0	0	0	0	0	0	0
KS-063	6.10	7.00	0	1	0	0	0	0	0	0	0
KS-063	7.00	10.00	0	5	0	0	0	0	0	0	0
KS-063	10.00	13.00	0	2.5	0	0	0	0	0	0	0
KS-063	13.00	15.70	0	2.5	0	0	0	0	0	0	0
KS-063	45.10	46.68	0	5	0	0	0	0	0	0	0
KS-063	46.68	50.00	0	10	0	0	0	0	0	0	0
KS-063	50.00	53.00	0	10	0	0	0	0	0	0	0
KS-063	53.00	56.00	0	5	0	0	0	0	0	0	0
KS-063	56.00	59.30	0	5	0	0	0	0	0	0	0
KS-063	59.30	59.90	1	11	0	0	0	0	0	0	0
KS-063	96.00	99.00	1	3.5	0.001	0	0.001	0	0	0	0
KS-063	99.00	100.00	2.5	7.5	0	1	1	0	0	0	0
KS-063	100.00	101.55	1	3.5	0	0.001	0.001	0	0	0	0
KS-063	101.55	102.00	1	6	0	1	1	0	0	0	0
KS-063	102.00	105.00	1	3.5	0	0.001	0.001	0	0	0	0
KS-063	105.00	108.00	0	10	0	0.001	0.001	0	0	0	0
KS-063	108.00	109.70	0	2.5	0	0	0	0	0	0	0
KS-063	109.70	113.00	1	6	0	0	0	0	0	0	0
KS-063	113.00	116.00	1	11	1	1	2	0	0	0	0
KS-063	116.00	119.00	0	5	0	0	0	0	0	0	0



DDHS	FROM metres	TO metres	V3 (%)	V4 (%)	X1 (%)	X2 (%)	X3 (%)	CLEAV	Cu:Au (%/ppm)
KS-062	19.00	21.34	0	0	0	0	3	0	0.51875
KS-062	21.34	24.00	0	0	0	0	0	0	0.66
KS-062	24.00	28.30	0	0	0	0	2	0	1.21667
KS-062	28.30	29.20	0	0	0	0	0	0	0.68
KS-062	29.20	31.30	0	0	0	0	5	0	0.41
KS-062	31.30	36.15	0	0	0	0	2.5	0	0.3
KS-062	36.15	38.90	0	0	0	0	2.5	0	0.66
KS-062	38.90	42.67	0	0	0	0	2.5	0	0.17
KS-062	74.80	78.80	0	0	0	0	4.1	0	0.04694
KS-062	78.80	81.99	0	0	0	0	5.3	0	0.03333
KS-062	81.99	85.04	0	0	0	0	2.6	1	0.00769
KS-062	85.04	86.25	0	0	0	0	1	0	0.00556
KS-062	86.25	89.40	0	0	0	0	2.8	0	0.02632
KS-062	89.40	92.40	0	0	0	0	2.3	0	0.11667
KS-062	92.40	95.40	0	0	0	0	3.6	1	0.01368
KS-062	95.40	97.84	0	0	0	0	1	0	0.28
KS-062	138.85	140.25	0	0	0	0	2	3	0.92
KS-062	140.25	141.85	0	0	0	0	1	1	0.92
KS-062	141.85	144.85	0	0	0	0	1.7	1	1.02727
KS-062	144.85	147.15	0	0	0	0	1.3	1	0.34444
KS-062	147.15	150.85	0	0	0	0	7	1	0.36
KS-062	150.85	153.85	0	0	0	4	2.8	2	0.77647
KS-062	153.85	155.25	0	0	0	0	3	1	0.91579
KS-062	155.25	156.85	0	0	0	0	2.2	2	0.91579
KS-062	156.85	159.85	0	0	0	0	4.5	2	2.15556
KS-062	159.85	162.85	0	0	0	0	0.1	3	1.40588
KS-062	171.85	174.85	1.4	0	0	0.5	0	3	0.98667
KS-062	174.85	177.85	0	0	0	0	0.3	3	3.49091
KS-062	177.85	182.00	0	0	0	0	1	3	2.85714
KS-062	182.00	182.85	0	0	0	0	0	4	0.825
KS-063	6.10	7.00	0	0	0	0	0	0	0.36667
KS-063	7.00	10.00	0	0	0	0	0.5	3	0.7
KS-063	10.00	13.00	0	0	0	0	0	1	1.6
KS-063	13.00	15.70	0	0	0	0	0	1	1.3
KS-063	45.10	46.68	0	0	0	0	7	2	0.52
KS-063	46.68	50.00	0	0	0	0	0	1	0.17059
KS-063	50.00	53.00	0	0	0	0	0	1	0.2375
KS-063	53.00	56.00	0	0	0	0	0	1	0.2875
KS-063	56.00	59.30	0	0	0	0	0	1	0.36875
KS-063	59.30	59.90	0	0	0	0	0	1	0.92174
KS-063	96.00	99.00	0	0	0	0	0.1	3	1.64615
KS-063	99.00	100.00	0	0	0	0	0	3	2.76
KS-063	100.00	101.55	0	0	0	0	2	1	2.76
KS-063	101.55	102.00	0	0	0	0	0	3	2.76
KS-063	102.00	105.00	0	0	0	0	0.5	2	1.85714
KS-063	105.00	108.00	0	0	0	0	0.8	2	0.31636
KS-063	108.00	109.70	0	0	0	0	0.5	1	0.16316
KS-063	109.70	113.00	0	0	0	0	0.5	2	0.76286
KS-063	113.00	116.00	0	0	0	0	1	2	1.53514
KS-063	116.00	119.00	0	0	0	0	1	2	0.98868



DDHS	FROM metres	TO metres	INTRVAL	CU (%)	AU (ppm)	ZN (ppm)	PB (ppm)	AG (ppm)	RECOV (%)	ROCK\$	BX
KS-063	155.00	158.00	3.00	0.544	1.67	325	22	2.7	100	BRXX	
KS-063	158.00	161.00	3.00	0.504	0.41	207	16	3.5	100	BRXX	
KS-063	161.00	163.00	2.00	0.436	0.24	367	18	2.6	100	BRXX	
KS-063	163.00	165.30	2.30	0.520	0.26	670	22	2.4	100	BRXX	
KS-063	165.30	168.30	3.00	0.025	0.07	90	20	0.4	100	LAPP	
KS-063	168.30	171.00	2.70	0.408	0.91	295	32	1.2	100	BRXX	
KS-063	171.00	174.00	3.00	0.684	0.24	176	32	2.7	100	BRXX	
KS-063	174.00	177.00	3.00	0.526	0.14	188	28	1.2	100	BRXX	
KS-063	189.00	192.00	3.00	0.352	0.23	65	18	0.8	100	BRXX	
KS-063	192.00	195.00	3.00	0.456	0.12	40	14	1.0	100	BRXX	
KS-064	15.50	18.50	3	0.040	0.10				100	LAPP	
KS-064	18.50	20.50	2	0.061	0.15				100	LAPP	
KS-064	20.50	23.50	3	0.704	0.47				100	TFLP	
KS-064	23.50	26.50	3	0.820	0.29				100	TFLP	
KS-064	26.50	29.50	3	0.352	0.07				100	TFLP	
KS-064	29.50	32.50	3	0.352	0.12				100	TFLP	
KS-064	32.50	35.50	3	0.392	0.15				100	TFLP	40
KS-064	35.50	38.50	3	0.392	0.15				98	BRXX	
KS-064	68.65	72.00	3.35	0.568	0.34				73	TFLP	
KS-064	72.00	75.00	3	0.299	1.67				100	TFLP	
KS-064	75.00	78.00	3	0.228	0.11				98	TFLP	
KS-064	78.00	81.00	3	0.175	0.16				98	TFLP	
KS-064	81.00	84.00	3	0.238	0.15				98	TFLP	
KS-064	84.00	87.00	3	0.291	0.20				98	TFLP	
KS-064	87.00	90.00	3	0.091	0.09				98	TFLP	
KS-064	122.70	125.70	3	0.161	0.10				100	TFLP	
KS-064	125.70	128.70	3	0.129	0.13				100	TFLP	
KS-064	128.70	131.70	3	0.055	0.13				100	TFLP	
KS-064	131.70	134.70	3	0.057	0.05				100	TFLP	
KS-064	134.70	137.70	3	0.048	0.24				100	TFLP	
KS-064	137.70	140.70	3	0.049	0.03				98	TFLP	
KS-064	140.70	143.70	3	0.060	0.14				98	TFLP	
KS-064	173.80	176.80	3	0.804	0.82				90	PHPP	
KS-064	176.80	178.90	2.1	0.648	0.51				95	PHPP	
KS-064	178.90	180.20	1.3	0.540	0.16				96	PHPP	
KS-064	224.00	230.70	6.1	0.864	0.11				20		
KS-064	230.70	239.90	9.2	0.828	0.08				6		
KS-064	239.90	243.70	3.8	1.036	0.11				37		
KS-064	243.70	246.00	2.3	1.064	0.22				100	PHPP	
KS-064	246.00	246.55	0.55	0.652	0.11				95		
KS-064	246.55	249.00	2.45	0.007	0.23				98	LAAP	
KS-064	282.40	284.00	1.6	0.584	6.40				100	PHPP	
KS-064	284.00	286.00	2	0.472	0.36				98	PHPP	
KS-064	286.00	289.00	3	0.460	0.26				96	PHPP	
KS-064	289.00	291.20	2.2	0.428	0.23				95	PHPP	
KS-064	291.20	293.00	1.8	0.017	0.12				98	LAAP	
KS-064	293.00	294.90	1.9	0.018	0.20				98	LAAP	
KS-064	294.90	297.00	2.1	0.209	0.14				95	PHPP	
KS-064	297.00	300.60	3.6	0.256	0.07				39	PHPP	
KS-064	300.60	303.60	3	0.256	0.07				63	PHPP	

DDHS	FROM metres	TO metres	FB	FX	VF	QZR (%)	QZV (%)	QZT (%)	AHR (%)	AHV (%)	AHT (%)
KS-063	155.00	158.00		60		5	2.5	7.5	0	0	0
KS-063	158.00	161.00		60		5	2.5	7.5	0	0	0
KS-063	161.00	163.00		55		2.5	2.5	5	0	0	0
KS-063	163.00	165.30		55		20	2.5	22.5	0	0	0
KS-063	165.30	168.30		80		0	1	1	0	0	0
KS-063	168.30	171.00		60		20	2.5	22.5	0	0	0
KS-063	171.00	174.00		50		10	2.5	12.5	0	0	0
KS-063	174.00	177.00		60		20	2.5	22.5	0	0	0
KS-063	189.00	192.00		50		30	2.5	32.5	0	0	0
KS-063	192.00	195.00		60		30	1	31	0	0	0
KS-064	15.50	18.90		50		1	0	1	0	0	0
KS-064	18.50	20.50		60		0	0	0	0	0	0
KS-064	20.50	23.50				10	5	15	0	0	0
KS-064	23.50	26.50				20	2.5	22.5	0	0	0
KS-064	26.50	29.50		55		5	1	6	0	0	0
KS-064	29.50	32.50				0	1	1	0	0	0
KS-064	32.50	35.50		40		0	1	1	0	0	0
KS-064	35.50	38.50		60		0	10	10	0	0	0
KS-064	68.65	72.00				0	1	1	0	0	0
KS-064	72.00	75.00		55		0	1	1	0	0	0
KS-064	75.00	78.00		55		0	2.5	2.5	0	0	0
KS-064	78.00	81.00		45		10	1	11	0	0	0
KS-064	81.00	84.00		30		20	1	21	0	0	0
KS-064	84.00	87.00		50		20	0	20	0	0	0
KS-064	87.00	90.00				20	0.001	20.001	0	0	0
KS-064	122.70	125.70		40		0	1	1	0	0	0
KS-064	125.70	128.70		50		0	1	1	0	0	0
KS-064	128.70	131.70		30		0	2.5	2.5	0	0	0
KS-064	131.70	134.70		40		0	1	1	0	0	0
KS-064	134.70	137.70		50		0	0.1	0.1	0	0	0
KS-064	137.70	140.70		45		0	0.1	0.1	0	0	0
KS-064	140.70	143.70		65		2.5	0.1	2.6	0	0	0
KS-064	173.80	176.80		40		0	20	20	0	0	0
KS-064	176.80	178.90				0	30	30	0	0	0
KS-064	178.90	180.20		60		0	0	0	0	0	0
KS-064	224.60	230.70				0	0	0	0	0	0
KS-064	230.70	239.90				0	0	0	0	0	0
KS-064	239.90	243.70				0	0	0	0	0	0
KS-064	243.70	246.00		50		0	5	5	0	0	0
KS-064	246.00	246.55				0	0	0	0	0	0
KS-064	246.55	249.00				0	1	1	0	0	0
KS-064	282.40	284.00		47		10	1	11	0	0	0
KS-064	284.00	286.00		50		0	0	0	0	0	0
KS-064	286.00	289.00				0	2.5	2.5	0	0	0
KS-064	289.00	291.20		50		0	2.5	2.5	0	0	0
KS-064	291.20	293.00				0	1	1	0	0	0
KS-064	293.00	294.90				0	0	0	0	0	0
KS-064	294.90	297.00		45		0	0	0	0	0	0
KS-064	297.00	300.60				0	2.5	2.5	0	0	0
KS-064	300.60	303.60		50		0	1	1	0	0	0

DDHS	FROM metres	TO metres	GYR (%)	GYV (%)	GYT (%)	AHGYT (%)	SER (%)	SEV (%)	SET (%)	YSR (%)	YSV (%)
KS-063	155.00	158.00	0	0	0	0	5	0	5	0	0
KS-063	158.00	161.00	0	0	0	0	20	0	20	0	0
KS-063	161.00	163.00	0	0	0	0	30	0	30	0	0
KS-063	163.00	165.30	0	0	0	0	20	0	20	0	0
KS-063	165.30	168.30	0	0	0	0	30	0	30	0	0
KS-063	168.30	171.00	0	0	0	0	20	0	20	0	0
KS-063	171.00	174.00	0	0	0	0	20	0	20	0	0
KS-063	174.00	177.00	0	0	0	0	20	0	20	0	0
KS-063	189.00	192.00	0	0	0	0	30	0	30	0	0
KS-063	192.00	195.00	0	0	0	0	30	0	30	0	0
KS-064	15.50	18.50	0	0	0	0	30	0.001	30.001	0	0
KS-064	18.50	20.50	0	0	0	0	30	0	30	0	0
KS-064	20.50	23.50	0	0	0	0	10	0	10	0	0
KS-064	23.50	26.50	0	0	0	0	20	0	20	0	0
KS-064	26.50	29.50	0	0	0	0	30	0	30	0	0
KS-064	29.50	32.50	0	0	0	0	30	0	30	0	0
KS-064	32.50	35.50	0	0	0	0	40	0	40	0	0
KS-064	35.50	38.50	0	0	0	0	30	0	30	0	0
KS-064	68.65	72.00	0	0	0	0	40	0	40	0	0
KS-064	72.00	75.00	0	0	0	0	40	0	40	0	0
KS-064	75.00	78.00	0	0	0	0	40	0	40	0	0
KS-064	78.00	81.00	0	0	0	0	40	0	40	0	0
KS-064	81.00	84.00	0	0	0	0	30	0	30	0	0
KS-064	84.00	87.00	0	0	0	0	20	0	20	0	0
KS-064	87.00	90.00	0	0	0	0	30	0	30	0	0
KS-064	122.70	125.70	0	0	0	0	30	0	30	0	0
KS-064	125.70	128.70	0	0	0	0	30	0	30	0	0
KS-064	128.70	131.70	0	0	0	0	30	0	30	0	0
KS-064	131.70	134.70	0	0	0	0	30	0	30	0	0
KS-064	134.70	137.70	0	0	0	0	30	0	30	0	0
KS-064	137.70	140.70	0	0	0	0	30	0	30	0	0
KS-064	140.70	143.70	0	0	0	0	30	0	30	0	0
KS-064	173.80	176.80	0	0	0	0	10	0	10	0	0
KS-064	176.80	178.90	0	0	0	0	20	0	20	0	0
KS-064	178.90	180.20	0	0	0	0	20	0	20	0	0
KS-064	294.60	230.70	0	0	0	0	0	0	0	0	0
KS-064	230.70	239.90	0	0	0	0	0	0	0	0	0
KS-064	239.90	243.70	0	0	0	0	0	0	0	0	0
KS-064	243.70	246.00	0	0	0	0	20	0	20	0	0
KS-064	246.00	246.55	0	0	0	0	0	0	0	0	0
KS-064	246.55	249.00	0	0	0	0	0	0	0	0	0
KS-064	282.40	284.00	0	0	0	0	30	0	30	10	0
KS-064	284.00	286.00	0	0	0	0	20	1	21	20	0
KS-064	286.00	289.00	0	0	0	0	10	0	10	0	0
KS-064	289.00	291.20	0	0	0	0	10	2.5	12.5	0	0
KS-064	291.20	293.00	0	0	0	0	20	0	20	0	0
KS-064	293.00	294.90	0	0	0	0	10	0	10	0	0
KS-064	294.90	297.00	0	0	0	0	5	0	5	0	0
KS-064	297.00	300.60	0	0	0	0	10	0	10	0	0
KS-064	300.60	303.60	0	0	0	0	10	0	10	20	0

DDHS	FROM metres	TO metres	YST (%)	GSR (%)	GSV (%)	GST (%)	SYGST (%)	KAR (%)	KAV (%)	KAT (%)	CLR (%)
KS-063	155.00	158.00	0	0	0	0	5	20	0	20	10
KS-063	158.00	161.00	0	0	0	0	20	10	0	10	2.5
KS-063	161.00	163.00	0	0	0	0	30	10	0	10	2.5
KS-063	163.00	165.30	0	0	0	0	20	10	0	10	0.001
KS-063	165.30	168.30	0	0	0	0	30	2.5	0	2.5	0
KS-063	168.30	171.00	0	2.5	0	2.5	22.5	10	0	10	1
KS-063	171.00	174.00	0	0	0	0	20	10	0	10	0.001
KS-063	174.00	177.00	0	0	0	0	20	10	0	10	0
KS-063	189.00	192.00	0	0	0	0	30	2.5	0	2.5	0
KS-063	192.00	195.00	0	0	0	0	30	2.5	0	2.5	0
KS-064	15.50	18.50	0	0	0	0	30.001	10	0	10	10
KS-064	18.50	20.50	0	0	0	0	30	20	0	20	10
KS-064	20.50	23.50	0	0	0	0	10	5	0	5	30
KS-064	23.50	26.50	0	0	0	0	20	2.5	0	2.5	20
KS-064	26.50	29.50	0	2.5	0	2.5	32.5	0	5	5	1
KS-064	29.50	32.50	0	0	0	0	30	5	0	5	0
KS-064	32.50	35.50	0	0	0	0	40	10	0	10	0.001
KS-064	35.50	38.50	0	0	0	0	30	0	0	0	0
KS-064	68.65	72.00	0	0	0	0	40	0	0.001	0.001	0
KS-064	72.00	75.00	0	0	0	0	40	10	0.001	10.001	1
KS-064	75.00	78.00	0	1	0	1	41	0	0	0	0
KS-064	78.00	81.00	0	0	0	0	40	10	0	10	0.001
KS-064	81.00	84.00	0	0	0	0	30	2.5	0	2.5	0.001
KS-064	84.00	87.00	0	0	0	0	20	2.5	0.001	2.501	2.5
KS-064	87.00	90.00	0	0.001	0	0.001	30.001	10	0	10	0.001
KS-064	122.70	125.70	0	0	0	0	30	10	0	10	0
KS-064	125.70	128.70	0	0	0	0	30	20	0	20	0
KS-064	128.70	131.70	0	0	0	0	30	20	0	20	0
KS-064	131.70	134.70	0	0	0	0	30	10	0	10	0
KS-064	134.70	137.70	0	0	0	0	30	10	0	10	0
KS-064	137.70	140.70	0	0	0	0	30	10	0	10	0
KS-064	140.70	143.70	0	0	0	0	30	10	0	10	0
KS-064	173.80	176.80	0	20	0	20	30	0	0.001	0.001	0
KS-064	176.80	178.90	0	10	0	10	30	5	0.001	5.001	0
KS-064	178.90	180.20	0	20	0	20	40	2.5	0.001	2.501	0
KS-064	224.60	230.70	0	0	0	0	0	0	0	0	0
KS-064	230.70	239.90	0	0	0	0	0	0	0	0	0
KS-064	239.90	243.70	0	0	0	0	0	0	0	0	0
KS-064	243.70	246.00	0	0	0	0	20	20	0.001	20.001	0
KS-064	246.00	246.55	0	0	0	0	0	0	0	0	0
KS-064	246.55	249.00	0	0	0	0	0	0	0	0	30
KS-064	282.40	284.00	10	0	0	0	40	10	0	10	0
KS-064	284.00	286.00	20	0	0	0	41	0	0.001	0.001	0
KS-064	286.00	289.00	0	30	1	31	41	0	0.001	0.001	2.5
KS-064	289.00	291.20	0	30	1	31	43.5	0	0	0	0
KS-064	291.20	293.00	0	0	0	0	20	0	0	0	20
KS-064	293.00	294.90	0	0	0	0	10	0	0	0	30
KS-064	294.90	297.00	0	30	0	30	35	0	0.001	0.001	1
KS-064	297.00	300.60	0	30	0	30	40	0	0	0	1
KS-064	300.60	303.60	20	0	0	0	30	0	0.001	0.001	0





DDH\$	FROM metres	TO metres	PYV (%)	PYT (%)	CPR (%)	CPV (%)	CPT (%)	TTR (%)	TTV (%)	TTT (%)	BOV (%)
KS-063	155.00	158.00	1	3.5	1	1	2	0	0	0	0
KS-063	158.00	161.00	1	11	0.001	0.001	0.002	0	0	0	0
KS-063	161.00	163.00	1	2	1	0.001	1.001	0	0	0	0
KS-063	163.00	165.30	1	2	1	1	2	0	0	0	0
KS-063	165.30	168.30	1	11	0	0	0	0	0	0	0
KS-063	168.30	171.00	2.5	7.5	1	1	2	0	0	0	0
KS-063	171.00	174.00	1	11	1	2.5	3.5	0	0	0	0
KS-063	174.00	177.00	1	3.5	0	1	1	0	0	0	0
KS-063	189.00	192.00	1	6	0.001	0.001	0.002	0	0	0	0
KS-063	192.00	195.00	2.5	12.5	0.001	0.001	0.002	0	0	0	0
KS-064	15.50	18.50	1	6	0	0	0	0	0	0	0
KS-064	18.50	20.50	1	11	0	0	0	0	0	0	0
KS-064	20.50	23.50	1	21	0.001	0.001	0.002	0	0	0	0.5
KS-064	23.50	26.50	1	3.5	0	1	1	0	0	0	0.001
KS-064	26.50	29.50	1	6	0.001	0	0.001	0	0	0	0
KS-064	29.50	32.50	0.001	10.001	0.001	0	0.001	0	0	0	0
KS-064	32.50	35.50	2.5	7.5	0	0	0	0	0	0	0.5
KS-064	35.50	38.50	0	30	1	0	1	0	0	0	0.5
KS-064	68.65	72.00	1	11	1	0	1	0	0	0	0.001
KS-064	72.00	75.00	2.5	22.5	0	1	1	0	0	0	0
KS-064	75.00	78.00	2.5	22.5	0	0	0	0.001	0	0.001	0
KS-064	78.00	81.00	1	6	0	0.001	0.001	0	0	0	0
KS-064	81.00	84.00	0.5	5.5	0	0.001	0.001	0	0	0	0
KS-064	84.00	87.00	0	5	0	0.001	0.001	0	0	0	0.001
KS-064	87.00	90.00	0	10	0	0	0	0	0	0	0
KS-064	122.70	125.70	1	21	1	0.001	1.001	0	0	0	0
KS-064	125.70	128.70	0	5	1	0.001	1.001	0	0	0	0
KS-064	128.70	131.70	1	11	0	0.001	0.001	0	0	0	0
KS-064	131.70	134.70	1	6	0.1	0	0.1	0	0	0	0
KS-064	134.70	137.70	0	10	0	0	0	0	0	0	0
KS-064	137.70	140.70	0	10	0	0	0	0	0	0	0
KS-064	140.70	143.70	0	5	0	0	0	0	0	0	0
KS-064	173.80	176.80	2.5	7.5	0	1	1	0	0	0	0.1
KS-064	176.80	178.90	1	6	0	1	1	0	0	0	0
KS-064	178.90	180.20	0	2.5	0	1	1	0	0.001	0.001	0
KS-064	224.60	230.70	0	0	0	0	0	0	0	0	0
KS-064	230.70	239.90	0	0	0	0	0	0	0	0	0
KS-064	239.90	243.70	0	0	0	0	0	0	0	0	0
KS-064	243.70	246.00	5	15	1	2.5	3.5	0	0.001	0.001	0
KS-064	246.00	246.55	0	0	0	0	0	0	0	0	0
KS-064	246.55	249.00	0.001	0.001	0	0	0	0	0	0	0
KS-064	282.40	284.00	2.5	7.5	0	1	1	0	0	0	0
KS-064	284.00	286.00	1	6	0	1	1	0	0	0	0
KS-064	286.00	289.00	0	5	0.001	0.1	0.101	0	0	0	0
KS-064	289.00	291.20	1	11	0	1	1	0	0	0	0
KS-064	291.20	293.00	0.1	1.1	0	0	0	0	0	0	0
KS-064	293.00	294.90	1	2	0	0	0	0	0	0	0
KS-064	294.90	297.00	1	6	0	0	0	0	0	0	0
KS-064	297.00	300.60	1	6	0	0	0	0	0	0	0
KS-064	300.60	303.60	1	11	0	0	0	0	0.1	0.1	0

DDH\$	FROM metres	TO metres	MOV (%)	SLV (%)	GLV (%)	WDC (%)	JAC (%)	CCC (%)	GYLV (%)	V1 (%)	V2 (%)
KS-063	155.00	158.00	0	0	0	0	0.001	0	0	2.7	0
KS-063	158.00	161.00	0	0	0	0	0.001	0	0	2.6	0
KS-063	161.00	163.00	0	0	0	0	0	0	0	2.1	0
KS-063	163.00	165.30	0	0	0	0	0	0	0	2.9	0
KS-063	165.30	168.30	0	0	0	0	0	0	0	0	0
KS-063	168.30	171.00	0	0	0	0	0	0	0	2.7	0
KS-063	171.00	174.00	0	0	0	0	0	0	0	2.7	0
KS-063	174.00	177.00	0	0	0	0	0	0	0	1.6	0
KS-063	189.00	192.00	0	0	0	0	0.001	0	0	0.5	0
KS-063	192.00	195.00	0	0	0	0	0.001	0	0	2.7	0
KS-064	15.50	18.50	0	0	0	0	1	0	0	0	0
KS-064	18.50	20.50	0	0	0	0.001	1	0	0	0	0
KS-064	20.50	23.50	0	0	0	0	1	0.001	0	4.2	0
KS-064	23.50	26.50	0	0	0	0	1	0	0	1.6	0
KS-064	26.50	29.50	0	0	0	0	1	0	0	0.8	0
KS-064	29.50	32.50	0	0	0	0	1	0	0	0	0
KS-064	32.50	35.50	0	0	0	0	0.001	0	0	0.2	0
KS-064	35.50	38.50	0	0	0	0	2.5	0	0	0	0
KS-064	68.65	72.00	0	0	0	0	0.001	1	0	2	0
KS-064	72.00	75.00	0	0	0	0	0.001	0	0	0.8	0
KS-064	75.00	78.00	0	0	0	0	0.001	0	0	0.1	0
KS-064	78.00	81.00	0	0	0	0	0.001	0	0	0.6	0
KS-064	81.00	84.00	0	0	0	0	0	0	0	0.1	0
KS-064	84.00	87.00	0	0.001	0	0	0.001	0	0	0.6	0
KS-064	87.00	90.00	0	0	0	0	0	0	0	0	0
KS-064	122.70	125.70	0.001	0	0	0	0	0	0	0.3	0
KS-064	125.70	128.70	0	0.001	0	0	0.001	0	0	1.8	0
KS-064	128.70	131.70	0	0	0	0	0.001	0	0	0.9	0
KS-064	131.70	134.70	0.1	0	0	0	0	0	0	1.1	0
KS-064	134.70	137.70	0	0	0	0	0	0	0	0.2	0
KS-064	137.70	140.70	0	0	0	0	0	0	0	0.1	0
KS-064	140.70	143.70	0	0	0	0	0	0	0	0.8	0
KS-064	173.80	176.80	0	0	0	0	0.001	0.001	0	20	0
KS-064	176.80	178.90	0	0	0	0	0	0	0	30	0
KS-064	178.90	180.20	0	0	0	0	0	0.001	0	10	0
KS-064	224.60	230.70	0	0	0	0	0	0	0	0	0
KS-064	230.70	239.90	0	0	0	0	0	0	0	0	0
KS-064	239.90	243.70	0	0	0	0	0	0	0	0	0
KS-064	243.70	246.00	0	0	0	0	0	0	0	35	0
KS-064	246.00	246.55	0	0	0	0	0	0	0	0	0
KS-064	246.55	249.00	0	0	0	0	0	0	0	0	0
KS-064	282.40	284.00	0	1	0.001	0	0	0	0	1	2
KS-064	284.00	286.00	0	0	0	0	0.001	0	0	2.2	0
KS-064	286.00	289.00	0	0	0	0	0	0	0	0	0
KS-064	289.00	291.20	0	0	0	0	0.001	0	0	0	0
KS-064	291.20	293.00	0	0	0	0	0	0	0	0	0
KS-064	293.00	294.90	0	0	0	0	0	0	0	0	0
KS-064	294.90	297.00	0	0	0	0	0	0	0	0	0
KS-064	297.00	300.60	0	0	0	0	0	0	0	0	0
KS-064	300.60	303.60	0	0	0	0	0	0	0	0	0



DDHS	FROM metres	TO metres	V3 (%)	V4 (%)	X1 (%)	X2 (%)	X3 (%)	CLEAV	Cu:Au (%/ppm)
KS-063	155.00	158.00	0	0	0	0	2	3	0.32575
KS-063	158.00	161.00	0	0	0	0.1	1.2	3	1.22927
KS-063	161.00	163.00	0	0	0	0	0.2	3	1.81667
KS-063	163.00	165.30	0	0	0	0	2	3	2
KS-063	165.30	168.30	0	0	0	0	2.1	3	0.35714
KS-063	168.30	171.00	0	0	0	0	0.7	2	0.44835
KS-063	171.00	174.00	0	0	0	1.4	0	3	2.85
KS-063	174.00	177.00	0	0	0	0.1	1.2	3	3.75714
KS-063	189.00	192.00	0.5	0	0	0	0	3	1.53043
KS-063	192.00	195.00	1	0	0	0	0	3	3.8
KS-064	15.50	18.50	0	0	0	0.4	0	3	0.4
KS-064	18.50	20.50	0	0	0	0	0	3	0.40667
KS-064	20.50	23.50	0	0	0	0	1.5	1	1.49787
KS-064	23.50	26.50	0	0	0	0	0.6	1	2.82759
KS-064	26.50	29.50	0	0	0	0	0	3	5.02857
KS-064	29.50	32.50	0	0	0	0	0	4	2.93333
KS-064	32.50	35.50	0.4	0	0	0	0.4	5	2.61333
KS-064	35.50	38.50	0	0	0	0	0	4	2.61333
KS-064	68.65	72.00	0	0	0	0	0	4	1.67059
KS-064	72.00	75.00	0.5	0	0	0	0.8	4	0.17904
KS-064	75.00	78.00	0.2	0	0	0	0	4	2.07273
KS-064	78.00	81.00	0.6	0	0	0	0	4	1.09375
KS-064	81.00	84.00	0	0	0	0	0.6	3	1.58667
KS-064	84.00	87.00	0	0	0	0	1	4	1.455
KS-064	87.00	90.00	0	0	0	0	0.8	5	1.01111
KS-064	122.70	125.70	0.9	0	0	0	0	6	1.61
KS-064	125.70	128.70	0	0	0	0	0.4	6	0.99231
KS-064	128.70	131.70	0	0	0	0	4	7	0.42308
KS-064	131.70	134.70	0	0	0	0	0	7	1.14
KS-064	134.70	137.70	0	0	0	0	2	7	0.2
KS-064	137.70	140.70	0	0	0	0	0	7	1.63333
KS-064	140.70	143.70	0	0	0	0	0	7	0.42857
KS-064	173.80	176.80	0	0	0	0	0	7	0.98049
KS-064	176.80	178.90	0	0	0	0	0	7	1.27059
KS-064	178.90	180.20	0	0	0	0	0	7	3.375
KS-064	224.60	230.70	0	0	0	0	0	0	7.85455
KS-064	230.70	239.90	0	0	0	0	0	0	10.35
KS-064	239.90	243.70	0	0	0	0	0	0	9.41818
KS-064	243.70	246.00	0	0	0	0	0	6	4.83636
KS-064	246.00	246.55	0	0	0	0	0	0	5.92727
KS-064	246.55	249.00	0	0	0	0	1	2	0.03043
KS-064	282.40	284.00	0	3.5	0	0	0	6	0.09125
KS-064	284.00	286.00	0	0	0	3.6	0	5	1.31111
KS-064	286.00	289.00	0	0	0	0	0	5	1.76923
KS-064	289.00	291.20	0	0	0	0	0	5	1.86087
KS-064	291.20	293.00	0	0	0	0	10	2	0.14167
KS-064	293.00	294.90	0	0	0	0	5	2	0.09
KS-064	294.90	297.00	0	0	0	0	0	5	1.49286
KS-064	297.00	300.60	0	0	0	0	0	5	3.65714
KS-064	300.60	303.60	0	0	0	0	0	5	3.65714

DDHS	FROM metres	TO metres	INTRVAL	CU (%)	AU (ppm)	ZN (ppm)	PB (ppm)	AG (ppm)	RECOV (%)	ROCKS	BX
KS-066	27.30	30.50	3.2	0.548	0.25	160	15	2.0	50	PHMG	
KS-066	30.50	36.50	6	0.041	0.25	20	6	2.6	27	PHMG	
KS-066	36.50	40.50	4	0.376	0.31	160	17	6.0	70	PHMG	
KS-066	41.50	44.50	3	0.085	0.01	305	5	0.1	93	ANPP	
KS-066	44.50	46.80	2.3	0.062	0.01	274	4	0.1	100	ANPP	
KS-066	46.80	51.00	4.2	0.920	0.35	133	36	1.0	80	PHMG	
KS-066	76.20	80.20	4	0.944	0.34	184	30	2.4	39	PHPP	
KS-066	80.20	84.20	4	1.020	0.38	44	8	2.5	73	PHPP	
KS-066	84.20	86.50	2.3	1.060	0.45	60	6	2.5	48	PHPP	
KS-066	86.50	89.95	3.45	1.140	0.39	220	7	2.2	65	PHPP	
KS-066	89.95	94.20	4.25	1.660	0.54	64	13	2.5	50	PHPP	
KS-066	94.20	97.20	3	1.560	0.51	40	20	2.1	60	PHPP	
KS-066	97.20	101.75	4.55	1.130	0.44	105	7	1.5	54	PHPP	
KS-066	128.00	131.00	3	0.368	0.60	1540	224	3.4	95	PHMG	
KS-066	131.00	134.00	3	0.520	0.31	72	14	1.3	99	PHFG	
KS-066	134.00	137.00	3	0.472	0.45	2130	100	4.2	98	PHFG	
KS-066	137.00	140.00	3	0.444	0.55	830	311	3.5	97	PHFG	
KS-066	140.00	143.00	3	0.278	0.22	118	21	1.5	60	PHFG	
KS-066	143.00	146.00	3	0.267	0.21	71	13	1.0	73	PHFG	
KS-066	146.00	149.00	3	0.097	0.08	153	9	0.4	80	PHFG	
KS-066	167.00	170.00	3	0.220	0.11				98	PHMG	
KS-066	170.00	173.00	3	0.281	0.16				93	PHMG	
KS-066	173.00	176.00	3	0.209	0.10				92		
KS-066	176.00	177.10	1.1	0.173	0.12				84		
KS-067	21.30	24.30	3	0.460	0.14	73	21	2.4	94	TUFF	
KS-067	24.30	27.30	3	0.241	0.30	67	34	2.1	98	TUFF	
KS-067	27.30	31.00	3.7	0.264	0.69	103	28	1.4	97	PHFG	
KS-067	31.00	34.00	3	0.488	0.28	170	25	2.7	96	TUFF	
KS-067	34.00	37.00	3	0.472	0.15	300	46	1.4	83	TUFF	
KS-067	37.00	40.00	3	0.756	0.14	156	11	0.9	95	PHPP	
KS-067	40.00	43.00	3	0.476	0.11	65	10	0.8	97	PHPP	
KS-067	84.00	87.00	3	0.177	0.17	110	8	0.3	93	PHPP	
KS-067	87.00	90.00	3	0.066	0.06	82	7	0.2	100	PHPP	
KS-067	90.00	93.00	3	0.205	0.10	92	9	0.5	100	TUFF	
KS-067	93.00	96.00	3	0.124	0.14	83	8	0.6	90	TUFF	
KS-067	96.00	99.00	3	0.108	0.07	33	5	0.3	100	TUFF	
KS-067	99.00	102.00	3	0.089	0.08	50	1	0.2	95	TUFF	
KS-067	102.00	105.00	3	0.123	0.10	70	3	0.3	100	TUFF	
KS-067	147.00	150.00	3	1.250	0.59	360	30	3.9	95	PHMG	
KS-067	150.00	153.00	3	1.240	0.75	125	16	1.7	85	PHPP	
KS-067	153.00	156.00	3	0.964	0.69	100	13	1.3	80	PHPP	
KS-067	156.00	159.00	3	1.020	0.58	153	14	0.9	87	PHPP	
KS-067	159.00	162.00	3	0.964	0.72	69	11	1.1	93	PHPP	
KS-067	162.00	165.00	3	0.652	1.31	270	300	1.8	93	PHPP	
KS-067	165.00	168.00	3	0.592	0.55	64	21	1.5	92	PHPP	
KS-067	212.40	215.50	3.1	0.349	0.52				90	PHPP	
KS-067	215.50	218.50	3	0.608	0.30				60	PHPP	
KS-067	218.50	222.00	3.5	0.624	0.21				70	PHPP	
KS-067	222.00	225.00	3	0.848	0.31				71	PHPP	
KS-067	225.00	228.10	3.1	0.308	0.14				75	LAAP	

DDH\$	FROM metres	TO metres	FB	FX	VF	QZR (%)	QZV (%)	QZT (%)	AHR (%)	AHV (%)	AHT (%)
KS-066	27.30	30.50		20		0	5	5	0	0	0
KS-066	30.50	36.50				0	0	0	0	0	0
KS-066	36.50	40.50		25		0	0	0	0	0	0
KS-066	41.50	44.50		60		0	1	1	0	0	0
KS-066	44.50	46.80				0	1	1	0	0	0
KS-066	46.80	51.00		50		0	10	10	0	0	0
KS-066	76.20	80.20		50		0	10	10	0	0	0
KS-066	80.20	84.20				0	10	10	0	0	0
KS-066	84.20	86.50		60		0	10	10	0	0	0
KS-066	86.50	89.95				0	10	10	0	0	0
KS-066	89.95	94.20				0	10	10	0	0	0
KS-066	94.20	97.20				0	10	10	0	0	0
KS-066	97.20	101.75				0	10	10	0	0	0
KS-066	128.00	131.00		57		1	5	6	0	0	0
KS-066	131.00	134.00		32		5	1	6	0	0	0
KS-066	134.00	137.00		45		10	5	15	0	0	0
KS-066	137.00	140.00		50		5	2.5	7.5	0	0	0
KS-066	140.00	143.00		35		0	2.5	2.5	0	0	0
KS-066	143.00	146.00		60		0	2.5	2.5	0	0	0
KS-066	146.00	149.00		60		5	2.5	7.5	0	0	0
KS-066	167.00	170.00		35		0	20	20	0	0	0
KS-066	170.00	173.00		45		10	2.5	12.5	0	0	0
KS-066	173.00	176.00				0	0	0	0	0	0
KS-066	176.00	177.10				0	0	0	0	0	0
KS-067	21.30	24.30		70		5	1	6	0	0	0
KS-067	24.30	27.30		80		20	2.5	22.5	0	0	0
KS-067	27.30	31.00		59		5	2.5	7.5	0	0	0
KS-067	31.00	34.00		50		30	2.5	32.5	0	0	0
KS-067	34.00	37.00		50		30	5	35	0	0	0
KS-067	37.00	40.00		65		20	5	25	0	0	0
KS-067	40.00	43.00				5	1	6	0	0	0
KS-067	84.00	87.00		65		30	5	35	0	0	0
KS-067	87.00	90.00		56		20	0	20	0	0	0
KS-067	90.00	93.00		57		10	2.5	12.5	0	0	0
KS-067	93.00	96.00		51		10	1	11	0	0	0
KS-067	96.00	99.00		65		10	1	11	0	0	0
KS-067	99.00	102.00		55		0	2.5	2.5	0	0	0
KS-067	102.00	105.00				0	2.5	2.5	0	0	0
KS-067	147.00	150.00		61		0	5	5	0	0	0
KS-067	150.00	153.00		60		0	20	20	0	0	0
KS-067	153.00	156.00		60		0	20	20	0	0	0
KS-067	156.00	159.00		60		0	30	30	0	0	0
KS-067	159.00	162.00		62		0	40	40	0	0	0
KS-067	162.00	165.00		70		0	70	70	0	0	0
KS-067	165.00	168.00				0	60	60	0	0	0
KS-067	212.40	215.50		80		0	1	1	0	0	0
KS-067	215.50	218.50				0	1	1	0	0	0
KS-067	218.50	222.00		70		0	0	0	0	0	0
KS-067	222.00	225.00				0	0	0	0	0	0
KS-067	225.00	228.10				0	1	1	0	0	0





DDHS	FROM metres	TO metres	CLV (%)	CLT (%)	CAR (%)	CAV (%)	CAT (%)	AKR (%)	AKV (%)	AKT (%)	MGR (%)
KS-066	27.30	30.50	0	1	0	0	0	0	0	0	0
KS-066	30.50	36.50	0	0	0	0	0	0	0	0	0
KS-066	36.50	40.50	0	0	0	0	0	0	0	0	0
KS-066	41.50	44.50	1	11	0	2.5	2.5	0	0	0	0
KS-066	44.50	46.80	1	11	0	2.5	2.5	0	0	0	0
KS-066	46.80	51.00	0	0	0	0	0	0	0	0	0
KS-066	76.20	80.20	0	0.001	0	0	0	0	0	0	0
KS-066	80.20	84.20	0	10	0	0	0	0	0	0	0
KS-066	84.20	86.50	0	2.5	0	0	0	0	0	0	0
KS-066	86.50	89.95	0	10	0	0	0	0	0	0	0
KS-066	89.95	94.20	0	5	0	0	0	0	0	0	0
KS-066	94.20	97.20	0	10	0	0	0	0	0	0	0
KS-066	97.20	101.75	0	10	0	0	0	0	0	0	0
KS-066	128.00	131.00	0	0	0	1	1	0	0	0	0
KS-066	131.00	134.00	0	0	0	0.001	0.001	0	0	0	0
KS-066	134.00	137.00	0	0	0	0.001	0.001	0	0	0	0
KS-066	137.00	140.00	0	0	0	0.1	0.1	0	0	0	0
KS-066	140.00	143.00	0	0	0	0	0	0	0	0	0
KS-066	143.00	146.00	0	0	0	0	0	1	0	1	0
KS-066	146.00	149.00	0.001	0.001	0	0	0	0.001	0	0.001	0
KS-066	167.00	170.00	0	0	0	1	1	0	0	0	0
KS-066	170.00	173.00	0	0	0	1	1	0	0	0	0
KS-066	173.00	176.00	0	0	0	0	0	0	0	0	0
KS-066	176.00	177.10	0	0	0	0	0	0	0	0	0
KS-067	21.30	24.30	0	0	0	0.001	0.001	0	0	0	0
KS-067	24.30	27.30	0	0	0	0	0	0	0	0	0
KS-067	27.30	31.00	0	0	0	0.001	0.001	0	0	0	0
KS-067	31.00	34.00	2.5	2.5	0	0.001	0.001	0	0	0	0
KS-067	34.00	37.00	0	0	0	0.001	0.001	0	0	0	0
KS-067	37.00	40.00	0	0	0	1	1	0	0	0	0
KS-067	40.00	43.00	0	0	0	0	0	0	0	0	0
KS-067	84.00	87.00	0	0	0	0	0	0	0	0	0
KS-067	87.00	90.00	0	0	0	0.1	0.1	0	0	0	0
KS-067	90.00	93.00	0	0	0	0	0	0	0	0	0
KS-067	93.00	96.00	0	0	0	0	0	0	0	0	0
KS-067	96.00	99.00	0	0	0	0	0	0	0	0	0
KS-067	99.00	102.00	0	0	0	0	0	0	0	0	0
KS-067	102.00	105.00	0	0	0	0	0	0	0	0	0
KS-067	147.00	150.00	0	0	0	0	0	0	0	0	0
KS-067	150.00	153.00	0	2.5	0	0	0	0	0	0	0
KS-067	153.00	156.00	0	0	0	0.001	0.001	0	0	0	0
KS-067	156.00	159.00	10	10	2.5	0	2.5	0	0	0	0
KS-067	159.00	162.00	0.5	0.5	0	1	1	0	0	0	0
KS-067	162.00	165.00	0	0	0	0	0	0	0	0	0
KS-067	165.00	168.00	1	1	0	0	0	0	0	0	0
KS-067	212.40	215.50	0	10	0	0	0	0	0	0	0
KS-067	215.50	218.50	2.5	12.5	0	0	0	0	0	0	0
KS-067	218.50	222.00	0	0	0	0	0	0	0	0	0
KS-067	222.00	225.00	0	0	0	0	0	0	0	0	0
KS-067	225.00	228.10	2.5	42.5	0	0	0	0	0	0	0







DDHS	FROM metres	TO metres	MOV (%)	SLV (%)	GLV (%)	WDC (%)	JAC (%)	CCC (%)	GYLV (%)	V1 (%)	V2 (%)
KS-066	27.30	30.50	0	0	0	0	1	1	0	0	0
KS-066	30.50	36.50	0	0	0	0	5	0	0	0	0
KS-066	36.50	40.50	0	0	0	0	5	0	0	0	0
KS-066	41.50	44.50	0	0	0	0	0	0	0	0	0
KS-066	44.50	46.80	0	0	0	0	1	0	0	0	0
KS-066	46.80	51.00	0	0	0	0	1	2.5	0	0	0
KS-066	76.20	80.20	0	0	0	0	0	0.001	0	0	0
KS-066	80.20	84.20	0	0	0	0	0	0.001	0	0	0
KS-066	84.20	86.50	0	0	0	0	0	0.5	0	10	0
KS-066	86.50	89.95	0	0	0	0	1	1	0	0	0
KS-066	89.95	94.20	0	0	0	0	0	2.5	0	10	0
KS-066	94.20	97.20	0	0	0	0	0	2.5	0	0	0
KS-066	97.20	101.75	0	0	0	0	0	2.5	0	10	0
KS-066	128.00	131.00	0	0.1	0.001	0	0	1	0	5	0
KS-066	131.00	134.00	0	0	0	0	0	0	0	0.6	0
KS-066	134.00	137.00	0.001	0.1	0.001	0	0	0	0	3.1	0
KS-066	137.00	140.00	0	0.1	0	0	0	0	0	3	0
KS-066	140.00	143.00	0	0	0	0	0	0.5	0	0	0
KS-066	143.00	146.00	0	0	0	0	0	0.001	0	3	0
KS-066	146.00	149.00	0	0	0	0	0	0	0	1.6	0
KS-066	167.00	170.00	0	0	0	0	0	0	0	2.1	0
KS-066	170.00	173.00	0	0	0	0	0	0	0	1.2	0
KS-066	173.00	176.00	0	0	0	0	0	0	0	0	0
KS-066	176.00	177.10	0	0	0	0	0	0	0	0	0
KS-067	21.30	24.30	0	0	0	0	1	1	0	0.3	0
KS-067	24.30	27.30	0	0	0	0	1	0.5	0	0.2	0
KS-067	27.30	31.00	0	0	0	0	1	0.5	0	1.8	0
KS-067	31.00	34.00	0	0	0	0	1	0.1	0	1.8	0
KS-067	34.00	37.00	0	0	0	0	1	0	0	2.2	0
KS-067	37.00	40.00	0	0	0	0	0	0.1	0	3.4	0
KS-067	40.00	43.00	0	0	0	0	1	1	0	0.9	0
KS-067	84.00	87.00	0	0	0	0	1	0.1	0	4.5	0
KS-067	87.00	90.00	0	0	0	0	0	0	0	0.2	0
KS-067	90.00	93.00	0.001	0	0	0	0.1	0	0	1.9	0
KS-067	93.00	96.00	0	0	0	0	0.001	0	0	0.2	0
KS-067	96.00	99.00	0	0	0	0	1	0.001	0	0	0
KS-067	99.00	102.00	0	0	0	0	0.001	0	0	0	0
KS-067	102.00	105.00	0	0	0	0	1	0	0	1.1	0
KS-067	147.00	150.00	0	0	0	0	0.5	1	0	5.3	0
KS-067	150.00	153.00	0	0	0	0	0	1	0	15	0
KS-067	153.00	156.00	0	0	0	0	0	0.1	0	15	0
KS-067	156.00	159.00	0	0	0	0	1	0.1	0	30	0
KS-067	159.00	162.00	0	0	0	0	0	0.5	0	38	0
KS-067	162.00	165.00	0	0	0	0	0	0.5	0	70	0
KS-067	165.00	168.00	0	0	0	0	0	0.5	0	70	0
KS-067	212.40	215.50	0	0	0	0	2.5	0.1	0	1	0
KS-067	215.50	218.50	0	0	0	0	0	0	0	1	0
KS-067	218.50	222.00	0	0	0	0	1	0	0	0	0
KS-067	222.00	225.00	0	0	0	0	1	0.5	0	0	0
KS-067	225.00	228.10	0	0	0	0	1	0.001	0	0	0

DDHS	FROM metres	TO metres	V3 (%)	V4 (%)	X1 (%)	X2 (%)	X3 (%)	CLEAV	Cu: Au (%/ppm)
KS-066	27.30	30.50	0	0	0	0	0	7	2.192
KS-066	30.50	36.50	0	0	0	0	0	7	0.164
KS-066	36.50	40.50	0	0	0	0	0	8	1.2129
KS-066	41.50	44.50	0	0	0	0	3.1	4	8.5
KS-066	44.50	46.80	0	0	0	0	3.2	3	6.2
KS-066	46.80	51.00	0	0	0	0	0	8	2.62857
KS-066	76.20	80.20	0	0	0	0	0	7	2.77647
KS-066	80.20	84.20	0	0	0	0	0	6	2.68421
KS-066	84.20	86.50	0	0	0	0	0	7	2.35556
KS-066	86.50	89.95	0	0	0	0	0	7	2.92308
KS-066	89.95	94.20	0	0	0	0	0	6	3.07407
KS-066	94.20	97.20	0	0	0	0	0	6	3.05882
KS-066	97.20	101.75	0	0	0	0	0	6	2.56818
KS-066	128.00	131.00	1.3	0.6	0	0	0	6	0.61333
KS-066	131.00	134.00	1.3	0	0	0	0	6	1.67742
KS-066	134.00	137.00	3.9	0	0	0	0.3	7	1.04889
KS-066	137.00	140.00	4.1	0	0	0	0.4	6	0.80727
KS-066	140.00	143.00	0	0	0	0	0	6	1.26364
KS-066	143.00	146.00	2	0	0	0	0	6	1.27143
KS-066	146.00	149.00	4	0	0	0	0	6	1.2125
KS-066	167.00	170.00	1.1	0	0	0.5	0	6	2
KS-066	170.00	173.00	2.5	0	0	1	0	6	1.75625
KS-066	173.00	176.00	0	0	0	0	0	0	2.09
KS-066	176.00	177.10	0	0	0	0	0	0	1.44167
KS-067	21.30	24.30	0.8	0	0	0	0.2	5	3.28571
KS-067	24.30	27.30	1	0	0	0	1.6	7	0.80333
KS-067	27.30	31.00	2.4	0	0	0	0	6	0.38261
KS-067	31.00	34.00	2.6	0	0	0	0	5	1.74286
KS-067	34.00	37.00	1.6	0	0	0	0	5	3.14667
KS-067	37.00	40.00	0.5	0	0	0	0.2	5	5.4
KS-067	40.00	43.00	0.5	0	0	0	0	6	4.32727
KS-067	84.00	87.00	0.9	0	0	0	0.3	6	1.04118
KS-067	87.00	90.00	0.2	0	0	0.1	0	6	1.1
KS-067	90.00	93.00	0.1	0	0	0	0	7	2.05
KS-067	93.00	96.00	0.7	0	0	0	0	7	0.88571
KS-067	96.00	99.00	0.3	0	0	0	1.1	7	1.54286
KS-067	99.00	102.00	0.3	0	0	0	0.3	7	1.1125
KS-067	102.00	105.00	0.1	0	0	0	0	7	1.23
KS-067	147.00	150.00	1.3	0	0	0	0.4	6	2.11864
KS-067	150.00	153.00	5	0	0	0	0	6	1.65333
KS-067	153.00	156.00	2.5	0	0	0	0	6	1.3971
KS-067	156.00	159.00	2.5	0	0	0	0	6	1.75862
KS-067	159.00	162.00	1.6	0	0	0	0	6	1.33889
KS-067	162.00	165.00	3.2	0	0	0	0	6	0.49771
KS-067	165.00	168.00	2.5	0	0	0	0	6	1.07636
KS-067	212.40	215.50	0	0	0	0	0	7	0.67115
KS-067	215.50	218.50	0	0	0	0	0	6	2.02667
KS-067	218.50	222.00	0	0	0	0	0	7	2.97143
KS-067	222.00	225.00	0	0	0	0	0	7	2.73548
KS-067	225.00	228.10	0	0	0	0	0	2	2.2

DDH\$	FROM metres	TO metres	INTRVAL	CU (%)	AU (ppm)	ZN (ppm)	PB (ppm)	AG (ppm)	RECOV (%)	ROCKS	BX
KS-067	228.10	231.00	2.9	0.544	0.21				76	PHPP	
KS-067	231.00	234.00	3	0.303	0.17				85	PHPP	
KS-067	246.00	249.00	3	0.370	0.66				100	PHPP	
KS-067	249.00	252.00	3	0.330	0.38				93	PHPP	
KS-067	252.00	256.30	4.3	0.151	0.16				98	PHPP	
KS-094	7.00	10.15	3.15	0.532	0.22				91	PHFG	
KS-094	16.00	19.00	3	0.038	0.14				87	LAPP	
KS-094	19.00	21.90	2.9	0.056	0.31				79	LAPP	
KS-094	21.90	25.00	3.1	0.680	1.81				91	TUFF	
KS-094	25.00	28.40	3.4	0.712	0.54				76	TUFF	
KS-094	28.40	31.00	2.6	0.996	0.26				92	PHFG	
KS-094	31.00	34.00	3	0.332	0.10				97	PHFG	
KS-094	34.00	37.00	3	0.568	0.18				94	PHFG	
KS-094	69.00	72.00	3	0.216	0.15				98	PHPP	
KS-094	72.00	74.10	2.1	0.376	0.17				100	PHPP	
KS-094	74.10	75.80	1.7	0.512	0.17				68	PHPP	
KS-094	75.80	76.90	1.1	0.025	0.05				100	LAPP	
KS-094	76.90	79.70	2.8	0.136	0.15				93	PHPP	
KS-094	79.70	83.00	3.3	0.284	0.13				77	PHPP	
KS-094	83.00	87.50	4.5	0.332	0.19				73	TFLP	
KS-094	87.50	90.30	2.8	0.036	0.07				82	LAPP	
KS-094	116.50	119.50	3	0.232	0.73				84	TFLP	
KS-094	119.50	121.10	1.6	0.130	0.39				75	PHPP	
KS-094	121.10	122.60	1.5	0.103	0.83				57	BNDK	
KS-094	122.60	125.50	2.9	0.235	0.66				92	TUFF	
KS-094	125.50	128.50	3	0.183	0.13				98	PHFG	
KS-094	128.50	131.50	3	0.055	0.05				97	TFLP	40
KS-094	131.50	134.50	3	0.137	0.06				92	TFLP	
KS-094	134.50	137.50	3	0.089	0.04				93	TFLP	
KS-094	167.00	170.00	3	0.085	0.29				89	TFLP	
KS-094	170.00	173.00	3	0.050	0.16				90	TFLP	
KS-094	173.00	176.00	3	0.050	0.12				93	TFLP	
KS-094	176.00	179.00	3	0.034	0.08				95	PHMG	
KS-094	179.00	182.00	3	0.029	0.07				100	PHMG	
KS-094	182.00	183.00	3	0.064	0.11				90	PHMG	
KS-094	185.00	188.00	3	0.129	0.11				98	PHMG	
KS-094	216.40	219.20	2.8	0.308	3.40				84	PHMG	
KS-094	219.20	219.90	0.7	0.048	0.10				86	ANDY	
KS-094	219.90	223.00	3.1	0.151	0.15				98	PHMG	
KS-094	223.00	226.00	3	0.050	0.07				92	PHMG	
KS-094	226.00	229.00	3	0.073	0.14				100	PHMG	
KS-094	229.00	232.00	3	0.051	0.08				93	PHMG	
KS-094	232.00	235.50	3.5	0.052	0.07				100	PHMG	
KS-094	235.50	238.50	3	0.328	0.14				70	PHMG	
KS-094	267.50	270.00	2.5	1.090	0.59				97	PHPP	
KS-094	270.00	273.00	3	1.090	0.54				90	PHPP	
KS-094	273.00	276.00	3	1.700	0.79				90	PHPP	
KS-094	276.00	279.50	3.5	1.170	0.53				46	PHPP	
KS-094	279.50	282.50	3	1.820	1.05				70	PHPP	
KS-094	282.50	285.60	3.1	1.460	0.71				95	PHPP	

DDHS	FROM metres	TO metres	FB	FX	VF	QZR (%)	QZV (%)	QZT (%)	AHR (%)	AHV (%)	AHT (%)
KS-067	228.10	231.00				0	1	1	0	0	0
KS-067	231.00	234.00		75		0	0	0	0	0	0
KS-067	246.00	249.00		75		0	10	10	0	0	0
KS-067	249.00	252.00		70		0	10	10	0	0	0
KS-067	252.00	256.30		70		2.5	10	12.5	0	0	0
KS-094	7.00	10.15		50		5	2.5	7.5	0	0	0
KS-094	16.00	19.00				0	0	0	0	0	0
KS-094	19.00	21.90				0	0	0	0	0	0
KS-094	21.90	25.00		5		5	5	10	0	0	0
KS-094	25.00	28.40				20	2.5	22.5	0	0	0
KS-094	28.40	31.00		5		20	5	25	0	0	0
KS-094	31.00	34.00				30	1	31	0	0	0
KS-094	34.00	37.00		15		10	2.5	12.5	0	0	0
KS-094	69.00	72.00		30		10	1	11	0	0	0
KS-094	72.00	74.10		20		20	2.5	22.5	0	0	0
KS-094	74.10	75.80		35		1	0	1	0	0	0
KS-094	75.80	76.90		16		0	0	0	0	0	0
KS-094	76.90	79.70		30		10	1	11	0	0	0
KS-094	79.70	83.00		30		30	1	31	0	0	0
KS-094	83.00	87.50		25		10	1	11	0	0	0
KS-094	87.50	90.30		30		0	0.1	0.1	0	0	0
KS-094	116.50	119.50		15		10	1	11	0	0	0
KS-094	119.50	121.10		10		5	1	6	0	0	0
KS-094	121.10	122.60		10		0	0	0	0	0	0
KS-094	122.60	125.50		10		5	1	6	0	0	0
KS-094	125.50	128.50		15		10	1	11	0	0	0
KS-094	128.50	131.50	5	35		0	0	0	0	0	0
KS-094	131.50	134.50		21		0	0	0	0	0	0
KS-094	134.50	137.50		25		0	0	0	0	0	0
KS-094	167.00	170.00		35		0	0	0	0	0	0
KS-094	170.00	173.00		30		0	0	0	0	0	0
KS-094	173.00	176.00		45		0	1	1	0	0	0
KS-094	176.00	179.00		40		0	0	0	0	0	0
KS-094	179.00	182.00		35		0	0	0	0	0	0
KS-094	182.00	185.00		50		0	0	0	0	0	0
KS-094	185.00	188.00		35		0	0.1	0.1	0	0	0
KS-094	216.40	219.20		35		0	0	0	0	0	0
KS-094	219.20	219.90				0	0	0	0	0	0
KS-094	219.90	223.00		40		0	0.5	0.5	0	0	0
KS-094	223.00	226.00		20		0	1	1	0	0	0
KS-094	226.00	229.00		30		0	1	1	0	0	0
KS-094	229.00	232.00		30		0	0	0	0	0	0
KS-094	232.00	235.50		37		0	0	0	0	0	0
KS-094	235.50	238.50				0	0	0	0	0	0
KS-094	267.50	270.00		55		0	30	30	0	0	0
KS-094	270.00	273.00		50		0	40	40	0	0	0
KS-094	273.00	276.00		50		0	40	40	0	0	0
KS-094	276.00	279.50		35		0	30	30	0	0	0
KS-094	279.50	282.50		65		0	60	60	0	0	0
KS-094	282.50	285.60		60		0	30	30	0	0	0

DDH\$	FROM metres	TO metres	GYR (%)	GYV (%)	GYT (%)	AHGYT (%)	SER (%)	SEV (%)	SET (%)	YSR (%)	YSV (%)
KS-067	228.10	231.00	0	0	0	0	40	0	40	0	0
KS-067	231.00	234.00	0	0	0	0	40	0	40	0	0
KS-067	246.00	249.00	0	0	0	0	20	0	20	20	0
KS-067	249.00	252.00	0	0	0	0	10	0	10	30	0
KS-067	252.00	256.30	0	0	0	0	10	0	10	30	0
KS-094	7.00	10.15	0	0	0	0	30	0	30	0	0
KS-094	16.00	19.00	0	0	0	0	20	0	20	0	0
KS-094	19.00	21.90	0	0	0	0	30	0	30	0	0
KS-094	21.90	25.00	0	0	0	0	10	0	10	0	0
KS-094	25.00	28.40	0	0	0	0	10	0	10	0	0
KS-094	28.40	31.00	0	0	0	0	30	0	30	0	0
KS-094	31.00	34.00	0	0	0	0	10	0	10	0	0
KS-094	34.00	37.00	0	0	0	0	20	0	20	0	0
KS-094	69.00	72.00	0	0	0	0	30	0	30	0	0
KS-094	72.00	74.10	0	0	0	0	30	0	30	0	0
KS-094	74.10	75.80	0	0	0	0	30	0	30	0	0
KS-094	75.80	76.90	0	0	0	0	30	0	30	0	0
KS-094	76.90	79.70	0	0	0	0	30	0	30	0	0
KS-094	79.70	83.00	0	0	0	0	30	0	30	0	0
KS-094	83.00	87.50	0	0	0	0	30	0	30	0	0
KS-094	87.50	90.30	0	0	0	0	30	0	30	0	0
KS-094	116.50	119.50	0	0	0	0	30	0	30	0	0
KS-094	119.50	121.10	0	0	0	0	30	0	30	0	0
KS-094	121.10	122.60	0	0	0	0	10	0	10	0	0
KS-094	122.60	125.50	0	0	0	0	30	0	30	0	0
KS-094	125.50	128.50	0	0	0	0	30	0	30	0	0
KS-094	128.50	131.50	0	0	0	0	40	0	40	0	0
KS-094	131.50	134.50	0	0	0	0	40	0	40	0	0
KS-094	134.50	137.50	0	0	0	0	40	0	40	0	0
KS-094	167.00	170.00	0	0	0	0	40	0	40	0	0
KS-094	170.00	173.00	0	0	0	0	40	0	40	0	0
KS-094	173.00	176.00	0	0	0	0	40	0	40	0	0
KS-094	176.00	179.00	0	0	0	0	40	0	40	0	0
KS-094	179.00	182.00	0	0	0	0	40	0	40	0	0
KS-094	182.00	185.00	0	0	0	0	40	0	40	0	0
KS-094	185.00	188.00	0	0	0	0	40	0	40	0	0
KS-094	216.40	219.20	0	0	0	0	40	0	40	0	0
KS-094	219.20	219.90	0	0	0	0	0	0	0	0	0
KS-094	219.90	223.00	0	0	0	0	40	0	40	0	0
KS-094	223.00	226.00	0	0	0	0	40	0	40	0	0
KS-094	226.00	229.00	0	0	0	0	40	0	40	0	0
KS-094	229.00	232.00	0	0	0	0	40	0	40	0	0
KS-094	232.00	235.50	0	0	0	0	40	0	40	0	0
KS-094	235.50	238.50	0	0	0	0	40	0	40	0	0
KS-094	267.50	270.00	0	0	0	0	40	0	40	0	0
KS-094	270.00	273.00	0	0	0	0	40	0	40	0	0
KS-094	273.00	276.00	0	0	0	0	40	0	40	0	0
KS-094	276.00	279.50	0	0	0	0	20	10	30	0	0
KS-094	279.50	282.50	0	0	0	0	20	0	20	0	0
KS-094	282.50	285.60	0	0	0	0	30	0	30	0	0

DDHS	FROM metres	TO metres	YST (%)	GSR (%)	GSV (%)	GST (%)	SYGST (%)	KAR (%)	KAV (%)	KAT (%)	CLR (%)
KS-067	228.10	231.00	0	0	0	0	40	0	1	1	0
KS-067	231.00	234.00	0	0	0	0	40	0	0	0	0
KS-067	246.00	249.00	20	0	0	0	40	0	0	0	0
KS-067	249.00	252.00	30	0.001	0	0.001	40.001	0	0	0	0
KS-067	252.00	256.30	30	0.1	0	0.1	40.1	0	0	0	0
KS-094	7.00	10.15	0	0	0	0	30	10	0	10	5
KS-094	16.00	19.00	0	0	0	0	20	20	0	20	10
KS-094	19.00	21.90	0	0	0	0	30	20	0	20	10
KS-094	21.90	25.00	0	0	0	0	10	0	0	0	10
KS-094	25.00	28.40	0	0	0	0	10	10	1	11	2.5
KS-094	28.40	31.00	0	0	0	0	30	0	0	0	5
KS-094	31.00	34.00	0	0	0	0	10	2.5	0	2.5	20
KS-094	34.00	37.00	0	0	0	0	20	5	0	5	10
KS-094	69.00	72.00	0	0	0	0	30	5	0	5	0
KS-094	72.00	74.10	0	0	0	0	30	2.5	0	2.5	0
KS-094	74.10	75.80	0	0	0	0	30	10	0.1	10.1	0
KS-094	75.80	76.90	0	0	0	0	30	10	0.001	10.001	0
KS-094	76.90	79.70	0	0	0	0	30	0.001	0	0.001	0
KS-094	79.70	83.00	0	0	0	0	30	0	0	0	0
KS-094	83.00	87.50	0	0	0	0	30	0	0	0	0
KS-094	87.50	90.30	0	10	0	10	40	10	0	10	2.5
KS-094	116.50	119.50	0	0	0	0	30	10	0	10	5
KS-094	119.50	121.10	0	0	0	0	30	5	0	5	5
KS-094	121.10	122.60	0	20	0	20	30	10	0	10	5
KS-094	122.60	125.50	0	0	0	0	30	10	0	10	0
KS-094	125.50	128.50	0	0	0	0	30	2.5	0.5	3	0
KS-094	128.50	131.50	0	0	0	0	40	5	0	5	0
KS-094	131.50	134.50	0	0	0	0	40	5	0	5	0
KS-094	134.50	137.50	0	0	0	0	40	0	0	0	0
KS-094	167.00	170.00	0	0	0	0	40	2.5	0	2.5	0
KS-094	170.00	173.00	0	0	0	0	40	2.5	0	2.5	0
KS-094	173.00	176.00	0	0	0	0	40	2.5	0	2.5	0
KS-094	176.00	179.00	0	0	0	0	40	2.5	0	2.5	0
KS-094	179.00	182.00	0	0	0	0	40	2.5	0	2.5	0
KS-094	182.00	185.00	0	0	0	0	40	2.5	0	2.5	0
KS-094	185.00	188.00	0	0	0	0	40	10	0	10	0
KS-094	216.40	219.20	0	0	0	0	40	2.5	0	2.5	0
KS-094	219.20	219.90	0	0	0	0	0	0	0	0	0
KS-094	219.90	223.00	0	0	0	0	40	2.5	0	2.5	0
KS-094	223.00	226.00	0	0	0	0	40	2.5	0	2.5	0
KS-094	226.00	229.00	0	0	0	0	40	2.5	0	2.5	0
KS-094	229.00	232.00	0	0	0	0	40	5	0	5	0
KS-094	232.00	235.50	0	10	0	10	50	0	0	0	0
KS-094	235.50	238.50	0	10	0	10	50	0	0	0	0
KS-094	267.50	270.00	0	0	0	0	40	0	0.001	0.001	1
KS-094	270.00	273.00	0	0	0	0	40	0	0	0	1
KS-094	273.00	276.00	0	0	0	0	40	0	0	0	1
KS-094	276.00	279.50	0	10	0	10	40	0	0	0	30
KS-094	279.50	282.50	0	2.5	0	2.5	22.5	0	0.001	0.001	1
KS-094	282.50	285.60	0	1	0	1	31	0	0	0	2.5

DDHS	FROM metres	TO metres	CLV (%)	CLT (%)	CAR (%)	CAV (%)	CAT (%)	AKR (%)	AKV (%)	AKT (%)	MGR (%)
KS-067	228.10	231.00	0	0	0	0	0	0	0	0	0
KS-067	231.00	234.00	0	0	0	0	0	0	0	0	0
KS-067	246.00	249.00	0	0	0	1	1	0	0	0	0
KS-067	249.00	252.00	0	0	0	1	1	0	0	0	0
KS-067	252.00	256.30	0	0	0	1	1	0	0	0	0
KS-094	7.00	10.15	1	6	0	0	0	0	0	0	0
KS-094	16.00	19.00	1	11	0	1	1	0	0	0	0
KS-094	19.00	21.90	1	11	0	0	0	0	0	0	0
KS-094	21.90	25.00	1	11	0	0	0	0	0	0	0
KS-094	25.00	28.40	1	3.5	0	0	0	0	0	0	0
KS-094	28.40	31.00	1	6	0	0	0	0	0	0	0
KS-094	31.00	34.00	0	20	0	0	0	0	0	0	0
KS-094	34.00	37.00	1	11	0	0	0	0	0	0	0
KS-094	69.00	72.00	0	0	0	0.001	0.001	0	0	0	0
KS-094	72.00	74.10	0	0	0	1	1	0	0	0	0
KS-094	74.10	75.80	0	0	0	0	0	0	0	0	0
KS-094	75.80	76.90	0	0	0	0	0	0	0	0	0
KS-094	76.90	79.70	0	0	0	0	0	0	0	0	0
KS-094	79.70	83.00	0	0	0	0	0	0	0	0	0
KS-094	83.00	87.50	0	0	0	0.001	0.001	0	0	0	0
KS-094	87.50	90.30	0	2.5	0	1	1	0	0	0	0
KS-094	116.50	119.50	1	6	0	0	0	0	0	0	0
KS-094	119.50	121.10	0	5	0	0	0	0	0	0	0
KS-094	121.10	122.60	0	5	0	1	1	0	0	0	0
KS-094	122.60	125.50	1	1	0	0	0	0	0	0	0
KS-094	125.50	128.50	1	1	0	0	0	0	0	0	0
KS-094	128.50	131.50	0	0	0	0.5	0.5	0	0	0	0
KS-094	131.50	134.50	0	0	1	1	2	0	0	0	0
KS-094	134.50	137.50	0	0	1	1	2	0	0	0	0
KS-094	167.00	170.00	0	0	0	1	1	0	0	0	0
KS-094	170.00	173.00	0	0	0	0	0	0	0	0	0
KS-094	173.00	176.00	0	0	0	1	1	0	0	0	0
KS-094	176.00	179.00	0	0	0	1	1	0	0	0	0
KS-094	179.00	182.00	0	0	0	1	1	0	0	0	0
KS-094	182.00	185.00	0	0	0	1	1	0	0	0	0
KS-094	185.00	188.00	0	0	0	0.5	0.5	0	0	0	0
KS-094	216.40	219.20	0	0	0	1	1	0	0	0	0
KS-094	219.20	219.90	0	0	5	0	5	0	0	0	10
KS-094	219.90	223.00	0	0	0	0.5	0.5	0	0	0	0
KS-094	223.00	226.00	0	0	0	1	1	0	0	0	0
KS-094	226.00	229.00	0	0	0	1	1	0	0	0	0
KS-094	229.00	232.00	0	0	0	1	1	0	0	0	0
KS-094	232.00	235.50	0	0	0	0	0	0	0	0	0
KS-094	235.50	238.50	2.5	2.5	0	0	0	0	0	0	0
KS-094	267.50	270.00	0	1	0	1	1	0	0	0	0
KS-094	270.00	273.00	0	1	0	0.001	0.001	0	0	0	0
KS-094	273.00	276.00	0	1	0	1	1	0	0	0	0
KS-094	276.00	279.50	1	31	0	1	1	0	0	0	0
KS-094	279.50	282.50	0	1	0	1	1	0	0	0	0
KS-094	282.50	285.60	0	2.5	0	0	0	0	0	0	0





DDHS	FROM metres	TO metres	PYV (%)	PYT (%)	CPR (%)	CPV (%)	CPT (%)	TTR (%)	TTV (%)	TTT (%)	BOV (%)
KS-067	228.10	231.00	1	11	0	0	0	0	0	0	0
KS-067	231.00	234.00	1	6	0	0	0	0	0	0	0
KS-067	246.00	249.00	2.5	12.5	1	1	2	0	0	0	0
KS-067	249.00	252.00	1	11	0	1	1	0	0	0	0
KS-067	252.00	256.30	2.5	12.5	0	0	0	0	0.1	0.1	0
KS-094	7.00	10.15	2.5	7.5	0	0	0	0	0	0	0.1
KS-094	16.00	19.00	0	1	0	0	0	0	0	0	0
KS-094	19.00	21.90	0	5	0	0	0	0	0	0	0
KS-094	21.90	25.00	1	3.5	0	0	0	0	0	0	0.5
KS-094	25.00	28.40	1	6	0	0.5	0.5	0	0	0	1
KS-094	28.40	31.00	2.5	7.5	1	0.5	1.5	0	0	0	0.5
KS-094	31.00	34.00	2.5	3.5	0	1	1	0	0	0	0
KS-094	34.00	37.00	2.5	3.5	1	0	1	0	0	0	0
KS-094	69.00	72.00	2.5	12.5	0	0.001	0.001	0	0	0	0
KS-094	72.00	74.10	2.5	12.5	0	0	0	0	0	0	0
KS-094	74.10	75.80	1	11	1	0	1	0	0	0	0
KS-094	75.80	76.90	0	5	0	0	0	0	0	0	0
KS-094	76.90	79.70	0	10	0.001	0	0.001	0	0	0	0
KS-094	79.70	83.00	0	10	0.001	0	0.001	0	0	0	0
KS-094	83.00	87.50	0.5	10.5	0	0.1	0.1	0	0	0	0
KS-094	87.50	90.30	0	5	0	0	0	0	0	0	0
KS-094	116.50	119.50	2.5	3.5	0	0.001	0.001	0	0	0	0
KS-094	119.50	121.10	0	2.5	0.1	0	0.1	0	0	0	0
KS-094	121.10	122.60	0	2.5	0	0	0	0	0	0	0
KS-094	122.60	125.50	0.5	10.5	1	0.1	1.1	0	0	0	0
KS-094	125.50	128.50	1	11	0.1	0	0.1	0	0	0	0
KS-094	128.50	131.50	0.5	10.5	0.5	0	0.5	0	0	0	0
KS-094	131.50	134.50	0.1	10.1	0	0	0	0	0	0	0
KS-094	134.50	137.50	0	10	0	0	0	0	0	0	0
KS-094	167.00	170.00	0.1	10.1	0	0	0	0	0	0	0
KS-094	170.00	173.00	0.5	10.5	0	0.001	0.001	0	0	0	0
KS-094	173.00	176.00	0.5	10.5	0	0	0	0	0	0	0
KS-094	176.00	179.00	0	10	0	0	0	0	0	0	0
KS-094	179.00	182.00	0	10	0	0	0	0	0	0	0
KS-094	182.00	185.00	0	10	0	0	0	0	0	0	0
KS-094	185.00	188.00	0	10	0	0	0	0	0	0	0
KS-094	216.40	219.20	2.5	5	0	0.5	0.5	0	0	0	0
KS-094	219.20	219.90	0	0	0	0	0	0	0	0	0
KS-094	219.90	223.00	1	11	0	0.1	0.1	0	0	0	0
KS-094	223.00	226.00	1	3.5	0	0.001	0.001	0	0	0	0
KS-094	226.00	229.00	1	3.5	0	0	0	0	0	0	0
KS-094	229.00	232.00	1	6	0.001	0	0.001	0	0	0	0
KS-094	232.00	235.50	1	3.5	0	0	0	0	0	0	0
KS-094	235.50	238.50	1	6	0	0	0	0	0	0	0
KS-094	267.50	270.00	10	20	0.001	2.5	2.501	0	0	0	0
KS-094	270.00	273.00	10	30	1	2.5	3.5	0	0	0	0
KS-094	273.00	276.00	10	30	1	2.5	3.5	0	0	0	0
KS-094	276.00	279.50	2.5	12.5	1	1	2	0	0	0	0
KS-094	279.50	282.50	10	15	0	2.5	2.5	0	0	0	0
KS-094	282.50	285.60	10	20	1	2.5	3.5	0	0	0	0

DDH\$	FROM metres	TO metres	MOV (%)	SLV (%)	GLV (%)	WDC (%)	JAC (%)	CCC (%)	GYLV (%)	V1 (%)	V2 (%)
KS-067	228.10	231.00	0	0	0	0	0	0.5	0	0	0
KS-067	231.00	234.00	0	0	0	0	2.5	0.5	0	0	0
KS-067	246.00	249.00	0	0.5	0.1	0	0	0	0	3.1	0
KS-067	249.00	252.00	0.001	0.1	0	0	0	0	0	3.1	0
KS-067	252.00	256.30	0	0	0.001	0	0	0	0	4	0
KS-094	7.00	10.15	0	0	0	0	2.5	1	0	1.5	0
KS-094	16.00	19.00	0	0	0	0	1	0	0	0	0
KS-094	19.00	21.90	0	0	0	0	1	0	0	0	0
KS-094	21.90	25.00	0	0	0	0	1	0.001	0	2.2	0
KS-094	25.00	28.40	0	0	0	0	1	0.001	0	1.2	0
KS-094	28.40	31.00	0	0	0	0	1	0.001	0	4.2	0
KS-094	31.00	34.00	0	0	0	0	1	0	0	0.4	0
KS-094	34.00	37.00	0	0	0	0	1	0	0	1.5	0
KS-094	69.00	72.00	0	0	0	0	0.001	0	0	0.3	0
KS-094	72.00	74.10	0	0	0	0	0.001	0	0	0.8	0
KS-094	74.10	75.80	0	0	0	0	0	0.1	0	1	0
KS-094	75.80	76.90	0	0	0	0	1	0	0	0	0
KS-094	76.90	79.70	0	0	0	0	0	0.1	0	0	0
KS-094	79.70	83.00	0	0.001	0	0	0.001	0.1	0	0.2	0
KS-094	83.00	87.50	0	0	0	0	0.001	0.1	0	1	0
KS-094	87.50	90.30	0	0	0	0	0.001	0	0	0	0
KS-094	116.50	119.50	0	0	0	0	1	0	0	0	0
KS-094	119.50	121.10	0	0	0	0	0.1	0	0	0	0
KS-094	121.10	122.60	0	0	0	0	1	0	0	0	0
KS-094	122.60	125.50	0.001	0	0	0	0.001	0	0	0.1	0
KS-094	125.50	128.50	0.001	0	0	0	0	0	0	0.6	0
KS-094	128.50	131.50	0.001	0	0	0	0	0	0	0	0
KS-094	131.50	134.50	0.1	0	0	0	0	0	0	0.6	0
KS-094	134.50	137.50	0.001	0	0	0	1	0	0	0.1	0
KS-094	167.00	170.00	0	0	0	0	0	0	0	0	0
KS-094	170.00	173.00	0	0	0	0	0	0	0	0	0
KS-094	173.00	176.00	0	0	0	0	0	0	0	0	0
KS-094	176.00	179.00	0	0.1	0	0	0	0	0	0	0
KS-094	179.00	182.00	0	0	0	0	0	0	0	0	0
KS-094	182.00	185.00	0	0	0	0	0	0	0	0	0
KS-094	185.00	188.00	0	0	0	0	0	0	0	0	0
KS-094	216.40	219.20	0	0	0.001	0	0	0	0	0	0
KS-094	219.20	219.90	0	0	0	0	0	0	0	0	0
KS-094	219.90	223.00	0	0	0.001	0	0	0	0	0	0
KS-094	223.00	226.00	0	0	0	0	0	0	0	0	0
KS-094	226.00	229.00	0	0	0	0	0	0	0	0	0
KS-094	229.00	232.00	0	0	0	0	0	0	0	0	0
KS-094	232.00	235.50	0	0	0	0	0	0	0	0.2	0
KS-094	235.50	238.50	0	0	0	0	0	0	0	0	0
KS-094	267.50	270.00	0	0	0	0	0	0	0	30	0
KS-094	270.00	273.00	0	0	0	0	0	0	0	45	0
KS-094	273.00	276.00	0	0	0	0	0	0	0	40	0
KS-094	276.00	279.50	0	0	0	0	0	0	0	30	0
KS-094	279.50	282.50	0	0	0	0	0	0	0	60	0
KS-094	282.50	285.60	0	0	0	0	0.001	0	0	30	0

DDHS	FROM metres	TO metres	V3 (%)	V4 (%)	X1 (%)	X2 (%)	X3 (%)	CLEAV	Cu:Au (%/ppm)
KS-067	228.10	231.00	0	0	0	0	0	7	2.59048
KS-067	231.00	234.00	2.5	0	0	0	0	7	1.78235
KS-067	246.00	249.00	1.9	8.7	0	0	0	7	0.56061
KS-067	249.00	252.00	1.1	0	0	0	0	6	0.86842
KS-067	252.00	256.30	3.5	0	0	0.2	0	6	0.94375
KS-094	7.00	10.15	1.1	0	0	0	0.2	3	2.41818
KS-094	16.00	19.00	0	0	0	0	16	1	0.27143
KS-094	19.00	21.90	0	0	0	0	0	0	0.18065
KS-094	21.90	25.00	0.8	0	0	0	2.5	2	0.37569
KS-094	25.00	28.40	0.7	0	0	0	0.9	1	1.31852
KS-094	28.40	31.00	0.6	0	0	0	2.7	2	3.83077
KS-094	31.00	34.00	0.9	0	0	0	0.5	2	3.32
KS-094	34.00	37.00	1.1	0	0	0	0.2	2	3.15556
KS-094	69.00	72.00	1.1	0	0	0	0.2	4	1.44
KS-094	72.00	74.10	1.2	0	0	0	0.2	4	2.21176
KS-094	74.10	75.80	1	0	0	0	0	5	3.01176
KS-094	75.80	76.90	0	0	0	0	0	5	0.5
KS-094	76.90	79.70	0	0	0	0.4	0	5	0.90667
KS-094	79.70	83.00	0	0	0	0	0.2	5	2.18462
KS-094	83.00	87.50	0.1	0	0	0	0	5	1.74737
KS-094	87.50	90.30	0	0	0	0	0.5	3	0.51429
KS-094	116.50	119.50	0.1	0	0	0	2.5	5	0.31781
KS-094	119.50	121.10	0	0	0	0	1.3	5	0.33333
KS-094	121.10	122.60	0	0	0	0	0	2	0.1241
KS-094	122.60	125.50	0.3	0	0	0	1.8	4	0.35606
KS-094	125.50	128.50	0.3	0	0	0	0.9	5	1.40769
KS-094	128.50	131.50	0.3	0	0	0	0.2	7	1.1
KS-094	131.50	134.50	0	0	0	0	0.3	7	2.28333
KS-094	134.50	137.50	0	0	0	0	0	7	2.225
KS-094	167.00	170.00	0	0	0	0.3	0	7	0.2931
KS-094	170.00	173.00	0	0	0	0	0	7	0.3125
KS-094	173.00	176.00	0	0	0	0	1	7	0.41667
KS-094	176.00	179.00	0.3	0	0	0	1.2	7	0.425
KS-094	179.00	182.00	0	0	0	0	0.9	7	0.41429
KS-094	182.00	185.00	0	0	0	0	0	7	0.58182
KS-094	185.00	188.00	0	0	0	0	0	7	1.17273
KS-094	216.40	219.20	2.8	0.2	0	0	0	7	0.09059
KS-094	219.20	219.90	0	0	0	0	0	0	0.48
KS-094	219.90	223.00	1	0	0	0.2	0	7	1.00667
KS-094	223.00	226.00	1.2	0	0	0	0	7	0.71429
KS-094	226.00	229.00	0	0	0	2	0	7	0.52143
KS-094	229.00	232.00	0	0	0	0	0.8	8	0.6375
KS-094	232.00	235.50	0.6	0	0	0	0.4	7	0.74286
KS-094	235.50	238.50	0	0	0	0	0	7	2.34286
KS-094	267.50	270.00	0	0	0	7	0	6	1.84746
KS-094	270.00	273.00	0	0	0	4	0	6	2.01852
KS-094	273.00	276.00	0	0	0	10	0	6	2.1519
KS-094	276.00	279.50	0	0	0	0	0	6	2.20755
KS-094	279.50	282.50	0	0	0	0	0	6	1.73333
KS-094	282.50	285.60	0	0	0	0	0	6	2.05634

DDHS	FROM metres	TO metres	INTRVAL	CU (%)	AU (ppm)	ZN (ppm)	PB (ppm)	AG (ppm)	RECOV (%)	ROCK\$	BX
KS-094	285.60	287.30	1.7	1.450	0.74				88	PHPP	
KS-094	317.00	318.50	1.5	0.860	0.31				100	PHPP	
KS-094	318.50	320.00	1.5	0.860	0.31				100	PHPP	
KS-094	320.00	323.00	3	1.130	0.32				100	PHPP	
KS-094	323.00	325.00	2	1.130	1.16				93	PHPP	
KS-094	325.00	328.00	3	1.150	0.35				93	PHMG	
KS-094	328.00	331.00	3	1.230	0.32				98	PHMG	
KS-094	331.00	334.00	3	1.000	0.44				97	PHMG	
KS-094	334.00	337.00	3	1.020	0.33				98	PHMG	
KS-094	366.30	369.00	2.7	0.644	0.22				100	PHPP	
KS-094	369.00	372.00	3	0.604	0.19				95	PHPP	
KS-094	372.00	375.00	3	0.436	0.13				95	TFLP	
KS-094	375.00	378.00	3	0.752	0.13				100	TFLP	
KS-094	378.00	382.30	4.3	0.680	0.24				98	PHPP	
KS-094	382.30	385.20	2.9	0.109	0.04				98	LAAP	
KS-094	385.20	387.60	2.4	0.536	0.16				92	PHPP	
87-4	3.30	4.90	1.6	0.008	0.005	156		0.1	22	LAAP	
87-4	4.90	6.00	1.1	0.016	0.005	36		0.4	54	PHFG	
87-4	6.00	8.00	2	0.148	0.22	261		1.3	96	PHFG	
87-4	8.00	10.40	2.4	0.037	0.10	39		0.8	44	PHFG	
87-4	10.40	11.90	1.5	0.072	0.005	46		0.7	88	PHFG	
87-4	11.90	13.40	1.5	0.146	0.005	217		1.0	86	PHFG	
87-4	13.40	14.90	1.5	0.151	0.005	133		0.1	99	PHFG	
87-4	73.40	75.40	2	0.057	0.13	584		2.8	80	PHFG	
87-4	75.40	76.60	1.2	0.106	0.06	400		3.4	84	PHFG	
87-4	76.60	77.80	1.2	0.114	0.005	514		4.1	91	PHFG	
87-4	77.80	79.80	2	0.049	0.005	179		1.4	91	PHFG	
87-4	79.80	81.80	2	0.031	0.005	225		0.4	84	PHFG	70
87-4	81.80	83.80	2	0.053	0.005	282		0.7	96	FRAG	60
87-4	83.80	85.80	2	0.069	0.005	156		0.9	93	FRAG	
87-4	85.80	87.80	2	0.033	0.005	107		0.1	100	PHFG	
87-4	87.80	89.80	2	0.017	0.005	134		0.1	100	FRAG	
87-4	89.80	91.80	2	0.023	0.005	188		0.1	100	FRAG	
87-4	91.80	93.30	1.5	0.023	0.005	256		0.1	90	TFAH	

DDHS	FROM metres	TO metres	FB	FX	VF	QZR (%)	QZV (%)	QZT (%)	AHR (%)	AHV (%)	AHT (%)
KS-094	285.60	287.30		40		0	40	40	0	0	0
KS-094	317.00	318.50		10		0	5	5	0	0	0
KS-094	318.50	320.00		10		20	10	30	0	0	0
KS-094	320.00	323.00		5		0	50	50	0	0	0
KS-094	323.00	325.00				0	10	10	0	0	0
KS-094	325.00	328.00		5		0	5	5	0	0	0
KS-094	328.00	331.00		10		0	10	10	0	0	0
KS-094	331.00	334.00		5		0	5	5	0	0	0
KS-094	334.00	337.00		5		0	5	5	0	0	0
KS-094	366.30	369.00		5		0	2.5	2.5	10	0	10
KS-094	369.00	372.00		10		0	10	10	20	0	20
KS-094	372.00	375.00				0	5	5	20	0	20
KS-094	375.00	378.00				0	10	10	20	0	20
KS-094	378.00	382.30		5		0	10	10	30	0	30
KS-094	382.30	385.20		5		0	2.5	2.5	0	0	0
KS-094	385.20	387.60		5		0	5	5	20	0	20
87-4	3.30	4.90		60		0	5	5	0	0	0
87-4	4.90	6.00		75		0	0	0	0	0	0
87-4	6.00	8.00		80		0	0	0	0	0	0
87-4	8.00	10.40		80		0	0	0	0	0	0
87-4	10.40	11.90		58		0	0	0	0	0	0
87-4	11.90	13.40		70		0	0	0	0	0	0
87-4	13.40	14.90		55		0	0	0	0	0	0
87-4	73.40	75.40				0	0	0	0	0	0
87-4	75.40	76.60				0	1	1	0	0	0
87-4	76.60	77.80				2.5	0	2.5	0	0	0
87-4	77.80	79.80				1	0	1	0	0	0
87-4	79.80	81.80				0	0	0	0	0	0
87-4	81.80	83.80				0	1	1	0	0	0
87-4	83.80	85.80				1	1	2	0	0	0
87-4	85.80	87.80				0	0	0	0	0	0
87-4	87.80	89.80				0	0	0	0	0	0
87-4	89.80	91.80				0	0	0	0	0	0
87-4	91.80	93.30				0	0	0	0	0	0





DDHS	FROM metres	TO metres	CLV (%)	CLT (%)	CAR (%)	CAV (%)	CAT (%)	AKR (%)	AKV (%)	AKT (%)	MGR (%)
KS-094	285.60	287.30	0	1	0	0	0	0	0	0	0
KS-094	317.00	318.50	0	0	0	1	1	0	0	0	0
KS-094	318.50	320.00	0	0	0	1	1	0	0	0	0
KS-094	320.00	323.00	0	0	0	0	0	0	0	0	0
KS-094	323.00	325.00	0	0	0	0.001	0.001	0	0	0	0
KS-094	325.00	328.00	0	0	0.001	1	1.001	0	0	0	0
KS-094	328.00	331.00	0	0	1	0	1	0	0	0	0
KS-094	331.00	334.00	0	0	0	2.5	2.5	0	0	0	0
KS-094	334.00	337.00	0	0	0	1	1	0	0	0	0
KS-094	366.30	369.00	0	0	1	0	1	0	0	0	0
KS-094	369.00	372.00	0	0	1	0	1	0	0	0	0
KS-094	372.00	375.00	0	0	1	1	2	0	0	0	0
KS-094	375.00	378.00	0	0	0	0.5	0.5	0	0	0	0
KS-094	378.00	382.30	0	0	0	1	1	0	0	0	0
KS-094	382.30	385.20	1	6	0	0	0	1	0	1	0
KS-094	385.20	387.60	0	0	0	1	1	0	0	0	0
87-4	3.30	4.90	1	21	0	1	1	0	0	0	0
87-4	4.90	6.00	0	0	0	0	0	0	0	0	0
87-4	6.00	8.00	0	0	0	0	0	0	0	0	0
87-4	8.00	10.40	0	0	0	0	0	0	0	0	0
87-4	10.40	11.90	0	0	0	0	0	0	0	0	0
87-4	11.90	13.40	0	0	0	0	0	0	0	0	0
87-4	13.40	14.90	1	1	0	0	0	0	0	0	0
87-4	73.40	75.40	0	2.5	0	1	1	0	0	0	0
87-4	75.40	76.60	0	1	5	2.5	7.5	0	0	0	0
87-4	76.60	77.80	0	0.5	0	2.5	2.5	0	0	0	0
87-4	77.80	79.80	0.1	0.1	0	1	1	0	0	0	0
87-4	79.80	81.80	0	0	0	2.5	2.5	0	0	0	0
87-4	81.80	83.80	0	0	0	0.5	0.5	0	0	0	0
87-4	83.80	85.80	0	0	0	0.5	0.5	0	0	0	0
87-4	85.80	87.80	0	0	0	1	1	0	0	0	0
87-4	87.80	89.80	0	5	0	0	0	0	0	0	0
87-4	89.80	91.80	0	10	0	0	0	0	0	0	0
87-4	91.80	93.30	0	2.5	0	0	0	0	0	0	0





DDH\$	FROM metres	TO metres	PYV (%)	PYT (%)	CPR (%)	CPV (%)	CPT (%)	TTR (%)	TTV (%)	TTT (%)	BOV (%)
KS-094	285.60	287.30	10	20	2.5	1	3.5	0	0	0	0
KS-094	317.00	318.50	0	2.5	0	1	1	0	0	0	0
KS-094	318.50	320.00	2.5	7.5	1	1	2	0	0	0	0
KS-094	320.00	323.00	5	7.5	0	1	1	0	0	0	0
KS-094	323.00	325.00	1	6	1	1	2	0	0	0	0
KS-094	325.00	328.00	1	11	0.001	1	1.001	0	0	0	0
KS-094	328.00	331.00	2.5	7.5	1	2.5	3.5	0	0	0	0
KS-094	331.00	334.00	1	11	0.5	1	1.5	0	0	0	0
KS-094	334.00	337.00	1	11	1	0.5	1.5	0	0.001	0.001	0
KS-094	366.30	369.00	1	11	1	0.5	1.5	0	0	0	0
KS-094	369.00	372.00	1	11	1	0	1	0	0	0	0
KS-094	372.00	375.00	0	10	0	0	0	0	0	0	0
KS-094	375.00	378.00	1	11	1	0	1	0	0	0	0
KS-094	378.00	382.30	1	11	1	0	1	0	0	0	0
KS-094	382.30	385.20	1	1	0.001	0	0.001	0	0	0	0
KS-094	385.20	387.60	1	11	1	1	2	0	0	0	0
87-4	3.30	4.90	0	0	0	0	0	0	0	0	0
87-4	4.90	6.00	1	6	0	0	0	0	0	0	0
87-4	6.00	8.00	1	6	0	0	0	0	0	0	0
87-4	8.00	10.40	1	6	0	0	0	0	0	0	0
87-4	10.40	11.90	1	6	0	0	0	0	0	0	0
87-4	11.90	13.40	1	6	0	0	0	0	0	0	0
87-4	13.40	14.90	2.5	7.5	0	0.001	0.001	0	0	0	0
87-4	73.40	75.40	0	1	0	0	0	0	0	0	0
87-4	75.40	76.60	1	2	0.001	0	0.001	0	0	0	0
87-4	76.60	77.80	0.5	1.5	0	0	0	0	0	0	0
87-4	77.80	79.80	0	1	0	0	0	0	0	0	0
87-4	79.80	81.80	0	1	0	0	0	0	0	0	0
87-4	81.80	83.80	1	3.5	0	0	0	0	0	0	0
87-4	83.80	85.80	0.5	1.5	0	0	0	0	0	0	0
87-4	85.80	87.80	0	2.5	0	0	0	0	0	0	0
87-4	87.80	89.80	0.1	1.1	0	0	0	0	0	0	0
87-4	89.80	91.80	0	0.5	0	0	0	0	0	0	0
87-4	91.80	93.30	0	1	0	0	0	0	0	0	0

DDHS	FROM metres	TO metres	MOV (%)	SLV (%)	GLV (%)	WDC (%)	JAC (%)	CCC (%)	GYLV (%)	V1 (%)	V2 (%)
KS-094	285.60	287.30	0	0	0	0	1	0	0	0	0
KS-094	317.00	318.50	0	0	0	0	0	0	0	6	0
KS-094	318.50	320.00	0	0	0	0	0	0	0	10	0
KS-094	320.00	323.00	0	0	0	0	0	0	0	50	0
KS-094	323.00	325.00	0	0	0	0	0	0	1	15	0
KS-094	325.00	328.00	0	0	0	0	0	0	1	5	0
KS-094	328.00	331.00	0	0	0	0	0	0	1	9.3	0
KS-094	331.00	334.00	0	0	0	0	0	0	1	4.1	0
KS-094	334.00	337.00	0	0	0	0	0	0	1	2.9	0
KS-094	366.30	369.00	0	0	0	0	0	0.1	0	3.1	0
KS-094	369.00	372.00	0	0	0	0	0	0	0	10	0
KS-094	372.00	375.00	0	0	0	0	0	0	0	5	0
KS-094	375.00	378.00	0	0	0	0	0	0.5	0	5	0
KS-094	378.00	382.30	0.001	0	0	0	0	0	0	10	0
KS-094	382.30	385.20	0	0	0	0	0	0	2.5	2.5	0
KS-094	385.20	387.60	0	0	0	0	0	0	0	4	0
87-4	3.30	4.90	0	0	0	0	0	0	0	0	0
87-4	4.90	6.00	0	0	0	0	2.5	0	0	0	0
87-4	6.00	8.00	0	0	0.001	0	0	0.1	0	0	0
87-4	8.00	10.40	0	0	0	0	0	0	0	0	0
87-4	10.40	11.90	0	0	0	0	1	0	0	0	0
87-4	11.90	13.40	0	0	0	0	0.001	0	0	0	0
87-4	13.40	14.90	0	0	0.001	0	0.001	0	0	0	0
87-4	73.40	75.40	0	0	0	0	0	0	0	0	0
87-4	75.40	76.60	0	0	0	0	0	0	0	0	0.1
87-4	76.60	77.80	0	0	0	0	0	0	0	0	0
87-4	77.80	79.80	0	0	0	0	0	0	0	0	0
87-4	79.80	81.80	0	0	0	0	0	0	0	0	0
87-4	81.80	83.80	0	0	0	0	0	0	0	0	0
87-4	83.80	85.80	0	0	0	0	0	0	0	0	0
87-4	85.80	87.80	0	0	0	0	0	0	0	0	0
87-4	87.80	89.80	0	0	0	0	0.001	0	0	0	0
87-4	89.80	91.80	0	0	0	0	0.001	0	0	0	0
87-4	91.80	93.30	0	0	0	0	1	0	0	0	0

DDHS	FROM metres	TO metres	V3 (%)	V4 (%)	X1 (%)	X2 (%)	X3 (%)	CLEAV	Cu:Au (%/ppm)
KS-094	285.60	287.30	0	0	0	0	0	7	1.95946
KS-094	317.00	318.50	0	0	2.1	0	0	5	2.77419
KS-094	318.50	320.00	0	0	2.5	0	0	5	2.77419
KS-094	320.00	323.00	0	0	0.9	0	0	4	3.53125
KS-094	323.00	325.00	0	0	0.1	0	0	4	0.97414
KS-094	325.00	328.00	0	0	1.8	0.6	0	5	3.28571
KS-094	328.00	331.00	0.3	0	3.3	0	0	5	3.84375
KS-094	331.00	334.00	0.3	0	2.3	0	1.2	4	2.27273
KS-094	334.00	337.00	0	0	1.8	0.3	0	5	3.09091
KS-094	366.30	369.00	0	0	2.5	1	0	8	2.92727
KS-094	369.00	372.00	0	0	0	0	0	7	3.17895
KS-094	372.00	375.00	0	0	1.2	0	0	7	3.35385
KS-094	375.00	378.00	0	0	0.6	0	0	6	5.78462
KS-094	378.00	382.30	0	0	0.4	0	0	7	2.83333
KS-094	382.30	385.20	0	0	0.8	0	1.3	5	2.725
KS-094	385.20	387.60	0	0	1.2	0	0	6	3.35
87-4	3.30	4.90	1	0	0	0	5.5	3	1.6
87-4	4.90	6.00	1	0	0	0	0	7	3.2
87-4	6.00	8.00	1	0	0	0	0	7	0.67273
87-4	8.00	10.40	1	0	0	0	0	7	0.37
87-4	10.40	11.90	1	0	0	0	0	7	14.4
87-4	11.90	13.40	1	0.1	0	1	0	7	29.2
87-4	13.40	14.90	0	0	0	0	0	6	30.2
87-4	73.40	75.40	0	0	0	0	0	0	0.43846
87-4	75.40	76.60	0	0	0	0	0	0	1.76667
87-4	76.60	77.80	0	0	0	0	0	1	22.8
87-4	77.80	79.80	0	0	0	0	0	0	9.8
87-4	79.80	81.80	0	0	0	0	0	0	6.2
87-4	81.80	83.80	0	0	0	0	0	0	10.6
87-4	83.80	85.80	0	0	0	0	0	0	13.8
87-4	85.80	87.80	0	0	0	0	0	0	6.6
87-4	87.80	89.80	0	0	0	0	0	0	3.4
87-4	89.80	91.80	0	0	0	0	0	0	4.6
87-4	91.80	93.30	0	0	0	0	0	0	4.6

DDH\$	FROM metres	TO metres	CU (%)	AU (ppm)	CU:AU (%/ppm)	RECOV (%)	ROCK\$	BX	FB	FX	VF
KS-101	59.00	62.00	0.017	0.70	0.024	100	CONG				
KS-101	62.00	65.00	0.043	0.43	0.100	100	CONG				
KS-101	65.00	68.00	0.059	0.18	0.328	100	CONG			40	
KS-101	68.00	71.00	0.038	0.53	0.072	100	CONG				
KS-101	71.00	74.00	0.051	1.55	0.033	100	CONG				
KS-101	74.00	76.90	0.028	2.15	0.013	100	CONG			40	
KS-101	76.90	77.40	0.071	0.50	0.142	100	LAPP			55	
KS-101	77.40	78.90	0.071	0.50	0.142	100	CONG			70	
KS-101	78.90	81.90	0.012	0.04	0.300	100	TRAC			55	
KS-101	120.40	123.40	0.022	0.29	0.076	100	TURB	10			
KS-101	123.40	126.40	0.026	0.07	0.371	100	TURB	5			
KS-101	126.40	129.40	0.018	0.02	0.900	100	TURB	5			
KS-101	129.40	132.40	0.013	0.02	0.650	100	TURB	5			
KS-101	132.40	135.40	0.012	0.06	0.200	100	TURB	5			
KS-101	135.40	138.40	0.008	0.08	0.100	100	TURB	30			
KS-101	138.40	141.40	0.017	0.04	0.425	98	TURB	5			
KS-102	22.00	24.60	0.074	0.10	0.740	85	PHMG			40	
KS-102	31.00	34.00	0.014	0.01	1.400	90	ANPP				
KS-102	34.00	37.00	0.013	0.01	1.300	50	ANPP			50	
KS-102	37.00	40.00	0.090	0.12	0.750	98	PHPP			55	
KS-102	40.00	43.00	0.019	0.01	1.900	82	TRAC			60	
KS-102	43.80	47.00	0.056	0.23	0.243	87	PHPP			50	
KS-102	47.00	50.00	0.044	0.13	0.338	93	PHPP			65	
KS-102	50.00	53.50	0.051	0.23	0.222	58	PHPP				
KS-102	91.00	94.00	0.025	0.19	0.132	98	PHFG			65	
KS-102	94.00	97.00	0.024	0.12	0.200	95	TFAH			35	
KS-102	97.00	100.00	0.003	0.15	0.020	95	TFAH			45	
KS-102	100.00	103.00	0.029	0.20	0.145	90	TFAH	30	50	50	
KS-102	103.00	106.00	0.055	0.29	0.190	92	TFAH			40	
KS-102	106.00	109.00	0.038	0.19	0.200	100	TFAH	30			
KS-102	109.00	112.00	0.029	0.18	0.161	100	TFAH	37			
KS-102	112.00	115.00	0.031	0.18	0.172	98	TFAH	50	3	47	
KS-102	152.00	155.00	0.009	0.16	0.056	100	SACO	15			
KS-102	155.00	158.00	0.007	0.05	0.140	93	SACO	21			
KS-102	158.00	161.00	0.007	0.04	0.175	97	SACO	20			
KS-102	161.00	164.00	0.014	0.20	0.070	92	SACO	20			
KS-102	164.00	167.00	0.014	0.21	0.067	97	SACO	20			
KS-102	167.00	169.30	0.014	0.15	0.093	91	SACO	25			
KS-102	169.30	172.00	0.005	0.05	0.100	93	ANPP				
KS-102	172.00	175.00	0.002	0.02	0.100	97	ANPP				
KS-104	19.00	22.00	0.780	0.33	2.364	93	PHMG			70	
KS-104	22.00	24.40	0.604	0.16	3.775	96	PHMG			60	
KS-104	24.40	27.60	0.152	0.11	1.382	58	PHMG			5	
KS-104	27.60	30.80	0.217	0.11	1.973	100	PHMG			60	
KS-104	30.80	33.50	1.045	0.25	4.180	54	PHMG				
KS-104	33.50	36.30	0.140	0.05	2.800	71	ANDY				
KS-104	36.30	39.30	0.440	0.17	2.588	71	PHMG			50	
KS-104	79.00	82.00	0.187	0.12	1.558	89	PHMG			70	
KS-104	82.00	84.60	0.201	0.20	1.005	95	PHMG			60	
KS-104	84.60	87.50	0.154	0.13	1.185	97	PHFG			60	
KS-104	87.50	90.50	0.003	0.01	0.300	94	ANPP			80	
KS-104	90.50	93.50	0.005	0.01	0.500	95	ANPP			50	
KS-104	93.50	96.50	0.012	0.03	0.400	90	ANPP				
KS-104	96.50	99.50	0.013	0.01	1.300	95	ANPP			50	
KS-102	102.10	105.00	0.040	0.17	0.235	70	PHMG			60	
KS-104	136.30	139.10	0.140	0.09	1.556	100	TFAH	35			
KS-104	139.10	142.00	0.017	0.14	0.121	94	TFAH	60			

DDHS	FROM metres	TO metres	QZR (%)	QZV (%)	QZT (%)	AHR (%)	AHV (%)	AHT (%)	GYR (%)	GYV (%)	GYT (%)
KS-101	59.00	62.00	0.5	2.5	3	0	0	0	0	0	0
KS-101	62.00	65.00	0	2.5	2.5	0	0	0	0	0	0
KS-101	65.00	68.00	0	1	1	0	0	0	0	0	0
KS-101	68.00	71.00	5	2.5	7.5	0	0	0	0	0	0
KS-101	71.00	74.00	10	5	15	0	0	0	0	0	0
KS-101	74.00	76.90	10	5	15	0	0	0	0	0	0
KS-101	76.90	77.40	0	0	0	0	0	0	0	0	0
KS-101	77.40	78.90	10	2.5	12.5	0	0	0	0	0	0
KS-101	78.90	81.90	0	1	1	0	0	0	0	0	0
KS-101	120.40	123.40	0	0.001	0.001	0	0	0	0	0	0
KS-101	123.40	126.40	0	0	0	0	0	0	0	0	0
KS-101	126.40	129.40	0	0	0	0	0	0	0	0	0
KS-101	129.40	132.40	0	0	0	0	0	0	0	0	0
KS-101	132.40	135.40	0	0.001	0.001	0	0	0	0	0	0
KS-101	135.40	138.40	0	0	0	0	0	0	0	0	0
KS-101	138.40	141.40	0	0	0	0	0	0	0	0	0
KS-102	22.00	24.60	0	1	1	0	0	0	0	0	0
KS-102	31.00	34.00	0	0.5	0.5	0	0	0	0	0	0
KS-102	34.00	37.00	0	1	1	0	0	0	0	0	0
KS-102	37.00	40.00	10	1	11	0	0	0	0	0	0
KS-102	40.00	43.00	0	0	0	0	0	0	0	0	0
KS-102	43.00	47.00	0	1	1	0	0	0	0	0	0
KS-102	47.00	50.00	0	1	1	0	0	0	0	0	0
KS-102	50.00	53.50	0	1	1	0	0	0	0	0	0
KS-102	91.00	94.00	0	1	1	0	0	0	0	0	0
KS-102	94.00	97.00	0	0.1	0.1	0	0	0	0	0	0
KS-102	97.00	100.00	0	0.5	0.5	0	0	0	0	0	0
KS-102	100.00	103.00	0	0	0	0	0	0	0	0	0
KS-102	103.00	106.00	0	0	0	0	0	0	0	0	0
KS-102	106.00	109.00	0	0.5	0.5	0	0	0	0	0	0
KS-102	109.00	112.00	0	0	0	0	0	0	0	0	0
KS-102	112.00	115.00	0	0.5	0.5	0	0	0	0	0	0
KS-102	152.00	155.00	0	1	1	0	0	0	0	0	0
KS-102	155.00	158.00	0	0.5	0.5	0	0	0	0	0	0
KS-102	158.00	161.00	0	0	0	0	0	0	0	0	0
KS-102	161.00	164.00	0	0.5	0.5	0	0	0	0	0	0
KS-102	164.00	167.00	0	0.5	0.5	0	0	0	0	0	0
KS-102	167.00	169.30	0	0	0	0	0	0	0	0	0
KS-102	169.30	172.00	0	1	1	0	0	0	0	0	0
KS-102	172.00	175.00	0	0.5	0.5	0	0	0	0	0	0
KS-104	19.00	22.00	0	2	2	0	0	0	0	0.001	0.001
KS-104	22.00	24.40	0	40	40	0	0	0	0	0	0
KS-104	24.40	27.60	0	2.5	2.5	0	0	0	0	0	0
KS-104	27.60	30.80	0	0.5	0.5	0	0	0	0	0	0
KS-104	30.80	33.50	0	30	30	0	0	0	0	0	0
KS-104	33.50	36.30	0	0	0	0	0	0	0	0	0
KS-104	36.30	39.30	0	0	0	0	0	0	0	0	0
KS-104	79.00	82.00	0	5	5	0	0	0	0	0	0
KS-104	82.00	84.60	0	5	5	0	0	0	0	0	0
KS-104	84.60	87.50	0	2.5	2.5	0	0	0	0	0	0
KS-104	87.50	90.50	0	1	1	0	0	0	0	0	0
KS-104	90.50	93.50	0	5	5	0	0	0	0	0	0
KS-104	93.50	96.50	0	5	5	0	0	0	0	0	0
KS-104	96.50	99.50	0	1	1	0	0	0	0	0	0
KS-102	102.10	105.00	0	0	0	0	0	0	0	0	0
KS-104	136.30	139.10	0	0	0	0	0	0	0	0	0
KS-104	139.10	142.00	0	1	1	0	0	0	0	0	0

DDHS	FROM metres	TO metres	AHGYT (%)	SER (%)	SEV (%)	SET (%)	YSR (%)	YSV (%)	YST (%)	GSR (%)	GSV (%)
KS-101	59.00	62.00	0	10	0	10	0	0	0	0	0
KS-101	62.00	65.00	0	30	0	30	0	0	0	0	0
KS-101	65.00	68.00	0	30	0	30	0	0	0	0	0
KS-101	68.00	71.00	0	30	0	30	0	0	0	0	0
KS-101	71.00	74.00	0	20	0	20	0	0	0	0	0
KS-101	74.00	76.90	0	20	0	20	0	0	0	0	0
KS-101	76.90	77.40	0	40	0	40	0	0	0	0	0
KS-101	77.40	78.90	0	20	0	20	0	0	0	0	0
KS-101	78.90	81.90	0	30	0	30	0	0	0	0	0
KS-101	120.40	123.40	0	0	0	0	0	0	0	0	0
KS-101	123.40	126.40	0	0	0	0	0	0	0	0	0
KS-101	126.40	129.40	0	0	0	0	0	0	0	0	0
KS-101	129.40	132.40	0	0	0	0	0	0	0	0	0
KS-101	132.40	135.40	0	0	0.1	0.1	0	0	0	0	0
KS-101	135.40	138.40	0	0	0.001	0.001	0	0	0	0	0
KS-101	138.40	141.40	0	0	0	0	0	0	0	0	0
KS-102	22.00	24.60	0	10	5	15	30	0	30	0	0
KS-102	31.00	34.00	0	30	0	30	0	0	0	0	0
KS-102	34.00	37.00	0	30	0	30	0	0	0	0	0
KS-102	37.00	40.00	0	30	0	30	0	0	0	0	0
KS-102	40.00	43.00	0	30	0	30	0	0	0	0	0
KS-102	43.00	47.00	0	10	5	15	30	0	30	0	0
KS-102	47.00	50.00	0	5	1	6	30	0	30	0	0
KS-102	50.00	53.50	0	30	5	35	0	0	0	0	0
KS-102	91.00	94.00	0	20	1	21	0	0	0	0	0
KS-102	94.00	97.90	0	30	1	31	0	0	0	0	0
KS-102	97.00	100.00	0	30	1	31	0	0	0	0	0
KS-102	100.00	103.00	0	30	1	31	0	0	0	0	0
KS-102	103.00	106.00	0	30	0	30	0	0	0	0	0
KS-102	106.00	109.00	0	30	0.1	30.1	0	0	0	0	0
KS-102	109.00	112.00	0	30	0	30	0	0	0	0	0
KS-102	112.00	115.00	0	30	0	30	0	0	0	0	0
KS-102	152.00	155.00	0	30	0	30	0	0	0	0	0
KS-102	155.00	158.00	0	20	0	20	0	0	0	0	0
KS-102	158.00	161.00	0	20	0	20	0	0	0	0	0
KS-102	161.00	164.00	0	10	0	10	0	0	0	0	0
KS-102	164.00	167.00	0	20	0	20	0	0	0	0	0
KS-102	167.00	169.30	0	20	0	20	0	0	0	0	0
KS-102	169.30	172.00	0	30	0	30	0	0	0	0	0
KS-102	172.00	175.00	0	30	0	30	0	0	0	0	0
KS-104	19.00	22.00	0.001	30	0	30	0	0	0	0	0
KS-104	22.00	24.40	0	30	0	30	0	0	0	0	0
KS-104	24.40	27.60	0	40	0	40	0	0	0	0	0
KS-104	27.60	30.80	0	60	0	60	0	0	0	0	0
KS-104	30.80	33.50	0	30	0	30	0	0	0	0	0
KS-104	33.50	36.30	0	0	0	0	0	0	0	0	0
KS-104	36.30	39.30	0	40	1	41	0	0	0	0	0
KS-104	79.00	82.00	0	20	1	21	20	0	20	0	0
KS-104	82.00	84.60	0	10	1	11	30	0	30	0	0
KS-104	84.60	87.50	0	30	1	31	0	0	0	0	0
KS-104	87.50	90.50	0	30	0	30	0	0	0	0	0
KS-104	90.50	93.50	0	30	0	30	0	0	0	0	0
KS-104	93.50	96.50	0	30	0	30	0	0	0	0	0
KS-104	96.50	99.50	0	30	0	30	0	0	0	0	0
KS-102	102.10	105.00	0	20	1	21	10	0	10	0	0
KS-104	136.30	139.10	0	30	0.5	30.5	2.5	0	2.5	0	0
KS-104	139.10	142.00	0	30	1	31	5	0	5	0	0

DDHS	FROM metres	TO metres	GST (%)	SYGST (%)	KAR (%)	KAV (%)	KAT (%)	CLR (%)	CLV (%)	CLT (%)	CAR (%)
KS-101	59.00	62.00	0	10	20	0	20	0	0	0	2.5
KS-101	62.00	65.00	0	30	10	0	10	0	0	0	2.5
KS-101	65.00	68.00	0	30	2.5	0	2.5	0	0	0	0
KS-101	68.00	71.00	0	30	2.5	0	2.5	0	0	0	0
KS-101	71.00	74.00	0	20	0	0	0	0	0	0	1
KS-101	74.00	76.90	0	20	2.5	0	2.5	0	0	0	0
KS-101	76.90	77.40	0	40	5	0	5	0	0	0	0
KS-101	77.40	78.90	0	20	0	0	0	0	0	0	0
KS-101	78.90	81.90	0	30	10	0	10	1	0	1	0
KS-101	120.40	123.40	0	0	0	0	0	0	0	0	0
KS-101	123.40	126.40	0	0	0	0	0	0	0	0	0
KS-101	126.40	129.40	0	0	0	0	0	0	0	0	0
KS-101	129.40	132.40	0	0	0	0	0	0	0	0	0
KS-101	132.40	135.40	0	0.1	0	0	0	0	0	0	0
KS-101	135.40	138.40	0	0.001	0	0	0	0	0	0	0
KS-101	138.40	141.40	0	0	0	0	0	0	0	0	0
KS-102	22.00	24.60	0	45	0.001	0	0.001	0	0	0	0
KS-102	31.00	34.00	0	30	5	0.001	5.001	5	0	5	2.5
KS-102	34.00	37.00	0	30	5	0	5	10	0	10	0
KS-102	37.00	40.00	0	30	0	0.5	0.5	0	0	0	0
KS-102	40.00	43.00	0	30	0	0	0	10	0.1	10.1	0
KS-102	43.80	47.00	0	45	0	0	0	0	0	0	0.001
KS-102	47.00	50.00	0	36	0	0	0	0	0	0	0
KS-102	50.00	53.50	0	35	0	0.5	0.5	0	0	0	0
KS-102	91.00	94.00	0	21	20	0	20	0	0	0	0
KS-102	94.00	97.00	0	31	0	0	0	0	0	0	0
KS-102	97.00	100.00	0	31	0	0	0	0	0	0	0
KS-102	100.00	103.00	0	31	0	0	0	0	0	0	0
KS-102	103.00	106.00	0	30	2.5	0	2.5	0	0	0	0
KS-102	106.00	109.00	0	30.1	0	0	0	0	0	0	0
KS-102	109.00	112.00	0	30	0	0	0	0	0	0	0
KS-102	112.00	115.00	0	30	0	0	0	0	0	0	0
KS-102	152.00	155.00	0	30	0	0	0	0	0	0	1
KS-102	155.00	158.00	0	20	0	0	0	0	0	0	1
KS-102	158.00	161.00	0	20	0	0	0	0	0	0	1
KS-102	161.00	164.00	0	10	0	0	0	0	0	0	1
KS-102	164.00	167.00	0	20	0	0	0	0	0	0	1
KS-102	167.00	169.30	0	20	0	0	0	0	0	0	1
KS-102	169.30	172.00	0	30	10	0	10	10	0.1	10.1	5
KS-102	172.00	175.00	0	30	2.5	0	2.5	10	0	10	0
KS-104	19.00	22.00	0	30	2.5	0	2.5	0	0	0	0
KS-104	22.00	24.40	0	30	0	0	0	0	0.1	0.1	0
KS-104	24.40	27.00	0	40	10	0	10	0	0	0	0
KS-104	27.60	30.80	0	60	2.5	0	2.5	0	0	0	0
KS-104	30.80	33.50	0	30	0	0.001	0.001	0	0	0	0
KS-104	33.50	36.30	0	0	0	0	0	0	0	0	2.5
KS-104	36.30	39.30	0	41	0	1	1	0	0	0	0
KS-104	79.00	82.00	0	41	0	0	0	0	0	0	0
KS-104	82.00	84.60	0	41	0	0	0	0	0	0	0
KS-104	84.60	87.50	0	31	0	0	0	0	0	0	0
KS-104	87.50	90.50	0	30	5	0	5	10	1	11	0
KS-104	90.50	93.50	0	30	0	0	0	20	1	21	0
KS-104	93.50	96.50	0	30	0	0	0	20	1	21	0
KS-104	96.50	99.50	0	30	5	0	5	10	1	11	0
KS-102	102.10	105.00	0	31	2.5	0	2.5	0	0	0	0
KS-104	136.30	139.10	0	33	0	0	0	0	0	0	0
KS-104	139.10	142.00	0	36	0	0	0	0	0	0	0



DDHS	FROM metres	TO metres	CAV (%)	CAT (%)	AKR (%)	AKV (%)	AKT (%)	MGR (%)	MGV (%)	MGT (%)	HER (%)
KS-101	59.00	62.00	1	3.5	0	0	0	0	0	0	0
KS-101	62.00	65.00	1	3.5	0	0	0	0	0	0	0
KS-101	65.00	68.00	1	1	0	0	0	0	0	0	0
KS-101	68.00	71.00	1	1	0	0	0	0	0	0	0
KS-101	71.00	74.00	0	1	0	0	0	0	0	0	0
KS-101	74.00	76.90	2.5	2.5	0	0	0	0	0	0	0
KS-101	76.90	77.40	0.5	0.5	0	0	0	0	0	0	0
KS-101	77.40	78.90	0.1	0.1	0	0	0	0	0	0	0
KS-101	78.90	81.90	2.5	2.5	0	0	0	0	0	0	0
KS-101	120.40	123.40	1	1	0	0	0	0	0	0	0
KS-101	123.40	126.40	1	1	0	0	0	0	0	0	0
KS-101	126.40	129.40	1	1	0	0	0	0	0	0	0
KS-101	129.40	132.40	1	1	0	0	0	0	0	0	0
KS-101	132.40	135.40	1	1	0	0	0	0	0	0	0
KS-101	135.40	138.40	2.5	2.5	0	0	0	0	0	0	0
KS-101	138.40	141.40	0	0	0	0	0	0	0	0	0
KS-102	22.00	24.60	0	0	0	0	0	0	0	0	0
KS-102	31.00	34.00	0.5	3	0	0	0	0	0	0	0
KS-102	34.00	37.00	0	0	0	0	0	0	0	0	0
KS-102	37.00	40.00	0.5	0.5	0	0	0	0	0	0	0
KS-102	40.00	43.00	0.5	0.5	0	0	0	0	0	0	0
KS-102	43.80	47.00	0.5	0.501	0	0	0	0	0	0	0
KS-102	47.00	50.00	1	1	0	0	0	0	0	0	0
KS-102	50.00	53.50	1	1	0	0	0	0	0	0	0
KS-102	91.00	94.00	0.5	0.5	0	0	0	0	0	0	0
KS-102	94.00	97.90	0.5	0.5	0	0	0	0	0	0	0
KS-102	97.00	100.00	2.5	2.5	0	0	0	0	0	0	0
KS-102	100.00	103.00	1	1	0	0	0	0	0	0	0
KS-102	103.00	106.00	0.1	0.1	0	0	0	0	0	0	0
KS-102	106.00	109.00	0.1	0.1	0	0	0	0	0	0	0
KS-102	109.00	112.00	0.5	0.5	0	0	0	0	0	0	0
KS-102	112.00	115.00	0.1	0.1	0	0	0	0	0	0	0
KS-102	152.00	155.00	1	2	0	0	0	0	0	0	0
KS-102	155.00	158.00	1	2	0	0	0	0	0	0	0
KS-102	158.00	161.00	0.5	1.5	0	0	0	0	0	0	0
KS-102	161.00	164.00	2.5	3.5	0	0	0	0	0	0	0
KS-102	164.00	167.00	1	2	0	0	0	0	0	0	0
KS-102	167.00	169.30	0.1	1.1	0	0	0	0	0	0	0
KS-102	169.30	172.00	0	5	0	0	0	0	0	0	0
KS-102	172.00	175.00	2.5	2.5	0	0	0	0	0	0	0
KS-104	19.00	22.00	0.1	0.1	0	0.001	0.001	0	0	0	0
KS-104	22.00	24.40	0	0	0	1	1	0	0	0	0
KS-104	24.40	27.60	0	0	0	0	0	0	0	0	0
KS-104	27.60	30.80	0	0	0	0	0	0	0	0	0
KS-104	30.80	33.50	0	0	0	0	0	0	0	0	0
KS-104	33.50	36.30	0	2.5	0	0	0	5	0	5	5
KS-104	36.30	39.30	0	0	0	0	0	0	0	0	0
KS-104	79.00	82.00	0	0	0	0	0	0	0	0	0
KS-104	82.00	84.60	0	0	0	0	0	0	0	0	0
KS-104	84.60	87.50	0	0	0	0	0	0	0	0	0
KS-104	87.50	90.50	2.5	2.5	0	0	0	0	0	0	0
KS-104	90.50	93.50	5	5	0	0	0	0	0	0	0
KS-104	93.50	96.50	5	5	0	0	0	0	0	0	0.5
KS-104	96.50	99.50	1	1	0	0	0	0	0	0	0
KS-102	102.10	105.00	0.5	0.5	0	0	0	0	0	0	0
KS-104	136.30	139.10	1	1	0	0	0	0	0	0	0
KS-104	139.10	142.00	1	1	0	0	0	0	0	0	0

DDHS	FROM metres	TO metres	HEV (%)	HET (%)	RUR (%)	RUV (%)	RUT (%)	PYR (%)	PYV (%)	PYT (%)	CPR (%)
KS-101	59.00	62.00	0	0	2.5	2.5	5	5	1	6	0
KS-101	62.00	65.00	0	0	0	2.5	2.5	10	1	11	0
KS-101	65.00	68.00	0	0	0	1	1	5	0.1	5.1	0
KS-101	68.00	71.00	0	0	0	0	0	10	1	11	0
KS-101	71.00	74.00	0	0	0	0	0	10	0.5	10.5	0
KS-101	74.00	76.90	0	0	0	0	0	10	2.5	12.5	0
KS-101	76.90	77.40	0	0	0	0	0	5	0	5	0
KS-101	77.40	78.90	0	0	0	0	0	10	0.5	10.5	0
KS-101	78.90	81.90	0	0	0	0	0	2.5	0.1	2.6	0
KS-101	120.40	123.40	0	0	0	0	0	5	0.5	5.5	0
KS-101	123.40	126.40	0	0	0	0	0	5	0	5	0
KS-101	126.40	129.40	0	0	0	0	0	5	0	5	0
KS-101	129.40	132.40	0	0	0	0	0	5	0	5	0
KS-101	132.40	135.40	0	0	0	0	0	5	0.001	5.001	0
KS-101	135.40	138.40	0	0	0	0	0	5	0.001	5.001	0
KS-101	138.40	141.40	0	0	0	0	0	2.5	0	2.5	0
KS-102	22.00	24.60	0	0	0	0	0	5	2.5	7.5	0
KS-102	31.00	34.00	0	0	0	0	0	0	0	0	0
KS-102	34.00	37.00	0	0	0	0	0	0	0	0	0
KS-102	37.00	40.00	0	0	0	0	0	10	1	11	0
KS-102	40.00	43.00	0	0	0	0	0	0	0	0	0
KS-102	43.00	47.00	0	0	0	0	0	10	1	11	0
KS-102	47.00	50.00	0	0	0	0	0	10	1	11	0
KS-102	50.00	53.50	0	0	0	0	0	10	5	15	0
KS-102	91.00	94.00	0	0	0	0	0	10	0.5	10.5	0
KS-102	94.00	97.90	0	0	0	0	0	5	1	6	0
KS-102	97.00	100.00	0	0	0	0	0	2.5	1	3.5	0
KS-102	100.00	103.00	0	0	0	0	0	1	2.5	3.5	0
KS-102	103.00	106.00	0	0	0	0	0	5	1	6	0
KS-102	106.00	109.00	0	0	0	0	0	5	1	6	0
KS-102	109.00	112.00	0	0	0	0	0	2.5	1	3.5	0
KS-102	112.00	115.00	0	0	0	0	0	5	1	6	0
KS-102	152.00	155.00	0	0	30	0	30	10	0.1	10.1	0
KS-102	155.00	158.00	0	0	20	0	20	5	0.001	5.001	0
KS-102	158.00	161.00	0	0	20	1	21	1	0.001	1.001	0
KS-102	161.00	164.00	0	0	0	0	0	5	0.001	5.001	0
KS-102	164.00	167.00	0	0	0	0	0	5	0.5	5.5	0
KS-102	167.00	169.30	0	0	0	0	0	5	0.5	5.5	0
KS-102	169.30	172.00	0	0	0	0	0	2.5	0	2.5	0
KS-102	172.00	175.00	0	0	0	0	0	0.5	0	0.5	0
KS-104	19.00	22.00	0	0	0	0	0	5	5	10	1
KS-104	22.00	24.40	0	0	0	0	0	5	2.5	7.5	1
KS-104	24.40	27.60	0	0	0	0	0	10	2.5	12.5	0
KS-104	27.60	30.80	0	0	0	0	0	10	0.5	10.5	0
KS-104	30.80	33.50	0	0	0	0	0	2.5	5	7.5	0
KS-104	33.50	36.30	0	5	0	0	0	0	0	0	0
KS-104	36.30	39.30	0	0	0	0	0	10	2.5	12.5	0
KS-104	79.00	82.00	0	0	0	0	0	10	2.5	12.5	0
KS-104	82.00	84.60	0	0	0	0	0	10	5	15	0.1
KS-104	84.60	87.50	0.001	0.001	0	0	0	10	5	15	0.001
KS-104	87.50	90.50	0	0	0	0	0	0	0	0	0
KS-104	90.50	93.50	0	0	0	0	0	0	0	0	0
KS-104	93.50	96.50	0.1	0.6	0	0	0	0	0	0	0
KS-104	96.50	99.50	0	0	0	0	0	0.1	0	0.1	0
KS-102	102.10	105.00	0	0	0	0	0	10	1	11	0
KS-104	136.30	139.10	0	0	0	0	0	5	1	6	0
KS-104	139.10	142.00	0	0	0	0	0	10	2.5	12.5	0

DDH\$	FROM metres	TO metres	CPV (%)	CPT (%)	TTR (%)	TTV (%)	TTT (%)	BOV (%)	MOV (%)	SLV (%)	GLV (%)
KS-101	59.00	62.00	0	0	0	0	0	0	0	0	0
KS-101	62.00	65.00	0	0	0	0	0	0	0	0	0
KS-101	65.00	68.00	0.001	0.001	0	0	0	0	0	0	0
KS-101	68.00	71.00	0	0	0	0	0	0	0	0	0
KS-101	71.00	74.00	0.1	0.1	0	0	0	0	0	0	0
KS-101	74.00	76.90	0	0	0	0	0	0	0	0	0
KS-101	76.90	77.40	0	0	0	0	0	0	0	0	0
KS-101	77.40	78.90	0.001	0.001	0	0	0	0	0	0	0
KS-101	78.90	81.90	0	0	0	0	0	0	0	0.001	0.001
KS-101	120.40	123.40	0	0	0	0	0	0	0	0	0
KS-101	123.40	126.40	0	0	0	0	0	0	0	0	0
KS-101	126.40	129.40	0	0	0	0	0	0	0	0	0
KS-101	129.40	132.40	0	0	0	0	0	0	0	0	0
KS-101	132.40	135.40	0	0	0	0	0	0	0	0	0
KS-101	135.40	138.40	0	0	0	0	0	0	0	0	0
KS-101	138.40	141.40	0	0	0	0	0	0	0	0	0
KS-102	22.00	24.60	0	0	0	0.1	0.1	0	0	0	0
KS-102	31.00	34.00	0	0	0	0	0	0	0	0	0
KS-102	34.00	37.00	0	0	0	0	0	0	0	0	0
KS-102	37.00	40.00	0	0	0	0.001	0.001	0	0.001	0	0
KS-102	40.00	43.00	0	0	0	0	0	0	0	0	0
KS-102	43.80	47.00	0	0	0	0.001	0.001	0	0	0	0
KS-102	47.00	50.00	0	0	0	0	0	0	0	0	0
KS-102	50.00	53.50	0	0	0	0	0	0	0	0	0
KS-102	91.00	94.00	0	0	0	0	0	0	0	0	0
KS-102	94.00	97.00	0	0	0	0.1	0.1	0	0	0	0
KS-102	97.00	100.00	0	0	0	0.001	0.001	0	0	0	0
KS-102	100.00	103.00	0	0	0	0	0	0	0	0	0
KS-102	103.00	106.00	0	0	0	0.001	0.001	0	0	0	0
KS-102	106.00	109.00	0	0	0	0.1	0.1	0	0	0	0
KS-102	109.00	112.00	0	0	0	0	0	0	0	0	0
KS-102	112.00	115.00	0	0	0	0	0	0	0	0	0
KS-102	152.00	155.00	0	0	0	0	0	0	0.001	0	0
KS-102	155.00	158.00	0	0	0	0	0	0	0	0	0
KS-102	158.00	161.00	0	0	0	0	0	0	0	0	0
KS-102	161.00	164.00	0	0	0	0	0	0	0	0	0
KS-102	164.00	167.00	0	0	0	0	0	0	0	0	0
KS-102	167.00	169.30	0	0	0	0	0	0	0	0	0
KS-102	169.30	172.00	0	0	0	0	0	0	0	0	0
KS-102	172.00	175.00	0	0	0	0	0	0	0	0	0
KS-104	19.00	22.00	1	2	0	0.001	0.001	0	0	0	0
KS-104	22.00	24.40	0.5	1.5	0	0.1	0.1	0	0.001	0	0
KS-104	24.40	27.60	0	0	0	0.1	0.1	0	0	0	0
KS-104	27.60	30.80	0.1	0.1	0	0	0	0	0	0	0
KS-104	30.80	33.50	1	1	0	0.1	0.1	0.001	0	0	0
KS-104	33.50	36.30	0	0	0	0	0	0	0	0	0
KS-104	36.30	39.30	0	0	0	0	0	0	0.001	0	0
KS-104	79.00	82.00	0.5	0.5	0	0.001	0.001	0	0	0	0
KS-104	82.00	84.60	1	1.1	0	0.001	0.001	0	0	0	0
KS-104	84.60	87.50	0.5	0.501	0	0.1	0.1	0	0	0	0
KS-104	87.50	90.50	0	0	0	0	0	0	0	0	0
KS-104	90.50	93.50	0	0	0	0	0	0	0	0	0
KS-104	93.50	96.50	0	0	0	0	0	0	0	0	0
KS-104	96.50	99.50	0	0	0	0	0	0	0	0	0
KS-102	102.10	105.00	0	0	0	0	0	0	0	0	0
KS-104	136.30	139.10	0	0	0	0.1	0.1	0	0	0	0
KS-104	139.10	142.00	0	0	0	0.1	0.1	0	0	0	0



DDHS	FROM metres	TO metres	X2 (%)	X3 (%)	CLEAV
KS-101	59.00	62.00	0	0	3
KS-101	62.00	65.00	0	0	2
KS-101	65.00	68.00	0	2.2	3
KS-101	68.00	71.00	0	0.1	2
KS-101	71.00	74.00	0	0.1	2
KS-101	74.00	76.90	0	0.1	4
KS-101	76.90	77.40	0	0	5
KS-101	77.40	78.90	0	0	3
KS-101	78.90	81.90	0	1.4	3
KS-101	120.40	123.40	0	1.2	1
KS-101	123.40	126.40	0	1	1
KS-101	126.40	129.40	0	0.5	1
KS-101	129.40	132.40	0	1	1
KS-101	132.40	135.40	0	1.1	1
KS-101	135.40	138.40	0	1	1
KS-101	138.40	141.40	0	0.1	1
KS-102	22.00	24.60	0	0	4
KS-102	31.00	34.00	0	1.1	3
KS-102	34.00	37.00	0	1.7	3
KS-102	37.00	40.00	0	0	4
KS-102	40.00	43.00	0	1.7	4
KS-102	43.80	47.00	0.7	0	5
KS-102	47.00	50.00	0	1	5
KS-102	50.00	53.50	0	1.1	5
KS-102	91.00	94.00	0	0	5
KS-102	94.00	97.00	0	0.2	5
KS-102	97.00	100.00	0	1.7	4
KS-102	100.00	103.00	0	2.5	4
KS-102	103.00	106.00	0	0.1	4
KS-102	106.00	109.00	0	0.1	4
KS-102	109.00	112.00	0	0.2	4
KS-102	112.00	115.00	0	0.1	4
KS-102	152.00	155.00	0	1.3	2
KS-102	155.00	158.00	0	2.1	2
KS-102	158.00	161.00	0	0.3	2
KS-102	161.00	164.00	0	2	2
KS-102	164.00	167.00	0	0.8	2
KS-102	167.00	169.30	0	0.1	2
KS-102	169.30	172.00	0	5.2	3
KS-102	172.00	175.00	0	3.4	2
KS-104	19.00	22.00	0	0	7
KS-104	22.00	24.40	0	0	7
KS-104	24.40	27.60	0	0	8
KS-104	27.60	30.80	0	0	7
KS-104	30.80	33.50	0	0	7
KS-104	33.50	36.30	0	0	0
KS-104	36.30	39.30	0	0	6
KS-104	79.00	82.00	0	0	6
KS-104	82.00	84.60	0	0	6
KS-104	84.60	87.50	0	0	5
KS-104	87.50	90.50	0	1.9	4
KS-104	90.50	93.50	0	16	3
KS-104	93.50	96.50	0	3.2	3
KS-104	96.50	99.50	0	1.6	5
KS-102	102.10	105.00	0	1	6
KS-104	136.30	139.10	1.2	0.2	4
KS-104	139.10	142.00	1.8	0.1	3

DDHS	FROM metres	TO metres	CU (%)	AU (ppm)	CU:AU (%/ppm)	RECOV (%)	ROCK\$	BX	FB	FX	VF
KS-104	142.00	145.00	0.036	0.17	0.212	97	TFAH	50			
KS-104	145.00	148.00	0.056	0.19	0.295	97	TFAH	35	10	45	
KS-104	148.00	151.00	0.052	0.13	0.400	96	TFAH	30	0	30	
KS-104	151.00	154.00	0.032	0.10	0.320	100	TFAH	40	0	40	
KS-104	154.00	157.00	0.020	0.12	0.167	97	TFAH	35	0	35	
KS-104	195.10	198.00	0.036	0.22	0.164	98	CONG			50	
KS-104	198.00	291.00	0.012	0.12	0.100	95	CONG			20	
KS-104	201.00	203.85	0.036	0.39	0.092	92	CONG			40	
KS-104	203.85	207.00	0.015	0.18	0.083	95	SAND			50	
KS-104	207.00	211.60	0.012	0.18	0.067	97	SAND			60	
KS-104	211.60	215.00	0.002	0.02	0.100	94	ANPP				
KS-104	215.00	217.50	0.001	0.01	0.100	92	ANPP				
KS-104	233.00	236.00	0.004	0.01	0.400	95	ANPP				
KS-104	236.00	239.00	0.006	0.01	0.600	100	ANPP				
KS-104	239.00	240.80	0.007	0.01	0.700	83	ANPP				
KS-119	24.54	32.61	0.048	0.16	0.300	8	TUFF			85	
KS-119	32.61	41.26	0.124	0.29	0.428	14	TUFF			75	
KS-119	41.26	47.85	0.241	0.30	0.803	22	TUFF				
KS-119	80.00	83.00	1.090	0.42	2.595	59	TUFF			45	
KS-119	83.00	90.45	0.968	0.49	1.976	30	TUFF			40	
KS-119	90.45	95.09	1.350	0.32	4.219	36	TUFF				
KS-119	95.09	98.00	0.888	0.31	2.865	78	TUFF				
KS-119	98.00	101.00	0.848	0.30	2.827	78	TUFF			55	
KS-119	101.00	105.76	0.246	0.13	1.892	60	PHMG			22	
KS-119	142.00	145.00	0.340	0.18	1.889	100	PHFG			60	
KS-119	145.00	148.00	0.584	0.41	1.424	100	PHFG			60	
KS-119	148.00	151.00	0.496	0.34	1.459	100	PHFG			48	
KS-119	151.00	154.00	0.632	0.26	2.431	100	PHFG			49	
KS-119	154.00	157.00	0.536	0.20	2.680	100	PHFG			70	
KS-119	157.00	160.00	0.488	0.21	2.324	100	PHFG			55	
KS-119	160.00	162.76	0.480	0.24	2.000	100	PHFG			50	
KS-119	202.00	205.75	0.404	0.17	2.376	68	PHMG			62	
KS-119	205.75	208.00	0.592	0.18	3.289	95	PHFG			65	
KS-119	208.00	211.00	0.420	0.12	3.500	98	PHFG			70	
KS-119	211.00	214.00	0.392	0.24	1.633	100	PHFG			65	
KS-119	214.00	217.00	0.512	0.19	2.695	100	PHFG			50	
KS-119	217.00	220.00	0.444	0.18	2.467	95	PHFG			40	
KS-119	220.00	223.00	0.576	0.21	2.743	95	PHFG				
KS-119	223.00	226.00	0.612	0.27	2.267	100	PHFG			70	
KS-119	251.00	254.00	0.042	0.11	0.382	80	PHFG			70	
KS-119	254.00	256.00	0.056	0.13	0.431	60	PHFG				
KS-119	256.00	258.17	0.080	0.13	0.615	60	PHFG				
KS-120	18.70	20.42	0.006	0.08	0.075	76	PHMG			70	
KS-120	20.42	23.46	0.008	0.08	0.100	53	PHMG			55	
KS-120	23.46	26.51	0.010	0.09	0.111	92	PHMG			50	
KS-120	26.51	29.56	0.105	0.10	1.050	100	PHMG			55	
KS-120	29.56	31.50	0.121	0.23	0.526	80	PHMG			40	
KS-120	31.50	34.50	0.117	0.26	0.450	98	PHMG			50	
KS-120	34.50	36.00	0.091	0.11	0.827	87	PHMG			50	
KS-120	36.00	38.40	0.069	0.10	0.690	98	PHMG			40	
KS-120	75.00	78.00	0.572	0.16	3.575	93	PHMG			20	
KS-120	78.00	81.00	0.520	0.18	2.889	98	PHMG			20	
KS-120	81.00	84.00	0.460	0.21	2.190	83	PHMG			20	
KS-120	84.00	87.00	0.368	0.14	2.629	93	PHMG			10	
KS-120	87.00	90.00	0.440	0.11	4.000	95	PHMG			28	
KS-120	90.00	93.57	0.352	0.11	3.200	81	PHMG			30	
KS-120	93.57	96.30	0.069	0.02	3.450	98	ANDY				









DDHS	FROM metres	TO metres	CAV (%)	CAT (%)	AKR (%)	AKV (%)	AKT (%)	MGR (%)	MGV (%)	MGT (%)	HER (%)
KS-104	142.00	145.00	1	1	0	0	0	0	0	0	0
KS-104	145.00	148.00	2.5	2.5	0	0	0	0	0	0	0
KS-104	148.00	151.00	1	1	0	0	0	0	0	0	0
KS-104	151.00	154.00	1	1	0	0	0	0	0	0	0
KS-104	154.00	157.00	1	1	0	0	0	0	0	0	0
KS-104	195.10	198.00	0.1	0.1	0	0	0	0	0	0	0
KS-104	199.00	201.00	1	1	0	0	0	0	0	0	0
KS-104	201.00	203.85	2.5	2.5	0	0	0	0	0	0	0
KS-104	203.85	207.00	0.5	0.5	0	0	0	0	0	0	0
KS-104	207.00	211.60	1	1	0	0	0	0	0	0	0
KS-104	211.60	215.00	2.5	2.5	0	0	0	0	0	0	0
KS-104	215.00	217.50	2.5	2.5	0	0	0	0	0	0	0
KS-104	233.00	236.00	0	0	0	0	0	0	0	0	0
KS-104	236.00	239.00	0	0	0	0	0	0	0	0	0
KS-104	239.00	240.80	0	0	0	0	0	0	0	0	0
KS-119	24.54	32.61	0	0	0	0	0	0	0	0	0
KS-119	32.61	41.26	0	0	0	0	0	0	0	0	0
KS-119	41.26	47.85	0	0	0	0	0	0	0	0	0
KS-119	80.00	83.00	0	0	0	0	0	0	0	0	0
KS-119	83.00	90.45	0	0	0	0	0	0	0	0	0
KS-119	90.45	95.09	0	0	0	0	0	0	0	0	0
KS-119	95.09	98.00	0	0	0	0	0	0	0	0	0
KS-119	98.00	101.00	0	0	0.5	0	0.5	0	0	0	0
KS-119	101.00	105.76	0	0	0	0	0	0	0	0	0
KS-119	142.00	145.00	0	0	0	0.1	0.1	0	0	0	0
KS-119	145.00	148.00	0	0	0	0.1	0.1	0	0	0	0
KS-119	148.00	151.00	0	0	0	0	0	0	0	0	0
KS-119	151.00	154.00	0	0	0	0.001	0.001	0	0	0	0
KS-119	154.00	157.00	0	0	0	0.5	0.5	0	0	0	0
KS-119	157.00	160.00	0	0	0	0.5	0.5	0	0	0	0
KS-119	160.00	162.76	0	0	0	0.1	0.1	0	0	0	0
KS-119	202.00	205.75	0	0	0	0	0	0	0	0	0
KS-119	205.75	208.00	0.1	0.1	0	0	0	0	0	0	0
KS-119	208.00	211.00	0	0	0	0	0	0	0	0	0
KS-119	211.00	214.00	0	0	0	0	0	0	0	0	0
KS-119	214.00	217.00	0.1	0.1	0	0	0	0	0	0	0
KS-119	217.00	220.00	0	0	0	0	0	0	0	0	0
KS-119	220.00	223.00	0	0	0	0	0	0	0	0	0
KS-119	223.00	226.00	0.001	0.001	0	0	0	0	0	0	0
KS-119	251.00	254.00	2.5	2.5	0	0	0	0	0	0	0
KS-119	254.00	256.00	1	1	0	0	0	0	0	0	0
KS-119	256.00	258.17	0	0	0	0	0	0	0	0	0
KS-120	18.70	20.42	0	0	0	0	0	0	0	0	0
KS-120	20.42	23.46	0	0	0	0	0	0	0	0	0
KS-120	23.46	26.51	0	0	0	0	0	0	0	0	0
KS-120	26.51	29.56	0	0	0	0	0	0	0	0	0
KS-120	29.56	31.90	0	0	0	0	0	0	0	0	0
KS-120	31.50	34.50	0	0	0	0	0	0	0	0	0
KS-120	34.50	36.00	0	0	0	0	0	0	0	0	0
KS-120	36.00	38.40	0	0	0	0	0	0	0	0	0
KS-120	75.00	78.00	0	0	0	0.5	0.5	0	0	0	0
KS-120	78.00	81.00	0	0	0	0	0	0	0	0	0
KS-120	81.00	84.00	0	0	0	0	0	0	0	0	0
KS-120	84.00	87.00	0	0	0	0	0	0	0	0	0
KS-120	87.00	90.00	0	0	0	0	0	0	0	0	0
KS-120	90.00	93.57	0	0	0	0	0	0	0	0	0
KS-120	93.57	96.30	2.5	2.5	0	0	0	5	0	5	0







DDHS	FROM metres	TO metres	X2 (%)	X3 (%)	CLEAV
KS-104	142.00	145.00	1.4	0.1	3
KS-104	145.00	148.00	2.1	1	4
KS-104	148.00	151.00	1.2	0	4
KS-104	151.00	154.00	1.1	0	4
KS-104	154.00	157.00	1.3	0.8	4
KS-104	195.10	198.00	0.1	0	5
KS-104	198.00	201.00	0	0.6	5
KS-104	201.00	203.85	0	1.7	5
KS-104	203.85	207.00	0	1.2	5
KS-104	207.00	211.60	0	1.9	4
KS-104	211.60	215.00	0	3.2	3
KS-104	215.00	217.50	0	3.9	3
KS-104	233.00	236.00	0	0	0
KS-104	236.00	239.00	0	0	0
KS-104	239.00	240.80	0	0	0
KS-119	24.54	32.61	0	0	5
KS-119	32.61	41.26	0	0	5
KS-119	41.26	47.85	0	0	5
KS-119	80.00	83.00	0	0	5
KS-119	83.00	90.45	0	0	5
KS-119	90.45	95.09	0	0	6
KS-119	95.09	98.00	0	0	6
KS-119	98.00	101.00	0	0	5
KS-119	101.00	105.76	0	0	5
KS-119	142.00	145.00	0	0	6
KS-119	145.00	148.00	0	0	5
KS-119	148.00	151.00	0	1.5	6
KS-119	151.00	154.00	0	0.2	7
KS-119	154.00	157.00	0	0.5	5
KS-119	157.00	160.00	0	0.5	6
KS-119	160.00	162.76	0	0	6
KS-119	202.00	205.75	0	2.5	6
KS-119	205.75	208.00	0	0	6
KS-119	208.00	211.00	0	0	6
KS-119	211.00	214.00	0	0	6
KS-119	214.00	217.00	0	0	6
KS-119	217.00	220.00	0	0	5
KS-119	220.00	223.00	0	0	5
KS-119	223.00	226.00	0	0	6
KS-119	251.00	254.00	5	0	4
KS-119	254.00	256.00	5	0	4
KS-119	256.00	258.17	2.5	0	4
KS-120	18.70	20.42	0	0	6
KS-120	20.42	23.46	0	0	6
KS-120	23.46	26.51	0	0	6
KS-120	26.51	29.56	0	0	6
KS-120	29.56	31.50	0	0	7
KS-120	31.50	34.50	0	0	6
KS-120	34.50	36.00	0	0	6
KS-120	36.00	38.40	0	0	6
KS-120	75.00	78.00	0	0	6
KS-120	78.00	81.00	0	0	6
KS-120	81.00	84.00	0	0	6
KS-120	84.00	87.00	0	0	6
KS-120	87.00	90.00	0	0	6
KS-120	90.00	93.57	0	0	6
KS-120	93.57	96.30	0	0	1

DDH\$	FROM metres	TO metres	CU (%)	AU (ppm)	CU:AU (%/ppm)	RECOV (%)	ROCK\$	BX	FB	FX	VF
KS-120	135.00	138.00	0.245	0.21	1.167	100	PHPP			60	
KS-120	138.00	141.00	0.227	0.12	1.892	98	PHMG			60	
KS-120	141.00	142.80	0.217	0.16	1.356	94	PHMG			60	
KS-120	142.80	144.85	0.154	0.16	0.963	94	PHMG			60	
KS-120	144.85	148.00	0.004	0.02	0.200	92	ANPP			50	
KS-120	148.00	150.75	0.002	0.01	0.200	95	ANPP			52	
KS-120	150.75	154.00	0.046	0.09	0.511	97	PHMG			60	
KS-120	154.00	157.00	0.056	0.12	0.467	97	PHMG			60	
KS-120	196.00	199.00	0.018	0.17	0.106	98	PHMG			20	
KS-120	199.00	202.00	0.051	0.18	0.283	100	PHMG	15		60	
KS-120	202.00	205.00	0.020	0.15	0.133	100	PHMG			60	
KS-120	205.00	206.55	0.047	0.18	0.261	100	PHFG	45	0	45	
KS-120	206.55	209.00	0.015	0.10	0.150	97	TFCO	35	0	35	
KS-120	209.00	212.00	0.007	0.13	0.054	93	TFCO	30			
KS-120	212.00	213.90	0.006	0.09	0.067	92	VLCO				
KS-120	213.90	217.00	0.009	0.09	0.100	100	PHMG				
KS-123	4.00	7.00	0.057	0.09	0.633	98	BRXX			40	
KS-123	7.00	10.00	0.058	0.09	0.644	100	BRXX			66	
KS-123	10.00	13.00	0.134	0.11	1.218	100	BRXX				
KS-123	13.00	16.00	0.073	0.14	0.521	100	BRXX				
KS-123	50.55	60.05	0.420	0.19	2.211	19	PHMG			60	
KS-123	60.05	63.09	0.396	0.21	1.886	50	PHFG			70	
KS-123	63.09	66.14	0.264	0.15	1.760	66	PHMG			40	
KS-123	66.14	69.19	0.456	0.12	3.800	28	PHMG			63	
KS-123	69.19	72.24	0.244	0.12	2.033	100	PHMG			40	
KS-123	110.64	114.91	0.804	0.40	2.010	12	PHFG				
KS-123	114.91	124.05				0	XCOR				
KS-123	124.05	127.71	1.070	0.54	1.981	20	PHFG				
KS-123	127.71	130.15	1.870	0.84	2.226	86	PHFG				
KS-123	168.90	171.90	0.708	0.43	1.647	100	PHFG			40	
KS-123	171.90	174.90	0.508	0.28	1.814	100	PHFG			50	
KS-123	174.90	176.90	0.524	0.30	1.747	100	PHFG			45	
KS-123	176.90	178.92	0.632	0.26	2.431	97	PHFG			65	
KS-123	178.92	181.97	0.736	0.33	2.230	84	PHFG				
KS-123	181.97	185.01	0.652	0.30	2.173	97	PHFG				
KS-123	185.01	187.40	0.684	0.37	1.849	97	PHFG				
KS-123	187.40	190.40	0.197	0.16	1.231	98	PHMG			60	
KS-123	229.00	232.00	0.648	0.38	1.705	100	PHFG				
KS-123	232.00	235.00	0.752	0.57	1.319	100	PHFG			50	
KS-123	235.00	236.83	0.556	0.17	3.271	100	PHMG				
KS-123	236.83	238.50	0.556	0.24	2.317	100	PHMG			55	
KS-123	238.50	241.15	0.038	0.02	1.900	100	ANDY				
KS-123	241.15	244.15	0.648	0.16	4.050	100	PHMG			60	
KS-123	244.15	247.15	0.636	0.28	2.271	100	PHMG			60	
KS-123	247.15	250.15	0.628	0.34	1.847	100	PHMG			30	
KS-123	286.15	289.15	0.700	0.38	1.842	100	PHMG			60	
KS-123	289.15	291.15	0.936	0.33	2.836	100	PHMG			50	
KS-123	291.15	293.20	0.576	0.48	1.200	100	PHMG			55	
KS-123	293.20	296.20	0.468	0.20	2.340	100	PHMG			60	
KS-123	296.20	298.20	0.352	0.21	1.676	100	PHMG			55	
KS-123	298.20	299.70	0.283	0.18	1.572	100	PHMG			65	
KS-123	299.70	302.70	0.002	0.02	0.100	100	ANPP			65	
KS-123	302.70	314.75	0.002	0.02	0.100	100	ANPP				
KS-123	314.75	317.75	0.079	0.12	0.658	100	PHMG			60	
KS-125	10.55	13.55	0.058	0.11	0.527	93	PHMG			60	
KS-125	13.55	17.00	0.063	0.09	0.700	96	PHMG			65	
KS-125	17.00	20.00	0.035	0.13	0.269	97	BRXX				

DDHS	FROM metres	TO metres	QZR (%)	QZV (%)	QZT (%)	AHR (%)	AHV (%)	AHT (%)	GYR (%)	GYV (%)	GYT (%)
KS-120	135.00	138.00	0	10	10	0	0	0	0	0	0
KS-120	138.00	141.00	0	5	5	0	0	0	0	0	0
KS-120	141.00	142.80	0	5	5	0	0	0	0	0	0
KS-120	142.80	144.85	0	5	5	0	0	0	0	0	0
KS-120	144.85	148.00	0	10	10	0	0	0	0	0	0
KS-120	148.00	150.75	0	5	5	0	0	0	0	0	0
KS-120	150.75	154.00	0	5	5	0	0	0	0	0	0
KS-120	154.00	157.00	0	5	5	0	0	0	0	0	0
KS-120	196.00	199.00	0	2.5	2.5	0	0	0	0	0	0
KS-120	199.00	202.00	0	2.5	2.5	0	0	0	0	0	0
KS-120	202.00	205.00	0	2.5	2.5	0	0	0	0	0	0
KS-120	205.00	206.55	0	0	0	0	0	0	0	0	0
KS-120	206.55	209.00	0	1	1	0	0	0	0	0	0
KS-120	209.00	212.00	0	1	1	0	0	0	0	0	0
KS-120	212.00	213.90	0	1	1	0	0	0	0	0	0
KS-120	213.90	217.00	0	2.5	2.5	0	0	0	0	0	0
KS-123	4.00	7.00	4	1	5	0	0	0	0	0	0
KS-123	7.00	10.00	40	1	41	0	0	0	0	0	0
KS-123	10.00	13.00	50	0	50	0	0	0	0	0	0
KS-123	13.00	16.00	50	2.5	52.5	0	0	0	0	0	0
KS-123	50.55	60.05	0	1	1	0	0	0	0	0	0
KS-123	60.05	63.09	0	1	1	0	0	0	0	0	0
KS-123	63.09	66.14	0	2.5	2.5	0	0	0	0	0	0
KS-123	66.14	69.19	10	1	11	0	0	0	0	0	0
KS-123	69.19	72.24	20	2.5	22.5	0	0	0	0	0	0
KS-123	110.64	114.91	0	2.5	2.5	0	0	0	0	0	0
KS-123	114.91	124.05	0	0	0	0	0	0	0	0	0
KS-123	124.05	127.71	0	5	5	0	0	0	0	0	0
KS-123	127.71	130.15	0	5	5	0	0	0	0	0	0
KS-123	168.90	171.90	0	5	5	0	0	0	2.5	5	7.5
KS-123	171.90	174.90	0	2.5	2.5	0	0	0	0	2.5	2.5
KS-123	174.90	176.90	0	2.5	2.5	0	0	0	0	2.5	2.5
KS-123	176.90	178.92	0	2.5	2.5	0	0	0	0	1	1
KS-123	178.92	181.97	0	2.5	2.5	0	0	0	0	0	0
KS-123	181.97	185.01	5	2.5	7.5	0	0	0	0	0	0
KS-123	185.01	187.40	2.5	2.5	5	0	0	0	0	0	0
KS-123	187.40	190.40	0	1	1	0	0	0	0	0	0
KS-123	229.00	232.00	0	5	5	0	0	0	2.5	0.5	3
KS-123	232.00	235.00	0	5	5	0	0	0	0	2.5	2.5
KS-123	235.00	236.83	10	5	15	0	0	0	0	0	0
KS-123	236.83	238.50	0	5	5	0	0	0	0	0	0
KS-123	238.50	241.15	0	0	0	0	0	0	0	0	0
KS-123	241.15	244.15	0	10	10	0	0	0	0	2.5	2.5
KS-123	244.15	247.15	0	10	10	0	0	0	5	5	10
KS-123	247.15	250.15	0	10	10	0	0	0	5	5	10
KS-123	286.15	289.15	0	30	30	0	0	0	5	5	10
KS-123	289.15	291.15	0	10	10	0	0	0	10	2.5	12.5
KS-123	291.15	293.20	0	10	10	0	0	0	5	5	10
KS-123	293.20	296.20	2.5	10	12.5	0	0	0	0	2.5	2.5
KS-123	296.20	298.20	5	10	15	0	0	0	0	0.5	0.5
KS-123	298.20	299.70	10	2.5	12.5	0	0	0	0	0	0
KS-123	299.70	302.70	0	1	1	0	0	0	0	0	0
KS-123	302.70	314.75	0	0	0	0	0	0	0	0	0
KS-123	314.75	317.75	0	1	1	0	0	0	0	0	0
KS-125	10.55	13.55	10	1	11	0	0	0	0	0	0
KS-125	13.55	17.00	10	0	10	0	0	0	0	0	0
KS-125	17.00	20.00	50	2.5	52.5	0	0	0	0	0	0



DDHS	FROM metres	TO metres	AHGYT (%)	SER (%)	SEV (%)	SET (%)	YSR (%)	YSV (%)	YST (%)	GSR (%)	GSV (%)
KS-120	135.00	138.00	0	2.5	0.5	3	30	0	30	0	0
KS-120	138.00	141.00	0	5	0.1	5.1	30	0	30	0	0
KS-120	141.00	142.80	0	10	0.1	10.1	30	0	30	0	0
KS-120	142.80	144.85	0	30	0	30	0	0	0	0	0
KS-120	144.85	148.00	0	30	0	30	0	0	0	0	0
KS-120	148.00	150.75	0	30	0	30	0	0	0	0	0
KS-120	150.75	154.00	0	10	0	10	30	0	30	1	0
KS-120	154.00	157.00	0	10	0	10	30	0	30	0	0
KS-120	196.00	199.00	0	20	0.5	20.5	10	0	10	0	0
KS-120	199.00	202.00	0	30	0	30	2.5	0	2.5	0	0
KS-120	202.00	205.00	0	30	1	31	2.5	0	2.5	0	0
KS-120	205.00	206.55	0	30	1	31	2.5	0	2.5	0	0
KS-120	206.55	209.00	0	30	0	30	5	0	5	0	0
KS-120	209.00	212.00	0	10	1	11	30	0	30	0	0
KS-120	212.00	213.90	0	10	1	11	30	0	30	0	0
KS-120	213.90	217.00	0	30	1	31	0	0	0	0	0
KS-123	4.00	7.00	0	20	0	20	0	0	0	0	0
KS-123	7.00	10.00	0	20	0.5	20.5	0	0	0	0	0
KS-123	10.00	13.00	0	10	0	10	10	0	10	0	0
KS-123	13.00	16.00	0	20	0	20	0	0	0	0	0
KS-123	50.55	60.05	0	10	0	10	10	0	10	20	0
KS-123	60.05	63.09	0	10	0	10	30	0	30	0	0
KS-123	63.09	66.14	0	5	1	6	30	0	30	0	0
KS-123	66.14	69.19	0	10	0	10	20	0	20	0	0
KS-123	69.19	72.24	0	10	1	11	30	0	30	0	0
KS-123	110.64	114.91	0	10	0	10	0	0	0	30	0
KS-123	114.91	124.05	0	0	0	0	0	0	0	0	0
KS-123	124.05	127.71	0	10	0	10	0	0	0	30	0
KS-123	127.71	130.15	0	10	0	10	0	0	0	30	0
KS-123	168.90	171.90	7.5	10	1	11	0	0	0	20	0
KS-123	171.90	174.90	2.5	10	0	10	20	0	20	10	0
KS-123	174.90	176.90	2.5	10	0	10	30	0	30	0	0
KS-123	176.90	178.92	1	10	0	10	30	0	30	0	0
KS-123	178.92	181.97	0	10	0	10	30	0	30	0	0
KS-123	181.97	185.01	0	20	0	20	20	0	20	0	0
KS-123	185.01	187.40	0	10	0	10	20	0	20	20	0
KS-123	187.40	190.40	0	30	0	30	0	0	0	0	0
KS-123	229.00	232.00	3	10	0	10	1	0	1	5	0
KS-123	232.00	235.00	2.5	10	0	10	0	0	0	0	0
KS-123	235.00	236.83	0	30	0	30	0	0	0	0	0
KS-123	236.83	238.50	0	20	2.5	22.5	20	0	20	10	0
KS-123	238.50	241.15	0	0	0	0	0	0	0	0	0
KS-123	241.15	244.15	2.5	30	0	30	0	0	0	0	0
KS-123	244.15	247.15	10	20	0	20	0	0	0	10	0
KS-123	247.15	250.15	10	30	0	30	0	0	0	0	0
KS-123	286.15	289.15	10	10	2.5	12.5	10	0	10	10	0
KS-123	289.15	291.15	12.5	10	2.5	12.5	10	0	10	0	0
KS-123	291.15	293.20	10	30	0	30	0	0	0	10	0
KS-123	293.20	296.20	2.5	30	0	30	10	0	10	0	0
KS-123	296.20	298.20	0.5	30	0	30	0	0	0	0	0
KS-123	298.20	299.70	0	20	0	20	10	0	10	0	0
KS-123	299.70	302.70	0	30	0	30	0	0	0	0	0
KS-123	302.70	314.75	0	0	0	0	0	0	0	0	0
KS-123	314.75	317.75	0	20	0	20	20	0	20	0	0
KS-125	10.55	13.55	0	40	0	40	0	0	0	0	0
KS-125	13.55	17.00	0	40	0	40	0	0	0	0	0
KS-125	17.00	20.00	0	20	1	21	0	0	0	0	0

DDHS	FROM metres	TO metres	GST (%)	SYGST (%)	KAR (%)	KAV (%)	KAT (%)	CLR (%)	CLV (%)	CLT (%)	CAR (%)
KS-120	135.00	138.00	0	33	0	0	0	0	0	0	0
KS-120	138.00	141.00	0	35.1	5	0	5	0	0	0	0
KS-120	141.00	142.80	0	40.1	5	0	5	0	0	0	0
KS-120	142.80	144.85	0	30	0	0	0	0	0.001	0.001	0
KS-120	144.85	148.00	0	30	0	0	0	10	5	15	0
KS-120	148.00	150.75	0	30	0	0	0	10	2.5	12.5	0
KS-120	150.75	154.00	1	41	0	0	0	0	0	0	0
KS-120	154.00	157.00	0	40	0	2.5	2.5	0	0	0	0
KS-120	196.00	199.00	0	30.5	0	0	0	0	0	0	0
KS-120	199.00	202.00	0	32.5	0	0	0	0	0	0	0
KS-120	202.00	205.00	0	33.5	0	0	0	0	0	0	0
KS-120	205.00	206.55	0	33.5	0	0	0	0	0	0	0
KS-120	206.55	209.00	0	35	0	0	0	0	0	0	0
KS-120	209.00	212.00	0	41	0	0	0	0	0	0	0
KS-120	212.00	213.90	0	41	0	0	0	0	0	0	0
KS-120	213.90	217.00	0	31	0	0	0	0	0	0	0
KS-123	4.00	7.00	0	20	10	0	10	0	0	0	0
KS-123	7.00	10.00	0	20.5	1	0	1	0	0	0	0
KS-123	10.00	13.00	0	20	0	0	0	0	0	0	0
KS-123	13.00	16.00	0	20	0	0.5	0.5	0	0	0	0
KS-123	50.55	60.05	20	40	0	1	1	0	0.1	0.1	0
KS-123	60.05	63.09	0	40	0	0	0	0	0	0	0
KS-123	63.09	66.14	0	36	0	0.5	0.5	0	0	0	0
KS-123	66.14	69.19	0	30	0	1	1	0	0	0	0
KS-123	69.19	72.24	0	41	0	0	0	0	0	0	0
KS-123	110.64	114.91	30	40	0	0	0	0	2.5	2.5	0
KS-123	114.91	124.05	0	0	0	0	0	0	0	0	0
KS-123	124.05	127.71	30	40	0	0	0	0	0	0	0
KS-123	127.71	130.15	30	40	0	0	0	0	0	0	0
KS-123	168.90	171.90	20	31	10	0	10	20	1	21	0
KS-123	171.90	174.90	10	40	0	0	0	10	1	11	0
KS-123	174.90	176.90	0	40	0	0	0	0	1	1	0
KS-123	176.90	178.92	0	40	0	0	0	0	0	0	0
KS-123	178.92	181.97	0	40	0	0	0	0	0	0	0
KS-123	181.97	185.01	0	40	0	0	0	10	1	11	0
KS-123	185.01	187.40	20	50	0	0	0	2.5	1	3.5	0
KS-123	187.40	190.40	0	30	0	0	0	0	0	0	0
KS-123	229.00	232.00	5	16	10	0	10	10	0.1	10.1	0
KS-123	232.00	235.00	0	10	20	0	20	10	0	10	0
KS-123	235.00	236.83	0	30	2.5	0	2.5	0	0.001	0.001	0
KS-123	236.83	238.50	10	52.5	0	0	0	10	1	11	0
KS-123	238.50	241.15	0	0	0	0	0	0	0	0	10
KS-123	241.15	244.15	0	36	10	0	10	5	0	5	0
KS-123	244.15	247.15	10	30	20	0	20	10	1	11	0
KS-123	247.15	250.15	0	30	10	0	10	0	0	0	0
KS-123	286.15	289.15	10	32.5	30	0	30	5	1	6	0
KS-123	289.15	291.15	0	22.5	30	0	30	0	0.5	0.5	0
KS-123	291.15	293.20	10	40	0	0	0	5	1	6	0
KS-123	293.20	296.20	0	40	10	0	10	0	0	0	0
KS-123	296.20	298.20	0	30	0	0	0	0	0	0	0
KS-123	298.20	299.70	0	30	10	0	10	10	0	10	0
KS-123	299.70	302.70	0	30	0	0	0	30	1	31	0
KS-123	302.70	314.75	0	0	0	0	0	0	0	0	0
KS-123	314.75	317.75	0	40	0	0	0	0	0.001	0.001	0
KS-125	10.55	13.55	0	40	2.5	0	2.5	0	0	0	0
KS-125	13.55	17.00	0	40	5	0	5	0	0	0	0
KS-125	17.00	20.00	0	21	0	0.001	0.001	0	0	0	0

DDHS	FROM metres	TO metres	CAV (%)	CAT (%)	AKR (%)	AKV (%)	AKT (%)	MGR (%)	MGV (%)	MGT (%)	HER (%)
KS-120	135.00	138.00	0.1	0.1	0	0	0	0	0	0	0
KS-120	138.00	141.00	0	0	0	0	0	0	0	0	0
KS-120	141.00	142.80	0	0	0	0	0	0	0	0	0
KS-120	142.80	144.85	0	0	0	0	0	0	0	0	0
KS-120	144.85	148.00	2.5	2.5	0	0	0	0	0	0	0
KS-120	148.00	150.75	2.5	2.5	0	0	0	0	0	0	0
KS-120	150.75	154.00	1	1	0	0	0	0	0	0	0
KS-120	154.00	157.00	0	0	0	0	0	0	0	0	0
KS-120	196.00	199.00	2.5	2.5	0	0	0	0	0	0	0
KS-120	199.00	202.00	2.5	2.5	0	0	0	0	0	0	0
KS-120	202.00	205.00	2.5	2.5	0	0	0	0	0	0	0
KS-120	205.00	206.55	2.5	2.5	0	0	0	0	0	0	0
KS-120	206.55	209.00	2.5	2.5	0	0	0	0	0	0	0
KS-120	209.00	212.00	2.5	2.5	0	0	0	0	0	0	0
KS-120	212.00	213.90	2.5	2.5	0	0	0	0	0	0	0
KS-120	213.90	217.00	5	5	0	0	0	0	0	0	0
KS-123	4.00	7.00	0	0	0	0	0	0	0	0	0
KS-123	7.00	10.00	0	0	0	0	0	0	0	0	0
KS-123	10.00	12.00	0	0	0	0	0	0	0	0	0
KS-123	13.00	16.00	0	0	0	0	0	0	0	0	0
KS-123	50.55	60.05	0	0	0	0	0	0	0	0	0
KS-123	60.05	63.09	0	0	0	0	0	0	0	0	0
KS-123	63.09	66.14	0	0	0	0	0	0	0	0	0
KS-123	66.14	69.19	0	0	0	0	0	0	0	0	0
KS-123	69.19	72.24	0	0	0	1	1	0	0	0	0
KS-123	110.64	114.91	0	0	0	0	0	0	0	0	0
KS-123	114.91	124.05	0	0	0	0	0	0	0	0	0
KS-123	124.05	127.71	0	0	0	0	0	0	0	0	0
KS-123	127.71	130.15	0	0	0	0	0	0	0	0	0
KS-123	168.90	171.90	0	0	0	0	0	0	0	0	0
KS-123	171.90	174.90	1	1	0	0	0	0	0	0	0
KS-123	174.90	176.90	1	1	0	0	0	0	0	0	0
KS-123	176.90	178.92	1	1	0	0	0	0	0	0	0
KS-123	178.92	181.97	0	0	0	0	0	0	0	0	0
KS-123	181.97	185.01	0	0	0	0	0	0	0	0	0
KS-123	185.01	187.40	0	0	0	0	0	0	0	0	0
KS-123	187.40	190.40	1	1	0	0	0	0	0	0	0
KS-123	229.00	232.00	1	1	0	0	0	0	0	0	2.5
KS-123	232.00	235.00	0	0	0	0	0	0	0	0	0
KS-123	235.00	236.83	0	0	0	0	0	0	0	0	0
KS-123	236.83	238.50	0	0	0	0	0	0	0	0	0
KS-123	238.50	241.15	0	10	0	0	0	10	0	10	0
KS-123	241.15	244.15	1	1	0	0	0	0	0	0	0
KS-123	244.15	247.15	1	1	0	0	0	0	0	0	0
KS-123	247.15	250.15	0	0	0	0	0	0	0	0	0
KS-123	286.15	289.15	0	0	0	0	0	0	0	0	0
KS-123	289.15	291.15	0	0	0	0	0	0	0	0	0
KS-123	291.15	293.20	0	0	0	0	0	0	0	0	0
KS-123	293.20	296.20	0	0	0	0	0	0	0	0	0
KS-123	296.20	298.20	0	0	0	0	0	0	0	0	0
KS-123	298.20	299.70	0	0	0	0	0	0	0	0	0
KS-123	299.70	302.70	1	1	0	0	0	0	0	0	0
KS-123	302.70	314.75	0	0	0	0	0	0	0	0	0
KS-123	314.75	317.75	1	1	0	0	0	0	0	0	0
KS-125	10.55	13.55	0	0	0	0	0	0	0	0	0
KS-125	13.55	17.00	0	0	0	0	0	0	0	0	0
KS-125	17.00	20.00	0.001	0.001	0	0	0	0	0	0	0

DDHS	FROM metres	TO metres	HEV (%)	HET (%)	RUR (%)	RUV (%)	RUT (%)	PYR (%)	PYV (%)	PYT (%)	CPR (%)
KS-120	135.00	138.00	0	0	0	0	0	10	1	11	0
KS-120	138.00	141.00	0	0	0	0	0	5	2.5	7.5	0
KS-120	141.00	142.80	0	0	0	0	0	10	2.5	12.5	0
KS-120	142.80	144.85	0.001	0.001	0	0	0	5	1	6	0
KS-120	144.85	148.00	1	1	0	0	0	0	0	0	0
KS-120	148.00	150.75	0	0	0	0	0	0	0	0	0
KS-120	150.75	154.00	0	0	0	0	0	5	1	6	0
KS-120	154.00	157.00	0	0	0	0	0	10	5	15	0
KS-120	196.00	199.00	0	0	0	0	0	10	2.5	12.5	0
KS-120	199.00	202.00	0	0	0	0	0	5	1	6	0
KS-120	202.00	205.00	0	0	0	0	0	10	1	11	0
KS-120	205.00	206.55	0	0	0	0	0	5	1	6	0
KS-120	206.55	209.00	0	0	0	0	0	5	1	6	0
KS-120	209.00	212.00	0	0	0	0	0	10	0.5	10.5	0
KS-120	212.00	213.90	0	0	0	0	0	5	1	6	0
KS-120	213.90	217.00	0	0	0	0	0	5	2.5	7.5	0
KS-123	4.00	7.00	0	0	0	0	0	5	0	5	0
KS-123	7.00	10.00	0	0	0	0	0	5	0	5	0
KS-123	10.00	13.00	0	0	0	0	0	2.5	0.1	2.6	0
KS-123	13.00	16.00	0	0	0	0	0	5	0.5	5.5	0
KS-123	50.55	60.05	0	0	0	0	0	5	1	6	0
KS-123	60.05	63.09	0	0	0	0	0	2.5	1	3.5	0
KS-123	63.09	66.14	0	0	0	0	0	2.5	1	3.5	0
KS-123	66.14	69.19	0	0	0	0	0	5	2.5	7.5	0
KS-123	69.19	72.24	1	1	0	0	0	5	1	6	0
KS-123	110.64	114.91	2.5	2.5	0	0	0	5	2.5	7.5	0
KS-123	114.91	124.05	0	0	0	0	0	0	0	0	0
KS-123	124.05	127.71	5	5	0	0	0	0	2.5	2.5	0
KS-123	127.71	130.15	1	1	0	0	0	2.5	2.5	5	0
KS-123	168.90	171.90	1	1	0	0	0	2.5	2.5	5	1
KS-123	171.90	174.90	0	0	0	0	0	2.5	2.5	5	0.5
KS-123	174.90	176.90	0	0	0	0	0	5	1	6	0.5
KS-123	176.90	178.92	0	0	0	0	0	10	5	15	0
KS-123	178.92	181.97	0	0	0	0	0	10	2.5	12.5	0.5
KS-123	181.97	185.01	0	0	0	0	0	10	2.5	12.5	0.5
KS-123	185.01	187.40	0	0	0	0	0	5	1	6	0.5
KS-123	187.40	190.40	0	0	0	0	0	5	1	6	0
KS-123	229.00	232.00	2.5	5	0	0	0	5	2.5	7.5	0.5
KS-123	232.00	235.00	1	1	0	0	0	2.5	2.5	5	1
KS-123	235.00	236.83	0	0	0	0	0	2.5	2.5	5	1
KS-123	236.83	238.50	1	1	0	0	0	5	0	5	0
KS-123	238.50	241.15	0	0	0	0	0	0	0	0	0
KS-123	241.15	244.15	0	0	0	0	0	10	5	15	0
KS-123	244.15	247.15	0.5	0.5	0	0	0	5	5	10	1
KS-123	247.15	250.15	0	0	0	0	0	2.5	1	3.5	0
KS-123	286.15	289.15	0	0	0	0	0	5	2.5	7.5	0
KS-123	289.15	291.15	0	0	0	0	0	2.5	2.5	5	0
KS-123	291.15	293.20	0	0	0	0	0	10	2.5	12.5	0
KS-123	293.20	296.20	0	0	0	0	0	10	1	11	1
KS-123	296.20	298.20	0	0	0	0	0	5	1	6	0
KS-123	298.20	299.70	0	0	0	0	0	5	1	6	0.5
KS-123	299.70	302.70	0	0	0	0	0	0	0	0	0
KS-123	302.70	314.75	0	0	0	0	0	0	0	0	0
KS-123	314.75	317.75	0	0	0	0	0	10	2.5	12.5	0
KS-125	10.55	13.55	0	0	0	0	0	5	0.5	5.5	0
KS-125	13.55	17.00	0	0	0	0	0	5	0	5	0
KS-125	17.00	20.00	0	0	0	0	0	10	1	11	0



[illegible]

DDHS	FROM metres	TO metres	X2 (%)	X3 (%)	CLEAV
KS-120	135.00	138.00	0.5	0	6
KS-120	138.00	141.00	0	0	6
KS-120	141.00	142.80	0	0	6
KS-120	142.80	144.85	0	0.5	6
KS-120	144.85	148.00	0	10	4
KS-120	148.00	150.75	0	9	4
KS-120	150.75	154.00	0.2	0	6
KS-120	154.00	157.00	2.1	0	6
KS-120	196.00	199.00	2.1	0	5
KS-120	199.00	202.00	0.9	0	6
KS-120	202.00	205.00	2.8	0.3	5
KS-120	205.00	206.55	4.2	0	6
KS-120	206.55	209.00	2.6	0	5
KS-120	209.00	212.00	2.2	0.3	5
KS-120	212.00	213.90	3.5	0	4
KS-120	213.90	217.00	4.3	0.5	4
KS-123	4.00	7.00	0	0	4
KS-123	7.00	10.00	0	0	4
KS-123	10.00	13.00	0	0	4
KS-123	13.00	16.00	0	1	4
KS-123	50.55	60.05	0	1	5
KS-123	60.05	63.09	0	0	5
KS-123	63.09	66.14	0	0	6
KS-123	66.14	69.19	0	0	6
KS-123	69.19	72.24	0	0	4
KS-123	110.64	114.91	0	0	5
KS-123	114.91	124.05	0	0	0
KS-123	124.05	127.71	0	0	6
KS-123	127.71	130.15	0	0	6
KS-123	168.90	171.90	0	0	5
KS-123	171.90	174.90	0	0	5
KS-123	174.90	176.90	0	0	6
KS-123	176.90	178.92	0	0	6
KS-123	178.92	181.97	0	0	6
KS-123	181.97	185.01	0	0	5
KS-123	185.01	187.40	0	0	5
KS-123	187.40	190.40	0	0	6
KS-123	229.00	232.00	0	0	5
KS-123	232.00	235.00	0	2	5
KS-123	235.00	236.83	0	0	5
KS-123	236.83	238.50	0	0	7
KS-123	238.50	241.15	0	0	0
KS-123	241.15	244.15	0	0	6
KS-123	244.15	247.15	0	0	6
KS-123	247.15	250.15	0	0	6
KS-123	286.15	289.15	0	0	6
KS-123	289.15	291.15	0	0	6
KS-123	291.15	293.20	0	0	7
KS-123	293.20	296.20	0	0	6
KS-123	296.20	298.20	0	0	7
KS-123	298.20	299.70	0	0	6
KS-123	299.70	302.70	0	1	4
KS-123	302.70	314.75	0	0	0
KS-123	314.75	317.75	0	1	7
KS-125	10.55	13.55	0	0	4
KS-125	13.55	17.00	0	0	5
KS-125	17.00	20.00	0	2.5	5

DDH\$	FROM metres	TO metres	CU (%)	AU (ppm)	CU:AU (%/ppm)	RECOV (%)	ROCK\$	BX	FB	FX	VF
KS-125	20.00	23.00	0.042	0.11	0.382	97	BRXX				
KS-125	23.00	26.00	0.046	0.08	0.575	87	BRXX			65	
KS-125	26.00	29.00	0.050	0.09	0.556	98	BRXX			70	
KS-125	29.00	32.00	0.044	0.08	0.550	93	BRXX				
KS-125	69.00	72.00	0.163	0.23	0.709	87	PHFG			60	
KS-125	72.00	75.00	0.158	0.18	0.878	92	PHFG			60	
KS-125	75.00	78.90	0.162	0.20	0.810	90	PHFG			63	
KS-125	78.90	84.43	0.068	0.09	0.756	38	PHMG			61	
KS-125	84.43	89.72	0.290	0.20	1.450	60	PHFG			50	
KS-125	127.10	130.15				0	XCOR				
KS-125	130.15	133.20	0.644	0.14	4.600	40	TUFF				
KS-125	133.20	140.30	0.636	0.24	2.650	17	TUFF				
KS-125	140.30	143.00	0.744	0.23	3.235	96	TUFF				
KS-125	143.00	146.00	0.764	0.23	3.322	97	PHFG			55	
KS-125	185.00	188.00	0.672	0.35	1.920	100	PHFG			75	
KS-125	188.00	191.00	0.600	1.16	0.517	100	PHFG				
KS-125	191.00	194.00	0.566	0.33	1.715	100	PHFG			67	
KS-125	194.00	197.00	0.620	0.38	1.632	100	PHFG			50	
KS-125	197.00	200.00	0.552	0.39	1.415	100	PHFG			65	
KS-125	200.00	203.00	0.584	0.35	1.669	100	PHFG			55	
KS-125	203.00	206.00	0.592	0.37	1.600	100	PHFG			45	
KS-125	243.00	246.00	0.712	0.29	2.455	90	PHFG				
KS-125	246.00	249.00	1.400	0.56	2.500	94	PHFG				
KS-125	249.00	252.00	0.904	0.29	3.117	94	PHFG				
KS-125	252.00	255.00	0.624	0.36	1.733	96	PHFG				
KS-125	255.00	258.00	0.564	0.36	1.567	98	PHFG				
KS-125	258.00	259.60	0.624	0.36	1.733	98	PHFG			55	
KS-125	262.40	265.00	0.728	0.27	2.696	99	PHFG			70	
KS-125	301.00	304.00	0.608	0.34	1.788	99	PHFG				
KS-125	304.00	307.00	0.624	0.41	1.522	98	PHFG				
KS-125	307.00	310.00	0.564	0.32	1.763	99	PHFG				
KS-125	310.00	313.00	0.444	0.24	1.850	98	PHFG			70	
KS-125	313.00	316.00	0.540	0.32	1.688	99	PHFG			52	
KS-125	316.00	319.00	0.440	0.26	1.692	96	PHMG			35	
KS-125	319.00	322.00	0.360	0.21	1.714	98	PHMG			70	
KS-125	362.00	365.00	0.048	0.19	0.253	99	PHFG			60	
KS-125	365.00	367.89	0.055	0.35	0.157	98	PHFG			60	
KS-132	81.05	84.10	0.011	0.05	0.220	55	TUFF			7	
KS-132	84.10	87.05	0.011	0.02	0.550	83	TUFF			10	
KS-132	87.05	88.40	0.017	0.02	0.850	98	FRAG			10	
KS-132	88.40	91.35	0.020	0.02	1.000	98	TUFF			10	
KS-132	117.30	120.30	0.034	0.12	0.283	100	TFAH	10	35	45	
KS-132	120.30	123.30	0.025	0.10	0.250	100	TFAH	30	25	55	
KS-132	123.30	125.30	0.045	0.16	0.281	100	TFAH	10	10	20	
KS-132	125.30	127.40	0.032	0.06	0.533	100	TFAH			45	
KS-132	127.40	129.40	0.027	0.07	0.386	100	PHFG			47	
KS-132	129.40	131.30	0.071	0.06	1.183	100	PHFG				
KS-132	131.30	134.30	0.065	0.08	0.813	100	TFAH				
KS-132	134.30	137.30	0.047	0.08	0.588	100	TFAH	65	55	10	
KS-132	137.30	140.30	0.087	0.08	1.088	100	TFAH	70			



DDHS	FROM metres	TO metres	QZR (%)	QZV (%)	QZT (%)	AHR (%)	AHV (%)	AHT (%)	GYR (%)	GYV (%)	GYT (%)
KS-125	20.00	23.00	50	1	51	0	0	0	0	0	0
KS-125	23.00	26.00	50	0.5	50.5	0	0	0	0	0	0
KS-125	26.00	29.00	50	1	51	0	0	0	0	0	0
KS-125	29.00	32.00	40	2.5	42.5	0	0	0	0	0	0
KS-125	69.00	72.00	0	2.5	2.5	0	0	0	0	0	0
KS-125	72.00	75.00	0	5	5	0	0	0	0	0	0
KS-125	75.00	78.90	0	0	0	0	0	0	0	0	0
KS-125	78.90	84.43	10	0	10	0	0	0	0	0	0
KS-125	84.43	89.72	0	0	0	0	0	0	0	0	0
KS-125	127.10	130.15	0	0	0	0	0	0	0	0	0
KS-125	130.15	133.20	10	1	11	0	0	0	0	0	0
KS-125	133.20	140.30	10	0	10	0	0	0	0	0	0
KS-125	140.30	143.00	0	5	5	0	2.5	2.5	0	2.5	2.5
KS-125	143.00	146.00	0	5	5	0	2.5	2.5	0	2.5	2.5
KS-125	185.00	188.00	0	20	20	10	0	10	0	0	0
KS-125	188.00	191.00	0	10	10	10	1	11	0	0	0
KS-125	191.00	194.00	0	20	20	5	2.5	7.5	0	0	0
KS-125	194.00	197.00	0	2.5	2.5	1	5	6	0	0	0
KS-125	197.00	200.00	0	5	5	0	2.5	2.5	0	0	0
KS-125	200.00	203.00	0	5	5	0	1	1	0	2.5	2.5
KS-125	203.00	206.00	0	5	5	0	5	5	0	0	0
KS-125	243.00	246.00	0	5	5	0	0	0	0	5	5
KS-125	246.00	249.00	0	5	5	5	0	5	0	0	0
KS-125	249.00	252.00	0	5	5	0	0	0	0	0	0
KS-125	252.00	255.00	0	5	5	2.5	5	7.5	0	5	5
KS-125	255.00	258.00	0	0	0	5	0	5	0	1	1
KS-125	258.00	259.60	0	5	5	0	0	0	0	2.5	2.5
KS-125	262.40	265.00	0	5	5	0	0	0	0	0	0
KS-125	301.00	304.00	0	5	5	0	2.5	2.5	0	0	0
KS-125	304.00	307.00	0	10	10	0	2.5	2.5	0	1	1
KS-125	307.00	310.00	0	2.5	2.5	0	1	1	0	0	0
KS-125	310.00	313.00	0	2.5	2.5	0	5	5	0	1	1
KS-125	313.00	316.00	0	2.5	2.5	0	2.5	2.5	0	0	0
KS-125	316.00	319.00	0	1	1	0	2.5	2.5	0	0	0
KS-125	319.00	322.00	10	1	11	0	0	0	0	0	0
KS-125	362.00	365.00	0	5	5	0	0	0	0	0	0
KS-125	365.00	367.89	0	2.5	2.5	0	0	0	0	0	0
KS-132	81.05	84.10	0	1	1	0	0	0	0	0	0
KS-132	84.10	87.05	0	1	1	0	0	0	0	0	0
KS-132	87.05	88.40	0	5	5	0	0	0	0	0	0
KS-132	88.40	91.35	0	0	0	0	0	0	0	0	0
KS-132	117.30	120.30	0	1	1	0	0	0	0	0	0
KS-132	120.30	123.30	0	0	0	0	0	0	0	0	0
KS-132	123.30	125.30	0	0	0	0	0	0	0	0	0
KS-132	125.30	127.40	0	0	0	0	0	0	0	0	0
KS-132	127.40	129.40	0	0	0	0	0	0	0	0	0
KS-132	129.40	131.30	0	0	0	0	0	0	0	0	0
KS-132	131.30	134.30	0	0	0	0	0	0	0	0	0
KS-132	134.30	137.30	0	0.5	0.5	0	0	0	0	0	0
KS-132	137.30	140.30	0	0.5	0.5	0	0	0	0	0	0

DDH\$	FROM metres	TO metres	AHGYT (%)	SER (%)	SEV (%)	SET (%)	YSR (%)	YSV (%)	YST (%)	GSR (%)	GSV (%)
KS-125	20.00	23.00	0	20	0	20	0	0	0	0	0
KS-125	23.00	26.00	0	20	0	20	0	0	0	0	0
KS-125	26.00	29.00	0	30	0	30	0	0	0	0	0
KS-125	29.00	32.00	0	40	0	40	0	0	0	0	0
KS-125	69.00	72.00	0	10	1	11	40	0	40	0	0
KS-125	72.00	75.00	0	10	2.5	12.5	40	0	40	0	0
KS-125	75.00	78.90	0	10	1	11	20	0	20	20	0
KS-125	78.90	84.43	0	30	0	30	0	0	0	0	0
KS-125	84.43	89.72	0	10	0	10	40	0	40	2.5	0
KS-125	127.10	130.15	0	10	0	0	0	0	0	0	0
KS-125	130.15	133.20	0	10	0	10	30	0	30	0	0
KS-125	133.20	140.30	0	10	0	10	20	0	20	20	0
KS-125	140.30	143.00	5	0	0	0	10	0	10	40	0
KS-125	143.00	146.00	5	0	0	0	20	0	20	20	0
KS-125	185.00	188.00	10	20	0	20	10	0	10	0.1	0
KS-125	188.00	191.00	11	10	0	10	20	0	20	20	0
KS-125	191.00	194.00	7.5	0	0	0	10	0	10	20	0
KS-125	194.00	197.00	6	10	0	10	10	0	10	30	0
KS-125	197.00	200.00	2.5	5	0	5	0	0	0	30	0
KS-125	200.00	203.00	3.5	10	0	10	20	0	20	10	0
KS-125	203.00	206.00	5	10	0	10	20	0	20	20	0
KS-125	243.00	246.00	5	10	0	10	0	0	0	20	0
KS-125	246.00	249.00	5	30	1	31	0	0	0	10	0
KS-125	249.00	252.00	0	10	1	11	0	0	0	10	0
KS-125	252.00	255.00	12.5	5	0	5	1	0	1	20	0
KS-125	255.00	258.00	6	10	1	11	5	0	5	20	0
KS-125	258.00	259.60	2.5	10	0	10	20	0	20	10	0
KS-125	262.40	265.00	0	20	0	20	10	0	10	10	0
KS-125	301.00	304.00	2.5	10	0	10	5	0	5	20	0
KS-125	304.00	307.00	3.5	10	0	10	0	0	0	20	0
KS-125	307.00	310.00	1	0	1	1	0	0	0	20	0
KS-125	310.00	313.00	6	30	2.5	32.5	0	0	0	10	0
KS-125	313.00	316.00	2.5	30	0	30	0	0	0	2.5	0
KS-125	316.00	319.00	2.5	30	0	30	10	0	10	5	0
KS-125	319.00	322.00	0	30	0	30	0	0	0	0	0
KS-125	362.00	365.00	0	0	10	10	30	0	30	0	0
KS-125	365.00	367.89	0	0	10	10	30	0	30	0	0
KS-132	81.05	84.10	0	50	0	50	0	0	0	0	0
KS-132	84.10	87.05	0	50	0	50	0	0	0	0	0
KS-132	87.05	88.40	0	40	0	40	10	0	10	0	0
KS-132	88.40	91.35	0	60	0	60	0	0	0	0	0
KS-132	117.30	120.30	0	50	0	50	1	0	1	0	0
KS-132	120.30	123.30	0	50	0	50	0	0	0	0	0
KS-132	123.30	125.30	0	50	0	50	0	0	0	0	0
KS-132	125.30	127.40	0	50	0	50	0	0	0	0	0
KS-132	127.40	129.40	0	40	0	40	0	0	0	0	0
KS-132	129.40	131.30	0	40	0	40	0	0	0	0	0
KS-132	131.30	134.30	0	40	0	40	0	0	0	0	0
KS-132	134.30	137.30	0	40	1	41	0	0	0	0	0
KS-132	137.30	140.30	0	40	0	40	0	0	0	0	0

DDHS	FROM metres	TO metres	GST (%)	SYGST (%)	KAR (%)	KAV (%)	KAT (%)	CLR (%)	CLV (%)	CLT (%)	CAR (%)
KS-125	20.00	23.00	0	20	0	0	0	0	0	0	0
KS-125	23.00	26.00	0	20	2.5	0	2.5	0	0	0	0
KS-125	26.00	29.00	0	30	1	0	1	0	0	0	0
KS-125	29.00	32.00	0	40	0	0	0	1	0	1	0
KS-125	69.00	72.00	0	51	0	0	0	0	0	0	0
KS-125	72.00	75.00	0	52.5	0	0	0	0	0.1	0.1	0
KS-125	75.00	78.90	20	51	0	0.5	0.5	0	1	1	0
KS-125	78.90	84.43	0	30	20	0	20	0	0	0	0
KS-125	84.43	89.72	2.5	52.5	0	0	0	0	0	0	0
KS-125	127.10	130.15	0	0	0	0	0	0	0	0	0
KS-125	130.15	133.20	0	40	0	0	0	0	0	0	0
KS-125	133.20	140.30	20	50	0	0	0	0	0	0	0
KS-125	140.30	143.00	40	50	0	0.5	0.5	0	0.1	0.1	0
KS-125	143.00	146.00	20	40	10	0	10	0	1	1	0
KS-125	185.00	188.00	0.1	30.1	0	0	0	0	0	0	0
KS-125	188.00	191.00	20	50	0	0	0	0	1	1	0
KS-125	191.00	194.00	20	30	10	0	10	5	0	5	0
KS-125	194.00	197.00	30	50	0	0	0	10	1	11	0
KS-125	197.00	200.00	30	35	0	0	0	10	1	11	0
KS-125	200.00	203.00	10	40	0	0	0	2.5	0.5	3	0
KS-125	203.00	206.00	20	50	0	0	0	0	0.5	0.5	0
KS-125	243.00	246.00	20	30	0	0	0	5	1	6	0
KS-125	246.00	249.00	10	41	0	0	0	0	1	1	0
KS-125	249.00	252.00	10	21	0	0	0	5	1	6	0
KS-125	252.00	255.00	20	26	10	0	10	10	0	10	0
KS-125	255.00	258.00	20	36	0	0	0	0	1	1	0
KS-125	258.00	259.60	10	40	0	0	0	0	1	1	0
KS-125	262.40	265.00	10	40	0	0	0	1	0	1	0
KS-125	301.00	304.00	20	35	0	0	0	20	1	21	0
KS-125	304.00	307.00	20	30	10	0	10	0	0	0	0
KS-125	307.00	310.00	20	21	2.5	0	2.5	20	0.1	20.1	0
KS-125	310.00	313.00	10	42.5	0	0	0	0	0	0	0
KS-125	313.00	316.00	2.5	32.5	10	0	10	0	0.1	0.1	0
KS-125	316.00	319.00	5	45	0	0	0	0	0	0	0
KS-125	319.00	322.00	0	30	0	0	0	0	0.1	0.1	0
KS-125	362.00	365.00	0	40	0	0	0	0	0	0	0
KS-125	365.00	367.89	0	40	0	0	0	0	0	0	0
KS-132	81.05	84.10	0	50	0	0	0	0	0	0	0
KS-132	84.10	87.05	0	50	0	0	0	0	0	0	0
KS-132	87.05	88.40	0	50	0	0	0	0	0	0	0
KS-132	88.40	91.35	0	60	0	0	0	0	0	0	0
KS-132	117.30	120.30	0	51	0	0	0	0	0	0	0
KS-132	120.30	123.30	0	50	0	0	0	0	0	0	0
KS-132	123.30	125.30	0	50	0	0	0	0	0	0	0
KS-132	125.30	127.40	0	50	0	0	0	0	0	0	0
KS-132	127.40	129.40	0	40	0	0	0	0	0	0	0
KS-132	129.40	131.30	0	40	0	0	0	0	0	0	0
KS-132	131.30	134.30	0	40	0	0	0	0	0	0	0
KS-132	134.30	137.30	0	41	0	0	0	0	0	0	0
KS-132	137.30	140.30	0	40	0	0	0	0	0	0	0

DDH\$	FROM metres	TO metres	CAV (%)	CAT (%)	AKR (%)	AKV (%)	AKT (%)	MGR (%)	MGV (%)	MGT (%)	HER (%)
KS-125	20.00	23.00	0	0	0	0	0	0	0	0	0
KS-125	23.00	26.00	0	0	0	0	0	0	0	0	0
KS-125	26.00	29.00	0	0	0	0	0	0	0	0	0
KS-125	29.00	32.00	0	0	0	0	0	0	0	0	0
KS-125	69.00	72.00	0	0	0	1	1	0	0	0	0
KS-125	72.00	75.00	0	0	0	0.5	0.5	0	0	0	0
KS-125	75.00	78.90	0	0	0	0	0	0	0	0	0
KS-125	78.90	84.43	0	0	0	0	0	0	0	0	0
KS-125	84.43	89.72	0	0	0	0	0	0	0	0	0
KS-125	127.10	130.15	0	0	0	0	0	0	0	0	0
KS-125	130.15	133.20	0	0	0	0	0	0	0	0	0
KS-125	133.20	140.30	0	0	0	0	0	0	0	0	0
KS-125	140.30	143.00	0	0	0	0	0	0	0	0	0
KS-125	143.00	146.00	0	0	0	0	0	0	0	0	0
KS-125	185.00	188.00	0	0	0	0	0	0	0	0	0
KS-125	188.00	191.00	0	0	0	1	1	0	0	0	1
KS-125	191.00	194.00	0	0	0	0	0	2.5	1	3.5	0
KS-125	194.00	197.00	0	0	0	0.5	0.5	0	0	0	0
KS-125	197.00	200.00	0	0	0	0	0	0	0	0	0
KS-125	200.00	203.00	0	0	0	0	0	0	0	0	0
KS-125	203.00	206.00	0	0	0	0	0	0	0	0	0
KS-125	243.00	246.00	0	0	0	0	0	0	0	0	5
KS-125	246.00	249.00	0	0	0	0	0	0	0	0	0
KS-125	249.00	252.00	0	0	0	1	1	0	0	0	2.5
KS-125	252.00	255.00	0	0	0	0	0	0	0	0	2.5
KS-125	255.00	258.00	0	0	0	0	0	0	0	0	0
KS-125	258.00	259.60	1	1	0	0	0	0	0	0	0
KS-125	262.40	265.00	0	0	0	1	1	0	0	0	0
KS-125	301.00	304.00	0	0	0	1	1	0	0	0	0
KS-125	304.00	307.00	0	0	0	0	0	0	0	0	0
KS-125	307.00	310.00	0.5	0.5	0	0	0	0	0	0	0
KS-125	310.00	313.00	0	0	0	0.5	0.5	0	0	0	0
KS-125	313.00	316.00	0	0	0	0	0	0	0	0	0
KS-125	316.00	319.00	0	0	0	0	0	0	0	0	0
KS-125	319.00	322.00	0	0	0	0	0	0	0	0	0
KS-125	362.00	365.00	5	5	0	0	0	0	0	0	0
KS-125	365.00	367.89	5	5	0	0	0	0	0	0	0
KS-132	81.05	84.10	1	1	0	0	0	0	0	0	0
KS-132	84.10	87.05	1	1	0	0	0	0	0	0	0
KS-132	87.05	88.40	2.5	2.5	0	0	0	0	0	0	0
KS-132	88.40	91.35	0	0	0	0	0	0	0	0	0
KS-132	117.30	120.30	0	0	0	0	0	0	0	0	0
KS-132	120.30	123.30	0	0	0	0	0	0	0	0	0
KS-132	123.30	125.30	0	0	0	0	0	0	0	0	0
KS-132	125.30	127.40	0	0	0	0	0	0	0	0	0
KS-132	127.40	129.40	0	0	0	0	0	0	0	0	0
KS-132	129.40	131.30	0	0	0	0	0	0	0	0	0
KS-132	131.30	134.30	0.1	0.1	0	0	0	0	0	0	0
KS-132	134.30	137.30	0	0	0	0	0	0	0	0	0
KS-132	137.30	140.30	0.5	0.5	0	0	0	0	0	0	0

DDHS	FROM metres	TO metres	HEV (%)	HET (%)	RUR (%)	RUV (%)	RUT (%)	PYR (%)	PYV (%)	PYT (%)	CPR (%)
KS-125	20.00	23.00	0	0	0	0	0	5	0.1	5.1	0
KS-125	23.00	26.00	0	0	0	0	0	5	0.5	5.5	0
KS-125	26.00	29.00	0	0	0	0	0	10	0.1	10.1	0
KS-125	29.00	32.00	0	0	0	0	0	10	1	11	0
KS-125	69.00	72.00	0	0	0	0	0	1	5	6	0
KS-125	72.00	75.00	0	0	0	0	0	5	5	10	0
KS-125	75.00	78.90	0	0	0	0	0	5	5	10	0
KS-125	78.90	84.43	0	0	0	0	0	0	0	0	0
KS-125	84.43	89.72	0	0	0	0	0	5	0	5	0
KS-125	127.10	130.15	0	0	0	0	0	0	0	0	0
KS-125	130.15	133.20	0	0	0	0	0	2.5	2.5	5	0
KS-125	133.20	140.30	0	0	0	0	0	5	1	6	0
KS-125	140.30	143.00	0.1	0.1	0	0	0	2.5	2.5	5	0
KS-125	143.00	146.00	0.5	0.5	0	0	0	1	2.5	3.5	0.5
KS-125	185.00	188.00	2.5	2.5	0	0	0	5	5	10	1
KS-125	188.00	191.00	0	1	0	0	0	10	10	20	0.5
KS-125	191.00	194.00	1	1	0	0	0	0.5	2.5	3	0
KS-125	194.00	197.00	0.5	0.5	0	0	0	5	2.5	7.5	0
KS-125	197.00	200.00	1	1	0	0	0	2.5	1	3.5	1
KS-125	200.00	203.00	0	0	0	0	0	2.5	2.5	5	0.5
KS-125	203.00	206.00	1	1	0	0	0	2.5	1	3.5	0
KS-125	243.00	246.00	5	10	0	0	0	5	1	6	0
KS-125	246.00	249.00	5	5	0	0	0	10	10	20	0
KS-125	249.00	252.00	5	7.5	0	0	0	5	2.5	7.5	0
KS-125	252.00	255.00	5	7.5	0	0	0	0	1	1	0
KS-125	255.00	258.00	5	5	0	0	0	5	2.5	7.5	0
KS-125	258.00	259.60	2.5	2.5	0	0	0	5	1	6	0
KS-125	262.40	265.00	1	1	0	0	0	10	0	10	0
KS-125	301.00	304.00	2.5	2.5	0	0	0	2.5	1	3.5	0
KS-125	304.00	307.00	0	0	0	0	0	1	1	2	0.5
KS-125	307.00	310.00	0	0	0	0	0	5	1	6	0
KS-125	310.00	313.00	0	0	0	0	0	10	5	15	0
KS-125	313.00	316.00	0	0	0	0	0	5	2.5	7.5	0
KS-125	316.00	319.00	0	0	0	0	0	10	2.5	12.5	0
KS-125	319.00	322.00	0	0	0	0	0	10	1	11	1
KS-125	362.00	365.00	0	0	0	0	0	10	10	20	0
KS-125	365.00	367.89	0	0	0	0	0	5	1	6	0
KS-132	81.05	84.10	0	0	0	0	0	10	0	10	0
KS-132	84.10	87.05	0	0	0	0	0	5	0	5	0
KS-132	87.05	88.40	0	0	0	0	0	10	0	10	0
KS-132	88.40	91.35	0	0	0	0	0	0	0	0	0
KS-132	117.30	120.30	0	0	0	0	0	5	0.5	5.5	0
KS-132	120.30	123.30	0	0	0	0	0	5	0.1	5.1	0
KS-132	123.30	125.30	0	0	0	0	0	2.5	0.5	3	0
KS-132	125.30	127.40	0	0	0	0	0	2.5	0.1	2.6	0
KS-132	127.40	129.40	0	0	0	0	0	10	0	10	0
KS-132	129.40	131.30	0	0	0	0	0	10	0.1	10.1	0
KS-132	131.30	134.30	0	0	0	0	0	10	0.5	10.5	0
KS-132	134.30	137.30	0	0	0	0	0	10	0.5	10.5	0
KS-132	137.30	140.30	0	0	0	0	0	5	1	6	0





DDHS	FROM metres	TO metres	X2 (%)	X3 (%)	CLEAV
KS-125	20.00	23.00	0	0.1	3
KS-125	23.00	26.00	0	0	3
KS-125	26.00	29.00	0	1.5	4
KS-125	29.00	32.00	0	0.9	3
KS-125	69.00	72.00	1	0	5
KS-125	72.00	75.00	0	0.6	6
KS-125	75.00	78.90	0	0	5
KS-125	78.90	84.43	0	0	5
KS-125	84.43	89.72	0	0	6
KS-125	127.10	130.15	0	0	0
KS-125	120.15	133.20	0	0	4
KS-125	133.20	140.30	0	0	4
KS-125	140.30	143.00	0	0	4
KS-125	143.00	146.00	0	0	4
KS-125	185.00	188.00	0	0	7
KS-125	188.00	191.00	0	0	4
KS-125	191.00	194.00	0	0	5
KS-125	194.00	197.00	0	0	4
KS-125	197.00	200.00	0	0	4
KS-125	200.00	203.00	0	0	5
KS-125	203.00	206.00	0	0	4
KS-125	243.00	246.00	0	0	4
KS-125	246.00	249.00	0	0	5
KS-125	249.00	252.00	0	0	4
KS-125	252.00	255.00	0	0	4
KS-125	255.00	258.00	0	0	4
KS-125	258.00	259.60	0	0	5
KS-125	262.40	265.00	0	0	5
KS-125	301.00	304.00	0	0	4
KS-125	304.00	307.00	0	0	4
KS-125	307.00	310.00	0	0	4
KS-125	310.00	313.00	0	0	5
KS-125	313.00	316.00	0	0	5
KS-125	316.00	319.00	0	0	5
KS-125	319.00	322.00	0	0	6
KS-125	362.00	365.00	3.2	0	4
KS-125	365.00	367.89	3.2	0	4
KS-132	81.05	84.10	0	1	7
KS-132	84.10	87.05	0	1	7
KS-132	87.05	88.40	0	5.1	6
KS-132	88.40	91.35	0	0	6
KS-132	117.30	120.30	0	0	3
KS-132	120.30	123.30	0	0	3
KS-132	123.30	125.30	0	0	3
KS-132	125.30	127.40	0	0	3
KS-132	127.40	129.40	0	0	5
KS-132	129.40	131.30	0	0	4
KS-132	131.30	134.30	0.2	0	3
KS-132	134.30	137.30	0.5	0	3
KS-132	137.30	140.30	0.5	0	3